

**STRUCTURAL AND METAMORPHIC EVOLUTION
OF THE NORTH STAR LAKE AREA, MANITOBA**

by

Lawrence I. Norquay

**Presented to the University of Manitoba
in fulfillment of the
thesis requirement for the degree of
Master of Science
in
Geological Sciences**

Winnipeg, Manitoba, 1997

(c) Lawrence I. Norquay, 1997



**National Library
of Canada**

**Acquisitions and
Bibliographic Services**

**395 Wellington Street
Ottawa ON K1A 0N4
Canada**

**Bibliothèque nationale
du Canada**

**Acquisitions et
services bibliographiques**

**395, rue Wellington
Ottawa ON K1A 0N4
Canada**

Your file Votre référence

Our file Notre référence

The author has granted a non-exclusive licence allowing the National Library of Canada to reproduce, loan, distribute or sell copies of this thesis in microform, paper or electronic formats.

The author retains ownership of the copyright in this thesis. Neither the thesis nor substantial extracts from it may be printed or otherwise reproduced without the author's permission.

L'auteur a accordé une licence non exclusive permettant à la Bibliothèque nationale du Canada de reproduire, prêter, distribuer ou vendre des copies de cette thèse sous la forme de microfiche/film, de reproduction sur papier ou sur format électronique.

L'auteur conserve la propriété du droit d'auteur qui protège cette thèse. Ni la thèse ni des extraits substantiels de celle-ci ne doivent être imprimés ou autrement reproduits sans son autorisation.

0-612-23443-6

**THE UNIVERSITY OF MANITOBA
FACULTY OF GRADUATE STUDIES

COPYRIGHT PERMISSION PAGE**

**STRUCTURAL AND METAMORPHIC EVOLUTION OF
NORTH STAR LAKE AREA, MANITOBA**

by

LAWRENCE I. NORQUAY

**A Thesis/Practicum submitted to the Faculty of Graduate Studies of The University
of Manitoba in partial fulfillment of the requirements of the degree
MASTER of SCIENCE**

LAWRENCE I. NORQUAY 1997 (c)

**Permission has been granted to the Library of The University of Manitoba to lend or sell
copies of this thesis/practicum, to the National Library of Canada to microfilm this thesis
and to lend or sell copies of the film, and to Dissertations Abstracts International to publish
an abstract of this thesis/practicum.**

**The author reserves other publication rights, and neither this thesis/practicum nor
extensive extracts from it may be printed or otherwise reproduced without the author's
written permission.**

ABSTRACT

The North Star Lake area of northwestern Manitoba lies within the Flin Flon domain which, along with the Kisseynew domain, forms the internal zone of the Reindeer zone of the Early Proterozoic Trans-Hudson Orogen. The North Star Lake area consists predominantly of an Early Proterozoic assemblage of metavolcanic, metasedimentary and intrusive rocks.

The North Star Lake area has undergone polyphase deformation and metamorphism. The initial deformation in the North Star Lake area was the result of the accretion of the Flin Flon domain volcanic terrane that juxtaposed the juvenile arc assemblages of the Flin Flon domain by intraoceanic tectonics into an accretionary complex during the period of 1.88--1.87 Ga. Subsequent to the initial deformation, the North Star Lake area underwent a progressive deformational cycle (D_1 -- D_3) and a contemporaneous prograde--retrograde metamorphic cycle (M_1 -- M_3) during the period of 1.83--1.80 Ga.

The progressive deformation cycle was a result of south--southwest-directed thrusting during the closure of the Kisseynew basin. This resulted in the overthrusting of the Amisk collage of the Flin Flon domain by the Snow Lake arc segment of the Flin Flon domain and by the Kisseynew domain.

The progressive deformation produced a succession of folds (F_1 -- F_3) which initially formed perpendicular to the south--southwest-directed movement vector. Early folds (F_1 and

F₂) were reoriented towards parallelism with the direction of transport.

Metamorphism in the North Star Lake area followed a clockwise medium-pressure (Barrovian) P--T--t evolution with maximum pressure predating maximum temperature. Peak metamorphism is associated with the second phase of deformation and culminated at upper-amphibolite facies grade during the period of 1820--1805 Ma.

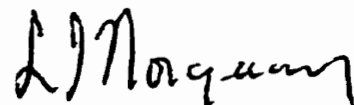
The final deformation in the North Star Lake area produced brittle--ductile and brittle structures under greenschist facies conditions. This phase of deformation occurred in a northwest--southeast stress regime and was probably the result of the terminal collision between the Reindeer zone and the Superior craton.

I hereby declare that I am the sole author of this thesis. I authorize the University of Manitoba to lend this thesis to other institutions or individuals for the purpose of scholarly research.

A handwritten signature in cursive script, reading "L I Norquay".

Lawrence I. Norquay

I further authorize the University of Manitoba to reproduce this thesis by photocopying or by other means, in total or in part, at the request of other institutions or individuals for the purpose of scholarly research.

A handwritten signature in cursive script, reading "L I Norquay".

Lawrence I. Norquay

The University of Manitoba requires the signatures of all persons using or photocopying this thesis. Please sign below, and give address and date.

DEDICATION

For my brother

**John Gavin Morquay
1966-1994**

All should know such a friend

ACKNOWLEDGMENTS

I would like to acknowledge two men, Dr. Norman M. Halden of the University of Manitoba and Dr. George H. Gale of Manitoba Energy and Mines. Each of these men, Dr. Halden, who was my thesis advisor, and Dr. Gale, whose ideas inspired this thesis, have served me well as both a mentor and a friend. For this I thank them.

I thank the faculty and staff of the Department of Geological Sciences at the University of Manitoba. I especially thank Dr. Allen C. Turnock for the hours he spent with myself and my thin sections in the petrography lab.

I thank colleagues at Manitoba Energy and Mines for their help and insight. I especially thank Martin Bieri, Tom Heine, Dave Prouse and Gerald Tremath; the Manitoba Energy and Mines geologists who were involved in the North Star Lake project. I also am thankful for the excellent assistance I received in the field during the course of the North Star Lake project from Zerai Andegorgs, Kyla Arden, Ayed Ayed, Eric Bjornson, Kathleen Dahlen, Marcia Hay, Ryan Hicks, Cameron Mitchell, Rolph Pippert, Christine Poschadel, John Roozendaal and Jason Underhill. I also thank all of the cartographers at Manitoba Energy and Mines for their help.

Finally, I thank my parents, Ian and Margaret Norquay, my family and my friends for their patience and support. Without these people this endeavour would have been impossible.

TABLE OF CONTENTS

Abstract.....	i
Dedication.....	v
Acknowledgments.....	vi
List of Figures.....	ix
List of Plates.....	xi
List of Tables.....	xiii
1. INTRODUCTION.....	1
1.1 Location.....	1
1.2 Significance.....	1
1.3 Statement of Objectives.....	2
2. REGIONAL GEOLOGIC SETTING.....	5
2.1 Geology and Tectonic Evolution of the Reindeer Zone.....	5
2.2.1 The Trans-Hudson Orogen.....	8
2.1.2 The Reindeer Zone.....	8
2.1.3 The Churchill--Superior Boundary Zone.....	11
2.1.4 The Wathaman--Chipewyan Batholith.....	12
2.1.5 Deformation and Metamorphism.....	13
2.1.6 Geochronology.....	14
2.2 General Geology of the Flin Flon and Kisseynew Domains.....	17
2.2.1 Flin Flon Domain Stratigraphy.....	17
2.2.2 Kisseynew Domain Stratigraphy.....	22
2.2.3 Early Deformation in the Flin Flon and Kisseynew Domains.....	25
2.2.4 Collision Tectonics, Deformation and Metamorphism in the Flin Flon and Kisseynew Domains.....	27
3. GEOLOGY OF THE NORTH STAR LAKE AREA.....	31
3.1 Introduction.....	31
3.2 Previous and Current Work.....	35
3.3 Procedure and Data Accumulation.....	36
3.4 Eastern Zone.....	36
3.5 Central Zone.....	37
3.5.1 East Shore of North Star Lake Area.....	38
3.5.2 Sausage Lake Area.....	41
3.3.3 Round Lake Area.....	43
3.6 Western Zone.....	44
3.7 Granitoid Rocks.....	53
3.7.1 Gants Lake Batholith.....	53
3.7.2 Granitic--Granodioritic Rocks.....	56
3.7.3 Norris Lake Pluton.....	56
3.7.4 Quartz-eye Porphyry.....	57
3.8 Ultramafic Intrusions.....	58
3.9 Diatremes.....	59

4. STRUCTURAL GEOLOGY OF THE NORTH STAR LAKE AREA.....	61
4.1 Introduction.....	61
4.2 Cleavage Classification.....	66
4.3 Fold Classification.....	68
4.4 Fault Rock Classification.....	70
4.5 Macroscopic Features.....	72
4.5.1 First Phase of Deformation (D_1)	72
4.5.2 Second Phase of Deformation (D_2)	82
4.5.3 Third Phase of Deformation (D_3)	91
4.5.4 Late Brittle and Brittle--Ductile Deformation (D_4).....	103
4.6 Equal Area Stereonet Analysis.....	108
4.6.1 First Phase of Deformation (D_1)	108
4.6.2 Second Phase of Deformation (D_2)	111
4.6.3 Third Phase of Deformation (D_3)	116
4.7 Microscopic Features.....	121
4.7.1 First Phase of Deformation (D_1)	121
4.7.2 Second Phase of Deformation (D_2)	125
4.7.3 Third Phase of Deformation (D_3)	130
5. METAMORPHISM IN THE NORTH STAR LAKE AREA.....	134
5.1 Introduction.....	134
5.2 Description of Metamorphic Events.....	136
5.2.1 First Phase of Metamorphism (M_1)	136
5.2.2 Second Phase of Metamorphism (M_2)	145
5.2.3 Third Phase of Metamorphism (M_3)	161
5.2.4 Fourth Phase of Metamorphism (M_4)	164
5.3 Geothermobarometry.....	167
5.4 Petrogenetic Grid.....	169
6. STRUCTURAL AND METAMORPHIC HISTORY OF THE NORTH STAR LAKE AREA.....	172
6.1 Introduction.....	172
6.2 Early Deformation in the North Star Lake Area.....	174
6.3 First Deformational Event (D_1) and First Metamorphic Event (M_1) in the North Star Lake Area	175
6.4 Second Deformational Event (D_2) and Second Metamorphic Event (M_2) in the North Star Lake Area	186
6.5 Third Deformational Event (D_3) and Third Metamorphic Event (M_3) in the North Star Lake Area	195
6.6 Late Deformation and Metamorphism in the North Star Lake Area.....	204
7. DISCUSSION AND CONCLUSIONS	
7.1 The Structural and Metamorphic Evolution of the North Star Lake Area Within the Context of the Trans-Hudson Orogen.....	205
7.1.1 Early Deformation.....	210
7.1.2 Collisional Tectonics, Deformation and Metamorphism.....	212
7.2 Conclusions.....	220

REFERENCES.....232

APPENDIX A.....242

List of Figures

1-1	Location of the North Star Lake area.....	3
1-2	Geology of Manitoba and the location of the Flin Flon--Snow Lake (Flin Flon) Volcanic belt.....	4
2-1	Major elements of the Trans-Hudson Orogen, other Early Proterozoic orogenic belts, and Archean cratons in North America.....	6
2-2	Lithotectonic domains of the Reindeer Zone, and other elements of the Trans-Hudson Orogen in Saskatchewan and Manitoba.....	7
2-3	Diagrammatic summary of geochronology data constraining the assembly of the crust in the internal zone of the Trans-Hudson Orogen in Manitoba.....	16
2-4	Major tectono-stratigraphic assemblages of the Flin Flon domain.....	18
2-5	Tectonic evolution of the Flin Flon domain (ca. 1.92--1.84 Ga).....	26
3-1	Geology of the North Star Lake area (after McGlynn, 1959).....	33
3-2	Geology of the North Star Lake area (after Norquay <i>et al.</i> , 1994a; 1994b).....	34
4-1	Structural geology schematic of the North Star Lake area.....	62
4-2	Structural subareas in the North Star Lake area.....	65
4-3	Type and spacing of cleavages.....	67
4-4	Classification of cleavages based on morphology.....	67
4-5	Classification of fold profiles using dip isogon patterns.....	69
4-6	Classification of fold orientations.....	69
4-7	Contoured equal area projection of poles to S_1 foliation (subareas 1, 2, 3 and 4).....	109
4-8	Equal area projection of F_1 orientation compared to S_1 maximum contour density (subareas 1, 2, 3 and 4).....	110
4-9	Contoured equal area projection of poles to S_1 (subarea 5).....	110
4-10	Equal area projection of orientation of F_2 axial planes (subareas 1, 2, 3 and 4).....	113
4-11	Equal area projection of poles to S_1 and girdle of poles to S_1 in the vicinity of Face Lake.....	113
4-12	Equal area projection of poles to S_1 and girdle of poles to S_1 in the vicinity of Round Lake.....	114

4-13	Equal area projection of F_{2n} fold axes (subarea 1) compared to girdle of poles to S_1 in vicinity of Face Lake.....	114
4-14	Equal area projection of F_{2n} fold axes (subarea 2) compared to girdle of poles to S_1 in vicinity of Round Lake.....	115
4-15	Equal area projection of F_{2n} orientation (subarea 5).....	115
4-16	Equal area projection of orientation of S_3 foliation and F_3 axial planes (subareas 6 and 7) ...	118
4-17	Equal area projection of orientation of F_{2n} fold axes (subareas 4, 6 and 7).....	118
4-18	Equal area projection of S_1 foliation and F_3 fold axes (subarea 6).....	119
4-19	Equal area projection of S_1 foliation and F_3 fold axes (subarea 7).....	119
4-20	Equal area projection of S_3 foliation, F_3 fold axes and F_3 axial planes (subarea 2)	120
4-21	Equal area projection of F_3 axial plane and F_3 fold axes (subarea 5).....	120
5-1	AFM projections for biotite and garnet zones.....	141
5-2	M_1 garnet compositional profile	142
5-3	M_2 garnet compositional profile	154
5-4	AFM projections showing assemblages coexisting with muscovite, quartz and H_2O in Barrovian-type (medium-pressure) metamorphism.....	155
5-5	ACF diagrams for medium-pressure facies series.....	156
5-6	Petrogenetic grid for the North Star Lake area.....	171
6-1	Displacement by progressive simple shear showing relationship of geometrical and geological elements.....	180
6-2	Development of reverse-slip creulations.....	188
6-3	Theory of the progressive evolution of fold shapes in single competent layers.....	196
6-4	The spectrum of fold shapes produced by buckling a competent layer in a less competent host material..	196
6-5	Models of folds developed in regularly alternating competent layers.....	201
7-1	Location of areas of recent studies in the eastern portion of the Flin Flon domain and southern flank of the Kisseynew domain.....	207
7-2	Dow Lake and Reed Lake areas.....	216
7-3	Reed Lake and southern File Lake areas.....	217
7-4	Diagram of the development of the North Star Lake area during the first phase of deformation.....	224
7-5	Diagram of the development of the North Star Lake area during the second phase of deformation.....	227
7-6	Diagram of the development of the North Star Lake area during the third phase of deformation.....	229
7-7	Plan view of the North Star Lake area during the fourth phase of deformation.....	231

List of Plates

4-1	Isoclinal F_1 . Amphibolite dyke in rhyolite	76
4-2	Tight F_1 with axial-planar schistosity. Folded S_0 contact between rhyolitic and dacitic rocks.....	76
4-3	Spaced cleavage (S_0) in rhyolite. Biotite-rich domains separate quartzo-feldspathic microlithons...	77
4-4	Gentle-plunging L_1 expressed as quartz-plagioclase aggregates.....	77
4-5	Pseudoconglomerate derived from layered psammopelitic rocks in hinge area of isoclinal F_1 ...	78
4-6	Layered psammopelitic rocks on limb of isoclinal F_1	78
4-7	Isoclinal F_1 in North--South zone. Amphibolite in psammopelitic rocks.....	79
4-8	Compositional (tectonic) layering or banding (S_1) in North--South zone.....	79
4-9	Mafic rock with well-developed foliation. Quartz veins both lie in and crosscut the foliation.....	80
4-10	Boudinaged mafic dyke or layer in North--South zone, extension parallel to fabric.....	80
4-11	Volcanoclastic rock proximal to North--South zone. Lithic fragments have undergone substantial flattening.....	81
4-12	Epidosite pods proximal to North--South zone, σ -type winged porphyroclast geometry indicates dextral simple shear.....	81
4-13	F_2 parallel fold. Amphibolite dyke in rhyolite	86
4-14	Tight, gentle-plunging F_2 in banded iron formation.....	86
4-15	Weak fracture cleavage (S_2) in rhyolite in hinge area of F_2 structure	87
4-16	Flat-lying spaced cleavage (S_1) in hinge area of F_2 structure	87
4-17	Volcanoclastic rock in F_2 hinge area. Lithic fragments have been flattened during D_1 and subsequently folded during D_2	88
4-18	Quartz rods define L_2 in felsic gneiss	88
4-19	Gneissosity in semipelite defines S_2 , axial-planar to F_2	89
4-20	Gneissosity defines L_2 as rods near circular in cross-section on the vertical face and elongate in cross-section on the horizontal face.....	89
4-21	Gneissosity in semipelite folded during D_2	90
4-22	Similar, tight to isoclinal F_2 folds fabric and compositional layering.....	90
4-23	F_3 open fold in foliated felsic rock, wavelength of several metres.....	95
4-24	F_3 open to tight fold in layered felsic and mafic rocks.....	95

4-25	F_3 crenulate folds in amphibolite with well-developed S_1/S_2 foliation	96
4-26	Moderately-developed biotite schistosity defines S_3 in micaceous felsic rock	96
4-27	F_3 chevron to tight parallel folds in felsic rocks with well-developed S_1/S_2 foliation	97
4-28	Quartz veins axial-planar to F_3 in foliated felsic intrusion.....	97
4-29	Symmetric F_3 cusped and lobate folds at contact between felsic intrusion and amphibolite dyke.....	98
4-30	Asymmetric F_3 cusped and lobate fold at contact between felsic intrusion and amphibolite dyke.....	98
4-31	F_3 box fold in banded intermediate and mafic rocks ..	99
4-32	Open Z conjugate of F_3 box fold	99
4-33	Tight Z-conjugate of F_3 box fold	100
4-34	Poorly-developed S-conjugate of F_3 box fold	100
4-35	F_{2a} folded by F_3 in banded iron formation	101
4-36	D_1/D_2 fabric in North--South zone folded by D_3	101
4-37	D_1/D_2 boudin folded by D_3	102
4-38	Ductile F_4 structure in amphibolite	105
4-39	Brittle--ductile F_4 structure in intermediate rock. Semi-brittle failure along short limb of F_4 structure.....	105
4-40	Brittle F_4 structure and sinistral brittle fault containing crush breccia and cataclasite in quartzo-feldspathic rock.....	106
4-41	Pseudotachylite in late brittle fault.....	106
4-42	Tension gashes in epidosite lenses proximal to fault zone indicate sinistral movement.....	107
4-43	Fine-grained brown biotite defines S_1 schistosity in felsic rock.....	123
4-44	Garnet overprints but is subsequently draped by S_1 schistosity in felsic rock.....	123
4-45	Quartz lenses in annealed felsic mylonite (<i>sensu lato</i>).....	124
4-46	Feldspar porphyroclast in felsic mylonite (<i>sensu lato</i>).....	124
4-47	Amphibole in hinge area of F_{2a} structure. View parallel to L_{2a}	127
4-48	Amphibole in hinge area of F_{2a} structure. View perpendicular to L_{2a}	127
4-49	Quartz rod in felsic rock. View parallel to L_{2a}	128
4-50	Quartz rod in felsic rock. View perpendicular to L_{2a}	128
4-51	Leucocratic component of gneissosity in felsic rock. View parallel to L_{2a}	129
4-52	Leucocratic component of gneissosity in felsic rock. View perpendicular to L_{2a}	129
4-53	F_3 crenulate fold in amphibolite	132
4-54	F_3 crenulate to box fold in amphibolite of North--South zone.....	132

4-55	Hinge area of tight flexural fold (F_3) in micaceous felsic rock.....	133
5-1	S_1 defined by biotite and muscovite in micaceous felsic rock.....	144
5-2	M_1 garnet with reaction halo; draped by biotite and muscovite.....	144
5-3	M_2 porphyroblasts overprint D_1/M_1 fabrics	158
5-4	M_2 garnet and biotite	158
5-5	M_2 assemblage of staurolite, biotite, muscovite and quartz.....	159
5-6	M_2 assemblage of kyanite, biotite, muscovite and quartz.....	159
5-7	D_2/M_2 fabric (assemblage of staurolite, biotite, muscovite and quartz) deformed by D_3	160
5-8	D_2/M_2 fabric (leucosome and melanosome material) deformed by D_3	160
5-9	Biotite and muscovite define S_3	163
5-10	F_3 crenulate fold overprinted by late garnet porphyroblast in amphibolite.....	163
5-11	Cataclasite; ductile fabric in North-- South zone overprinted by brittle deformation. Retrograde metamorphic assemblage.....	165
5-12	Weak S_1 fabric in micaceous felsic rock overprinted by late muscovite.....	165

List Of Tables

2-1	Flin Flon domain stratigraphy.....	21
2-2	Kisseynew domain stratigraphy.....	23
2-3	Stratigraphy of supracrustal rocks of the Kisseynew domain.....	24
4-1	Characteristics of the structural subareas in the North Star Lake area.....	64
4-2	Fold classification system based on interlimb angle.....	68
4-3	Textural classification of fault rocks.....	71
4-4	Fault rocks and style of faulting.....	71
7-1	Structural and metamorphic history of the North Star Lake area.....	208
7-2	Structural and metamorphic characteristics of areas proximal to the North Star Lake area.....	209

Chapter I

INTRODUCTION

1.1 Location

The North Star Lake area (NTS 63K/15) is bounded by latitudes $54^{\circ}48'45''$ and $54^{\circ}56'15''$ north and longitudes $100^{\circ}30'00''$ and $100^{\circ}38'45''$ west. It is located approximately 35 km west of the Town of Snow Lake, Manitoba and approximately 85 km east of the City of Flin Flon, Manitoba (Figure 1-1).

1.2 Significance

The North Star Lake area consists predominantly of an Early Proterozoic assemblage of metavolcanic, metasedimentary and intrusive rocks and is in the Flin Flon--Snow Lake Volcanic Belt near the contact with the Kisseynew Metasedimentary Gneiss Belt. The Flin Flon--Snow Lake Volcanic Belt is located in northern Manitoba and Saskatchewan (Figure 1-2) and is part of the Reindeer Zone of the Trans-Hudson Orogen.

In 1989, forest fires in northern Manitoba provided extensive new outcrop exposures in the North Star Lake area. In order to take advantage of these new outcrop exposures the North Star Lake area was included in the Strategic Outcrop Mapping Project (STOMP) of the Geological Services Branch of the Manitoba Department of Energy and Mines. The North Star

Lake area was mapped by the Manitoba Geological Services Branch during the period of 1990--1994 (Trembath et al., 1990; Norquay et al., 1991; Norquay et al., 1992; Norquay and Halden, 1992; Ayed and Halden, 1993; Norquay et al., 1993; Prouse and Gale, 1993; Norquay et al., 1994a, 1994b, 1994c).

Previous exploration indicated several areas with the potential to contain massive sulphide type deposits (G.H. Gale pers. com., 1989), as well as a large number of gold occurrences (Stockwell, 1935). Because of the economic potential of the North Star Lake area and the opportunity presented by the recent forest fire in the area, the North Star Lake project was initiated by the Geological Services Branch to coincide with other recent or ongoing regional mapping projects in the Flin Flon--Snow Lake Volcanic Belt.

1.3 Statement of Objectives

The objectives of this thesis are:

- 1) documentation of the structural and metamorphic properties of the rocks in the North Star Lake area.
- 2) interpretation of the structural and metamorphic history of the North Star Lake area.
- 3) discussion of the significance of the North Star Lake area structural and metamorphic history within the context of the Trans-Hudson Orogen.

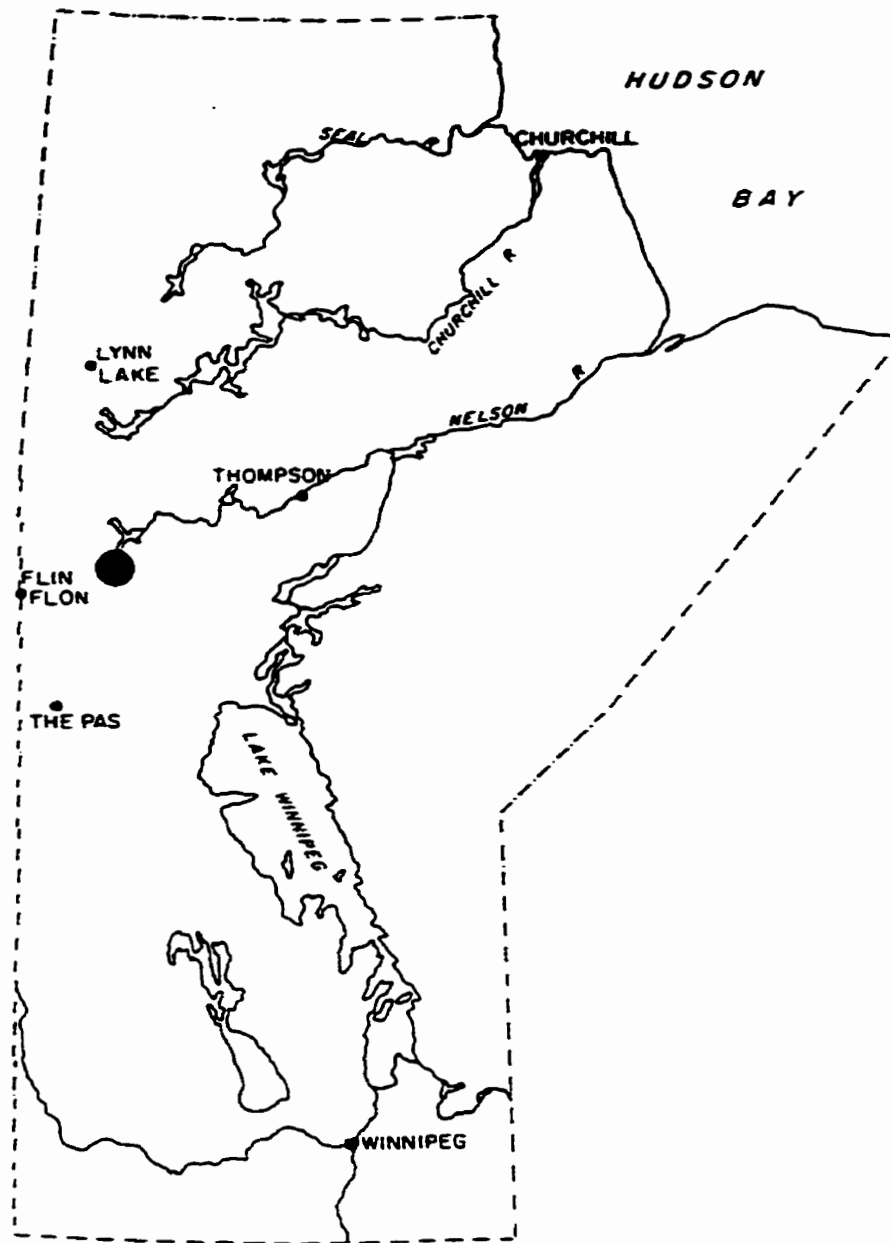


Figure 1-1. Location of the North Star Lake area (large dot).

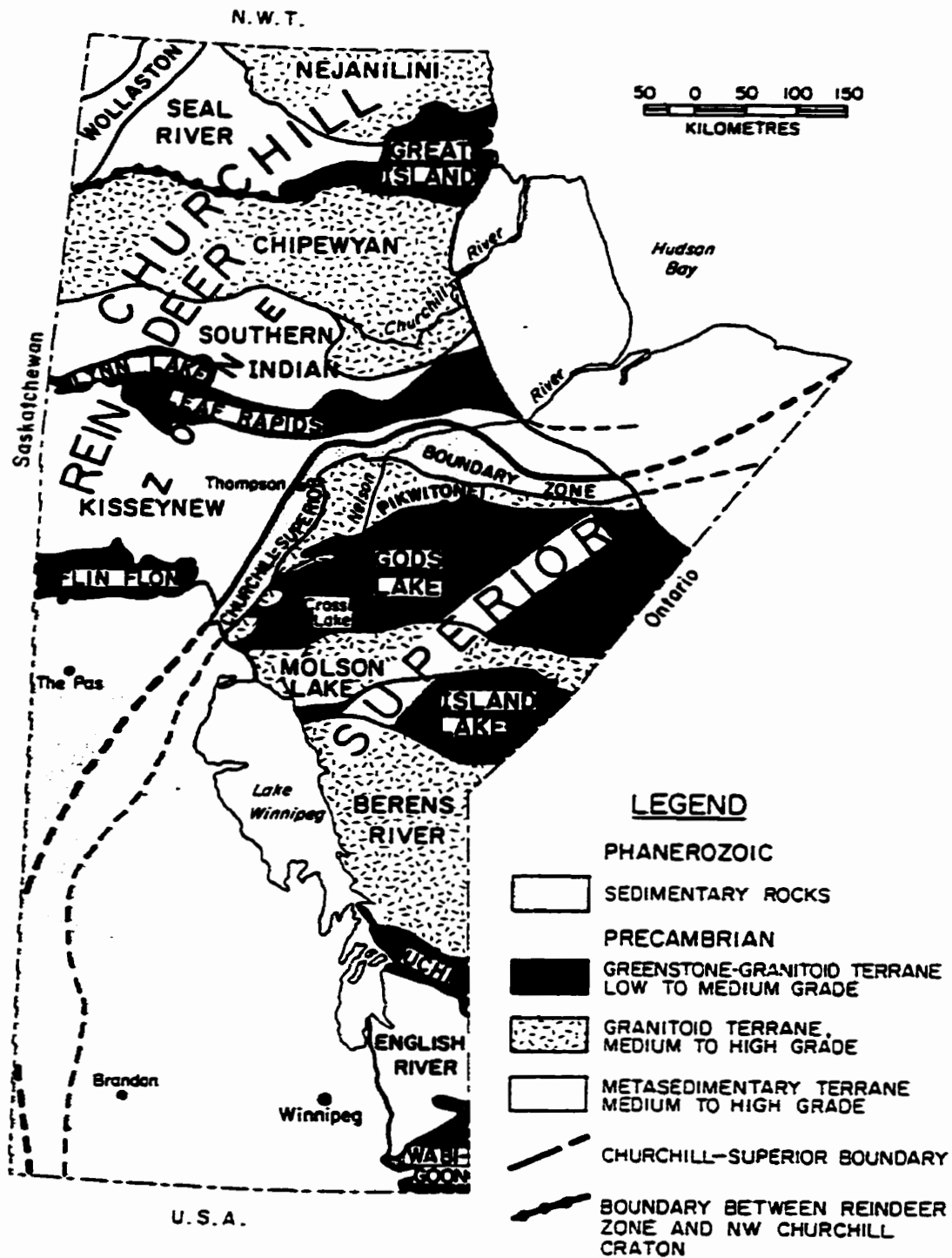


Figure 1-2. Geology of Manitoba and the location of the Flin Flon--Snow Lake (Flin Flon) Volcanic belt (from Weber, 1990).

Chapter II

REGIONAL GEOLOGIC SETTING

2.1 Geology and Tectonic Evolution of the Reindeer Zone

The Reindeer Zone of the Trans-Hudson Orogen (Figure 2-1) straddles northern Manitoba and Saskatchewan. First defined by Stauffer (1984) as The Reindeer Lake Zone; the Reindeer Zone (Figure 2-2) consists of a number of juvenile tectonic domains which lie between the Churchill--Superior Boundary Zone and the Wathaman--Chipewyan batholith (Stauffer, 1984; Lewry and Collerson, 1990). The Reindeer Zone is lithologically and structurally complex; it is a post-collisional collage of Early Proterozoic arc-related volcanic and plutonic rocks, volcanoclastic rocks and later arkosic molasse sedimentary rocks (Stauffer, 1990). The Reindeer Zone is up to 400 km in width and is dominated by juvenile material accreted during the Trans-Hudson Orogen (Hoffman, 1990).

The Reindeer Zone is situated in what was traditionally referred to as the Churchill Province of the Canadian Shield (Stockwell, 1961). The deformation that resulted in the structural trend that distinguishes the Churchill Province from other structural provinces of the Canadian Shield was referred to as the Hudsonian Orogeny (Stockwell, 1961). This orogeny has been incorporated into the more extensive Trans-Hudson Orogen (Hoffman, 1981).

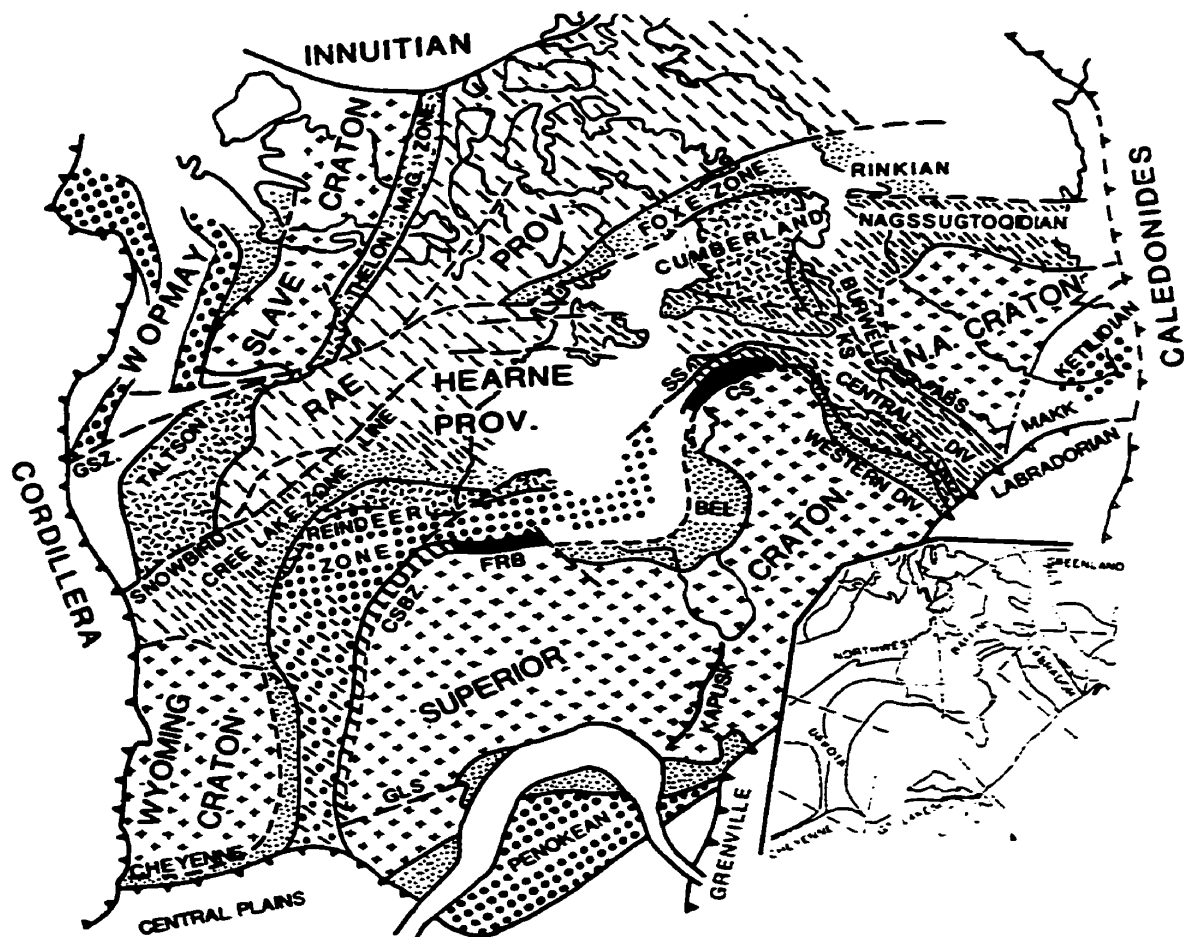


Figure 2-1. Major elements of the Trans-Hudson Orogen, other Early Proterozoic orogenic belts, and Archean cratons in North America.

Abbreviations: ABS, Abloviak shear zone; KS, Komaktorvik shear zone; SS, Sugluk suture; CS, Cape Smith belt; BEL, Belcher Islands area; FRB, Fox River belt; GLS, Great Lakes shear zone; GSZ, Great Slave shear zone; CSBZ, Churchill--Superior Boundary Zone; and MAKK, Makkovik belt.

Legend: crosses, little reworked Archean cratons; oblique dash, Archean continental crust variably reworked during Early Proterozoic orogeny; stipple, Early Proterozoic foreland fold/thrust belts; random ticks, major continental magmatic arc batholiths; heavy dots, mostly accreted juvenile Early Proterozoic arc terranes; black, predominantly mafic-ultramafic allochthons thrust over margins of the Superior craton (from Lewry and Collerson, 1990).

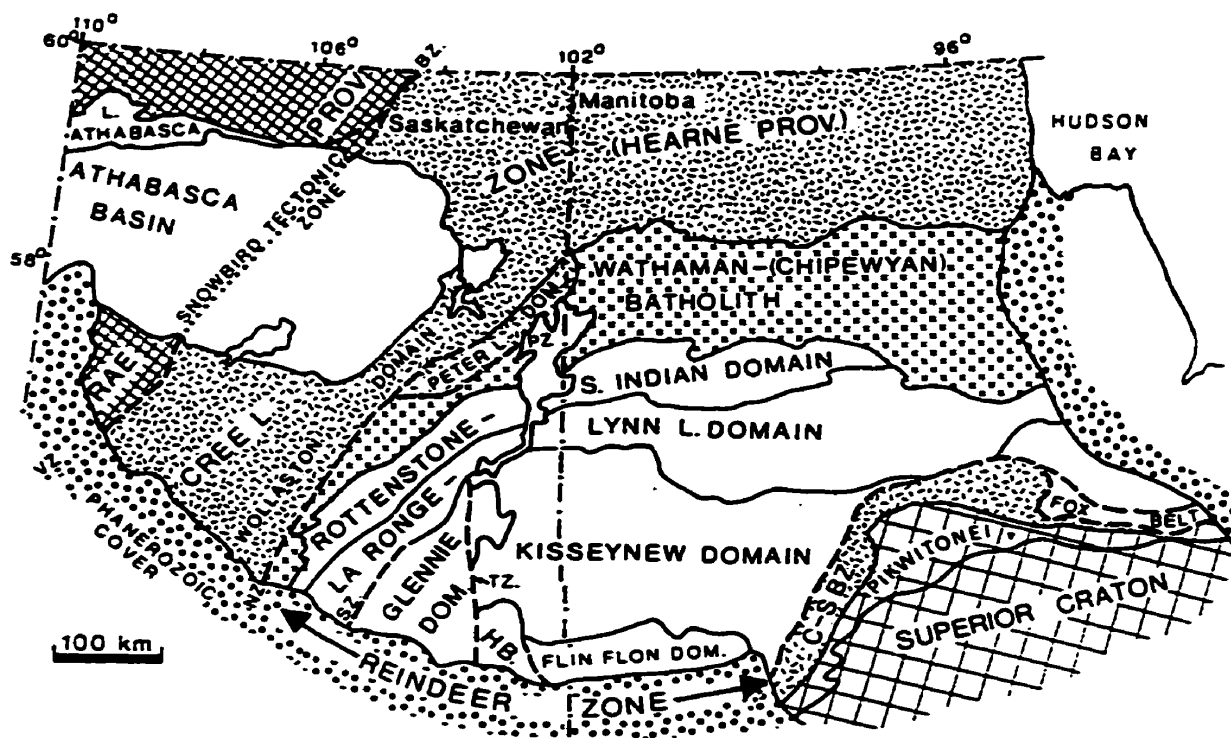


Figure 2-2. Lithotectonic domains of the Reindeer Zone, and other elements of the Trans-Hudson Orogen in Saskatchewan and Manitoba. Ornamented Precambrian components are mainly "ensialic" elements of the orogen and bounding cratons. Unornamented domains are mostly juvenile early proterozoic crustal elements. Heavy dashed lines indicate major ductile shear zones or brittle--ductile faults. **Abbreviations:** C-S BZ, Churchill--Superior Boundary Zone; HB, Hanson Lake Block; TZ, Tabernor fold/fault zone; SZ, Stanley fault/shear zone; NZ and PZ, Needle Falls and Parker Lake shear zones; and VZ and BZ, Virgin River and Black Lake shear zones (from Lewry et al., 1990).

2.1.1 The Trans-Hudson Orogen

The Trans-Hudson Orogen (Hoffman, 1981) is the dominant orogenic component of the Pan-American System (Lewry et al., 1987), a more extensive orogenic system. The evolution and development of the Pan-American System coincides with a major episode of the accretion of the North American continent and the Laurentian supercontinent during the Early Proterozoic (Hoffman, 1988).

The Trans-Hudson Orogen has been delineated in subsurface from South Dakota through to the edge of the Canadian Shield in Manitoba and Saskatchewan (Green et al., 1985; Klasner and King, 1990). The Trans-Hudson Orogen continues across the exposed shield and under the Hudson Bay basin and to at least the Cape Smith Belt in northern Quebec (Lewry and Collerson, 1990) (Figure 2-1).

Considerable evidence suggests that the evolution of the Reindeer Zone during the Trans-Hudson Orogen proceeded under uniformitarian plate tectonic processes (Lewry and Collerson, 1990). These processes or stages were: 1) initial continental rifting and passive margin development; 2) ensuing subduction; 3) arc generation and closure; 4) juvenile terrane accretion; and 5) terminal continental suturing at collisional plate boundaries.

2.1.2 The Reindeer Zone

The Reindeer Zone (Figure 2-2) has been defined as the

lithotectonic elements lying between the Churchill--Superior Boundary Zone and the Wathaman--Chipevyan batholith (Hoffman, 1990; Lewry *et al.*, 1990; Lewry and Collerson 1990) while other workers have included the Wathaman--Chipevyan batholith as part of the Reindeer Zone (Stauffer, 1984). The rocks of the Reindeer Zone are composed predominantly of mafic island-arc metavolcanic rocks and associated metasedimentary rocks (Stauffer, 1984).

Stauffer (1984) divided the Reindeer Zone into four lithostructural domains: 1) Flin Flon domain; 2) Kisseynew domain; 3) La Ronge (La Ronge--Lynn Lake) domain; and 4) Rottenstone (Rottenstone--South Indian) domain (Figure 2-2). The Reindeer Zone underwent plate-tectonic closure during the Early to Middle Proterozoic resulting in the formation of subduction zones with associated volcanic island-arcs and back- and fore-arc sedimentary basins followed by collision-generated deformation, metamorphism, and intrusion (Stauffer, 1984). The Glennie Lake domain, a terrane of possibly Archean origin (Green *et al.*, 1985), lies within the Reindeer zone (Figure 2-2).

The Flin Flon domain (Flin Flon--Snow Lake Volcanic Belt) is a complex assemblage of subaqueous and subordinate subaerial volcanic rocks with associated synvolcanic sedimentary rocks overlain by a sequence of terrestrial sedimentary rocks (Bailes *et al.*, 1987). The western portion of the Flin Flon domain is composed predominantly of basalt

and basaltic andesite with an island-arc tholeiite affinity and subordinate more-fractionated ferrobasalts as well as basalts with a back-arc affinity (Syme, 1990). According to Bailes (1971) the Flin Flon domain is comprised of four main sequences. These four sequences are: 1) the Amisk Group, a thick sequence of mafic to felsic volcanic rocks with associated intercalated sedimentary rocks; 2) the Post-Amisk Intrusive Group; 3) the Missi Group, a sequence of arkose, greywacke, and quartzite that unconformably overlies the Amisk Group and Post-Amisk Intrusive Group; and 4) the Post-Missi Intrusive Group.

The Kisseynew domain (Kisseynew Metasedimentary Gneiss Belt) is composed of highly deformed, predominantly amphibolite-grade gneisses (Stauffer, 1984). The Kisseynew domain contains five suites of supracrustal rocks that are the high-grade equivalents of stratigraphic groups recognised in the adjacent lower grade Flin Flon and La Ronge domains as well as various plutonic rocks that range from pre- to late-tectonic in age (Zwanzig, 1990).

In the southern--southeastern portion of the La Ronge domain (La Ronge--Lynn Lake Volcanic Belt), adjacent to the Kisseynew domain, the supracrustal rocks are predominantly island-arc volcanic rocks with associated intercalated sedimentary rocks (Stauffer, 1984). The volcanic rocks in the southern portion of the La Ronge domain in Manitoba consists of: 1) tholeiitic basalts; 2) "primitive" (magnesian) calc-

alkaline basalts; 3) felsic volcanic rocks; and 4) andesitic calc-alkaline rocks (Syme, 1990a).

The northwestern portion of the La Ronge domain, adjacent to the Rottenstone domain, is composed mainly of psammitic to pelitic metasedimentary rocks. These rocks have been interpreted as turbidites shed from the La Ronge domain island-arc (Stauffer, 1984).

Stauffer (1984) defined the Rottenstone domain as a terrane consisting of the Wathaman--Chipewyan batholith in the northwestern portion and the Tonalite--Migmatite complex in the southeast. Green et al. (1985) included the Tonalite--Migmatite complex with the Reindeer--South Indian Lakes belt; and interpreted this belt to be the remnant of a back-arc basin that separated the La Ronge domain from the Archean cratons to the northwest.

2.1.3 The Churchill--Superior Boundary Zone

The Churchill--Superior Boundary Zone lies to the southeast of the Reindeer Zone (Figure 2-2). It is a structurally complex zone that forms the northwest margin of the Archean Superior craton and is in fault or thrust contact with the Early Proterozoic Reindeer Zone to the northwest (Weber, 1990). The Churchill--Superior Boundary Zone has been divided into three segments: 1) the Thompson belt; 2) the Split Lake block; and 3) the Fox River belt (Weber and Scoates, 1978).

It has been suggested that most supracrustal rocks of the Churchill--Superior Boundary Zone were related to initial continental rifting. Recent evidence indicates that these supracrustal rocks are the result of marginal basin or back-arc basin rifting that was contemporaneous with the island-arc volcanism of the Reindeer Zone (Weber, 1990).

The thermotectonic overprinting of the rocks of the Churchill--Superior Boundary Zone was the result of the collisional tectonics of the Trans-Hudson Orogen (Weber, 1990). Bleeker (1990) presented a model of the structural evolution of the Thompson belt in which initial north--south or northwest--southeast thrusting of the juvenile material of the Thompson belt over the Archean Superior foreland evolved into sinistral transform motion.

To the southeast of the Churchill--Superior Boundary Zone is the Archean Superior craton. The Superior craton, outside of its margin that adjacent is to the Churchill--Superior Boundary Zone, was little reworked by the Trans-Hudson Orogen (Lewry and Collerson, 1990).

2.1.4 The Wathaman--Chipewyan Batholith

The monzogranite--granodiorite Wathaman--Chipewyan batholith (Figure 2-2) is everywhere emplaced between the reworked Archean Hearne Province to the northwest and the Reindeer Zone to the southeast. The Wathaman--Chipewyan batholith is interpreted as a continental margin magmatic-arc

(Lewry and Collerson, 1990). Based on geochemical and isotopic constraints, the Wathaman--Chipewyan batholith and the adjacent Baldock batholith are interpreted to be products of subduction-related plate tectonic processes; in contrast with the adjacent Thornsteinson batholith which is interpreted to be a younger, anorogenic intrusion (Halden et al., 1990).

Northwest of the Wathaman--Chipewyan batholith is the Hearne Province, consisting of continuous, variably reworked, Archean continental crust (Lewry and Collerson, 1990; Hoffman, 1990). The Archean basement is locally overlain and infolded with Early Proterozoic volcanic and sedimentary rocks of rifted margin environment and miogeoclinal and foreland basin sedimentary rocks (Lewry and Collerson, 1990).

2.1.5 Deformation and Metamorphism

The Reindeer Zone -- composed of Early Proterozoic volcanic island-arcs (Flin Flon and La Ronge domains) and their associated fore-arc (Kisseynew domain) and back-arc (Rottenstone domain) basins -- lies wedged between the Archean Superior craton to the east and the Archean portions of the Churchill and Wyoming cratons to the west (Green et al., 1985). The deformation in the Reindeer Zone is the result of extreme crustal shortening produced by fold and thrust stacking and the transportation of major allochthonous sheets (Lewry et al., 1990). Recent seismic data from LITHOPROBE Trans-Hudson Orogen Transect (Hajnal and Lewry eds., 1992;

1993; 1994; 1995) has provided a three-dimensional picture of the structural geology of the Reindeer Zone. LITHOPROBE seismic data indicate that the Reindeer Zone of western Superior boundary zone underwent significant crustal imbrication and was subsequently overthrust by the Superior craton (White and Lucas, 1994; White et al., 1994). Additional LITHOPROBE seismic data indicate that the south flank of the Kisseynew domain overlies the Flin Flon domain (Lucas et al., 1994b; White and Lucas, 1994).

The grade of regional metamorphism in the Reindeer Zone is highest in the central portion of the Kisseynew domain and decreases rapidly along the north and south margins into the Flin Flon and La Ronge domains (Bailes and McRitchie, 1978). The grade of regional metamorphism reaches upper-amphibolite facies in the Kisseynew domain (Zwanzig and Schledewitz, 1992) and can be as low as sub-greenschist in the Flin Flon domain (Bailes and Syme, 1987).

2.1.6 Geochronology

The geochronology of the formation and accretion of the crustal material of the Reindeer Zone has been described by Gordon et al. (1990). This formation and accretion occurred over a period of 85 Ma (Figure 2-3).

Island-arc volcanic activity in the La Ronge domain and island-arc and oceanic-rift volcanism in the Flin Flon domain began during the interval of 1.91--1.89 Ga (Figure 2-3a). The

Flin Flon domain underwent the construction of juvenile tholeiitic arcs, associated arc-rift and/or back-arc basins as well as the construction of contaminated arcs that involved a significant proportion of Archean crust (Lucas et al., 1994a). By 1.89 Ga volcanism in the Flin Flon area had evolved to calc-alkaline to alkaline and this continued to 1.88 Ga (Lucas et al., 1994a).

The second major magmatic episode occurred at approximately 1.875 Ga when isoclinally folded volcanic rocks in the La Ronge domain were intruded by tonalite and quartz diorite (Figure 2-3b). This was contemporaneous with the development of an 8 km thick rhyolitic caldera in the Rusty Lake belt to the southeast.

Extensive widespread plutonism occurred from 1.860 to 1.845 Ga (Figure 2-3c) and produced the Wathaman--Chipewyan batholith and numerous smaller intrusions. By this time Flin Flon domain had undergone isoclinal folding. Uplift, erosion and molasse sedimentation began at 1.85 Ga.

By 1.830 Ga magmatic activity in the Reindeer Zone continued (Figure 2-3d), but at a reduced scale with the emplacement of small sills in the Kisseynew domain, and subaerial volcanic activity and the emplacement of small plutons in the Flin Flon domain.

By 1.815 Ga north--south convergence had produced thrust faults in the Flin Flon domain and east--west recumbent isoclinal folds in the Kisseynew domain. In the central

portion of the Kisseynew domain high temperature--moderate pressure metamorphism reached its peak at 1.815 Ga, resulting in extensive anatexis (Figure 2-3e).

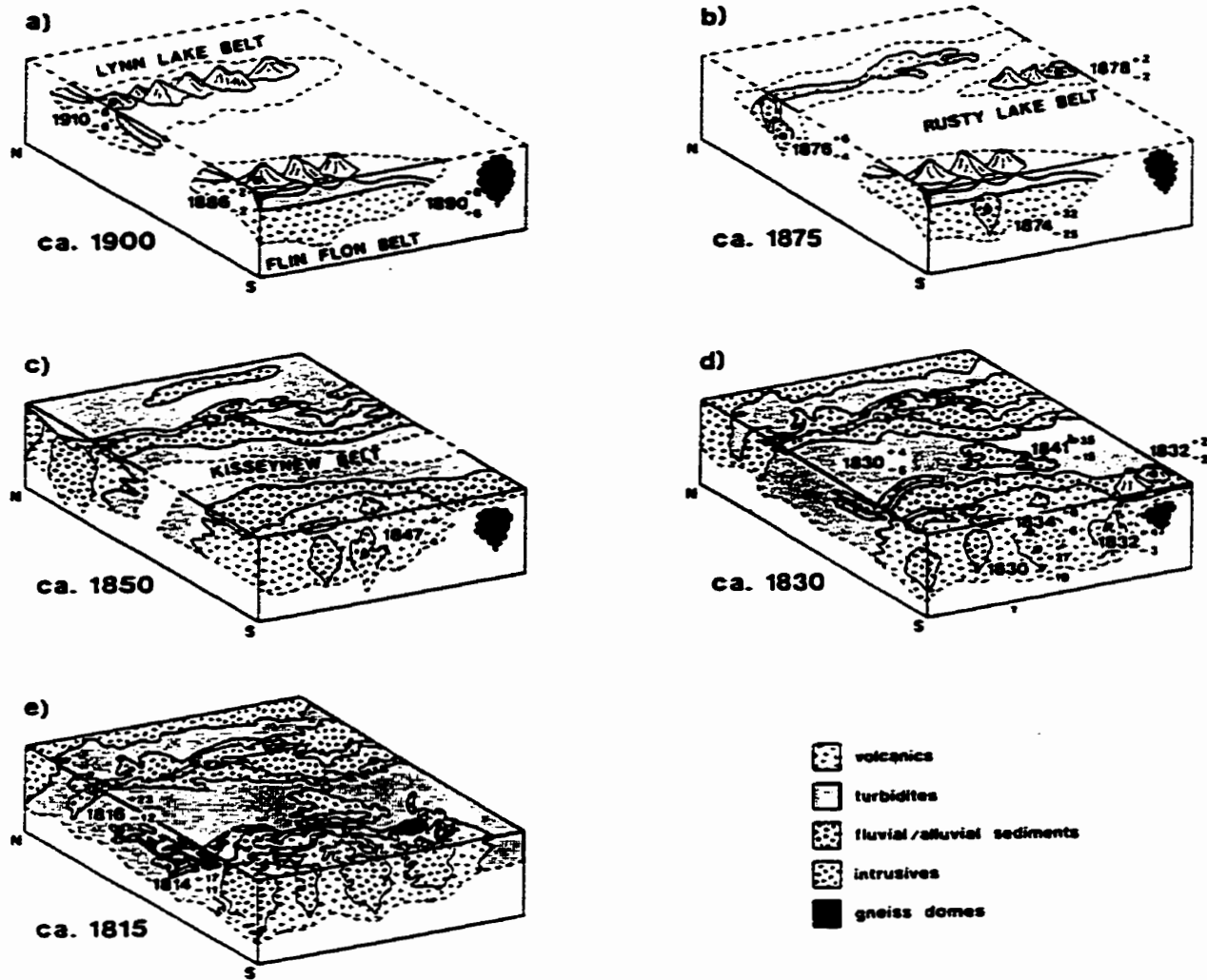


Figure 2-3. Diagrammatic summary of geochronology data constraining the assembly of the crust in the internal zone of the Trans-Hudson Orogen in Manitoba (from Gordon et al., 1990).

2.2 General Geology of the Flin Flon and Kisseynew Domains

2.2.1 Flin Flon Domain Stratigraphy

The exposed section of the Flin Flon domain is 250 km east--west and, in the Flin Flon area, 32--48 km north--south; to the south however, the volcanic belt is overlain by flat-lying Ordovician limestones and sandstones (Bailes et al., 1987). This results in the total length of the north--south dimension of the volcanic belt to be unknown.

At one time the Flin Flon domain was considered to be an Archean greenstone belt, similar to the greenstone belts of the Archean Superior Province. The area has since been recognized as an Early Proterozoic volcanic island-arc complex (Mukherjee et al., 1971; Stauffer, 1974; 1984; Green et al., 1985).

Lucas et al., (1996) have divided the Flin Flon domain into three major tectono-stratigraphic assemblages; the Hanson Lake block, the Amisk collage and the Snow Lake arc segment (Figure 2-4). The stratigraphy of the Flin Flon domain can be divided into four main groups (Bailes, 1971). From oldest to youngest these are: the Amisk Group; the Post-Amisk Intrusive Group; the Missi Group; and the Post-Missi Intrusive Group (Table 2-1).

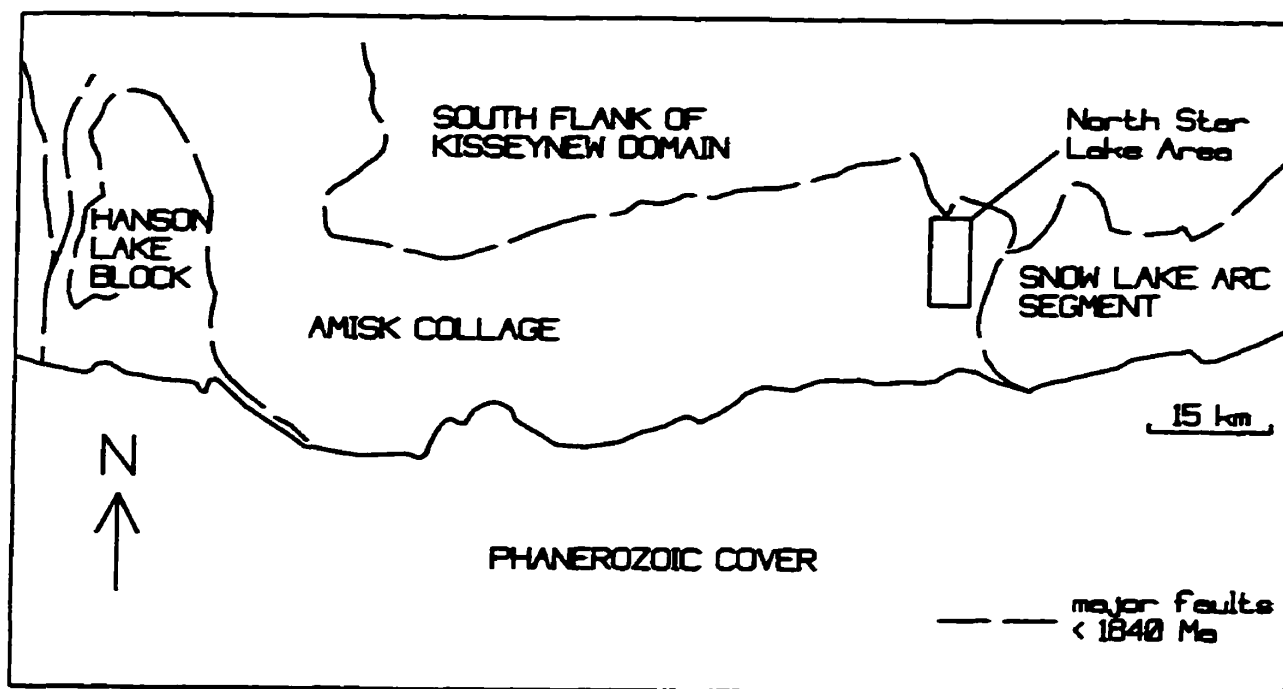


Figure 2-4. Major tectono-stratigraphic assemblages of the Flin Flon domain. The Amisk collage is in structural contact with the overlying Kisseynew domain and Snow Lake arc segment and the underlying Hanson Lake block (after Lucas et al., 1996).

Bailes (1971) further divided the Amisk Group into three smaller units (Table 2-1). The earliest volcanism consists of widespread mafic to intermediate flows (A1a) with the associated mafic to intermediate pyroclastics (A1b). Crosscutting the stratigraphy of unit A1 are mafic to intermediate feeder dykes and small intrusions.

The Amisk volcanism progressively became more felsic, more fragmental, and increasingly more localized (Bailes, 1971) resulting in the felsic volcanic rocks of unit A2. This

unit includes dacitic to rhyolitic flows and pyroclastics, and their quartz porphyry feeders. Brief periods of quiescence are noted by thin beds of tuffaceous, cherty or carbonaceous sediments (Bailes, 1971).

The Amisk volcanism was predominantly subaqueous with the mafic flows forming large shield volcanoes; only some of the later felsic volcanic rocks were possibly deposited in a subaerial environment (Bailes et al., 1987). In the Amisk Group volcanic rocks the full range of composition, from basalt to rhyolite, is seen and includes both tholeiitic and calc-alkaline suites (Syme et al., 1982).

The final unit (A3) included by Bailes (1971) in the Amisk Group are the sedimentary rocks derived by the erosion of pyroclastic deposits. These consist of thin beds of volcanoclastic sedimentary rocks and thicker, more extensive turbidite sequences. These rocks occur throughout the Amisk Group but are more commonly associated with unit A2, the felsic volcanic rocks (Bailes, 1971).

Upon cessation of the Amisk volcanism the volcanic pile was intruded by the Post-Amisk Intrusive Group (units A4 and A5) (Table 2-1). These units show a close spatial relationship and are possibly comagmatic (Bailes, 1971).

Overlying the Amisk Group are the sedimentary rocks of the Missi Group (Table 2-1). This unit (A6) consists of arkose, greywacke, quartzite, with some basal conglomerate.

There is evidence of a major break in geological history

between the Amisk and the Missi (Syme et al., 1982). This evidence is: the presence of a well developed regolith in the Amisk rocks near the contact with the Missi; an angular discordance between the Amisk and the Missi; and the presence in the Missi of granitic clasts eroded from the exposed roofs of Post-Amisk plutons.

The textures and sedimentary structures seen in the Missi Group indicate deposition in alluvial fan and alluvial plain environments (Syme et al., 1982). Some Missi Group rocks contain textures and sedimentary structures indicating deposition by fluvial processes (Bailes et al. 1987).

The Post-Missi Intrusive Group (Table 2-1) consists of large granitic intrusions. This group is further subdivided into unit A7, gneissic rocks; and unit A8, relatively unfoliated intrusive rocks.

Flin Flon Domain

Post-Missi Intrusive Group

- A8** Intrusive rocks of variable composition related to unit A7
- A7** Granodiorite and quartz diorite, generally gneissic. Large portions represent metasomatically granitized material

Missi Group

- A6** Arkose, greywacke, quartzite. Basal conglomerate common

Post-Amisk Group

- A5** Gabbro and diorite often with ultrabasic phases. Commonly differentiated. Includes rocks of several ages and diverse origins
- A4** "Quartz-eye" granite

Amisk Group

- A3** Argillite, greywacke, tuff. Turbidites common in eastern region
- A2** Rhyolite, dacite, quartz porphyry. Includes acidic crystal tuff and siliceous, carbonate-rich tuff
- A1** Mafic to intermediate volcanic rocks: a) pillowed varieties, and b) fragmental varieties. Includes many small related intrusions

Table 2-1. Flin Flon domain stratigraphy (after Bailes, 1971).

2.2.2 Kisseynew Domain Stratigraphy

The dimensions of the Kisseynew domain are 240 km in length, 140 km in width and in total comprise 35 000 square kilometres of metasedimentary rocks (Bailes and McRitchie, 1978).

Bailes (1971) divided the Kisseynew domain into four main groups. From oldest to youngest these are: the Basement Group; the Nokomos Group; the Sherridon Group; and the Post-Sherridon Intrusive Group (Table 2-2). Although more recent work has resulted in new correlations and nomenclature of stratigraphic relationships in the Kisseynew domain (Zwanzig and Schledewitz, 1992), Bailes' stratigraphic groups are included here for historical continuity.

Zwanzig and Schledewitz (1992) have developed a stratigraphic classification of the Kisseynew domain that attempts to correlate the stratigraphy of the south flank of the Kisseynew domain with that of the Flin Flon domain (Table 2-3).

Kisseynew domain

Post-Sherridon Intrusive Group

K6 Pyroxenite, gabbro

K5 Pink granodiorite gneiss, derived in part from unit K3

K4 White quartz monzonite and granodiorite, derived in part from unit K1

Sherridon Group

K3 Siliceous paragneiss derived from a monotonous sequence of arkosic to quartzitic sedimentary rocks, possibly equivalent to unit A6. Includes undifferentiated material transitional into unit K5

Nokomos Group

K2 Hornblende plagioclase gneiss

K1 Intermediate garnetiferous paragneisses derived from a repetitious sequence of greywacke and argillite, possibly equivalent to unit A3. Includes migmatitic and granitoid phases

Basement Group

K0 Variable sequence of granitized gneisses

Table 2-2. Kisseynew domain stratigraphy (after Bailes, 1971).

Amisk Group: fine grained amphibolites and felsic gneisses derived from metavolcanic and metasedimentary rocks;

Burntwood Suite: graphite-bearing garnet-biotite gneisses, migmatites and minor amphibolites that are the equivalent to greywacke-mudstone turbidites;

Unnamed Gneisses: fine- to coarse-grained amphibolite and felsic gneisses, probably highly recrystallized equivalents to the Amisk Group;

Sherridon Suite: predominantly quartz-rich rocks, a large part of which are also suspected to be equivalent to the Amisk Group;

Missi Group: quartz-rich metasedimentary gneiss, and metavolcanic rocks interpreted to be equivalent to the metasandstones in the Flin Flon area.

Table 2-3. Stratigraphy of supracrustal rocks of the Kisseynew domain (after Zwanzig and Schledewitz, 1992).

2.2.3 Early Deformation in the Flin Flon and Kisseynew Domains

The volcano-plutonic assemblages of the Flin Flon domain developed in a convergent margin tectonic environment during the period of 1.92--1.88 Ga (Figure 2-5a) and along with Archean crustal slices were amalgamated by the juxtaposition of the volcano-plutonic assemblages along shear zones to form an accretionary complex during the period of 1.88--1.87 Ga (Figure 2-5b) (Lucas *et al.*, 1994a; 1996). The amalgamation of this accretionary complex is considered to be the first major deformational event in the Amisk collage (Lucas *et al.*, 1994a). The accretionary complex was subsequently intruded by plutons related to a magmatic-arc or arcs and unconformably overlain by volcanic and sedimentary rocks during the period of 1.87--1.84 Ga (Figure 2-5c) (Lucas *et al.*, 1994a; 1996). Arc magmatism occurred in the Snow Lake arc segment during the period of 1.84 to 1.83 Ga (Lucas *et al.*, 1994a).

The amalgamation of the accretionary complex and the development of post-accretion magmatic-arc would have resulted in steeply-dipping stratigraphy and structures prior to the plutonism related to the arc magmatism (Figure 2-5c). Field evidence in the low-grade areas of the Amisk Collage suggests that early structures and fabrics would have been steepened during the development of the magmatic-arc (Lucas *et al.*, 1996). The heat advected into the accretionary complex by the plutonism associated with the arc magmatism would have resulted in extensive contact metamorphism (Lucas *et al.*,

1996).

Zwanzig and Schledewitz (1992) describe an early deformation in the southern flank of the Kiseynew domain that steepened stratigraphy and the margins of early plutons. This deformation occurred prior to the deposition of the 1.85--1.83 Ga Missi Group fluvial--alluvial sediments.

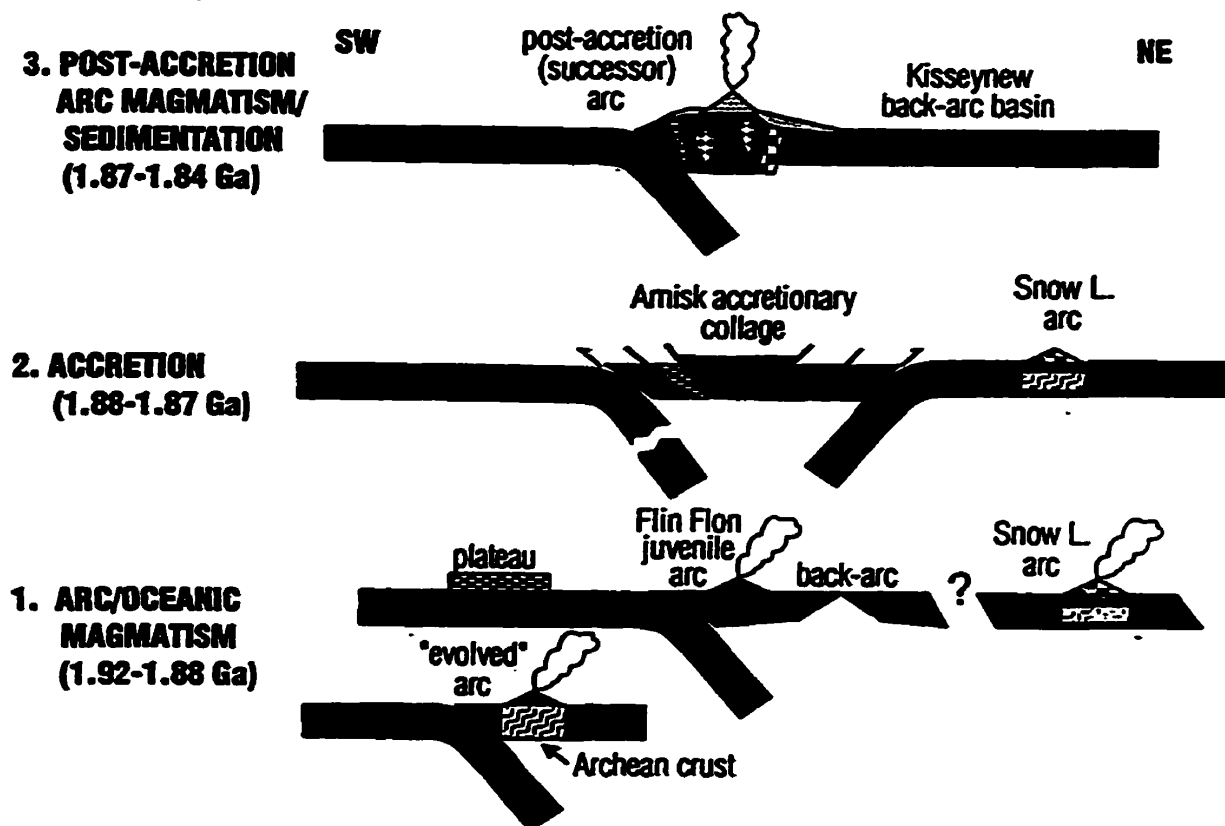


Figure 2-5. Tectonic evolution of the Flin Flon domain (ca. 1.92--1.84 Ga) (from Lucas et al., 1996)

2.2.4 Collision Tectonics, Deformation and Metamorphism in the Flin Flon and Kisseynew Domains

Progressive deformation in the Flin Flon domain and on the south flank of the Kisseynew domain occurred as a southwest-directed compressive deformation that may have lasted over a period of 30 Ma (Norman et al., 1995). This progressive deformation commenced as early as approximately 1840 Ma (Syme et al., 1995; Connors, 1996) or as late as approximately 1830 Ma (Norman et al., 1995) and continued to approximately 1800 Ma (Norman et al., 1995; Syme et al., 1995; Connors, 1996). This progressive deformation is associated with a prograde--retrograde metamorphic cycle (Zwanzig and Schledewitz, 1992; Krause and Williams, 1994a, 1994b, 1995; Norman et al., 1995; Connors, 1996) and was the result of collision tectonics during the convergence of the Flin Flon and Kisseynew domains. This convergence was achieved by the contraction of the Kisseynew basin in a southwest-directed fold--thrust belt and its subsequent overthrusting of the Flin Flon domain volcano-plutonic terrane (Zwanzig and Schledewitz, 1992; Norman et al., 1995; Connors, 1996).

Partitioning of deformation resulted in a concentration of non-coaxial strain along the boundary of the Flin Flon and Kisseynew domains (Norman et al., 1995; Connors, 1996) and in eastern portion of the Flin Flon domain (Krause and Williams, 1994a, 1994b, 1995; Connors, 1996). Seismic reflection profiles of the Trans-Hudson Orogen in Manitoba and Saskatchewan

obtained from the LITHOPROBE program data are interpreted as a series of stacked thrust sheets essentially confined to the crust (Lucas *et al.*, 1994b). On the southern flank of the Kiseynew domain seismic reflections are interpreted by Lucas *et al.* (1994b) as a stack of thrust sheets and fold nappes with a major footwall ramp at the northern margin of the Flin Flon domain. The structures that juxtapose the Flin Flon and Kiseynew domains are interpreted to have been localized near the ancestral Kiseynew sedimentary basin margin (Lucas *et al.*, 1994b; Norman *et al.*, 1995; Connors, 1996). Within the Flin Flon domain the Amisk collage is overthrust by the Snow Lake arc segment and underthrust by the Hanson Lake block (Lucas *et al.*, 1996).

The southern flank of the Kiseynew domain has undergone a southwest-directed, progressive, compressive deformation cycle that was coeval with a prograde--retrograde metamorphic cycle (Zwanzig and Schledewitz, 1992; Norman *et al.*, 1995). In the heterogeneous non-coaxial model of Norman *et al.* (1995) the progressive compressive deformation cycle on the south flank of the Kiseynew domain produced a succession of folds. The heterogeneous non-coaxial strain produced folds whose axes were originally oriented approximately perpendicular to the movement direction. With progressive deformation these fold axes were reoriented by transposition towards parallelism with the movement direction. The younger folds in low-strain domains are more open and less reoriented towards parallelism

than older folds while in high-strain domains transposition is more advanced and most folds approach parallelism.

In the model of Norman *et al.* (1995) the heterogeneous non-coaxial strain path for the Kiseynew domain had a southwesterly movement direction over the Flin Flon domain. The Flin Flon domain is interpreted to have behaved as a relatively rigid block. In the Kiseynew domain the high-strain zone is proximal to the contact with the Flin Flon domain while the intermediate- and low-strain zones are further removed.

The contact between the Kiseynew metasedimentary rocks and the Amisk volcano-plutonic assemblage lies along early faults (Syme *et al.*, 1995; Zwanzig, 1995a; Connors, 1996). In the Snow Lake arc segment of the Flin Flon domain the initial imbrication of the 1.85 Ga Kiseynew turbidites with the older volcano-plutonic assemblages occurred prior to the onset of the 1.84--1.83 Ga magmatism (Connors, 1996). This phase of deformation was characterized by southwest-directed thrusting and continued until approximately 1805 Ma (Connors, 1996).

Subsequent to the southwest-directed progressive deformation and the associated prograde--retrograde metamorphic cycle the Flin Flon and Kiseynew domains underwent northwest--southeast to east--west compression (Zwanzig and Schledewitz, 1992; Norman *et al.*, 1995; Syme *et al.*, 1995; Connors, 1996). This switch from southwest-directed transport to northwest--southeast compression is possibly the

result of the collision of the Reindeer zone with the Superior craton (Krause and Williams, 1994a, 1994b; Syme et al., 1995).

Late in their deformational and metamorphic history, the Flin Flon and Kisseynew domains underwent ductile to brittle deformation under waning-metamorphic conditions (Zwanzig and Schledewitz, 1992; Ryan and Williams, 1994, 1995; Norman et al., 1995; Syme et al., 1995; Connors; 1996). These <1800 Ma structures played a significant role in the segmentation of the Flin Flon and Kisseynew domains (Lucas et al., 1994a). In the southern flank of the Kisseynew domain these structures are interpreted to be the result of continued northwest--southeast (Zwanzig and Schledewitz, 1992) to east--west (Norman et al., 1995) compression.

Chapter III
GEOLOGY OF THE NORTH STAR LAKE AREA

3.1 Introduction

The Elbow Lake area (NTS 63K/15) was mapped during the period of 1949--1952 by J.C. McGlynn of the Geological Survey of Canada. McGlynn (1959) concluded that the supracrustal rocks in the vicinity of North Star Lake (Figure 3-1) could be divided into two major successions; an older group (unit 1) interpreted to consist predominantly of mafic volcanic rocks which were considered by McGlynn to be equivalent to the Amisk Group as defined by Bruce (1918), and a younger succession (units 2 and 3) interpreted to consist of sedimentary rocks overlain by mafic volcanic rocks which were also considered by McGlynn to be Amisk Group. McGlynn (1959) also mapped grey gneisses and migmatites, derived from mafic volcanic rocks and sedimentary rocks adjacent to the contact with a gneissic granodiorite batholith, as well as younger granitoid rocks.

Rocks belonging to unit 1 were described by McGlynn (1959) as being banded hornblende--plagioclase gneisses derived from mafic volcanic rocks. Rocks of units 2 and 3 were described as garnetiferous biotite schist and gneiss, and hornblende--plagioclase gneiss, respectively. Bailes (1971) considered units 2 and 3 to be part of the Kisseynew domain. Bailes (1971) describes unit 2 as "intermediate garnetiferous paragneisses derived from a repetitious sequence of greywacke

and argillite" while retaining McGlynn's classification of hornblende--plagioclase gneiss for the rocks of unit 3.

Geological mapping by Manitoba Geological Services Branch during the period of 1990-1994 has shown that the geology of the North Star Lake area (Figure 3-2) is composed predominantly of mafic to felsic metavolcanic and metasedimentary rocks (Trembath et al., 1990; Norquay et al., 1991, 1992, 1993, 1994). The supracrustal rocks of the North Star Lake area have been subdivided into three lithostratigraphic zones; the Eastern zone, the Central zone and the Western zone (Norquay et al., 1993, 1994). Along the western edge of the mapped area the supracrustal rocks have been intruded by a catazonal granitoid batholith (Gants Lake batholith). Epizonal granitoid intrusions (Norris Lake pluton and 'Quartz-eye' porphyry) have intruded the supracrustal rocks in the eastern portion of the mapped area.

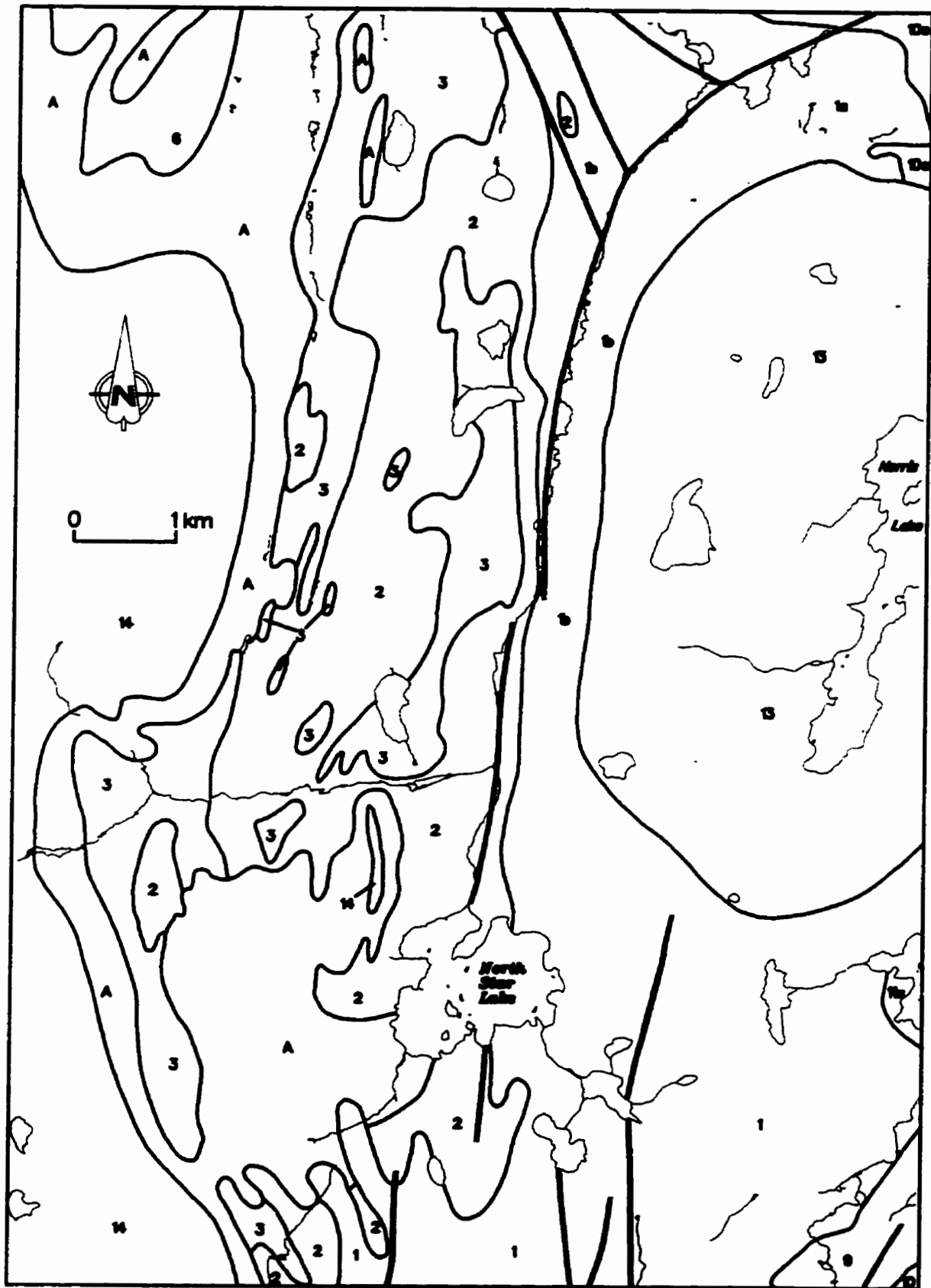
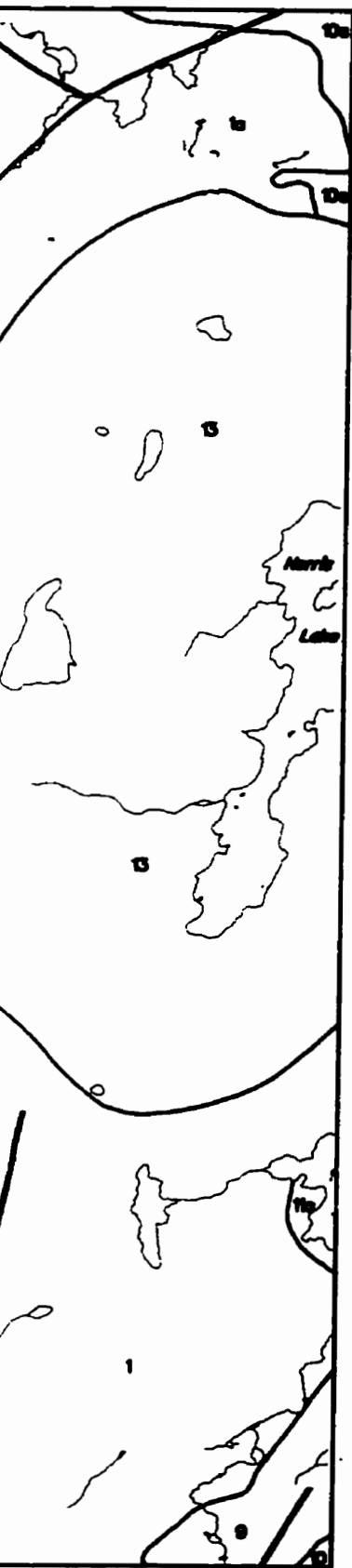


Figure 3-1.
(after McGl)





- 14** Gneissic biotite granodiorite
- 13** Gneissic hornblende-biotite quartz diorite to granodiorite
- 11** 'Quartz-eyes' granite
- 10** Meta-gabbro and meta-diorite; 10a, meta-pyroxenite
- 9** Porphyritic rhyolite and rhyolite
- 6** Hornblende-plagioclase gneiss, in part banded
- 3** Hornblende-plagioclase gneiss, probably altered volcanic rocks
- 2** Garnetiferous biotite schist and gneiss, garnetiferous staurolite gneiss
- 1** Basic volcanic rocks, pillow lavas, minor acidic volcanic rocks, minor pyroclastic rocks, cherts, iron formation; undifferentiated basic intrusions; 1a, basic volcanic rocks with thin bands of garnetiferous hornblende-plagioclase gneiss; 1b, banded hornblende-plagioclase gneiss
- A** Grey gneisses and migmatites derived from units 1, 2 and 3 by unit 14


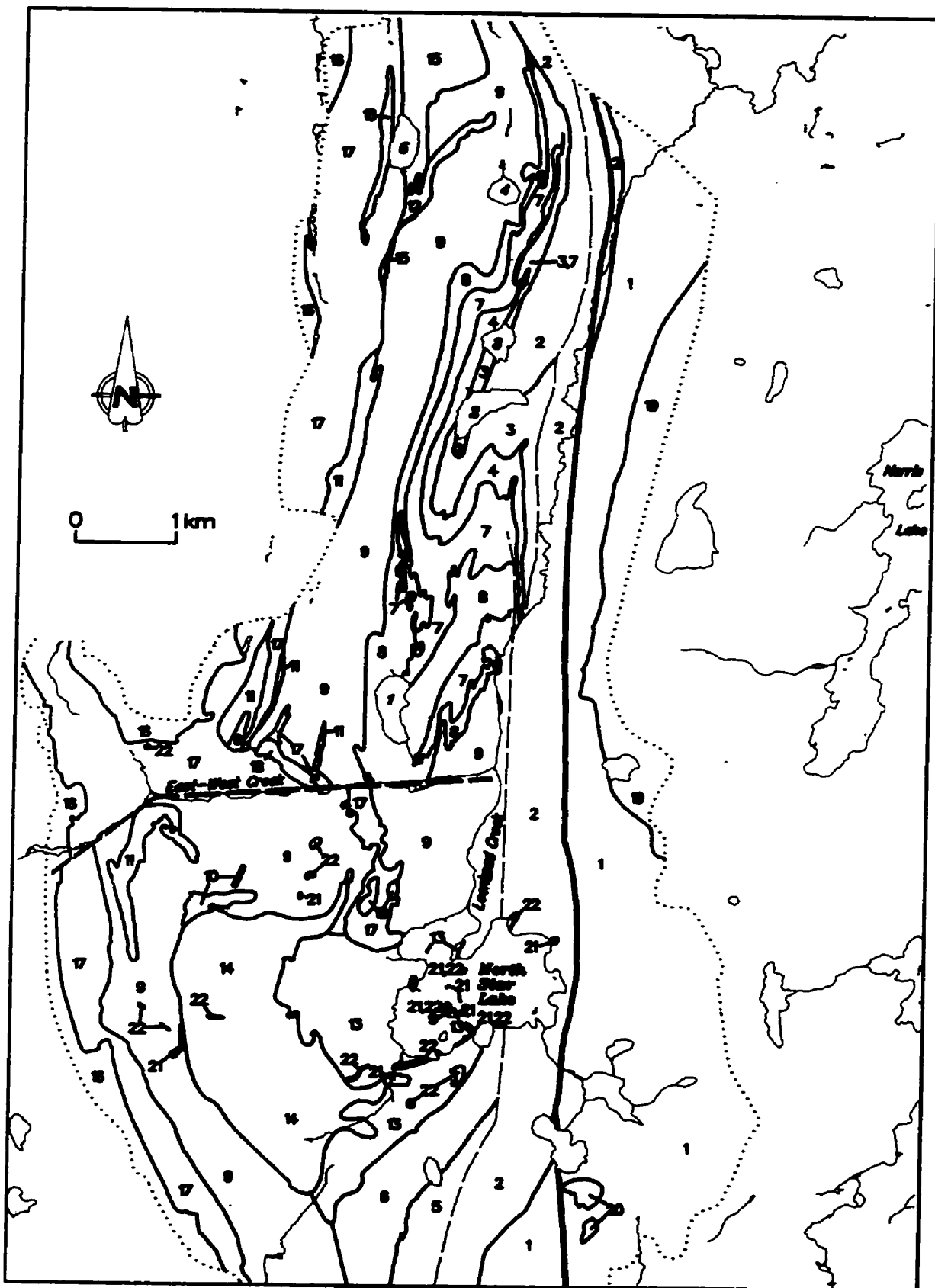
 Geological contact
 Fault

Figure 3-1. Geology of the North Star Lake Area (after McGlynn, 1959).





- 22 Diatreme
- 21 Ultramafic intr
- 20 'Quartz-eye' p
- 19 Norris Lake ph
- 18 Granitic-Gran
- 17 Contact aureol
- 16 Ganta Lake ba

Western Zone

- 15 Hornblende
- 14 Quartz feldspa
- 13 Felsic intrusion
- 12 Psammopelite,
- 11 Amphibolitic ro
- 10 Altered rocks
- 9 Lower rhyolite
- 8 Intermediate an
- rocks +/- irat
- 7 Upper rhyolite
- 6 Rhyolite dykes
- 5 Amphibolite, in

Central Zone

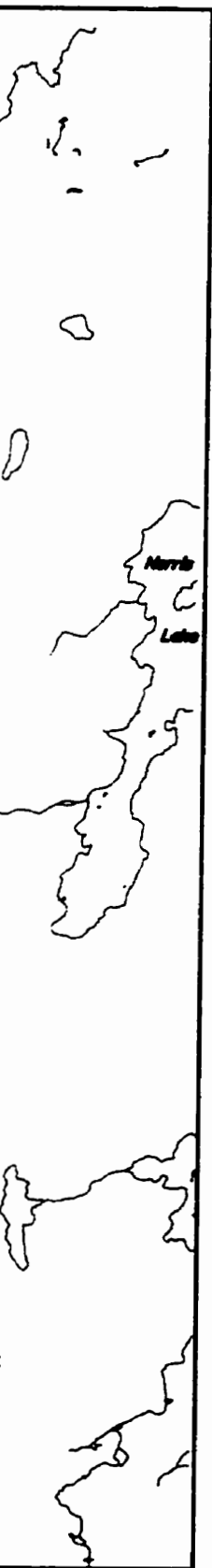
- 4 Amphibolite, qu
- 3 Mafic to felsic l
- rocks or layers
- 2 Mafic to felsic l
- and/or tectonit

Eastern Zone

- 1 Basalt, schistoa
- grained gabbroic
- intrusions

Figure 3-2.
(after Norqu)





- | | |
|---|---|
| <p>22 Diatreme</p> <p>21 Ultramafic intrusive rocks</p> <p>20 'Quartz-eye' porphyry</p> <p>19 Norris Lake pluton</p> <p>18 Granitic-Granodioritic rocks</p> <p>17 Contact aureoles; migmatite, gneissite</p> <p>16 Gants Lake batholith</p> <p>Western Zone</p> <p>15 Hornblende</p> <p>14 Quartz feldspar gneiss</p> <p>13 Felsic intrusion, fine- to medium-grained</p> <p>12 Psammopelite, grey-weathered</p> <p>11 Amphibolitic rocks</p> <p>10 Altered rocks</p> <p>9 Lower rhyolite</p> <p>8 Intermediate and mafic volcanic and sedimentary rocks +/- iron formation</p> <p>7 Upper rhyolite</p> <p>6 Rhyolite dykes and flows, mafic sedimentary rocks</p> <p>5 Amphibolite, in part layered, minor interlayered rhyolite</p> <p>Central Zone</p> <p>4 Amphibolite, quartz-rich, +/- epidote lenses</p> <p>3 Mafic to felsic layered and conglomeratic sedimentary rocks or layered and pseudoconglomeratic tectonites</p> <p>2 Mafic to felsic volcanic and sedimentary rocks and/or tectonites</p> <p>Eastern Zone</p> <p>1 Basalt, schistose mafic rocks, fine- to medium-grained gabbroic-dioritic rocks, minor rhyolitic intrusions</p> | <p>— Geological contact</p> <p>— Fault</p> <p>- - - Assumed fault</p> <p>- - - North-South zone structural break</p> <p>... Limit of mapping</p>
<p>Lakes</p> <p>1 Face Lake</p> <p>2 Sausage Lake</p> <p>3 Spruce Lake</p> <p>4 Round Lake</p> <p>5 Long Lake</p> |
|---|---|

Figure 3-2. Geology of the North Star Lake Area (after Norquay et al., 1994a; 1994b).



3.2 Previous and Current Work

The North Star Lake area has been mapped by the Geological Survey of Canada at a scale of 1:63 360 (McGlynn, 1959). The North Star Lake area lies immediately west of the File Lake area which has been mapped at a scale of 1:20 000 (Bailes, 1980), and immediately east of the Elbow Lake area was mapped at a scale of 1:20 000 as part of a current project by the Manitoba Geological Services Branch (Syme, 1990, 1991, 1992) and the Geological Survey of Canada (Whalen, 1991, 1992, 1993). The North Star Lake area lies immediately south of the Kississing Lake--Batty Lake area which is a current mapping project conducted by the Manitoba Geological Services Branch (Zwanzig and Schledewitz, 1992). Immediately south of the North Star Lake area is the Reed Lake area which is currently being studied by the Geological Survey of Canada and the Manitoba Geological Services Branch (Syme et al., 1995).

The Flin Flon--Snow Lake Volcanic Belt includes the North Star Lake area and is part of the southeastern portion of the Trans-Hudson Orogen. Seismic data of this portion of the Trans-Hudson Orogen was acquired during the period of 1991--1994 as part of the LITHOPROBE program (Hajnal and Lewry eds., 1992, 1993, 1994, 1995). Detailed geological studies of areas adjacent to the North Star Lake area were also part of the LITHOPROBE program (Norman et al., 1995; Connors, 1996).

3.3 Procedure and Data Accumulation

The North Star Lake area was mapped using 1:5000 scale air photographs. The air photographs used during the mapping project were taken from flight lines flown during June 1990. Oriented samples of mesoscopic structures were collected for the study of the structural evolution of the area. A suite of samples were collected for microprobe analysis in order to elucidate the metamorphic evolution of the North Star Lake area.

3.4 Eastern Zone

The mafic metavolcanic rocks of the Eastern zone (unit 1) (Figure 3-2) can be correlated with unit 1 of McGlynn (1959) (Figure 3-1); they consist predominantly of mafic flows and fine- to medium-grained mafic intrusive rocks. The mineral assemblage of the mafic rocks of the eastern zone consists predominantly of amphibole, plagioclase and quartz. Small intrusions of rhyolitic and granitic rocks occur throughout the eastern zone.

The mafic flows of the Eastern zone consist of foliated mafic volcanic rocks, massive to pillowed flows and brecciated flows. The mafic flows are predominantly aphanitic however, some flows are sparsely feldspar phyric. Primary volcanic features are often vague and indistinct.

The foliated mafic volcanic rocks are commonly layered or laminated and locally contain flow breccia or pyroclastic

material. These rocks are often intercalated with massive mafic flows and may represent deformed pillowed or brecciated flows.

The pillowed flows are characterized by well-defined pillowed selvages. The pillows range in size from 0.25 m to approximately 1.0 m in length. The pillows are commonly deformed and typically show length to width ratios of 10:1. Deformed quartz-filled amygdules are common in some flows. Locally aphanitic to fine-grained massive and/or pillowed flow are gradational into amoeboid pillows and subrounded breccia with variable amounts of <1 cm sized hyaloclastite material.

Throughout the Eastern zone there are fine-grained mafic dykes several metres to several tens of metres thick. The larger mafic intrusions commonly have medium-grained and locally coarse-grained centres. These mafic intrusive rocks are similar mineralogically and often similar texturally to the mafic flows and are interpreted to be related to the flows.

3.5 Central Zone

The Central zone (Figure 3-2) is considered to be a package that consists predominantly of layered sedimentary and amphibolitic rocks and subordinate volcanic rocks. The majority of the Central zone has been grouped into unit 2 (Mafic and felsic volcanic and sedimentary rocks and/or tectonites) and of consists of intermediate to felsic

psammopelitic to psammitic rocks, layered rhyolitic tuff, lapilli tuff and tuff breccia, layered amphibolite, quartz-rich amphibolite, mafic flows and chemical sedimentary rocks. The intermediate to felsic psammopelitic to psammitic rocks in the Central zone can be correlated to unit 2 of McGlynn (1959). The individual subunits in the Central zone exhibit remarkable continuity from the southern most portion of the mapped area, and can be traced northward until they are displaced by late brittle faults (Figure 3-2). Biotitic and amphibolitic rocks in the Central zone generally have a well-developed fabric and dislocated fold hinges are common in pelitic bands.

3.5.1 East Shore of North Star Lake Area

The rocks of the Central zone along the east shore of North Star Lake (Figure 3-2) are grouped into unit 2. These rocks have been subdivided into several subunits.

The brown-weathered psammitic and psammopelitic rocks of the Central zone are felsic to intermediate in composition. In general these rocks contain 5--10% biotite and/or amphibole and have variable garnet contents. Layers vary from a few centimetres to approximately 10 cm thick. White-weathered (rhyolitic) layers (<10 cm thick) are locally interlayered with psammopelitic layers.

Fine-grained, aphanitic, quartz crystal-bearing, white-weathered layers within several of the felsic units are

interpreted to be felsic tuffs.

A subunit of clastic rhyolite with white-weathered, angular blocks in a pale brown lapilli and tuff matrix can be followed northward until it is cut by a late brittle fault immediately east of North Star Lake. In the area immediately east of North Star Lake the unit is crudely layered with an eastern tuff breccia and a western lapilli tuff layer. The fragments decrease in size towards the south and the southernmost extent of this unit is well-layered (layers 30--50 cm thick) and does not contain fragments larger than 5 mm in length. This unit is interpreted to be volcanic or volcanoclastic in origin.

Two subunits of white-weathered, fine-grained rhyolitic rocks occur towards the western margin of the Central zone in the vicinity of North Star Lake. In general, these rocks are poorly-layered to massive, but locally have well-defined layers with variable quartz crystal (2--4 mm) contents. These rocks are interpreted to be rhyolite tuffs.

The amphibolitic rocks of the central zone include a fine-grained, quartz-rich (approximately 50% quartz), poorly-layered amphibolite, layered amphibolite, a thin unit of mafic schist and chemical sedimentary rocks and several units of interlayered mafic and felsic rocks.

The quartz-rich amphibolite is an indistinctly layered, dark green to black rock that consists of approximately 50% quartz and 50% amphibole.

The layered amphibolite has well-defined layers that are generally several centimetres to several tens of centimetres thick, but locally range up to 1 m thick. The layers contain variable amounts of porphyroblastic feldspar in a dark green matrix that consists predominantly of amphibole.

The mafic schist subunit is 2--4 m thick, light green in colour, well-layered and contains calc-silicate and sulphide layers. It occurs at the contact between rhyolite tuff and felsic psammitic rocks.

The interlayered amphibolite and felsic rocks are exposed southeast of North Star Lake and occur between mafic volcanic rocks and felsic rocks. Layer thickness varies from several centimetres to several tens of centimetres and are rarely greater than 50 cm thick. The amphibolites are pale green to dark green and are interlayered with felsic (volcanoclastic ?) rocks. Several layers of sulphide facies iron formation are interlayered with the mafic and felsic rocks of this subunit.

Mafic volcanic rocks include two distinctive basaltic subunits that can be traced for several thousand metres in the vicinity of North Star Lake and a dark green to black basaltic unit that can only be traced for several hundred metres in adjacent to the eastern zone mafic volcanic rocks.

In the area of North Star Lake the western-most of the two distinctive basaltic subunits consists of green-weathering, massive, pillowed and brecciated amygdaloidal flows and minor mafic schist. In the southernmost portion of

the mapped area this subunit consists predominantly of mafic schist with subordinate massive flow.

In the vicinity of North Star Lake the other distinctive basaltic subunit consists predominantly of brown-weathered, massive and amygdaloidal pillowed flow and variable (<30%) amounts of brown-weathered mafic schist. In the southernmost portion of the mapped area this subunit consists of approximately 60% mafic schist. All variations of this subunit contains up to 10% black amphibole (2x5 mm) and up to 10% white, 2--4 mm, feldspar porphyroblasts.

The dark green to black basaltic subunit consists of aphanitic to fine-grained massive, pillowed and brecciated flows and minor mafic schist. Locally, amygdules and flow lines are visible.

3.5.2 Sausage Lake Area

In the vicinity of Sausage Lake (Figure 3-2) the Central zone package consists of mafic to felsic layered and conglomeratic sedimentary rocks or layered and pseudoconglomeratic tectonites (unit 3) and amphibolite (unit 4).

Near the contact with the amphibolitic rocks (unit 4), the conglomeratic rocks of unit 3 are composed of polymodal basaltic fragmental rocks that contain up to cobble sized lithic fragments. These basaltic fragmental rocks predominantly contain amygdaloidal or porphyritic basaltic

fragments and commonly contain felsic lithic fragments.

Away from the contact the conglomeratic rocks of unit 3 are predominantly intermediate to felsic in composition. The conglomeratic rocks contain up to cobble sized intermediate to felsic fragments that constitute 20--50% of the rocks by volume. The matrix is fine-grained, composed of amphibole, biotite, feldspar and quartz and is commonly more mafic in composition than the fragments. Individual layers, defined by the range in size and the relative abundance of the larger fragments, vary in thickness from less than a metre to several tens of metres. Since the Central zone rocks in the Sausage Lake area are situated in the hinge area of a large isoclinal fold structure (Figure 3-2) these fragmental rocks may be the result of the transposition of layering.

The layered rocks of unit 3 are psammitic in appearance and are similar in composition and appearance to the matrix material of the conglomeratic rocks. Layering in these rocks is indistinct and individual layers can be followed only a few metres to a few tens of metres.

The amphibolite (unit 4) consists predominantly of medium-grey to black, fine-grained massive and pillowed mafic flows. Commonly, these rocks contain epidosite pods and lenses up to several tens of centimetres in diameter. Typically the foliation in the rocks wraps around, or is deflected by, the epidosite bodies.

Some sections of this unit consists of monotonous fine-

grained amphibolite. Other sections include quartz-rich amphibolite, amphibolite with wisps of plagioclase and quartz, amphibolite with pyroxene megacrysts (≤ 15 mm) and amphibolite composed of up to 60% plagioclase aggregates (≤ 1 cm). Other amphibolites have a gabbroic texture.

The amphibolites of this unit are composed of 50--80% amphibole with plagioclase, quartz and minor biotite. Locally, the amount of epidosite pods and lenses can range up to 10% of the rock.

3.5.3 Round Lake Area

The Central zone rocks in the Round Lake area (Figure 3-2) has been grouped into unit 2 and consist of intermediate to felsic psammitic and psammopelitic rocks, massive to layered rhyolite, amphibolite and interlayered mafic and felsic sedimentary rocks.

The psammitic and psammopelitic rocks in the Round Lake area are similar to the psammitic and psammopelitic rocks in the North Star Lake area. In the area proximal to Loonhead Creek (Figure 3-2) these rocks are brown-weathered, fine-grained, layered rocks composed of feldspar, quartz, biotite and amphibole. Elsewhere in the Round Lake area psammitic rocks are massive to indistinctly-layered, felsic rocks.

The rhyolitic rocks of the Central zone in the Round Lake area consist of aphanitic, massive to layered rhyolite and layered rhyolite with quartz or feldspar phenocrysts.

The amphibolites of the Central zone in the Round Lake area consist of fine-grained amphibolite, quartz-rich amphibolite, amphibolite with abundant plagioclase porphyroblasts, fine-grained layered amphibolite and amphibolite with abundant epidosite lenses and pods, and commonly with abundant quartz lenses. These amphibolites are similar to those in the Sausage Lake and North Star Lake areas.

Two subunits that are probably early mafic intrusions occur in the Round Lake area (Figure 3-2). The first is medium-grained and contains pyroxene megacrysts. The second is fine-grained, massive and commonly contains fine-grained garnet.

3.6 Western Zone

The rocks of the Western zone predominantly consist of felsic metavolcanic with subordinate felsic metasedimentary rocks and felsic intrusive rocks. These rocks can be loosely correlated with unit 2 of McGlynn (1959). Amphibolitic rocks commonly occur as layers in the felsic metavolcanic and metasedimentary rocks. The Western zone also contains a sequence of mafic to intermediate metasedimentary rocks with subordinate mafic metavolcanic rocks that can be correlated with unit 3 of McGlynn (1959).

South and southwest of North Star Lake (Figure 3-2) there is a sequence of fine-grained mafic rocks with interbedded

rhyolitic rocks (unit 5). The mafic rocks vary from fine-grained layered amphibolite to porphyritic amphibolite with 2 mm feldspar porphyroblasts in a fine-grained groundmass of feldspar and amphibole. The rhyolitic rocks are fine-grained and vary in texture from well-laminated to massive. The rhyolitic layers vary in thickness from a few centimetres to 5 metres.

Immediately west of unit 5 (Figure 3-2) is a unit of layered mafic rocks and variable amounts (25--100%) of extrusive and intrusive rhyolite (unit 6). These fine-grained rhyolites are variable in texture and colour from white massive rhyolite and intrusion breccia to pale brown layered rhyolite, lapilli tuff and tuff breccia. Locally, the layered mafic rocks are contained as rafts within the rhyolite.

The felsic metavolcanic and subordinate metasedimentary rocks in the Western zone have been divided into two units; the Upper Rhyolite (unit 7) and the Lower Rhyolite (unit 9). These unit names are based upon the relative structural position of the two units in the hinge area of a large fold in the vicinity of Face Lake (Figure 3-2). The sequence of mafic to intermediate metasedimentary and metavolcanic rocks (unit 8) is situated between the Upper Rhyolite and Lower Rhyolite and is commonly associated with iron formation.

The Upper Rhyolite (unit 7) is up to approximately 100 m thick and in a substantial portion of the mapped area lies immediately west of the Central zone sequence (Figure 3-2). It

consists of grey-white or cream to buff coloured rocks and includes: 1) aphanitic to fine-grained massive rocks with that commonly contain ovoid cavities; and 2) fine-grained, near massive to distinctly layered rocks.

In the area to the west and north of Sausage Lake (Figure 3-2) the Upper Rhyolite consists predominantly of massive rocks with ovoid cavities that are homogenous and weakly foliated. These rocks are composed predominantly of feldspar and quartz; 1 mm quartz phenocrysts ($\leq 3\%$) occur locally. The weak foliation is defined by fine-grained biotite ($< 5\%$). The cavities are usually less than 2 cm in length but can range up to 7 cm, have smooth inner surfaces with quartz lining and are commonly partially to completely filled by biotite. These cavities are possibly the result of preferential weathering of amygdules.

In the area south of Sausage Lake (Figure 3-2) the Upper Rhyolite consists predominantly of fine-grained near massive to layered rocks. These rocks are composed predominantly of quartz and feldspar with up to 10% biotite. These rocks have layers (1--10 cm) that are defined by recessive weathering and subtle changes in biotite content.

Outcrops are limited in the third dimension and often the foliation gives the impression of layers. This foliation (or planes of spaced cleavage/pressure solution) range from 3--20 cm apart and in some areas has a anastomosing pattern.

Iron formation occurs in a 100 metre thick sequence of

metasedimentary and metavolcanic rocks (unit 8). In the vicinity of Face Lake (Figure 3-2) the iron formation commonly consists of two bands, 1--10 m thick separated by 1--30 m of intermediate to mafic tuffaceous or metasedimentary rocks. In the area north of Face Lake only one band of iron formation has been observed. Individual layers of the iron formation range from 1 cm to 1.2 m thick. Compositional end members of the iron formation consist of a) quartz; b) garnet (95%) + amphibole--chlorite--quartz; c) amphibole--chlorite +/- quartz +/- feldspar; d) magnetite (5--60%) + quartz; and e) green fibrous amphibole. In the vicinity of Face Lake a felsic layer associated with the iron formation consists of plagioclase (50--90%), quartz (<50%), garnet (<5%), acicular amphibole (<3%), biotite (<10%) and magnetite. Commonly the iron formation layers are repeated by isoclinal folds.

The metavolcanic rocks of this unit consist of massive to amygdaloidal basaltic flows, pillowed basaltic flows, amphibolites derived from these flows, mafic tuffaceous rocks.

The flows and the amphibolites are fine grained, dark-grey to black and are composed of 50--80% amphibole, 20--45% plagioclase, and <5% quartz. The amygdaloidal flows grade into and resemble the massive portions of the flows but contain 5--35% subequant amygdules. These amygdules consist of plagioclase, quartz, and minor biotite and/or amphibole.

The pillowed flows have distinct to indistinct pillow outlines. Pillows vary in size from a few centimetres to 4 m.

Pillow rims are observed as 1--3 cm thick dark coloured concentric zones. Locally, the pillowed flows contain epidosite altered pillowed cores and epidosite lenses up to tens of centimetres in diameter.

The primary volcanic features are observed almost exclusively in the Face Lake--Sausage Lake area. The northern portion of the mapped area the rocks of this unit are massive monotonous amphibolites.

Tuffaceous or sedimentary rocks are distinguished by their indistinct to distinct layers. Possible graded beds occur in a mafic lapilli tuff northeast of Face Lake (Figure 3-2).

The Lower Rhyolite (unit 9) is approximately 600 m thick. The rocks of this unit are fine-grained and vary in colour from slightly pink/orange to cream and vary in texture from laminated to massive. The unit varies from massive and amygdaloidal rhyolite flows with subordinate tuffaceous rocks in the area north of Spruce Lake (Figure 3-2) to predominantly laminated rocks in the area of the East--West Creek. Layers of rusty-weathered rock are common in this unit.

In the northern portion of the mapped area the unit has been subdivided into three subunits: a) altered flows and pyroclastic rocks, b) flows and tuffaceous rocks, and c) amygdaloidal flows.

a) Altered flows and pyroclastic rocks.

These rhyolitic rocks are variably altered and vary in colour from grey to beige to cream and locally there are areas or layers of rusty-weathered sulphide-bearing rock. The rocks of this subunit consist of tuff, lapilli tuff, tuff breccia and flows. The upper contact of this subunit is well distinguished by a marked visual change from altered to relatively unaltered rock as well as a zone or layer of rusty-weathered rock up to 3 m thick.

The massive flow rocks and the blocks in the tuff breccia are aphanitic to fine-grained with a weak foliation. The tuffaceous rocks have a moderate to strong foliation. The less altered tuffaceous rocks are commonly indistinctly laminated. The laminae are defined by a variable biotite content that ranges up to 5% biotite. The more altered tuffaceous rocks contain up to 20% biotite and muscovite combined.

The uppermost portion of this subunit is well exposed west of Sausage Lake (Figure 3-2); it occurs as a 15 m thick distinctly layered zone of altered tuffaceous rocks and chemical sedimentary rocks. Locally, this zone contains layers that consist predominantly of quartz and muscovite with pale brown staurolite and pale red to slightly purple garnet. One 50 cm layer at this location contained up to 5% gahnite.

b) Flows and tuffaceous rocks

This subunit is composed rhyolite flow lobes, tuff and

lapilli tuff. In the area west of Spruce Lake the subunit consists predominantly of rhyolitic flows. Towards the south there is a gradual increase in the proportion of tuffaceous material. The rocks of this subunit are white, light-grey or cream coloured, and locally slightly pink. Some sections are reddish or orange stained.

The flows are cream coloured (commonly with an orange tint), aphanitic to fine grained. Locally, quartz and/or feldspar phenocrysts can range up to 1 mm in size. The flows include weakly foliated to massive flow lobes that are commonly 2--3 m thick. These lobes are generally lighter coloured and less foliated than the surrounding interflow material. The lobes contain biotite wisps and finely disseminated biotite (up to 5% biotite).

The interflow material is grey in colour and moderately foliated. This material contains up to 10% biotite as well as fine grained quartz, feldspar, +/- muscovite, +/- garnet. It commonly contains round lapilli sized (<5 mm) particles that are composed of feldspathic material with a biotite-rich core.

The tuffaceous rocks of this subunit are most common in the southern portion of the study area. These tuffaceous rocks are fine-grained, light-grey to cream in colour and weakly foliated. Layering is indistinct but locally can be distinguished by variations in the biotite and garnet contents. Individual layers range in thickness from 10 cm to

several metres. Biotite occurs as wisps that can grade into laminae. Overall biotite constitutes 5--10% of the rock.

c) Amygdaloidal flows

The amygdaloidal flows in this subunit are cream to white or grey in colour and are aphanitic to fine-grained. This subunit is composed predominantly of rhyolite lobes that commonly contain ovoid cavities up to 1 cm in length and wisps (<2 mm) composed of fine-grained biotite. The ovoid cavities are partially filled by biotite and quartz +/- garnet. The interflow material in this area is medium-grey in colour, fine-grained, locally garnetiferous and can contain up to 10% biotite.

In the southern portion of the mapped area altered rocks (unit 10) locally occur within unit 9 as small areas or bands or as larger areas with dimensions of several hundred metres (Figure 3-2). These areas are characterized by variable amounts of fine- to medium-grained biotite, staurolite, garnet, chlorite, quartz and muscovite.

Foliated, dark-grey, fine-grained amphibolitic rocks (unit 11) occur throughout the Lower Rhyolite and rarely in the Upper Rhyolite as layers several centimetres to several tens of metres thick. Locally, these rocks have a wispy texture defined by 1--15 mm white lenses that are aggregates of quartz and plagioclase.

Although amphibolitic layers are generally parallel to the foliation and layering in the rhyolitic rocks, the amphibolites also occur as slightly discordant sills and/or dykes. Definitive volcanic, sedimentary or intrusive features were not observed in these rocks.

Psammopelitic rocks (unit 12) occur as a 100 m thick sequence adjacent to unit 9 in the northern portion of the mapped area (Figure 3-2). These rocks are light to medium-grey, fine-grained, moderately foliated and vary from near massive to finely laminated. These rocks are composed of 75% feldspar, 10--20% biotite and 5--10% quartz. Locally these rocks are garnetiferous and red garnet aggregates up to 1 cm in size constitute up to 3% of the rock. The garnet commonly occurs in metamorphic aggregates with feldspar and biotite.

The intrusive rocks of the Western zone outcrop to the west of North Star Lake (Figure 3-2) and consist of fine-grained felsic intrusion (unit 13) and medium-grained quartz feldspar gneiss (unit 14). Both of these units are foliated.

The fine-grained felsic intrusion (unit 13) is situated west of North Star Lake (Figure 3-2) and consists predominantly of grey or white, fine-grained, massive to slightly foliated rocks that consist predominantly of feldspar and quartz with 10--15% biotite. The intrusive rocks contain felsic rafts and blocks, up to several tens of metres in size, that resemble felsic metavolcanic rocks. Mafic xenoliths within this unit are medium-grained, gneissic and range in

size from <1 to >10 m. The mafic xenoliths commonly exhibit a stronger foliation than the felsic intrusive rocks. Some of the xenoliths probably resemble boudinaged mafic dykes.

The quartz feldspar gneiss (unit 14) is a medium-grained, pink or grey felsic gneiss that is composed predominantly of quartz and feldspar with 20% biotite and 1% garnet. The gneiss has a weak to well-developed foliation as well as rods of quartz and feldspar that are 4--10 mm in length.

Hornblendite (unit 15) in the northern portion of the mapped area (Figure 3-2). Rocks of this unit are massive, fine- to medium-grained and weakly foliated. These rocks are composed of amphibole, plagioclase and minor quartz. These rocks are probably recrystallized mafic extrusive rocks however, a intrusive precursor is possible.

3.7 Granitoid Rocks

3.7.1 Gants Lake Batholith

The Gants Lake batholith (Whalen, 1992) was described by McGlynn (1959) as gneissic biotite granodiorite. The Gants Lake batholith (unit 16) is an elongate, north-trending intrusive body that occupies the entire western margin of the mapped area (Figure 3-2). Whalen (1992, 1993) described the Gants Lake batholith as a composite batholith. The various phases of this batholith are gabbro, gabbroic and tonalitic agmatite, tonalitic gneiss, and gneissic to slightly foliated biotite and biotite-hornblende granodiorite and granite

(Whalen, 1992). The various phases of the batholith range in age from >1870 Ma to <1850 Ma and there is great variation in metamorphic grade across the batholith (Whalen, 1993).

In the portion of the Gants Lake batholith adjacent to the North Star Lake area is described by Whalen (1993) as various compositionally banded to migmatitic gneisses, including grey tonalitic to quartz dioritic gneiss that contain abundant sheets of older deformed orthogneiss, and K-feldspar phyric migmatitic granodioritic gneiss. These orthogneisses grade towards the west into a mixed zone that contains the orthogneisses and abundant foliation-parallel younger biotite granodiorite and granite and subsequently into a terrane that contains rafts of orthogneiss within the less deformed granodiorite and granite (Whalen, 1993).

During the mapping of the North Star Lake area the slightly to moderately foliated biotite granodiorite and granite were mapped as granitoid rocks and the agmatitic and migmatitic terranes were mapped as the contact aureole (unit 17) of the Gants Lake batholith.

Contact Aureole

The contact aureole (unit 17) of the Gants Lake batholith is a zone up to 700 m in width (Figure 3-2). The volcanic and volcanoclastic sedimentary rocks of the contact aureole are mafic to felsic in composition and have undergone variable degrees of partial melting, lit--par--lit injection of

granitoid material, contamination, recrystallization, and intrusion by cross-cutting granitoid to aplitic material.

In the vicinity of the East--West Creek (Figure 3-2) the contact aureole contains a substantial intrusive component. In many areas the contact aureole is agmatitic with rafts of country surrounded by granitoid material. These rafts have undergone little to nil disruption from their pre-intrusion orientation. Other sections of the contact aureole consist of granitoid stocks up to several hundred metres in diameter.

In the northern portion of the mapped area (Figure 3-2) the country rocks in the western portion of the contact aureole appear to be intermediate to dacitic in composition and are commonly banded. This banding, and the variable compositions that reflect this banding, appear to be the result of contamination caused by extensive lit--par--lit injection of granodioritic material along the foliation. This section is also extensively intruded by irregular to cross-cutting felsic dikes.

The dacitic country rocks of the western section of the contact aureole are fine grained and composed of variable amounts of hornblende, plagioclase and quartz. The more intermediate country rocks of this section can be slightly garnetiferous with red garnet aggregates up to 1 cm in diameter.

In the northern portion of the mapped area the eastern portion of the contact aureole consists mainly of felsic

supracrustal rocks that have undergone variable amounts of partial melting, as well as injection of granodioritic material into the highly irregular foliation. The country rocks in this section are fine grained and composed of quartz, muscovite, feldspar and biotite, as well as variable amounts of garnet (often a purplish colour) and pale brown staurolite. Biotitic and garnetiferous mafic bands are common and these mafic layers are often boudinaged. Mafic xenoliths are present in the intrusive material. Cross-cutting felsic dikes are present but not common.

3.7.2 Granitic--Granodioritic Rocks

Within the contact aureole, both in the vicinity of the East--West Creek and in the northern portion of the mapped area, several stocks of granitoid material (unit 18) outcrop (Figure 3-2). These rocks are medium-grained, weakly foliated and resemble the rocks of the Gants Lake batholith. These rocks are probably related to the Gants Lake batholith however, this is not certain.

3.7.3 Norris Lake Pluton

The ca. 1.83 Ga (*cf.* Connors, 1996) Norris Lake pluton (Bailes, 1980) was described by McGlynn (1959) as gneissic hornblende-biotite quartz diorite. Bailes (1980) described the Norris Lake pluton as a texturally and compositionally homogenous white-weathering, medium-grained, equigranular,

plagioclase-rich (quartz-poor) leucotonalite. The Norris Lake pluton (unit 19) is an ellipsoid-shaped stock that lies in the eastern portion of the mapped area (Figure 3-2).

The Norris Lake pluton is massive and unfoliated except near the contact with the surrounding country rock. The pluton intrudes and displaces the surrounding country rock and deflects the earlier fabrics. The Norris Lake pluton is characterized by sharp, well defined contacts and no significant indication of assimilation of country rocks. Along the contacts with the surrounding country rocks, and in small dykes proximal to the pluton, the intrusive material contains numerous angular xenoliths.

3.7.4 Quartz-eye Porphyry

A pink-orange porphyry described by McGlynn (1959) as "quartz-eye granite" outcrops as several small stocks in the southern portion of the mapped area (Figure 3-2). This quartz-eye porphyry (unit 20) is unfoliated to weakly foliated and fine- to medium-grained. The quartz phenocrysts can range up to 10 mm in size and commonly can comprise up to 40% of the rock. Analysis by McGlynn (1959) found the average mineral content to be approximately 60% plagioclase, 35% quartz, with minor biotite, epidote and opaque minerals.

Near the contacts between the porphyry stocks and the surrounding country rock porphyry dykes intrude the country rock. These dykes are only found within 200 m of the contact.

Xenoliths of supracrustal rocks are absent from the intrusion. Locally there is some contact metamorphism of the mafic supracrustal country rocks in the vicinity of the contact.

3.8 Ultramafic Intrusions

Intrusions of ultramafic rocks (unit 21) and associated diatremes occur in the North Star Lake area (Figure 3-2). The largest ultramafic intrusive body underlies North Star Lake and corresponds with a large circular magnetically high area in the vicinity of North Star Lake (GSC Magnetic Anomaly Map C 21509 G, 1990). Smaller bodies of ultramafic rocks have intruded into diatremes proximal to North Star Lake.

These ultramafic rocks are unfoliated, coarse-grained hornblendite characterized by random mutual intergrowths of hornblende and biotite with interstitial feldspar, epidote and calcite (Ayed, 1994). Analysis by Ayed (1994) found the average mineral content of these ultramafic rocks to be approximately 55% hornblende, 25% biotite, 10% feldspar, 7% epidote, 3% calcite and minor muscovite and pyrite.

The intergrowth of hornblende and biotite in the ultramafic rocks may indicate high fluid pressures during crystallization. The presence of hydrous minerals and calcite in these rocks suggests the presence of volatiles, H₂O and CO₂, respectively. The fine-grained epidote in these rocks is anhedral to euhedral and prismatic, suggesting that the epidote is of a magmatic origin; crystallizing under

moderately high pressure conditions (Ayed, 1994).

3.9 Diatremes

Diatremes (unit 22) were first noted in the North Star Lake area (Figure 3-2) during the 1991 field season (Norquay *et al.*, 1991) and subsequently documented and described (Ayed and Halden, 1993; Ayed, 1994). The North Star Lake diatreme field contains at least 15 diatremes that range in size from several metres to >100 m and occur as near-circular to irregular-shaped features and as dykes (Ayed, 1994). The diatremes are associated with the ultramafic intrusion located in the vicinity of North Star Lake and their emplacement was locally and regionally controlled by country rock structure and the proximity of the ultramafic magmatism (Ayed, 1994).

The common texture of the diatremes is a fragment-supported breccia. The internal constituents of the diatremes consist of matrix and lithic fragments. The fragments are unsorted, subrounded to angular, and range in size from <1 cm to several metres. These fragments consist of the mafic and felsic intrusive rocks, felsic metavolcanic rocks and metasedimentary rocks that are the country rocks in the immediate area, and rare exotic lithic fragments (Ayed, 1994).

The fragments are surrounded by various proportions of three different matrix types (Ayed, 1994). These matrix types are: 1) a felsic matrix -- composed predominantly of quartz and feldspar, subordinate biotite and minor muscovite, garnet

and opaque minerals -- which is interpreted by Ayed (1994) to be rock flour derived from the country rocks; 2) a dioritic matrix, interpreted by Ayed (1994) to have possibly been formed by syntexis or represents a residual liquid derived from ultramafic fractionation; and 3) an ultramafic matrix, interpreted by Ayed (1994) to have been derived from ultramafic magma centred in the vicinity of North Star Lake.

Ayed (1994) states that matrix type is determined by the location of a diatreme relative to the ultramafic intrusion in the vicinity of North Star Lake and that the felsic matrix is the precursor to the other two matrix types. The felsic matrix is occurs in all but one diatreme and is commonly the only matrix type that occurs in diatremes distal to the ultramafic stock. The dioritic matrix occurs in two diatremes located approximately 1500 m from the ultramafic stock. The ultramafic matrix occurs in diatremes proximal to the ultramafic stock.

Chapter IV

STRUCTURAL GEOLOGY OF THE NORTH STAR LAKE AREA

4.1 Introduction

Several phases of ductile deformation have been identified in the North Star Lake area (Figure 4-1), three of which are particularly prominent. In addition, there have been several episodes of late brittle--ductile and brittle deformations. The ductile phases of deformation (D_1 -- D_3) are associated with a prograde--retrograde metamorphic cycle (M_1 -- M_3). Peak regional metamorphism (M_2) appears to have been associated with the second phase of deformation.

Fold style in the North Star Lake area ranges from similar, isoclinal, passive-flow folds that developed during the first phase of deformation (D_1) to parallel, open to tight, flexural folds developed during the third phase of deformation (D_3).

A north-trending structural break -- referred to as the North--South zone structural break -- transects the map area (Figure 4-1). There is a change in deformational style of the early deformation (D_1 and D_2) between those areas to the west and those to the east of the structural break.

The final phase of deformation in the area produced brittle--ductile to brittle structures. A major north-trending brittle fault zone transects the entire map area (Figure 4-1).

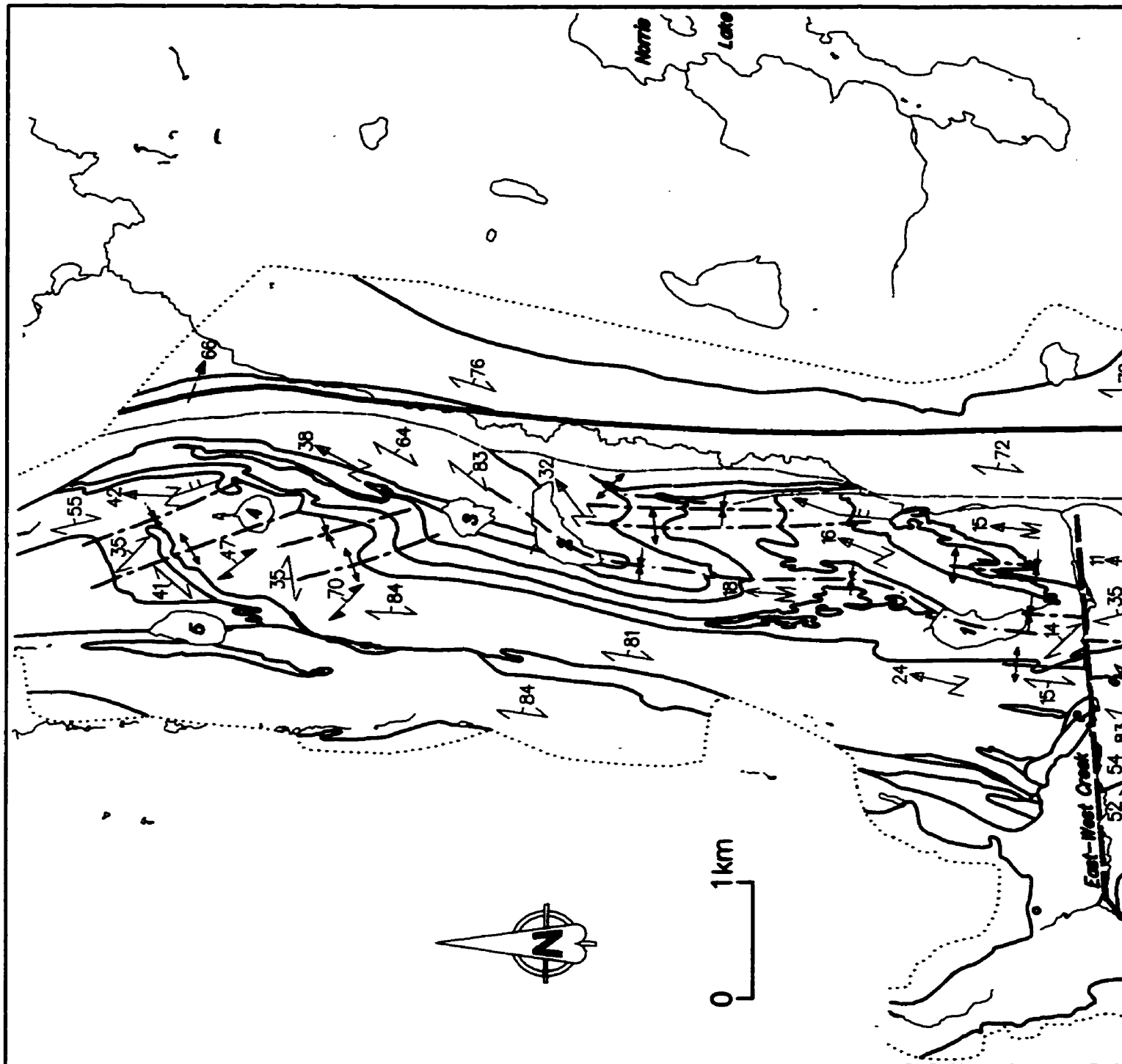


Figure 4-1. Strucl Lake area (after following page.



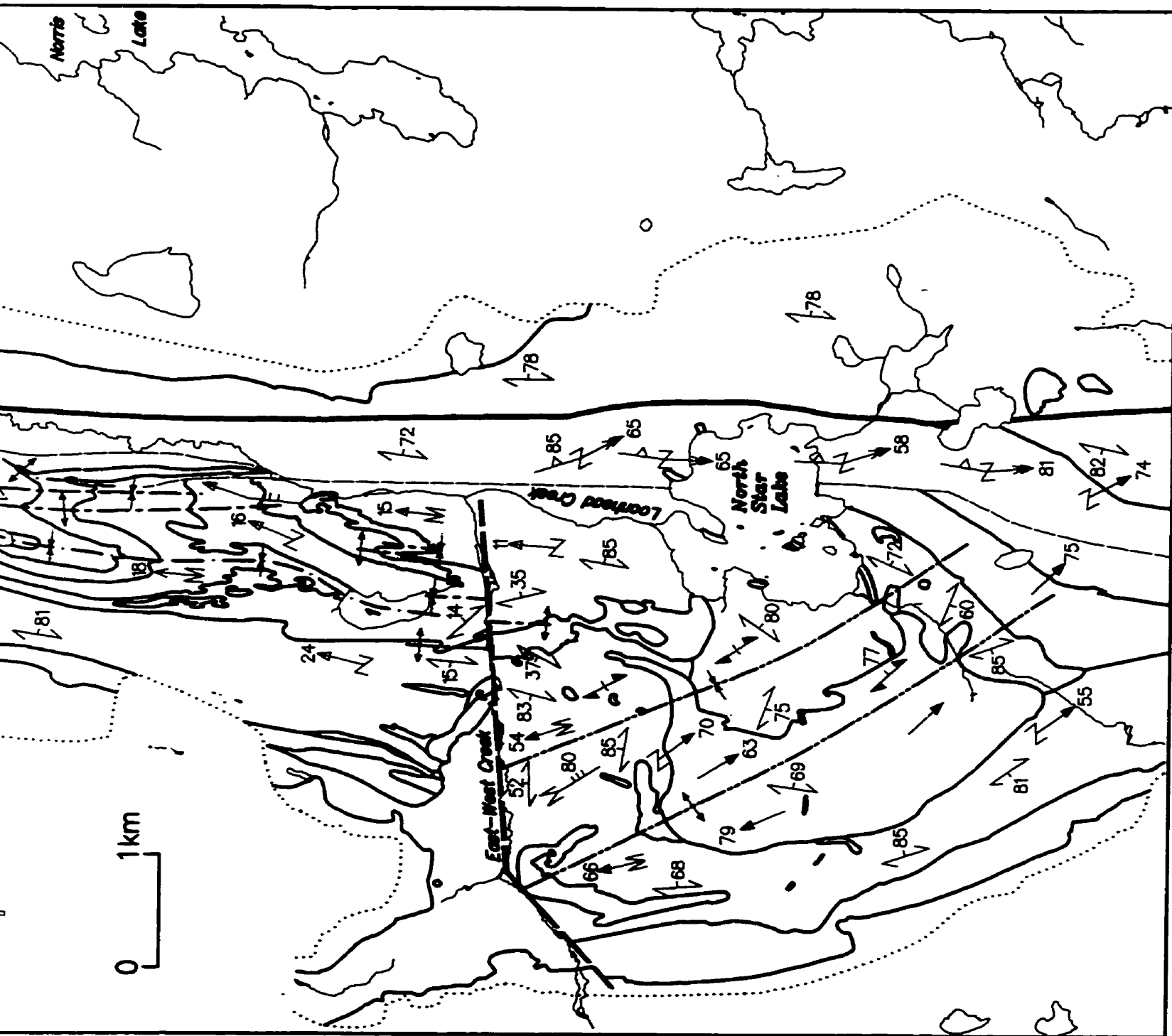


Figure 4-1. Structural geology schematic of the North Star Lake area (after Norquay et al., 1994a; 1994b); Legend on following page.



 S1 schistosity

 S3 schistosity

 F1 fold axis

 F2a fold axis

 F2b fold axis

 F3 fold axis

 F2a fold axial plane

 F2b fold axial plane

 F3 fold axial plane

 Synform

 Antiform

M S Z Minor fold asymmetry

 F1 fold axial trace

 F2a fold axial trace

 F3 fold axial trace

 Geological contact

 Fault

 Assumed fault

 North-South zone
structural break

 Limit of mapping

Lakes

1 Face Lake

2 Sausage Lake

3 Spruce Lake

4 Round Lake

5 Long Lake

The North Star Lake area has been divided into seven structural subareas (Figure 4-2) based on the orientation of the dominant structural trend and/or on the prominence of a specific generation of structure (Table 4-1).

subarea 1 (Face Lake area)

Predominantly upright, northerly-trending F_1 structures with axial-planar S_1 foliation. Gentle, northerly-plunging F_1 fold axes and L_1 lineation. Upright, northerly-trending F_2 structures. Gentle, northerly-plunging F_2 fold axes and L_2 lineation. Rare easterly-trending F_3 open folds.

subarea 2 (Round Lake area)

Predominantly upright, northerly-trending F_1 structures with axial-planar S_1 foliation. Gently-plunging F_1 fold axes and L_1 lineation. Upright, northerly-trending F_2 structures. Gentle, northerly-plunging F_2 fold axes and L_2 lineation. Easterly-trending F_3 open and crenulate folds.

subarea 3 (Sausage Lake area)

Upright, northeasterly-trending F_2 structures. Gentle to moderate, northeasterly-plunging F_2 fold axes and L_2 lineation.

subarea 4 (Creek Junction area)

Upright, northerly-trending F_2 structures. Gentle, northerly-plunging F_2 fold axes and L_2 lineation.

subarea 5 (North--South zone)

Upright, northerly-trending shear foliation (S_1). Upright, northerly-trending F_2 structures. Steep, southerly-plunging F_2 fold axes. Easterly-trending F_3 crenulate and box folds.

subarea 6 (South North Star area, northwest section)

Upright, northwesterly-trending F_3 structures. Moderate to steep, north- to northwesterly-plunging F_3 fold axes.

subarea 7 (South North Star area, southeast section)

Upright, northwesterly-trending F_3 structures. Moderate to steep, southeasterly-plunging F_3 fold axes.

Table 4-1. Characteristics of structural subareas in the North Star Lake area.

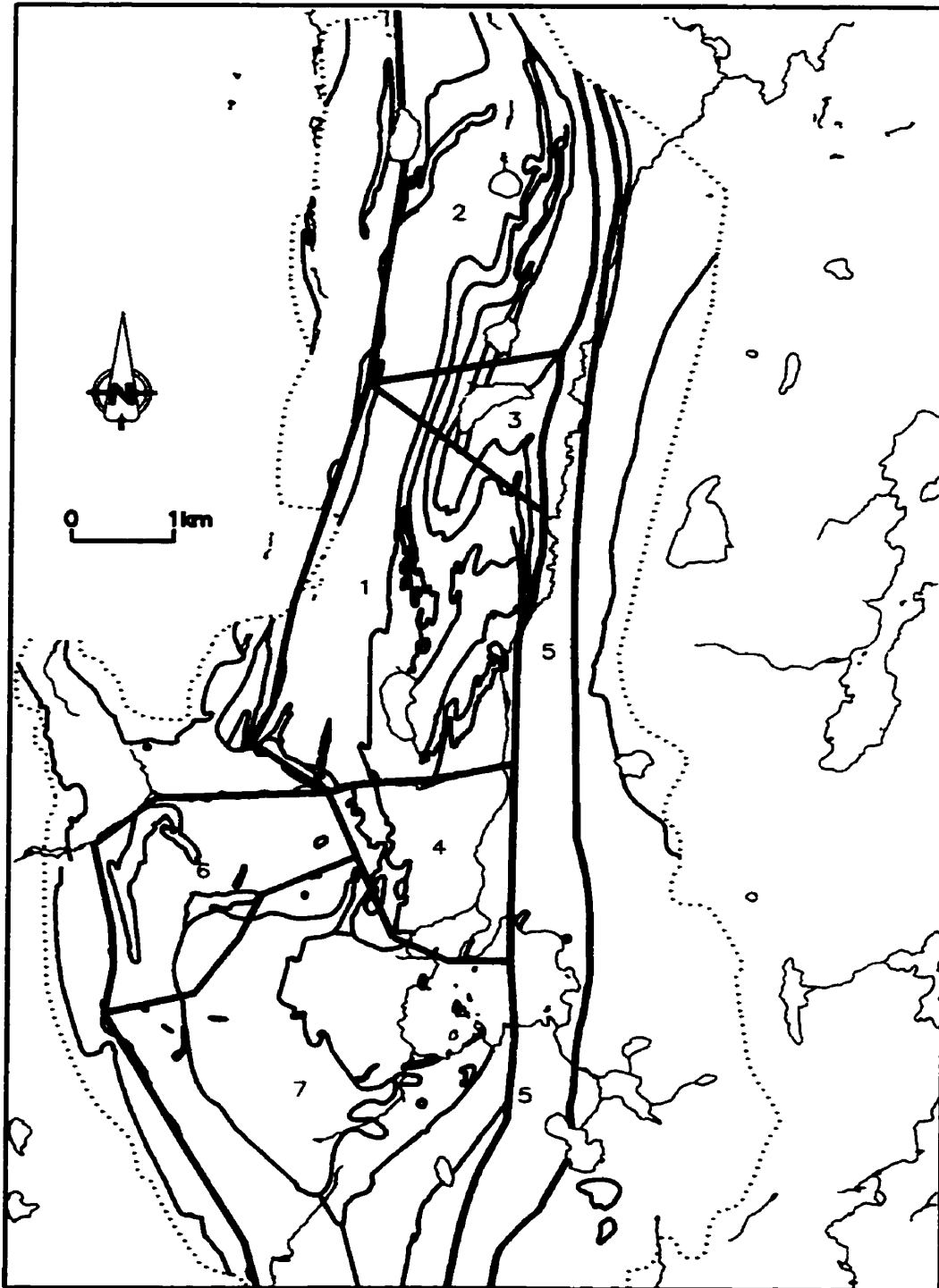


Figure 4-2. Structural subareas in the North Star Lake area (after Norquay et al., 1994a; 1994b).

4.2 Cleavage Classification

The wide variety of lithologies in the North Star Lake area has resulted in a wide variety of rock cleavage. For the purposes of discussion the cleavage classification of Powell (1979) is used (Figures 4-3, 4-4). In this classification foliations have a primary subdivision of continuous or spaced cleavages. Continuous cleavages are further subdivided into fine or coarse. Spaced cleavages are subdivided into crenulation or disjunctive, based upon whether or not the rock contained a pre-existing anisotropy.

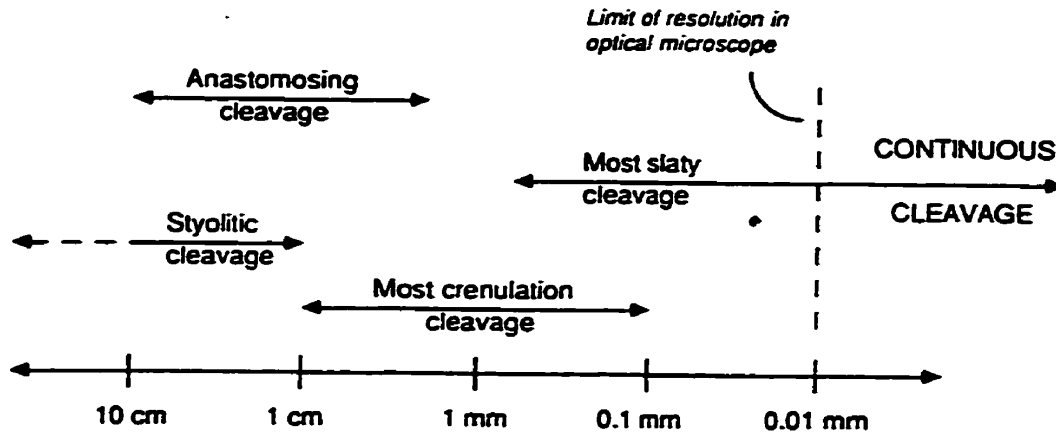


Figure 4-3. Type and spacing of cleavages (from Powell, 1979).

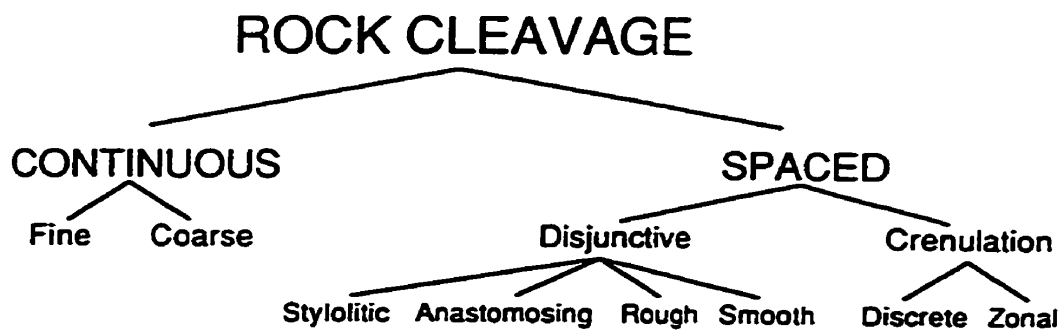


Figure 4-4. Classification of cleavages based upon morphology (from Powell, 1979).

4.3 Fold Classification

The wide variety of folding mechanisms experienced in the North Star Lake area has resulted in a wide variety in fold geometry and orientation. For the purposes of discussion the terminology used in this thesis will be summarized.

One of the first attempts to classify folds based on the fold geometry was made by Van Hise (1896) in which folds were classified as either parallel or similar. Fleuty (1964) developed a fold classification system base on the interlimb angle of the fold (Table 4-2). Ramsey (1967) developed a system of fold classification (Figure 4-5) based on the dip isogon method of Elliot (1965).

The terminology used to describe fold orientation will be that of Fleuty (1964) (Figure 4-6).

Interlimb angle	Description of fold
180--120°	Gentle
120--70°	Open
70--30°	Close
30--0°	Tight
0°	Isoclinal
Negative angles	Mushroom or Elastica

Table 4-2. Fold classification system based on interlimb angle (after Fleuty, 1964).

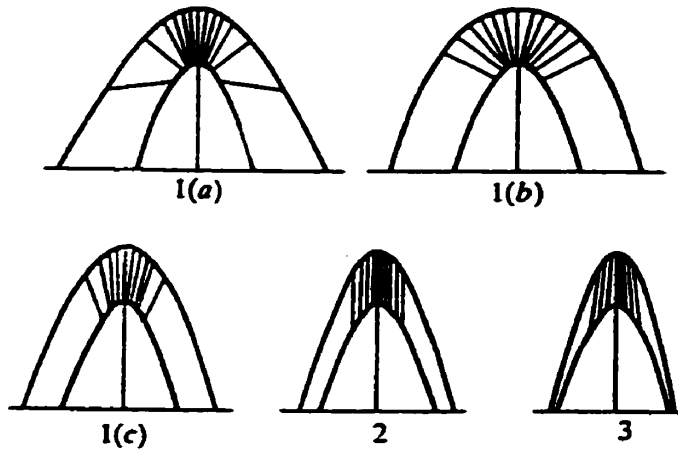


Figure 4-5. Classification of fold profiles using dip isogon patterns. 1(a) Strongly convergent, 1(b) parallel, 1(c) weakly convergent, 2 similar, 3 divergent (after Ramsey, 1967).

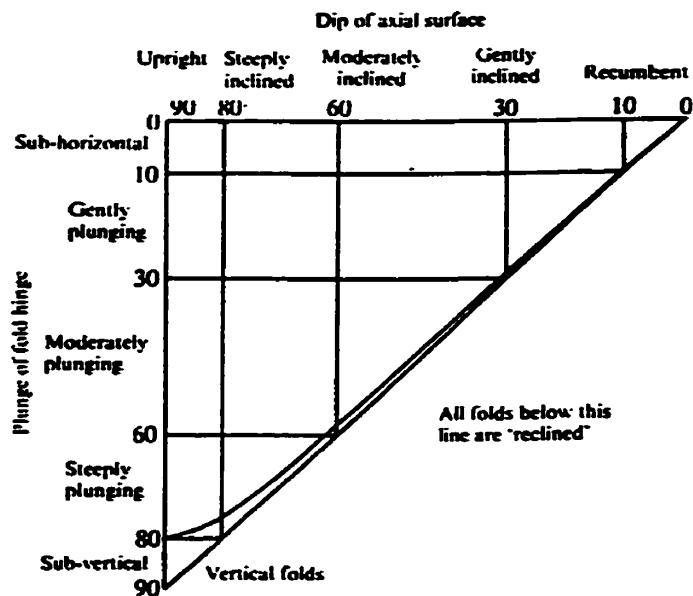


Figure 4-6. Classification of fold orientation (after Fleuty, 1964).

4.4 Fault Rock Classification

Sibson (1977) presented a classification of fault rocks based upon the textural characteristics of the rocks within the fault zone (Tables 4-3, 4-4). In this classification fault rocks have a primary subdivision of foliated or random-fabric. The primary subdivisions are further divided based upon the presence or absence of primary cohesion.

The fault rocks within the random-fabric subdivision essentially have a random shape and crystallographic fabric. The cataclasite (*sensu lato*) series is within the random-fabric subdivision.

The fault rocks of the foliated series have a foliated fabric, usually with a strong inosculating L--S fabric. The mylonite (*sensu lato*) series is within the foliated subdivision.

The fault mechanisms that result in the various fault rocks in quartzo-feldspathic crust are divided into two subdivisions (Sibson, 1977). The elasto-frictional (EF) regime exists at higher crustal levels where rock particles exhibit near-elastic behaviour, therefore deformation of rock material is friction-dominated. The quasi-plastic (QP) regime exists at lower crustal levels where deformation is dominated by crystal plasticity. The terms elasto-frictional and quasi-plastic may be loosely correlated with the more commonly used terms brittle and ductile, respectively.

		RANDOM - FABRIC	FOLIATED		
INCOHESIVE		FAULT BRECCIA (visible fragments >30% of rock mass)	?		
		FAULT COCKLE (visible fragments <30% of rock mass)	?		
CONESIVE	Glass/dust-filled glass	PSEUDOTACHYLITE	?		
	NATURE OF MATRIX Tectonic reduction in grain size dominates grain growth by recrystallization & metamorphism	CRUSH BRECCIA FINE CRUSH BRECCIA CRUSH MICROBRECCIA	(fragments > 0.5 cm) (0.1cm < frags. < 0.5cm) (fragments < 0.1 cm)	0 - 10%	PROPORTION OF MATRIX
		PROTOMylonite	PROTOMylonite	10 - 50%	
		CATACLASTITE	MYLONITE	50 - 90%	
	ULTRACATACLASTITE	ULTRAMylonite	90 - 100%		
Grain growth pronounced	?	BLASTOMylonite			

Table 4-3. Textural classification of fault rocks (from Sibson, 1977).

	Style of Faulting	Fault Rocks
ELASTICO-FRITIONAL	Brittle shearing of intact rock } sliding on existing planes	Pseudotachylite
	Cataclastic crush zones	Cataclasite-Ultracataclasite (& some pseudotachylite)
	Crush Melange	Crush breccias, microbreccias & protocataclasite
	Quasi-plastic shear zones	Phyllonitic mylonites & ultramylonites
QUASI-PLASTIC	Crush Melange with crude mylonitic foliation	Protomylonites

Table 4-4. Fault rocks and style of faulting (from Sibson, 1977).

4.5 Macroscopic Features

4.5.1 First Phase of Deformation (D_1)

The first phase of deformation (D_1) folded the primary layering (S_0) and produced similar, tight to isoclinal folds (F_1) which commonly have a well-developed axial-planar foliation (S_1) (Plate 4-1). These folds, which occur throughout the map area, commonly have small amplitudes and most commonly occur in the iron formation of unit 8 (Figure 3-1) where they have amplitudes of 10 cm to 1 m.

The F_1 structures generally are upright, northerly-trending with gentle plunges. A macroscopic northerly-plunging, northerly-trending F_1 structure with S-asymmetry (Face Lake synform) is defined by the outcrop pattern of units 2 through 4 and 7 through 9 north of Face Lake (Figure 4-1). The F_1 structures generally have gentle northerly-plunging fold axes in the southern portion of the map area and gentle southerly-plunging fold axes in the northern portion of the map area.

The S_1 foliation is the dominant fabric in the North Star Lake area. S_1 is commonly expressed as a schistosity (coarse continuous cleavage) in felsic rocks and is less developed in intermediate to mafic rocks (Plate 4-2). The S_1 schistosity is particularly well-developed in micaceous felsic rocks.

In quartzo-feldspathic rocks the (S_1) foliation is commonly expressed as a disjunctive spaced cleavage. This spaced cleavage is defined by thin (<5 mm) biotite-rich

domains that separate quartzo-feldspathic--disseminated biotite microlithons (≥ 1 cm) (Plate 4-3). The biotite-rich domains commonly undulate along both the horizontal and vertical axes.

A feature of D_1 is a lineation (L_1) that is commonly well-developed. L_1 is locally expressed in some mafic rocks as an alignment of plagioclase--quartz aggregates (Plate 4-4). Pillows, lithic fragments, and mineral aggregates define a $l>s$ fabric. Primary features such as pillows, amygdules and lithic fragments have undergone substantial flattening and stretching.

The layering in psammopelitic rocks and other well-layered rocks underwent transposition during D_1 . Locally, Pseudoconglomerate occurs in the hinge areas of F_1 structures (Plates 4-5 and 4-6).

In the area along, and immediately to the east of, Loonhead Creek and bounded to the east by a series of late brittle faults and to the west by the North--South zone structural break, thin lithologic units with layer-parallel foliation (S_1) strike generally north--south (Figure 4-1) and define a zone of concentrated deformation. Locally, tight to isoclinal folds (F_1) are preserved. These folds contain the S_1 foliation as an axial-planar fabric (Figure 4-7).

In this area -- referred to as the North--South zone -- fabrics suggest that at least a portion of the strain was in the form of ductile simple shear. The fabrics have undergone

substantial annealing however, rare examples of winged inclusion geometry suggest a dextral sense of shear.

The S_1 fabrics are mylonitic fabric in felsic rocks, compositional (tectonic) layering in intermediate to mafic rocks, and a well-developed foliation in mafic rocks. The mylonitic fabric is characterized by thin (<0.5 cm) lenses and veins, composed of very fine grained quartz and lying in the foliation. These quartz domains separate thin (<1.0 cm) aphanitic quartzo-feldspathic domains. The compositional (tectonic) layering or banding is characterized by lenses and discontinuous layers of mafic (melanocratic) material interlayered and interfingered with lenses and discontinuous layers of intermediate (mesocratic) material (Plate 4-8). The mafic rocks usually have a well-developed foliation and commonly contain quartz veins that both lie in and crosscut the foliation (Plate 4-9).

In some areas of the North--South zone primary features are preserved. These features have undergone substantial flattening, as well as extension in a direction parallel to the plane of flattening (Plate 4-10).

Proximal to, but outside of, the North--South zone strain fabrics (extensive flattening, folded boudinage and winged porphyroclast geometry) produced by the stress regime of the North--South zone are preserved and indicate flattening (Plate 4-11) as well as dextral simple shear (Plate 4-12).

Plates 4-1 through 4-12 (next six pages).

Plate 4-1. Isoclinal F_1 . Amphibolite dyke in rhyolite.

Plate 4-2. Tight F_1 with axial-planar schistosity. Folded S_0 contact between rhyolitic and dacitic rocks. Note schistosity is more developed in rhyolitic rock.

Plate 4-3. Spaced cleavage (S_1) in rhyolite. Biotite rich domains separate quartzo-feldspathic microlithons.

Plate 4-4. Gently-plunging L_1 expressed as quartz-plagioclase aggregates. Note lineation is parallel to S_1 spaced cleavage.

Plate 4-5. Pseudoconglomerate derived from layered psammopelitic rocks in hinge area of isoclinal F_1 .

Plate 4-6. Layered psammopelitic rocks on limb of isoclinal F_1 (same exposure as Plate 4-7).

Plate 4-7. Isoclinal F_1 in North--South zone. Amphibolite in psammopelitic rocks.

Plate 4-8. Compositional (tectonic) layering or banding (S_1) in North--South zone. Note discontinuity of layers or bands.

Plate 4-9. Mafic rock with well-developed foliation, quartz veins both lie and in crosscut the foliation.

Plate 4-10. Boudinaged mafic dyke or layer in North--South zone, extension parallel to fabric.

Plate 4-11. Volcanoclastic rock proximal to North--South zone. Lithic fragments have undergone substantial flattening.

Plate 4-12. Epidosite pods proximal to North--South zone, σ -type winged porphyroclast geometry indicates dextral simple shear.

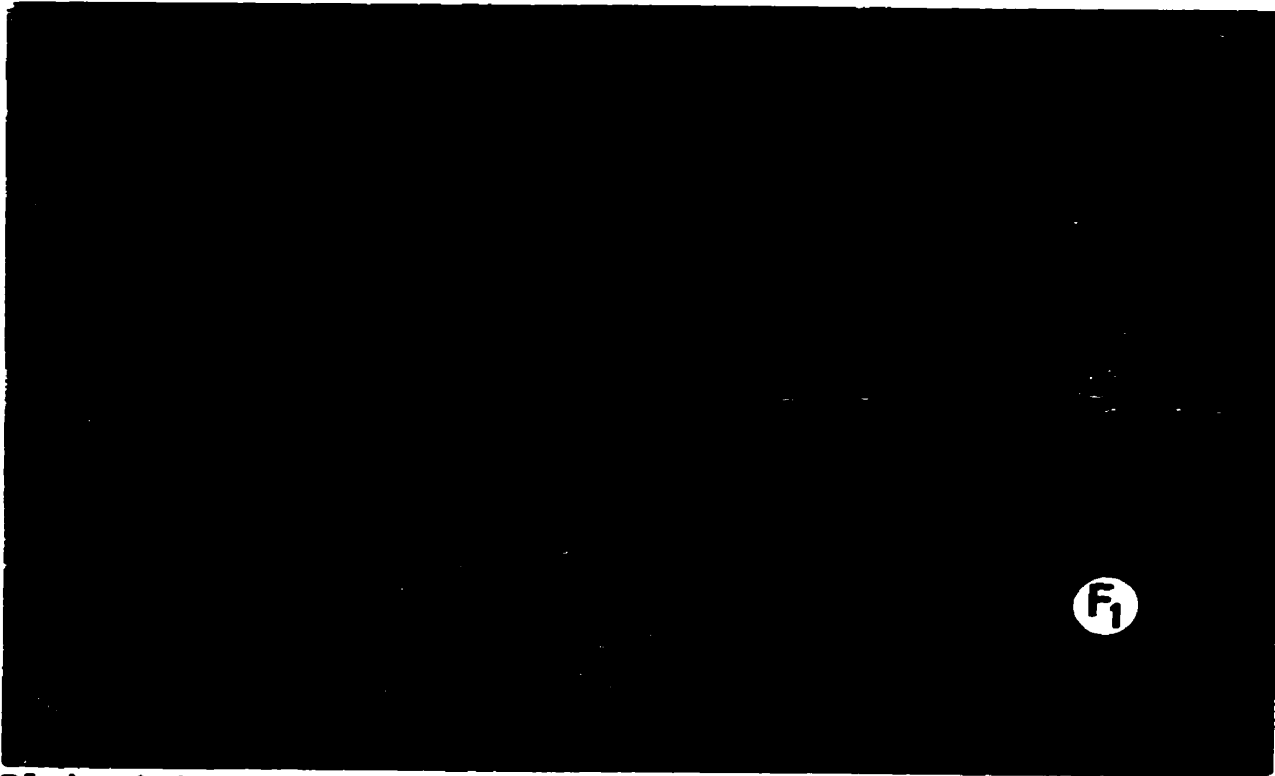


Plate 4-1

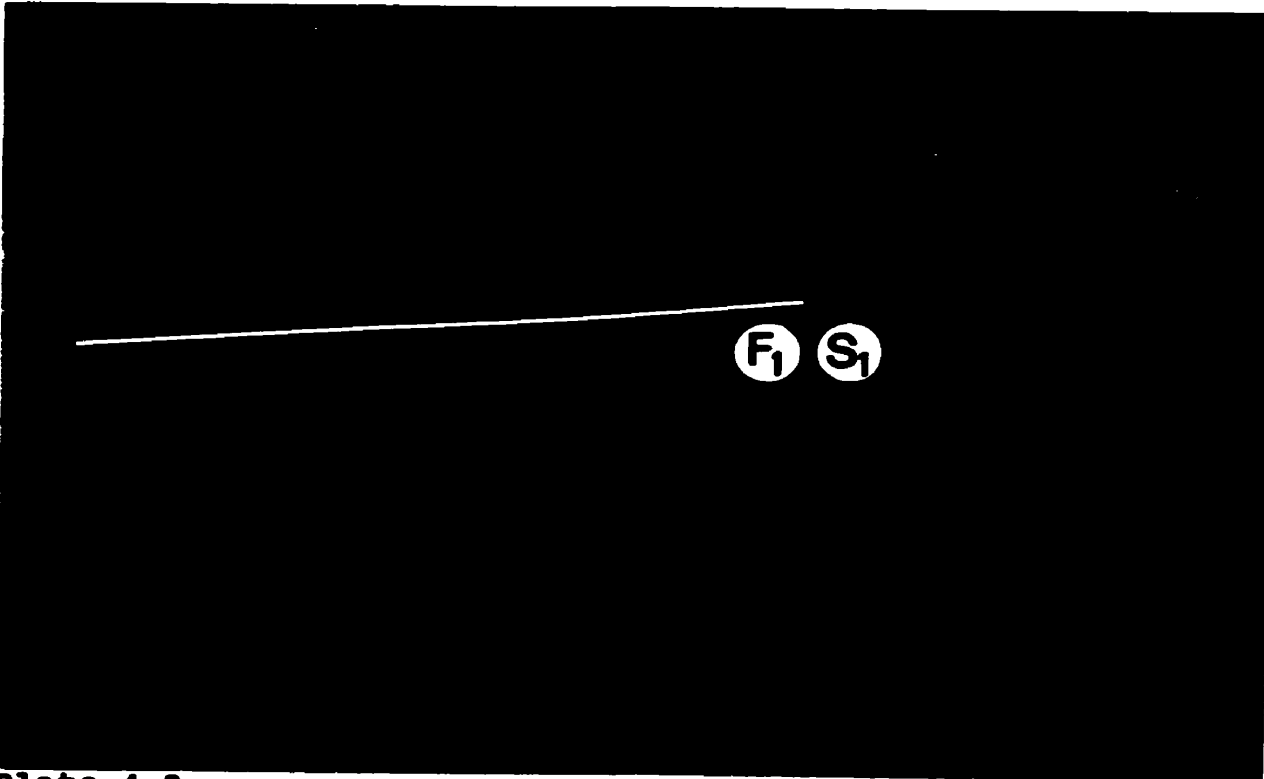


Plate 4-2

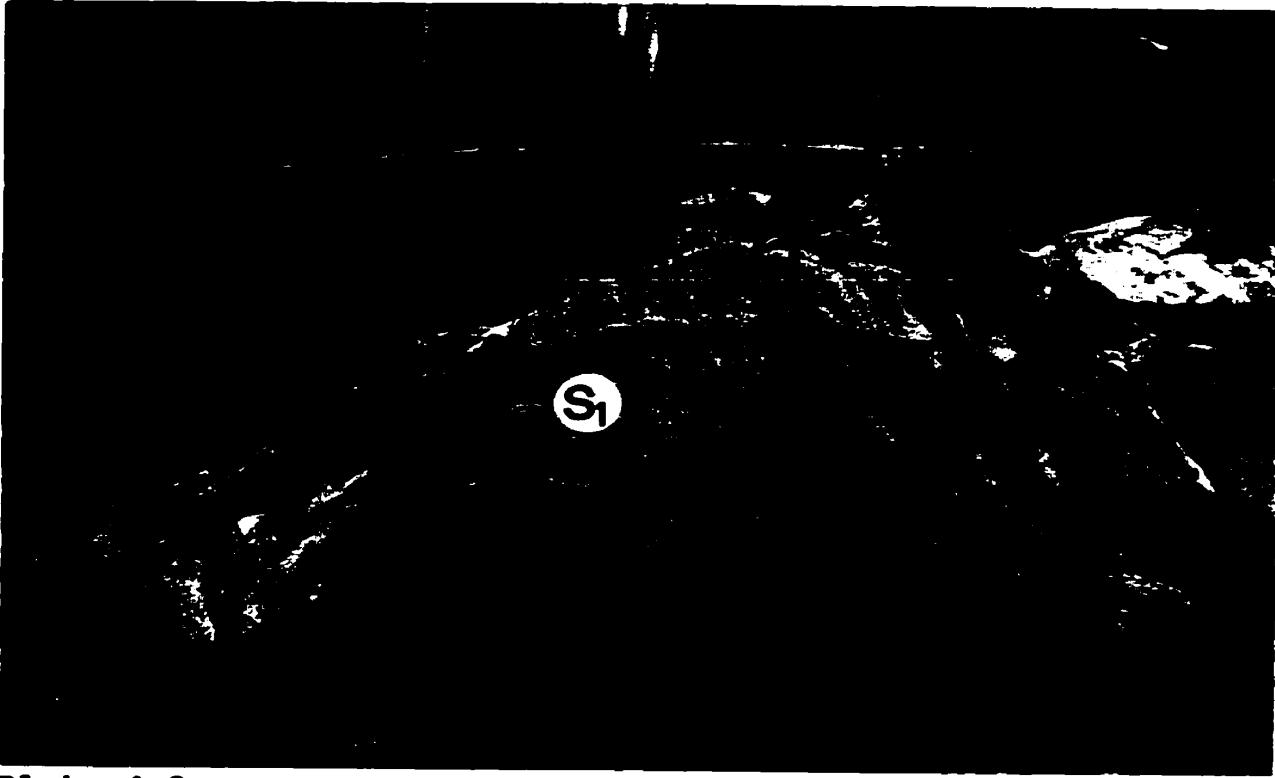


Plate 4-3

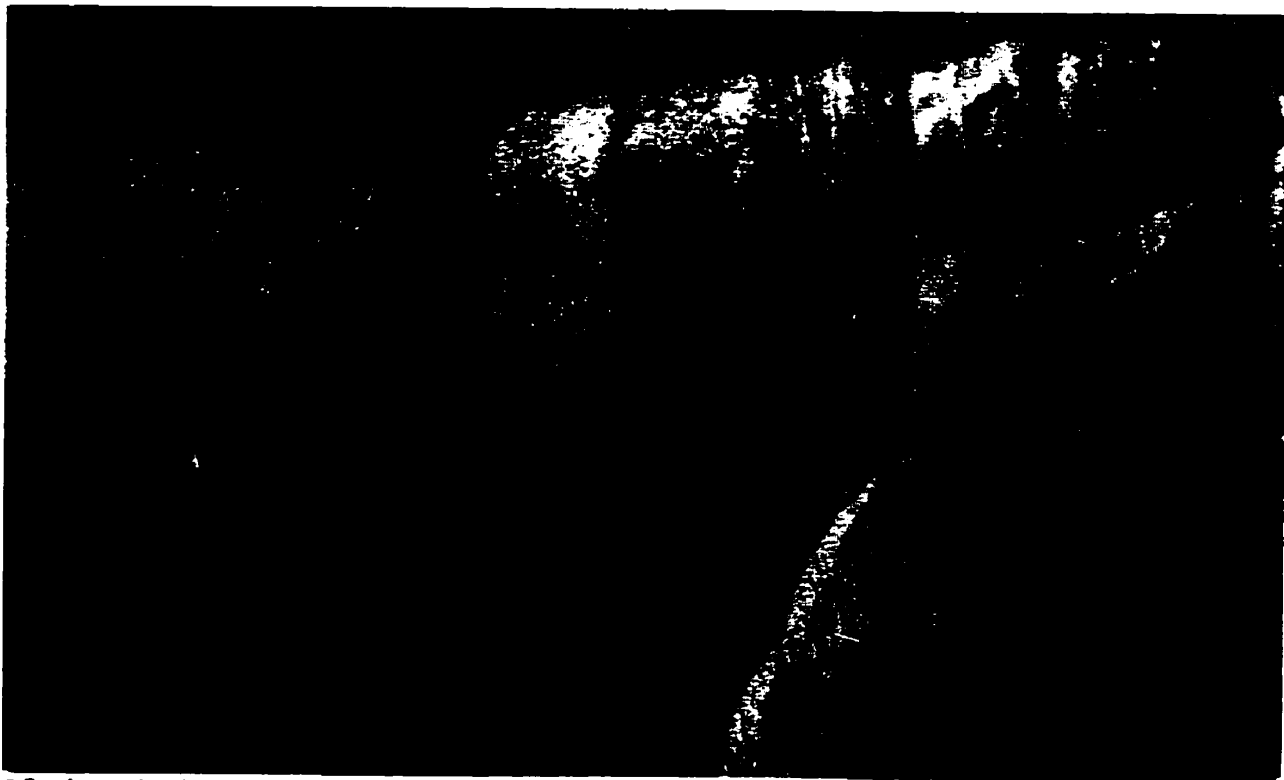


Plate 4-4

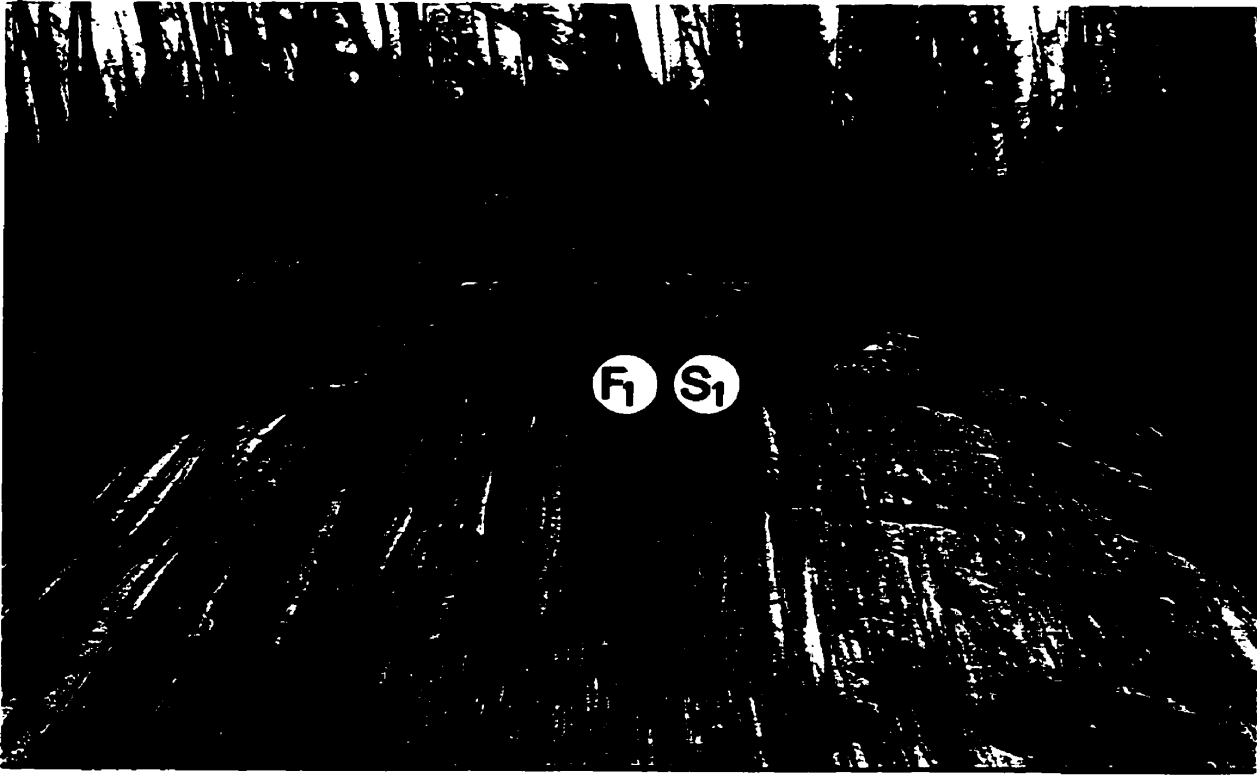


Plate 4-5

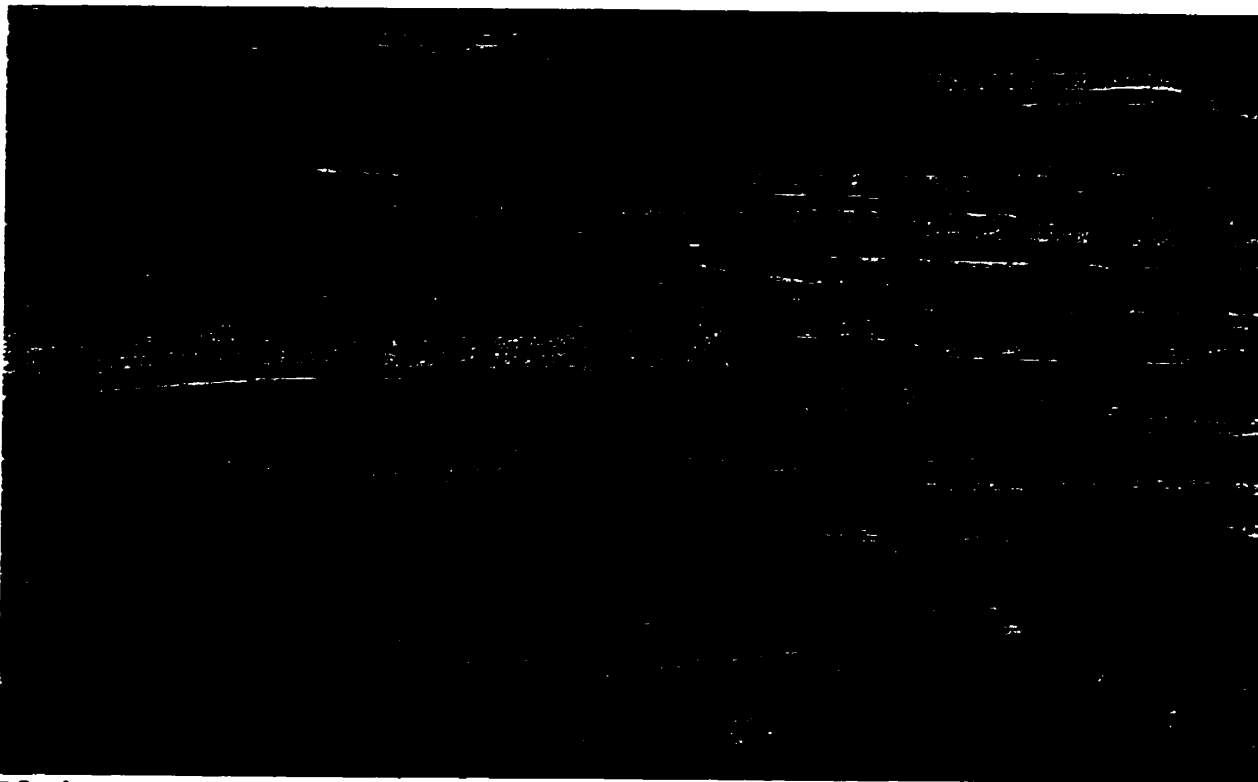


Plate 4-6



Plate 4-7

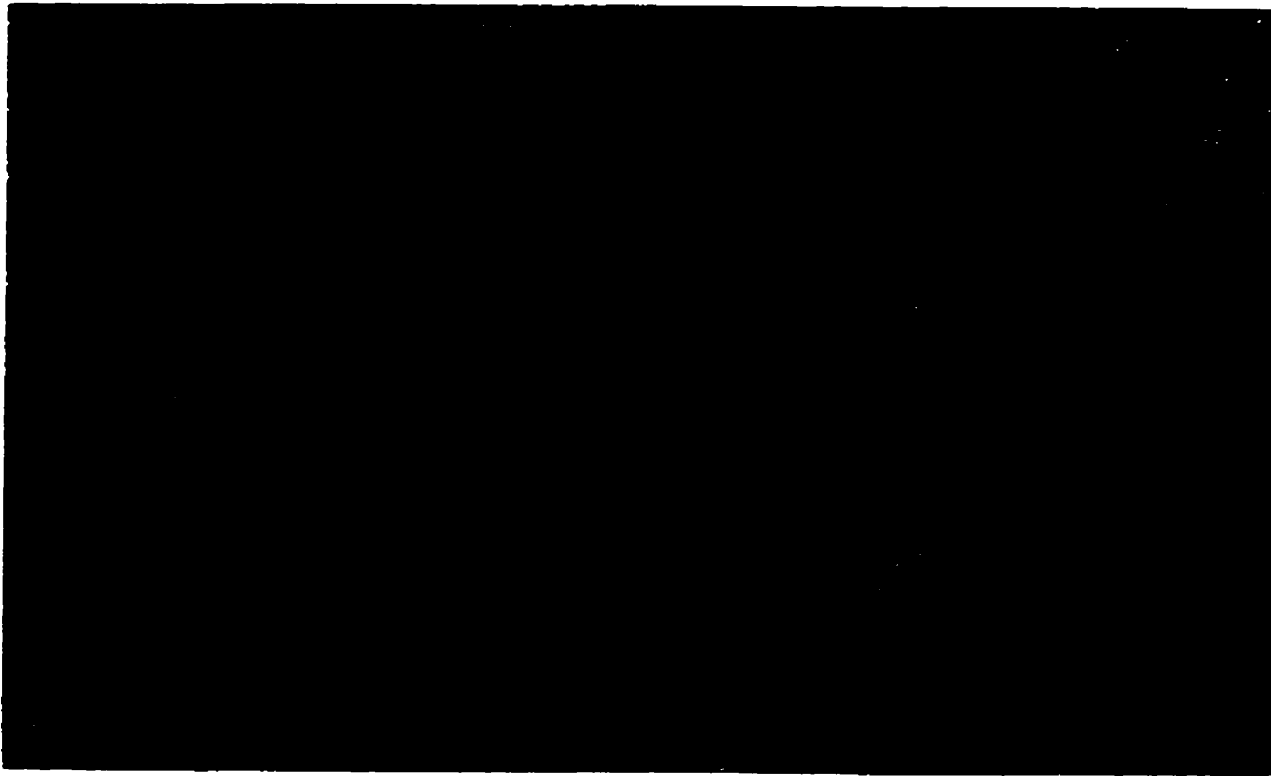


Plate 4-8

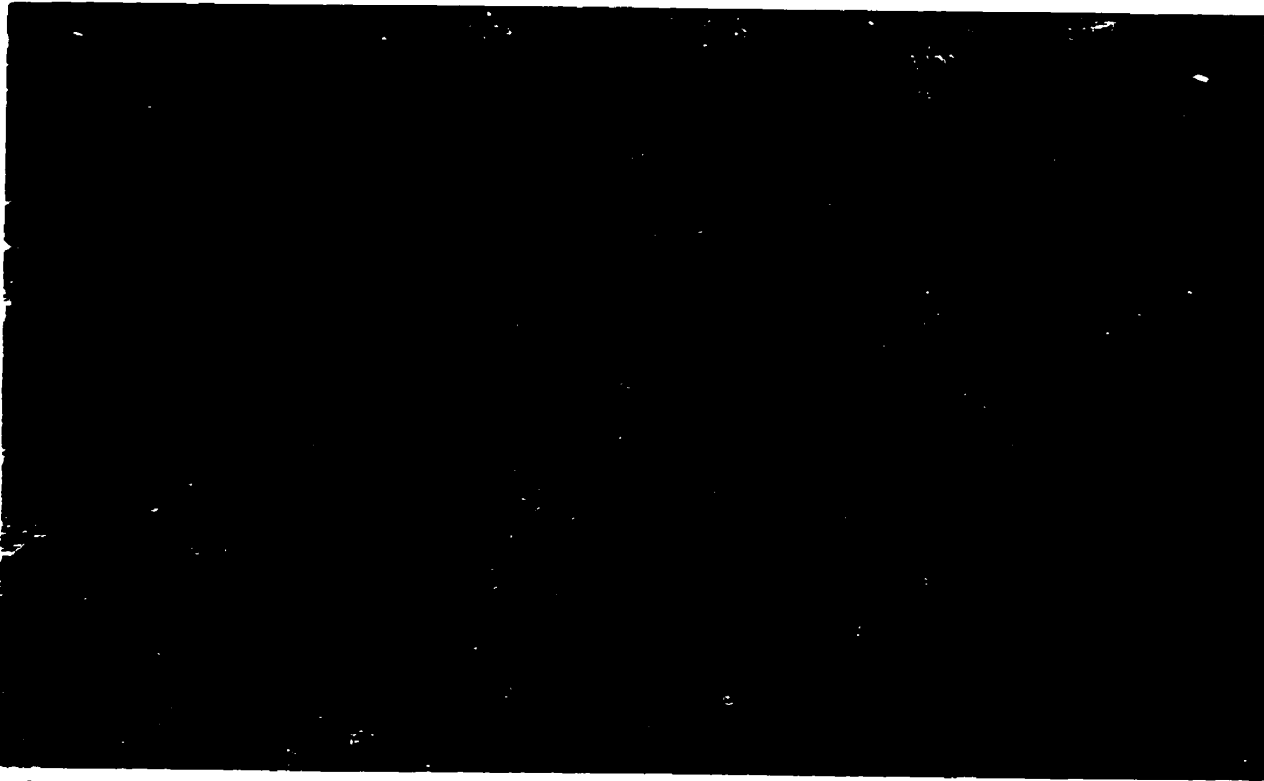


Plate 4-9

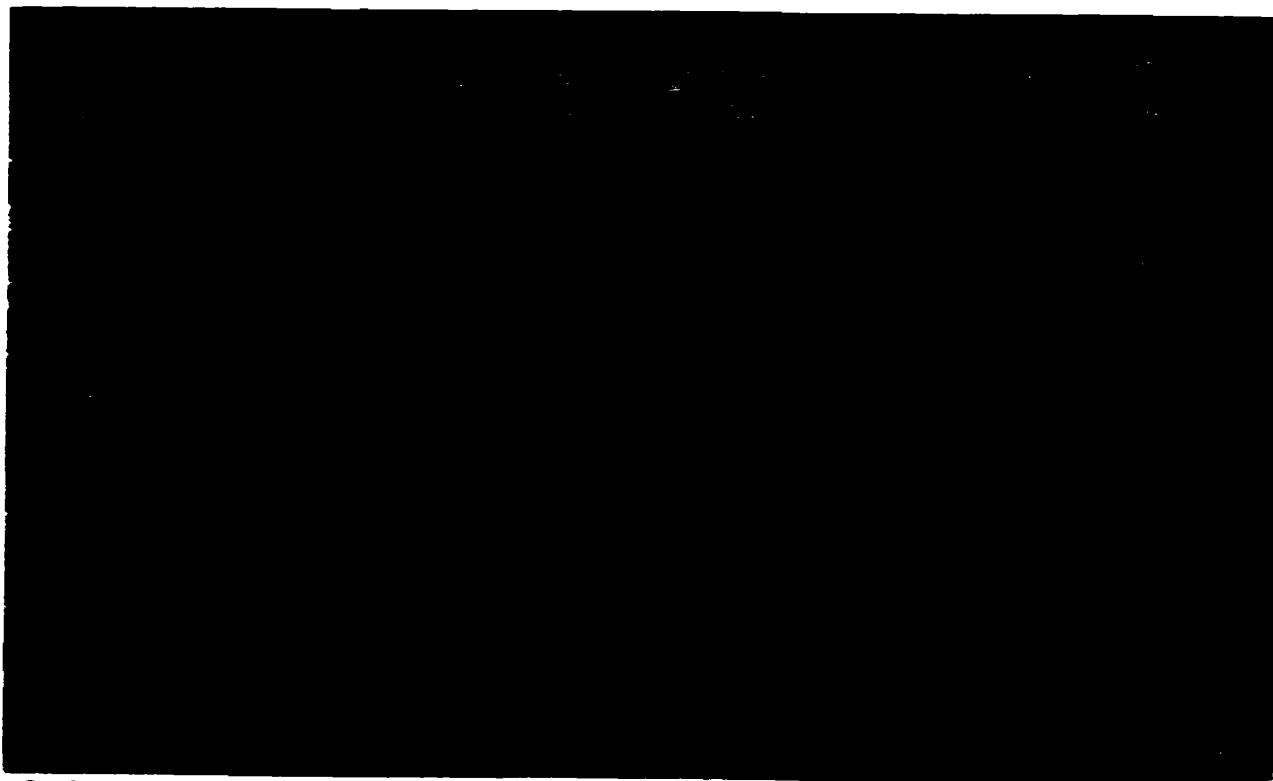


Plate 4-10

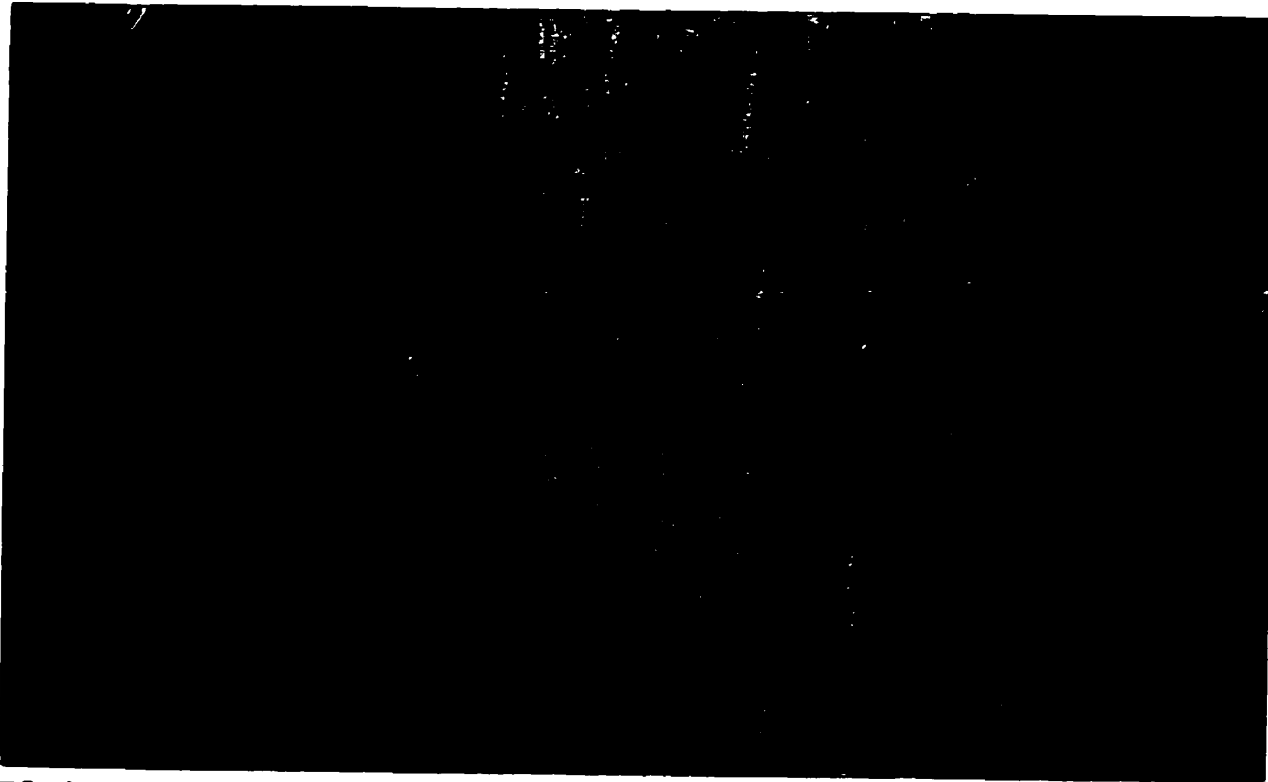


Plate 4-11

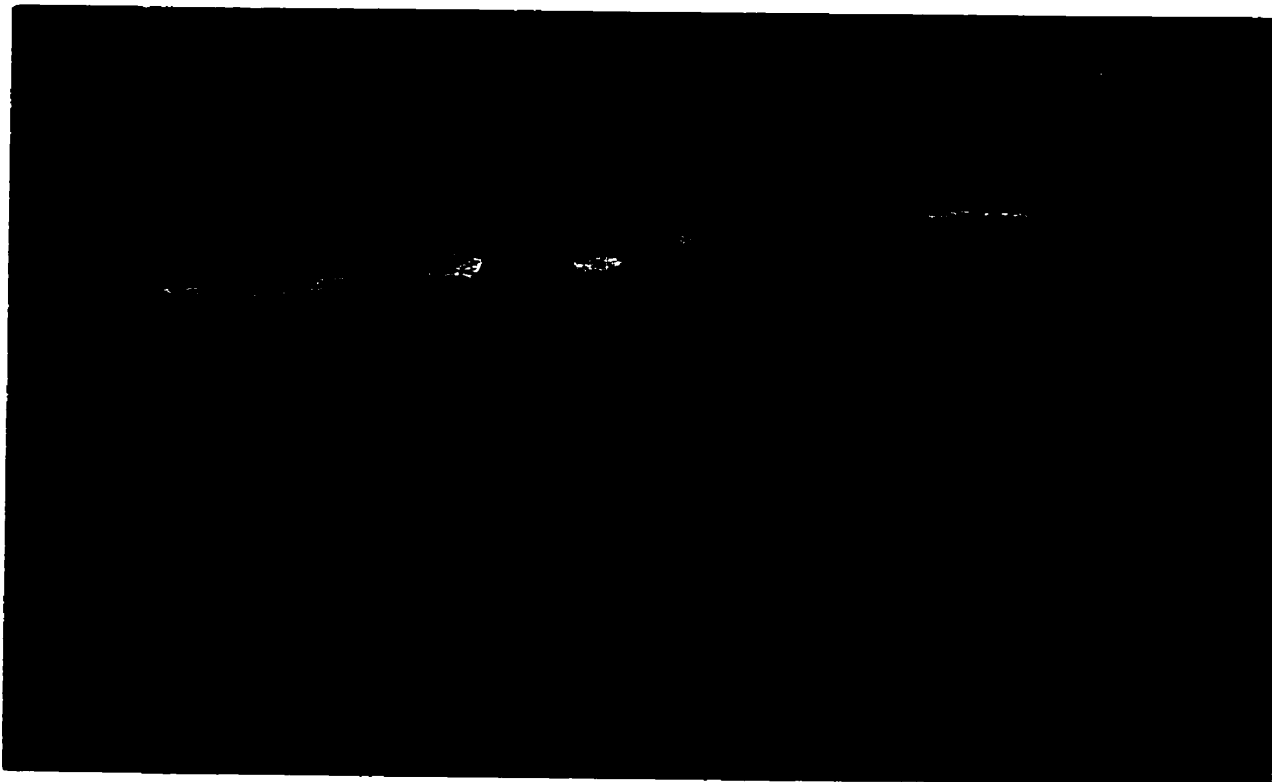


Plate 4-12

4.5.2 Second Phase of Deformation (D_2)

The second phase of deformation (D_2) produced open to tight folds (F_2) that generally have northerly-trending and moderately- to steeply-inclined, easterly-dipping axial planes. In the area west of the North--South zone structural break (Figure 4-1) the F_2 structures (F_{2a}) predominantly have northerly-trending, gently- to moderately-plunging fold axes while east of the structural break the F_2 structures (F_{2b}) have southerly-trending, moderately- to steeply-plunging fold axes.

In the area west of the structural break the most commonly recognized F_{2a} structures are minor folds that fold earlier S_0 and S_1 . The F_{2a} structures typically express Z-asymmetry with subordinate M- and S-asymmetry (Plate 4-13 and 4-14). A poorly-developed axial-planar fracture cleavage (S_{2a}) occurs locally in felsic rocks in the hinge area of minor F_{2a} structures (Plate 4-15).

A large F_{2a} fold pair is defined by units 7 through 9 between Face Lake and Loonhead Creek (Figure 4-1). On the long limbs of this D_2 synform and antiform pair minor folds predominantly have Z-asymmetry with subordinate M-asymmetry. Rare minor folds with S-asymmetry occur only on the short limbs of this fold pair.

F_1 minor structures and S_1 foliations have been refolded by F_{2a} . In the hinge areas of the F_{2a} structures, S_1 foliations and isoclinal F_1 structures are gently-inclined (Plate 4-16). In these hinge areas primary features that were flattened

during D_1 were subsequently folded during D_2 (Plate 4-17). Commonly, primary features are preserved only in the F_{2a} hinge areas. On the limbs of the F_{2a} structures the S_1 foliation is coplanar to near coplanar with the S_{2a} foliation.

A feature of D_2 was the development of a lineation (L_{2a}). In amphibolite this lineation is locally expressed as an alignment of amphibole crystals. In quartzo-feldspathic rocks L_{2a} is defined macroscopically by lenses of quartz aggregates (Figure 4-18). The L_{2a} fabric generally has a northerly gentle-plunge in the southern portion of the map area, and a northerly gentle- to moderate-plunge in the northern portion of the map area. L_{2a} can only be definitely recognized in the hinge areas of F_{2a} structures. In these hinge areas the orientation of L_{2a} is near-parallel to the F_{2a} axis (Figure 4-1).

Mineral assemblages and the orientation of minerals and mineral aggregates in the North Star Lake area indicate that the peak of metamorphism was approximately contemporaneous with D_2 . In amphibolite amphibole crystals locally define the L_{2a} fabric. In the Lower Rhyolite (unit 9) south of East--West Creek and west of Face Lake (Figure 4-1) semipelitic rocks have developed a prominent gneissosity (S_{2a}). The distribution of the gneissosity appears to have been controlled by compositional variations in the original lithologies (Plate 4-19). At some locations this gneissosity defines the L_{2a} fabric (Plate 4-20) however, at other locations the

gneissosity has been folded during D_2 (Plate 4-21).

In the area east of the structural break (the North--South zone) minor folds (F_{2b}) fold an older foliation or compositional layering. Locally, younger quartz veins lie within, and crosscut, the foliation and layering.

The minor folds of the North--South zone (F_{2b}) are similar, tight to isoclinal, and exclusively have Z-asymmetry (Plate 4-22). The axial planes of these folds have an orientation similar to those of F_{2a} however, these folds have southerly-trending, steeply-plunging fold axes (Figure 4-1).

The mafic rocks in the North--South zone usually have a well-developed foliation; here they commonly contain quartz veins that both lie in and crosscut the foliation. Although the quartz veins that lie in the foliation also lie in the foliation through the hinge of minor folds the age of these quartz veins relative to the foliation is uncertain.

Plates 4-13 through 4-22 (next five pages).

Plate 4-13. F_2 parallel fold. Amphibolite dyke in rhyolite. Note folded S_1 .

Plate 4-14. Tight, gently-plunging F_2 in banded iron formation.

Plate 4-15. Poorly-developed fracture cleavage S_2 in rhyolite in hinge area of F_2 structure.

Plate 4-16. Gently-inclined spaced cleavage (S_1) in hinge area of F_2 structure.

Plate 4-17. Volcanoclastic rock in F_2 hinge area. Lithic fragments have been flattened during D_1 and subsequently folded during D_2 .

Plate 4-18. Quartz rods define L_2 in felsic gneiss.

Plate 4-19. Gneissosity in semipelite defines S_2 , axial-planar to F_2 .

Plate 4-20. Gneissosity defines L_2 as rods near circular in cross-section on the vertical face and elongate in cross-section on the horizontal face.

Plate 4-21. Gneissosity in semipelite folded during D_2 .

Plate 4-22. Similar, tight to isoclinal (F_2) folds fabric and compositional layering. Note offset above fold.

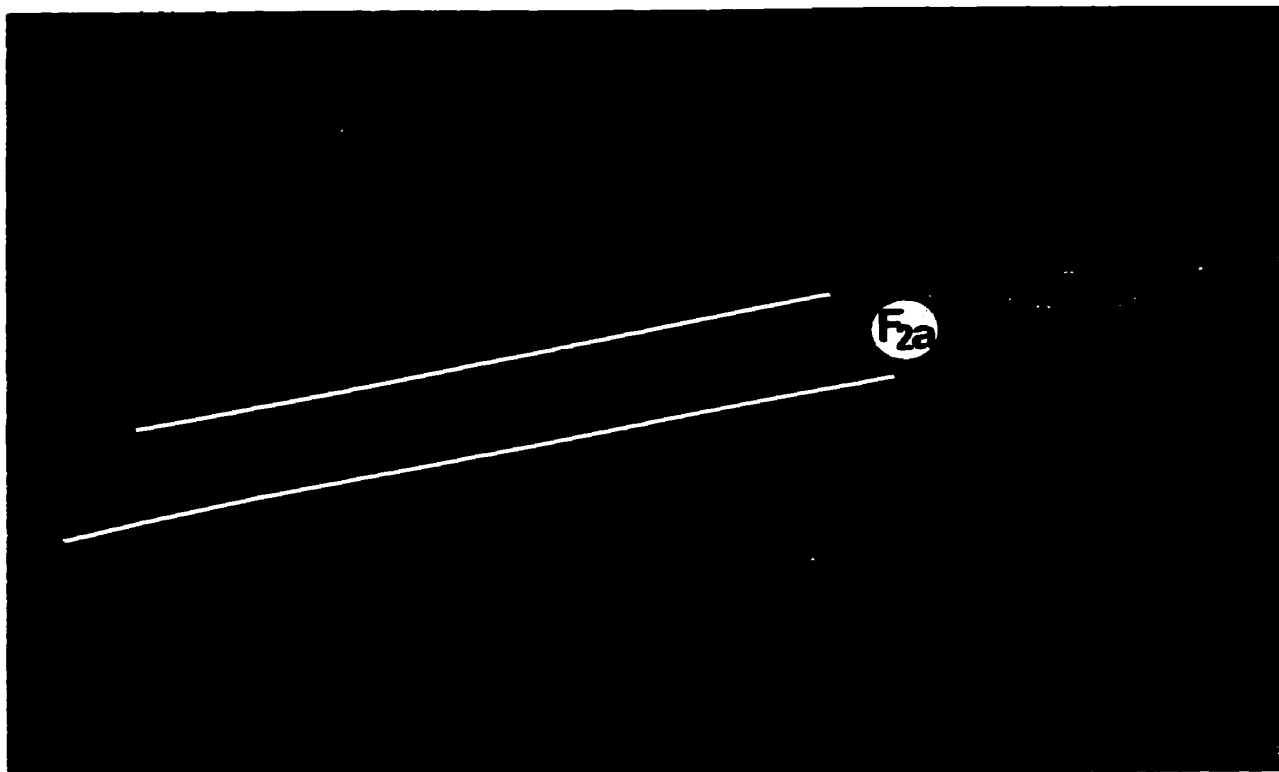


Plate 4-13

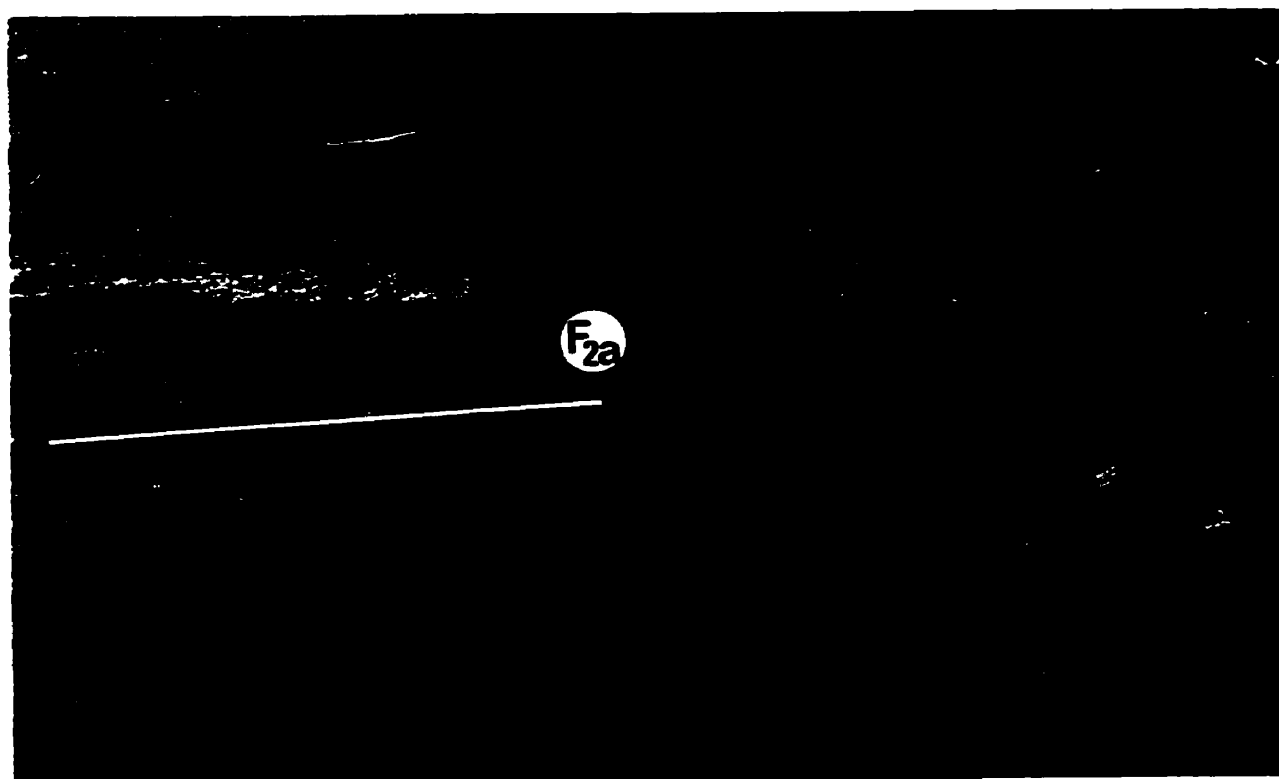


Plate 4-14

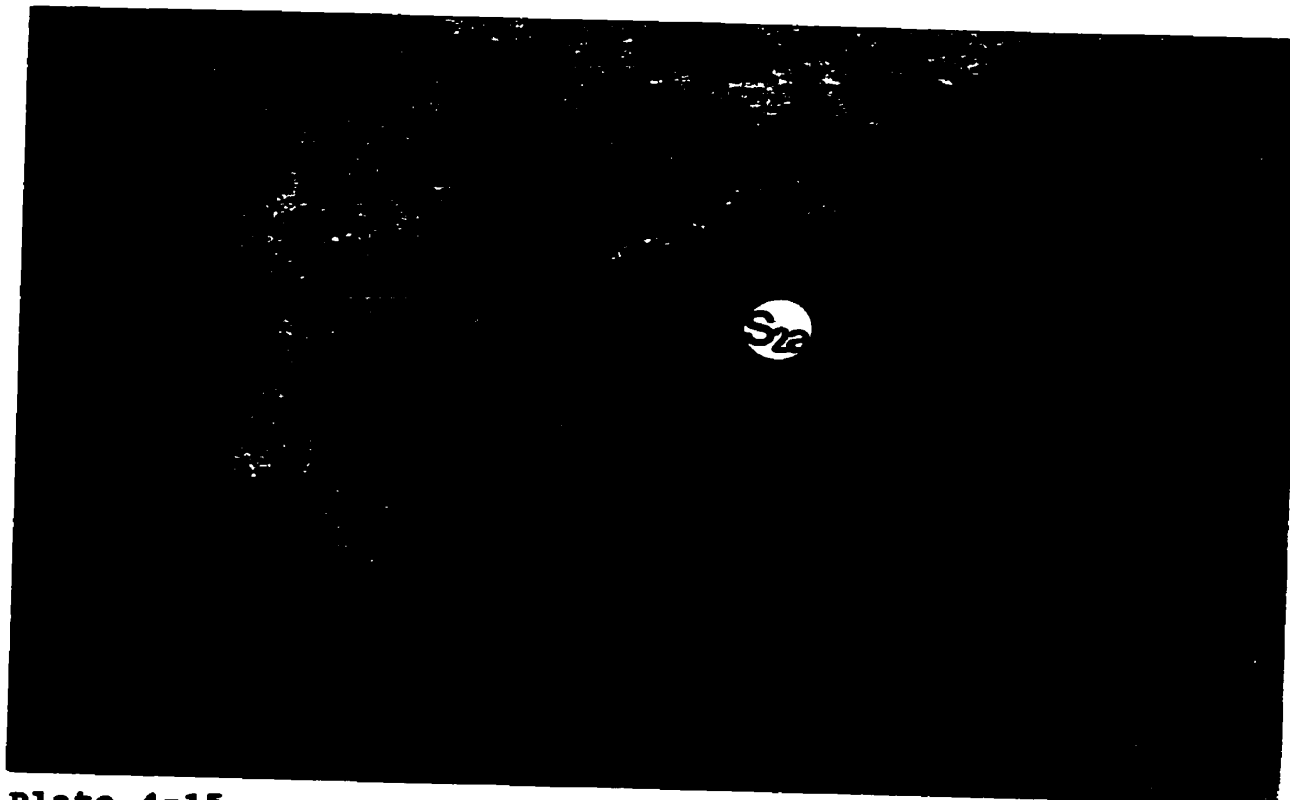


Plate 4-15

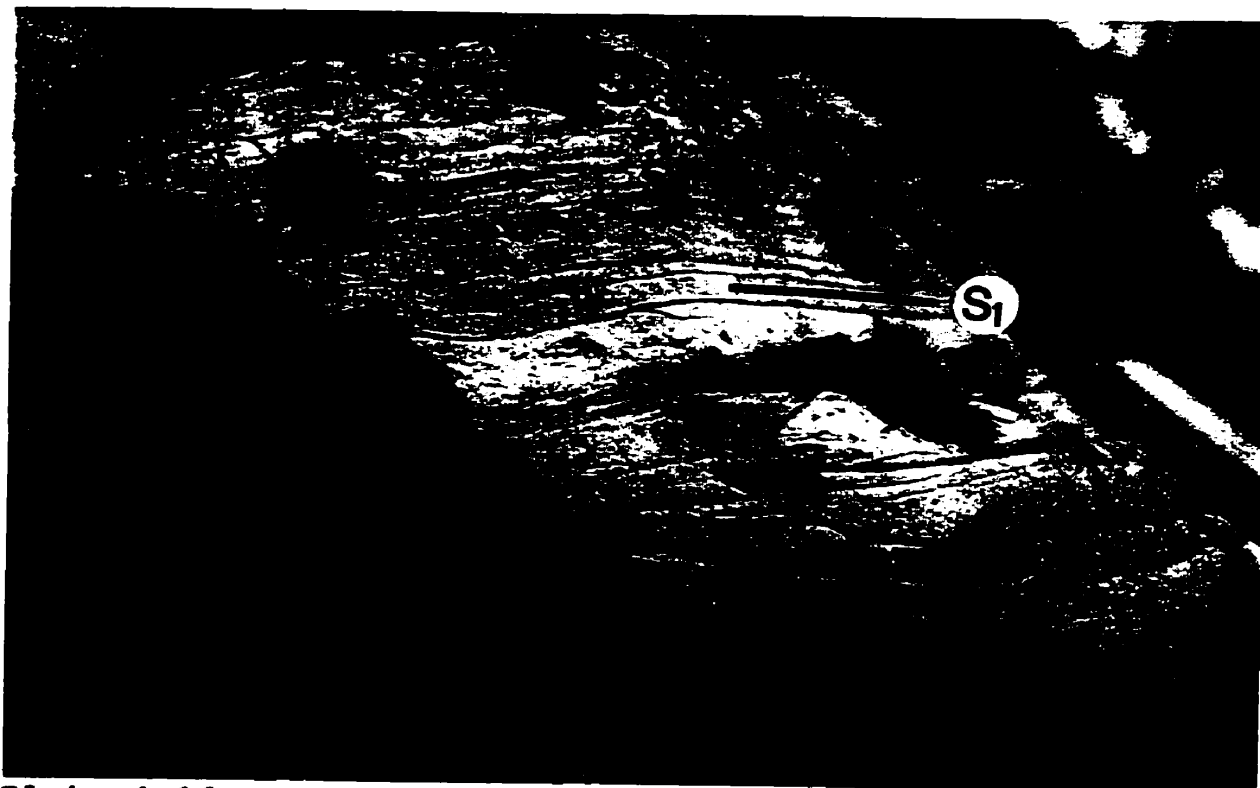


Plate 4-16

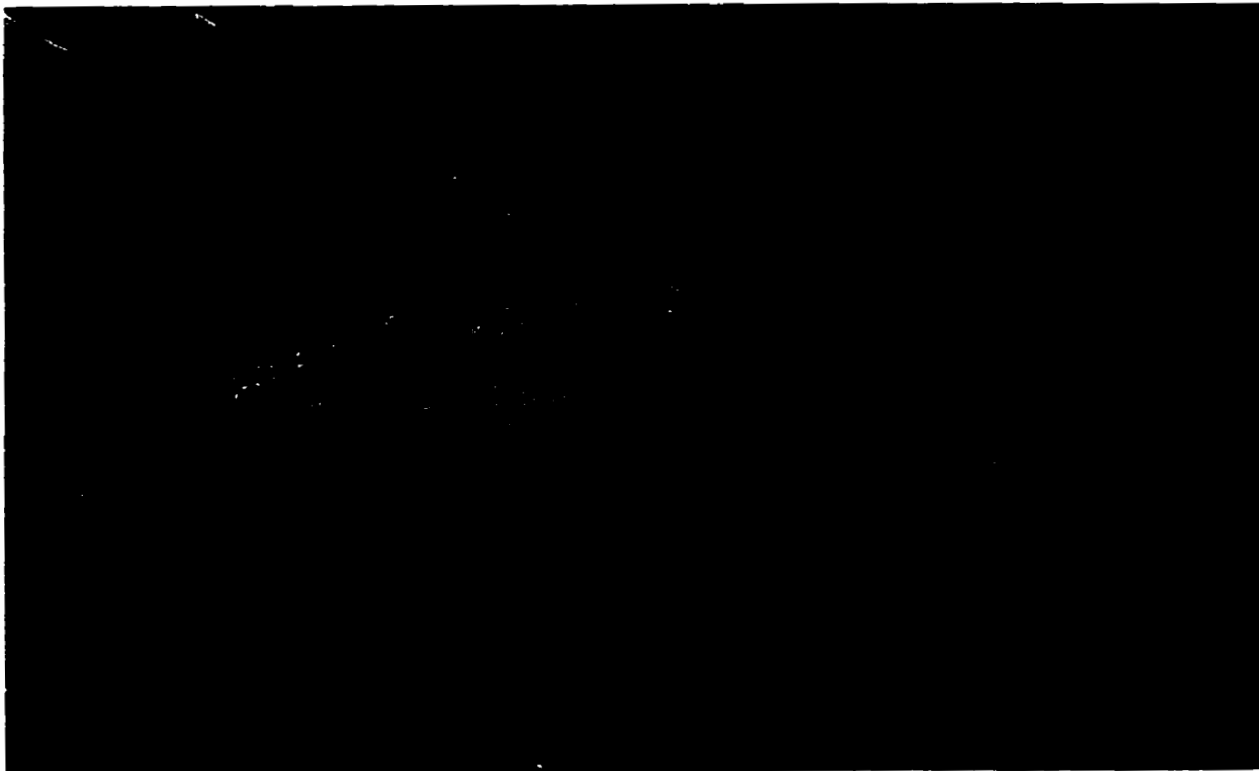


Plate 4-17

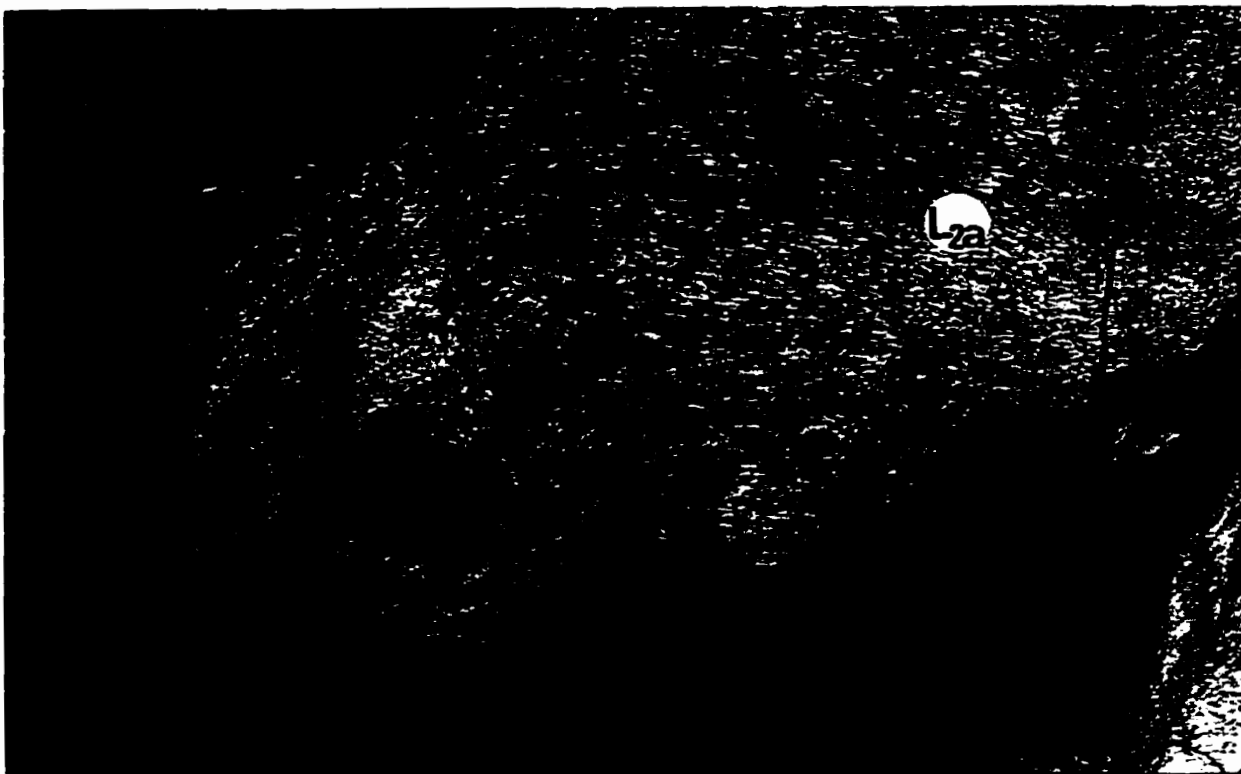


Plate 4-18

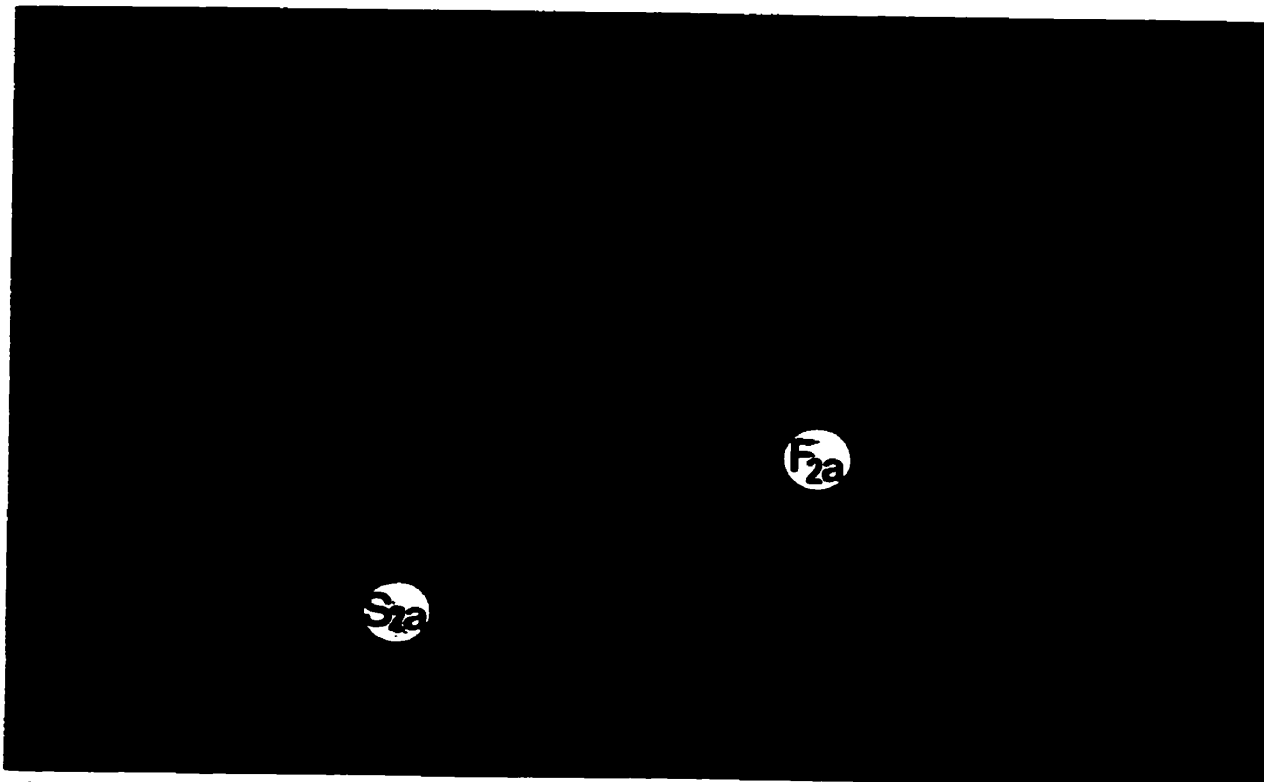


Plate 4-19

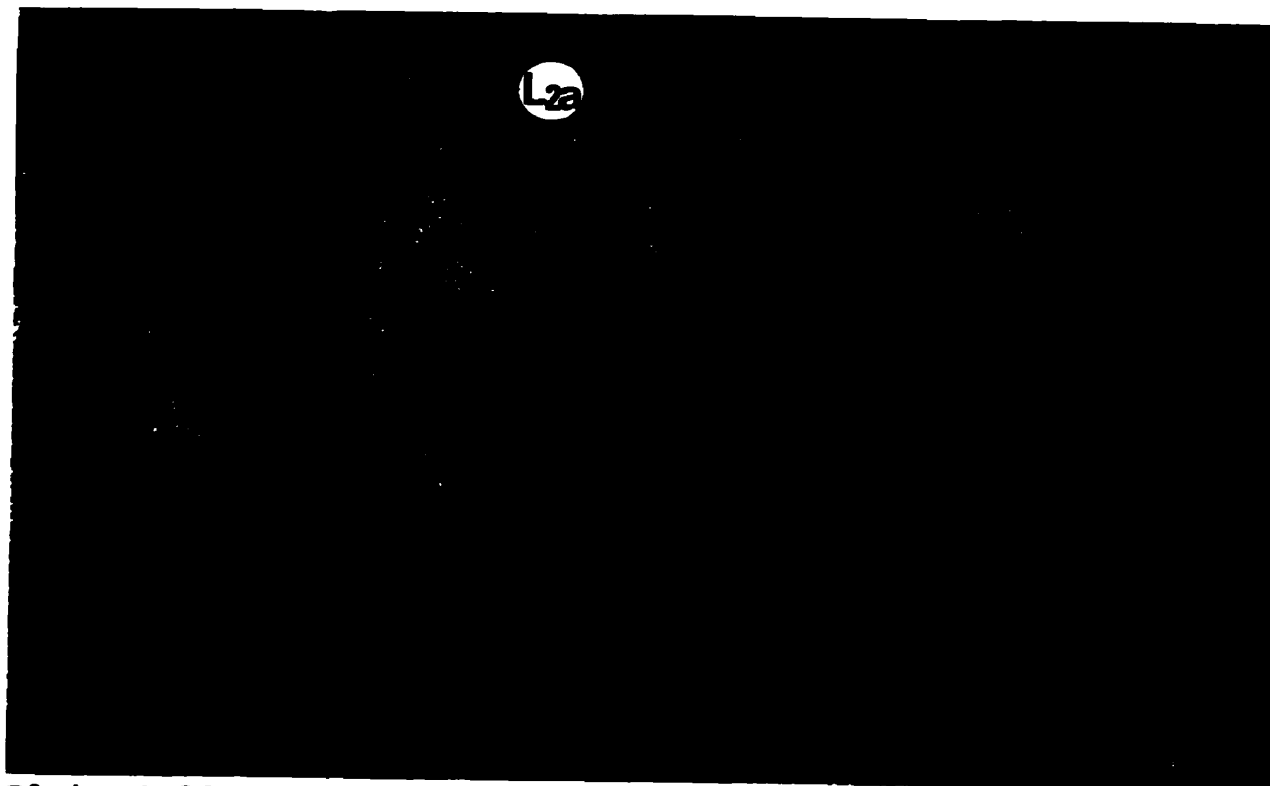


Plate 4-20

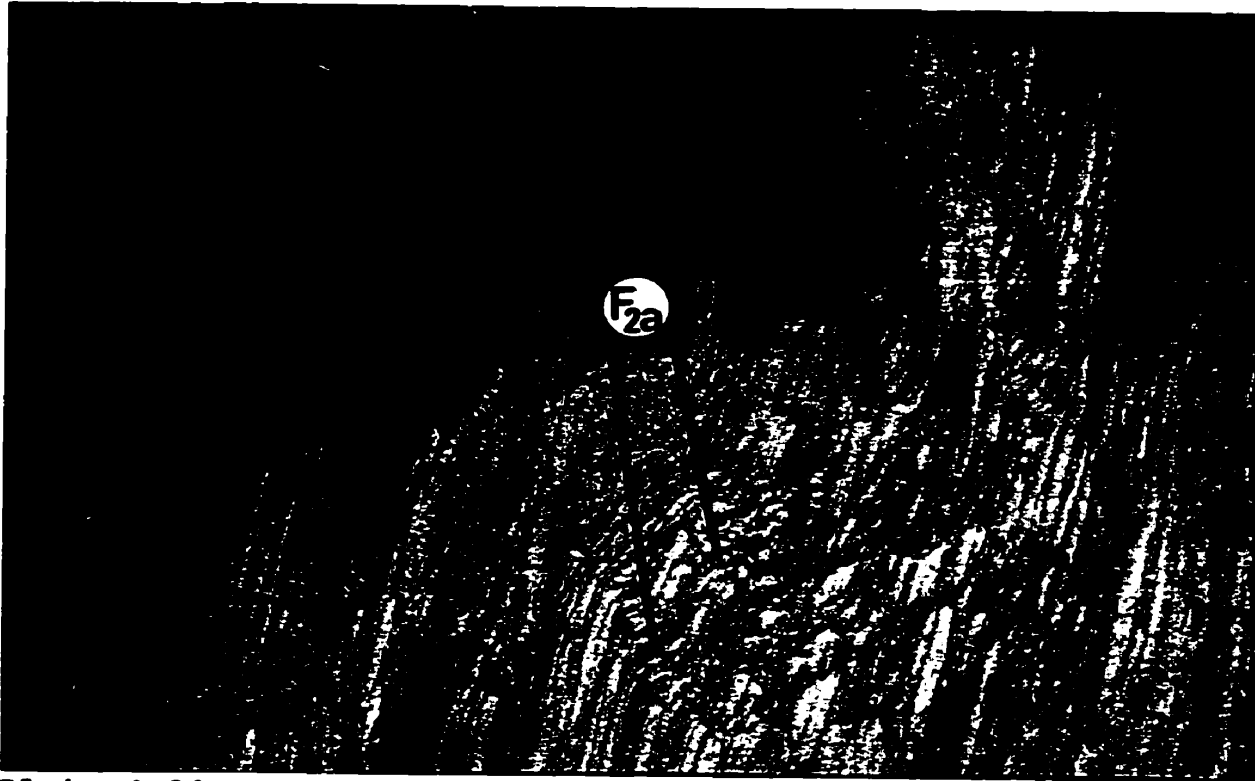


Plate 4-21

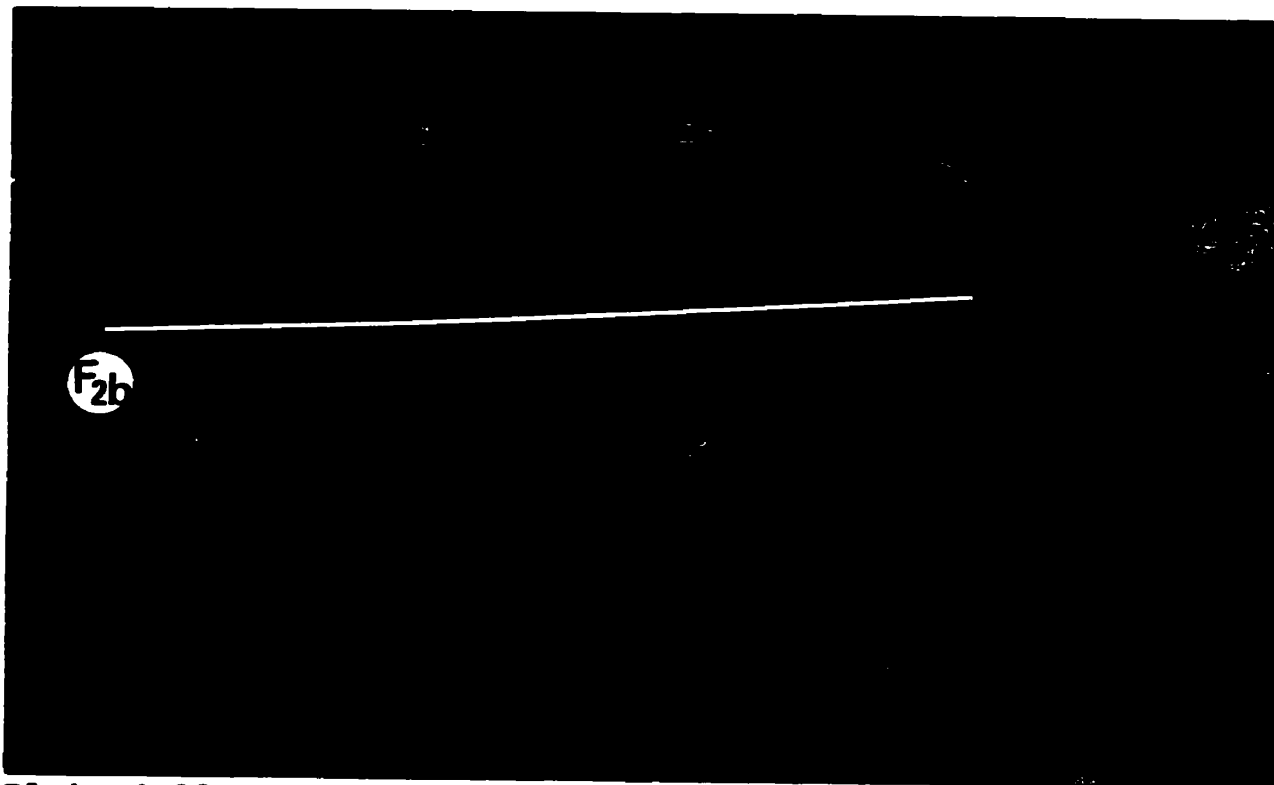


Plate 4-22

4.5.3 Third Phase of Deformation (D₃)

The third deformational event (D₃) folded older (D₁ and D₂) fabrics and structures and produced a new fabric (S₃) that developed locally in micaceous or amphibole-bearing rocks. This deformational event produced folds (F₃) that exhibit a variety of styles, but have similar orientations. This variation in fold style is the result of differing response to deformation of different lithologies. D₃ structures are preserved throughout the map area however, these structures are most-developed in the southern portion of the map area (Figure 4-1).

In the southern portion of the map area D₃ structures generally are oriented between 300° and 345° and are upright to steeply-inclined with northeasterly dips. The F₃ structures have moderately- to steeply-plunging fold axes. In the western portion of this area the F₃ fold axes have northwesterly-trending plunges whereas in eastern portion the F₃ fold axes have southeasterly-trending plunges (Figure 4-1).

In the northern portion of the map area D₃ structures generally are oriented between 270° and 330° and have steeply- to moderately-inclined, northerly to northeasterly dips. In this area the F₃ structures have easterly-trending, moderately- to steeply-plunging fold axes (Figure 4-1).

F₃ structures are commonly preserved as open folds with wavelengths that range from 1 m to several metres, fold the S₁/S₂ foliations and rotate the L₁/L₂ lineations (Plate 4-23).

Open to tight, parallel F_3 structures with wavelengths of approximately 1 m are preserved in layered mafic and felsic sequences (Plate 4-24). In these sequences the thickness of the felsic (relatively competent) layer is approximately 1 m, and is less than the thickness of the mafic (relatively incompetent) layers.

Well-developed examples of S_3 tend commonly occur in amphibolite that have a strong S_1 and/or S_2 foliation. In such cases S_3 is preserved as a near vertical crenulation cleavage that overprints the S_1/S_2 foliation. In such amphibolites F_3 is preserved as crenulate folds approximately 1 cm in wavelength (Plate 4-25). In micaceous felsic rocks S_3 is locally preserved as a weakly- to moderately-developed biotite schistosity (Plate 4-26).

Chevron folds (F_3) with an orientation similar to the crenulate folds have developed in micaceous quartzo-feldspathic rocks that are characterized by a well-developed earlier foliation (Plate 4-27). Locally F_3 chevron folds contain axial-planar quartz veins, pegmatitic or felsite dykes (Plate 4-28).

A further characteristic of the D_3 deformation is the development of cusped and lobate folds (F_3). These cusped and lobate folds have developed at the contacts between amphibolite dykes and the quartzo-feldspathic country rocks. This indicates a moderate competency difference between the quartzo-feldspathic country rock and the relatively

incompetent amphibolite dykes. These cusped and lobate folds have an orientation similar to the F_3 chevron folds and crenulate folds. The symmetry of the cusped and lobate fold is dependant upon the orientation of the amphibolite dyke and the F_3 axial plane (Plates 4-29 and 4-30).

Box folds (F_3) have overprinted the tectonic layering fabric of the banded intermediate to mafic rocks of the North--South zone (Plate 4-31). The various stages of development of these box folds are preserved. The Z-asymmetry conjugate folds are open to tight (Plates 4-32 and 4-33) while the S-asymmetry conjugate folds are commonly poorly developed (Plate 4-34).

The relative ages of the ductile deformational events are confirmed by fold interference patterns (Plate 4-35) and by the deformation of older fabrics (Plates 4-36 and 4-37).

Plates 4-23 through 4-37 (next eight pages)

Plate 4-23. F_3 open fold in foliated felsic rock, wavelength of several metres.

Plate 4-24. F_3 open to tight fold in layered felsic and mafic rocks. Note fold style in felsic layer varies from open (on convex side) to moderately tight (on concave side).

Plate 4-25. F_3 crenulate folds in amphibolite with well-developed S_1/S_2 foliation.

Plate 4-26. Moderately-developed biotite schistosity defines S_3 in micaceous felsic rock.

Plate 4-27. F_3 chevron to tight parallel folds in felsic rocks with well-developed S_1/S_2 foliation.

Plate 4-28. Quartz veins axial-planar to F_3 in foliated felsic intrusion.

Plate 4-29. Symmetric F_3 cusped and lobate folds at contact between felsic intrusion and amphibolite dyke.

Plate 4-30. Asymmetric F_3 cusped and lobate fold at contact between felsic intrusion and amphibolite dyke.

Plate 4-31. F_3 box fold in banded intermediate and mafic rocks.

Plate 4-32. Open Z-conjugate of F_3 box fold.

Plate 4-33. Tight Z-conjugate of F_3 box fold.

Plate 4-34. Poorly-developed S-conjugate of F_3 box fold.

Plate 4-35. F_{2a} folded by F_3 in banded iron formation. Note F_1 folded by F_{2a} in hinge zone of F_{2a} .

Plate 4-36. D_1/D_2 fabric in North--South zone folded by D_3 .

Plate 4-37. D_1/D_2 boudin folded by F_3 .

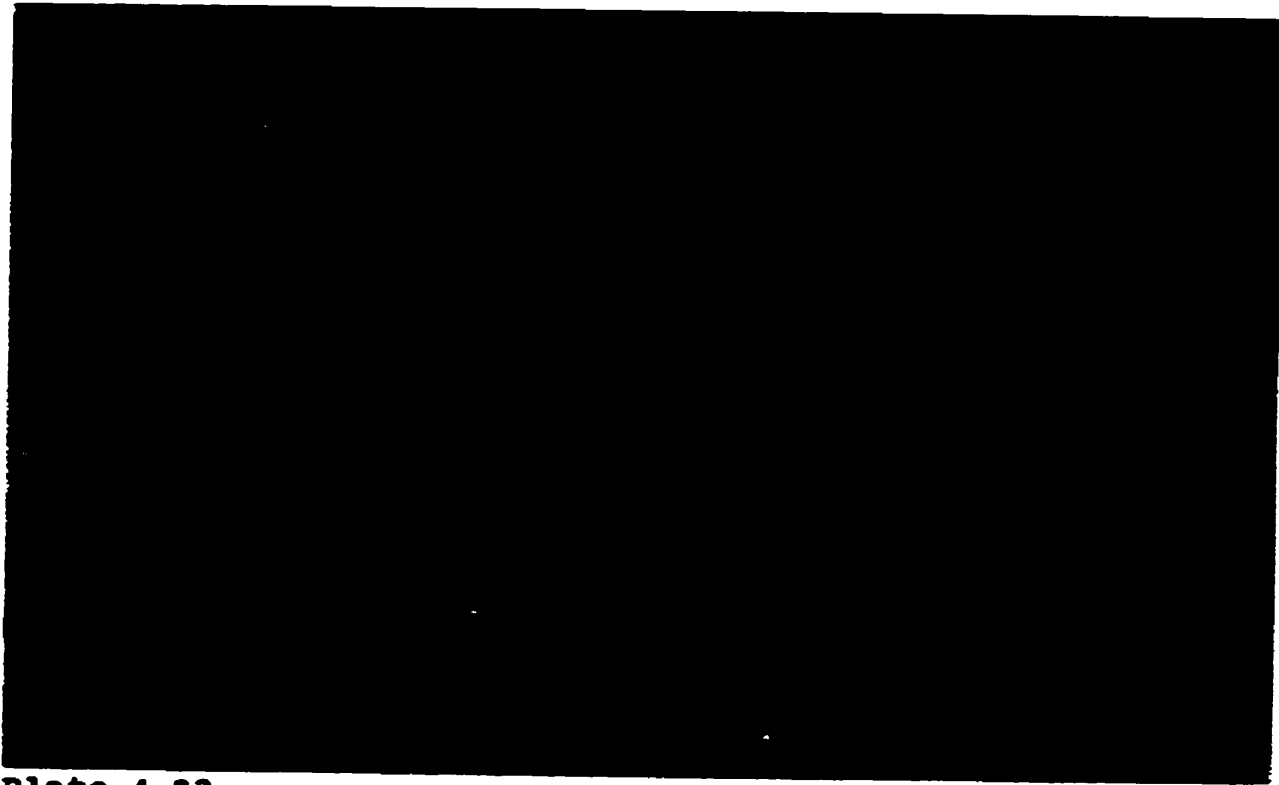


Plate 4-23

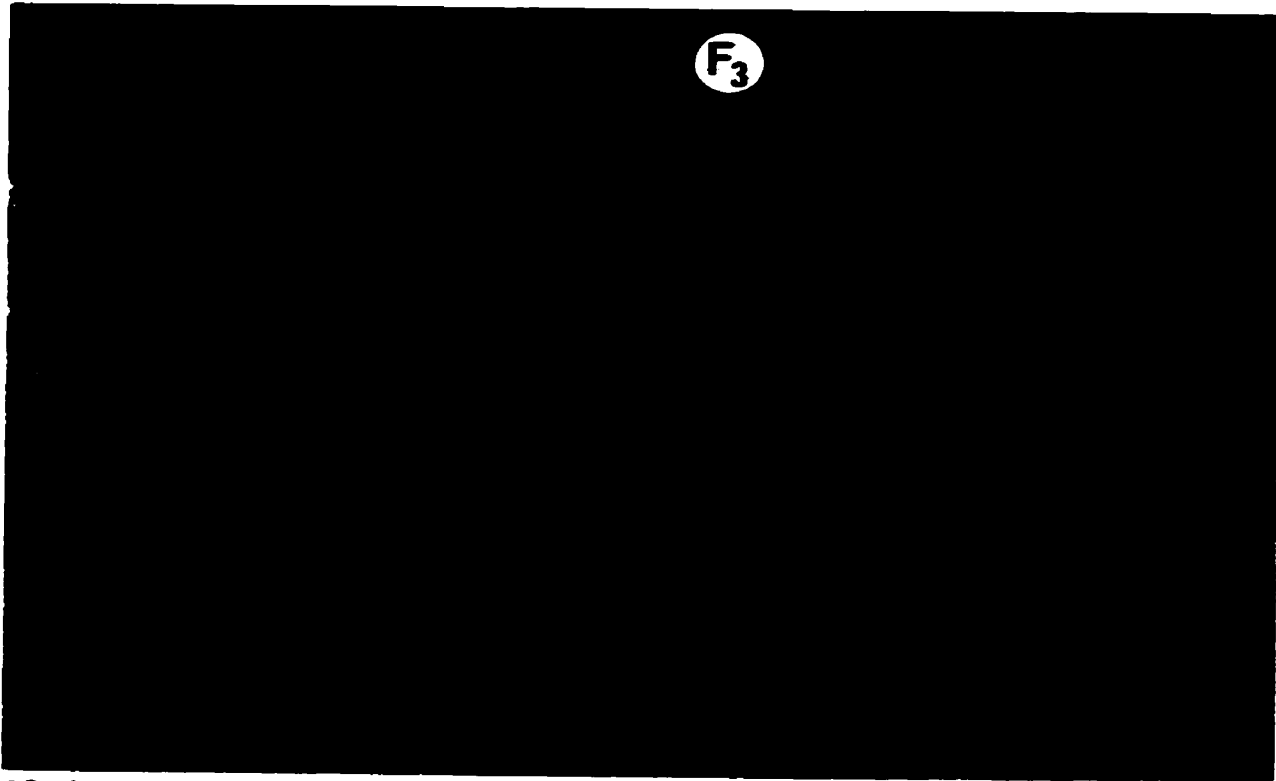


Plate 4-24

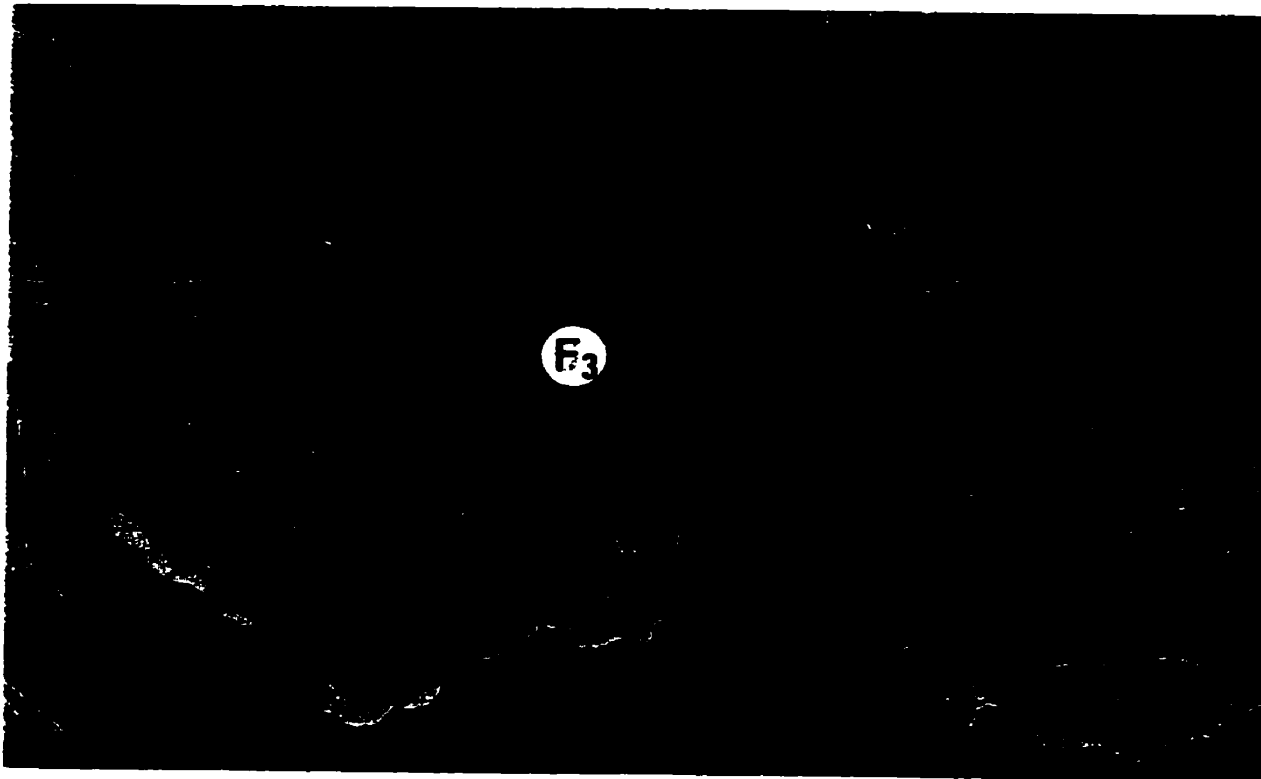


Plate 4-25

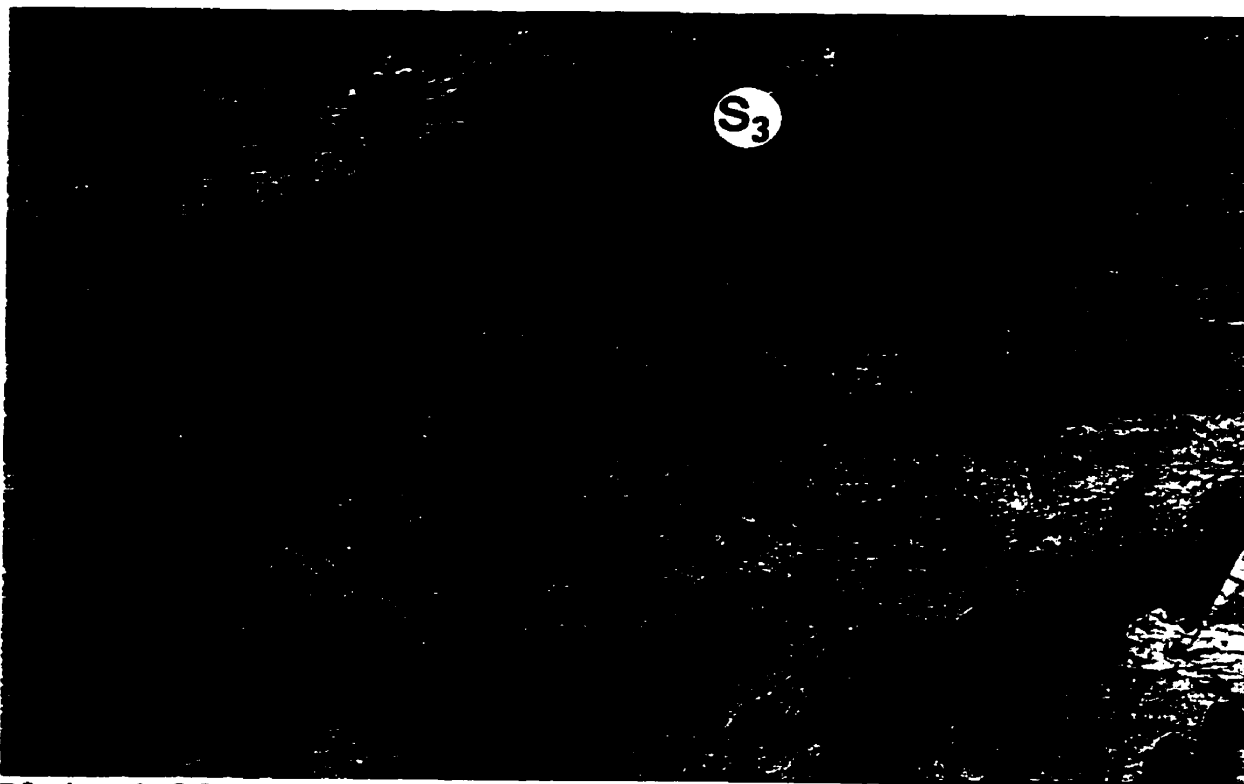


Plate 4-26

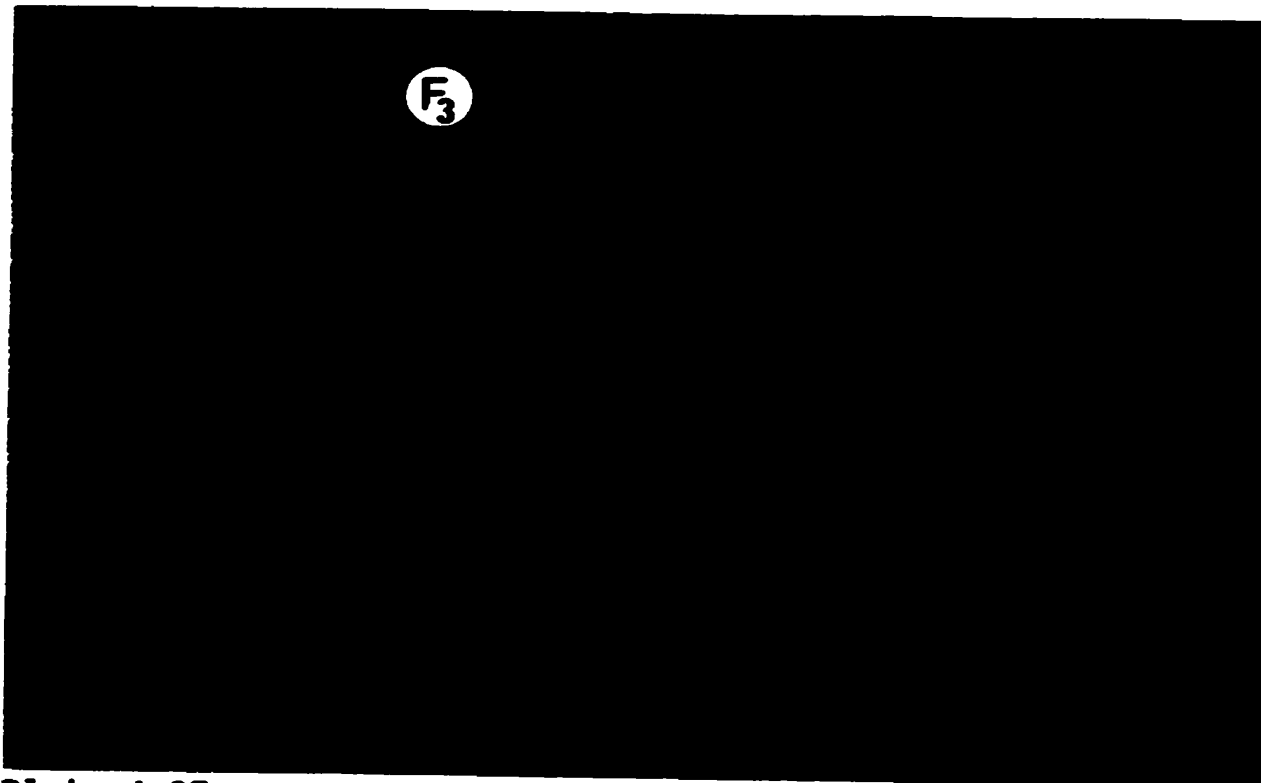


Plate 4-27

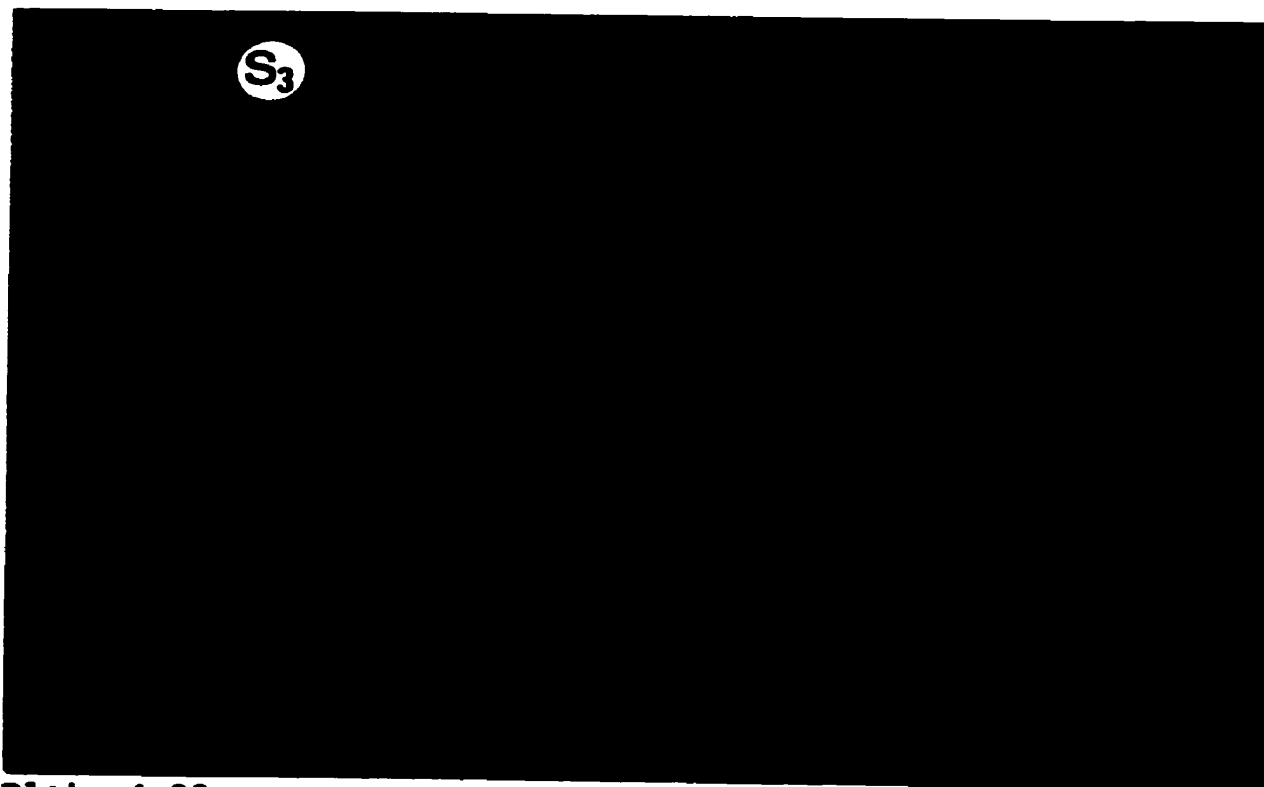


Plate 4-28

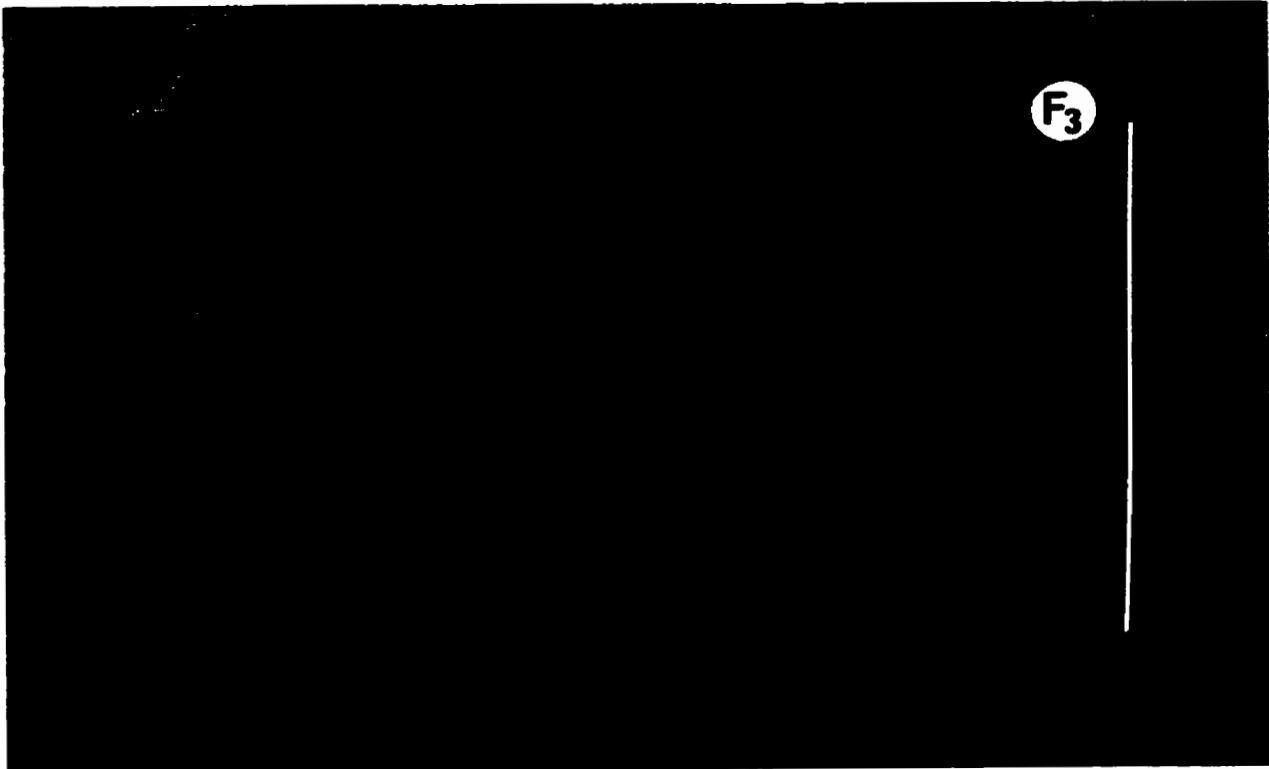


Plate 4-29

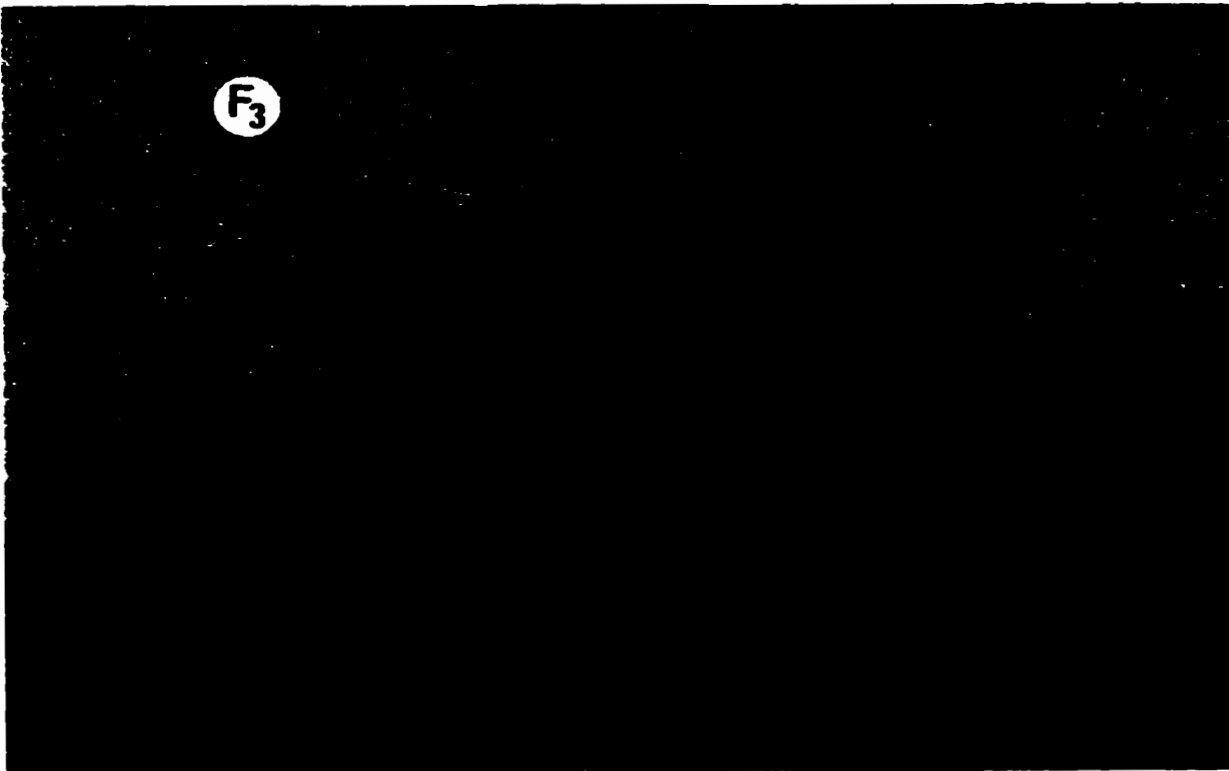


Plate 4-30

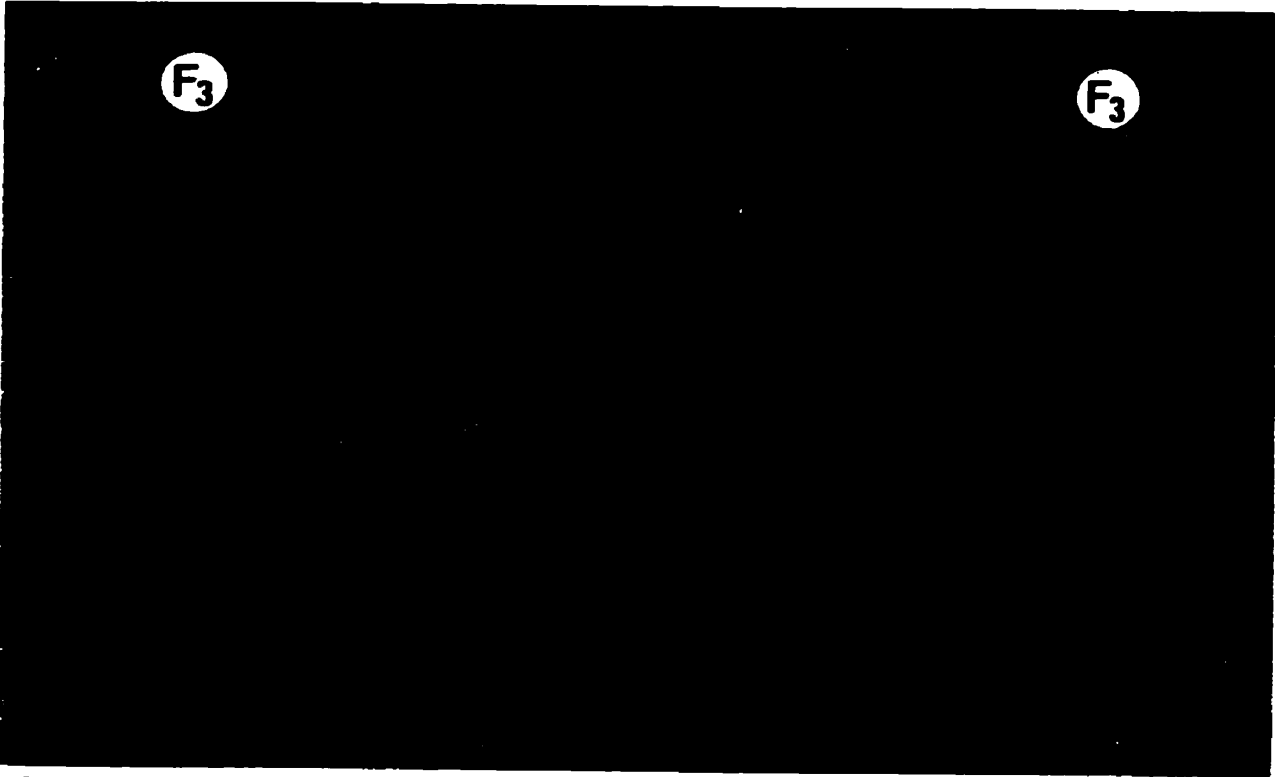


Plate 4-31

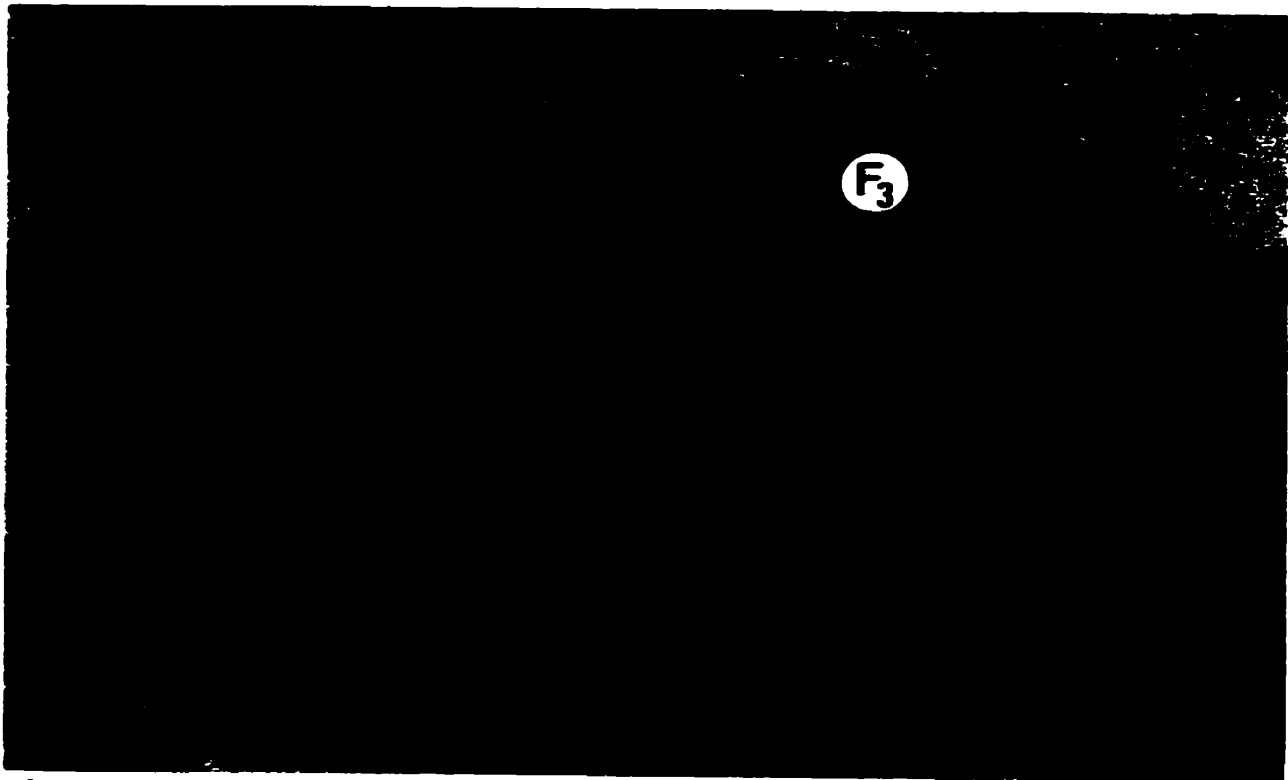


Plate 4-32

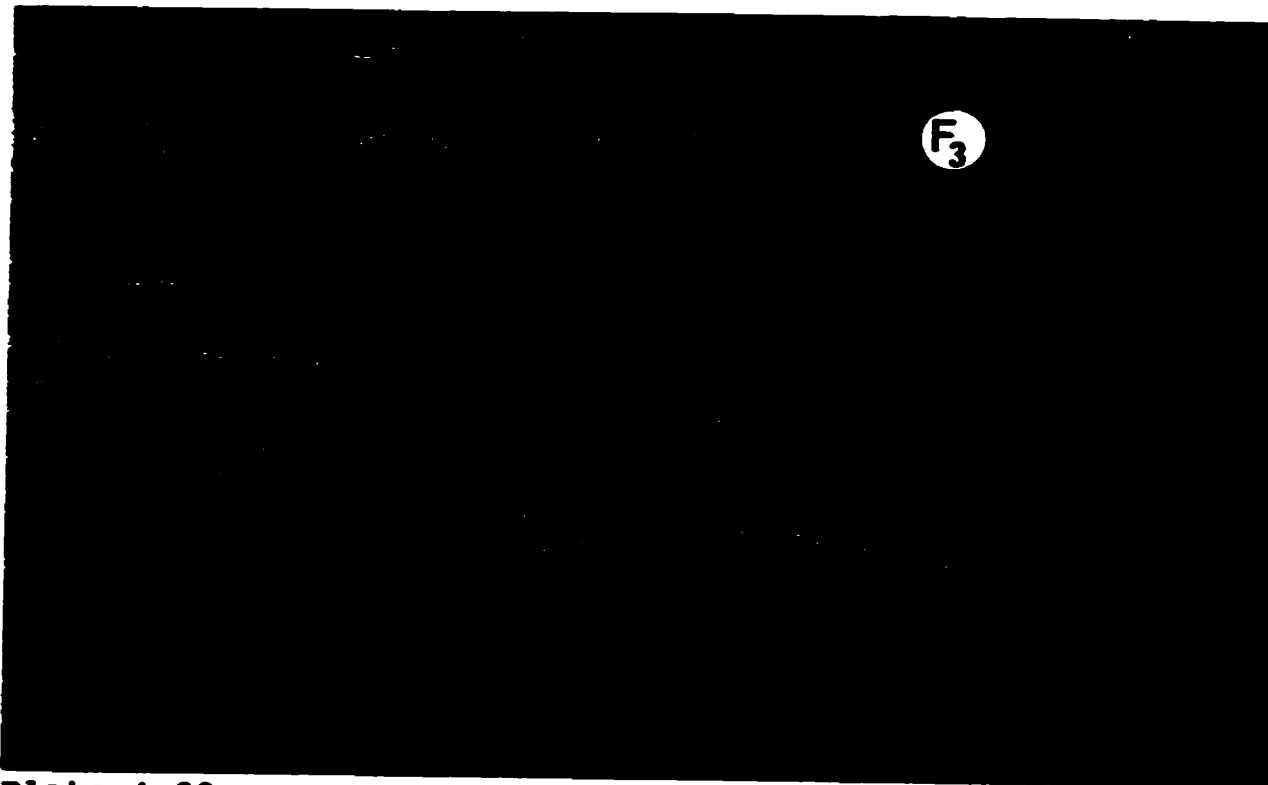


Plate 4-33

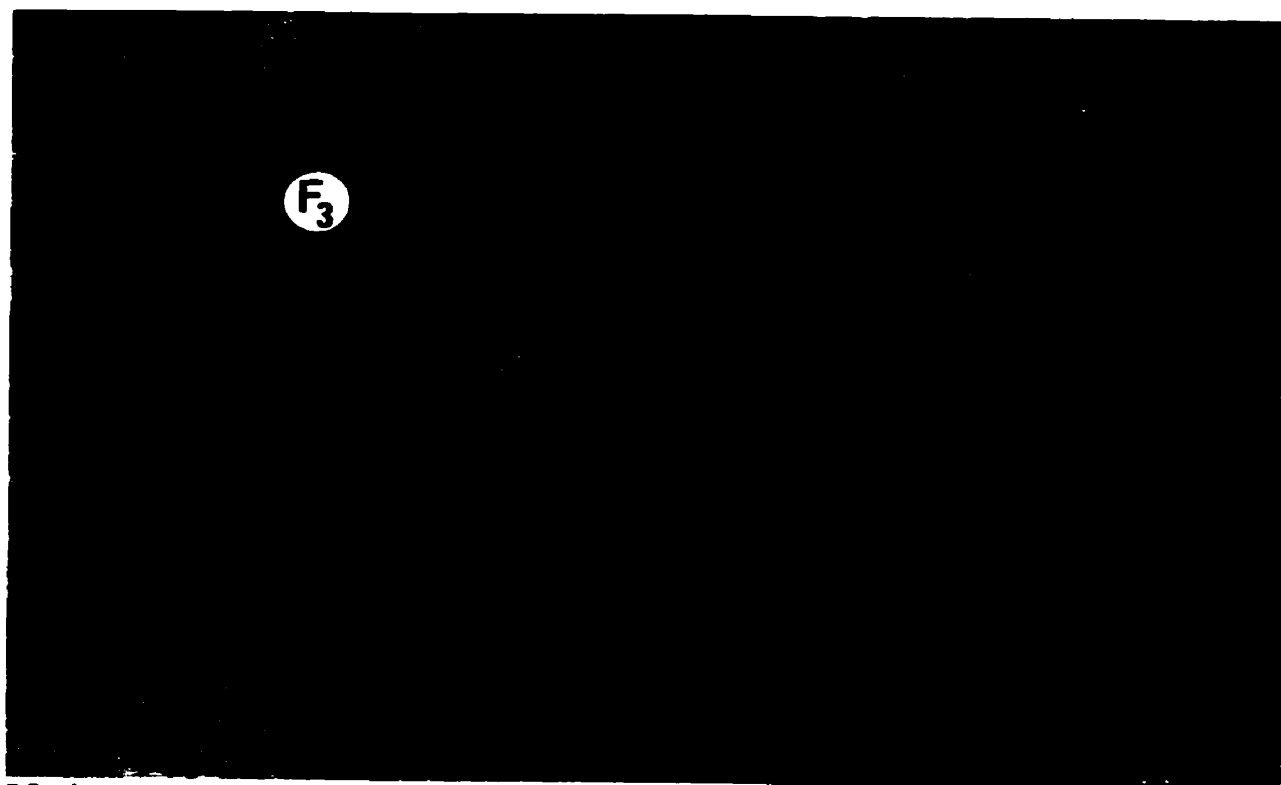


Plate 4-34

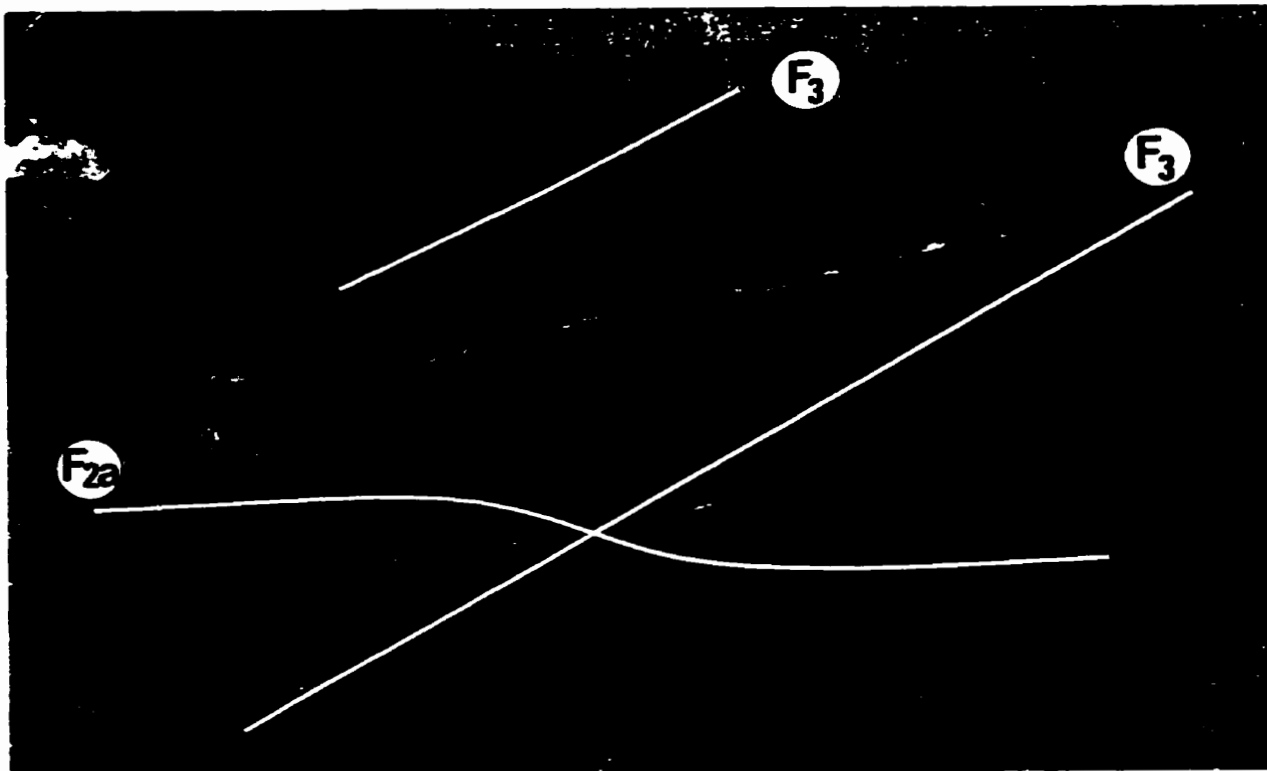


Plate 4-35

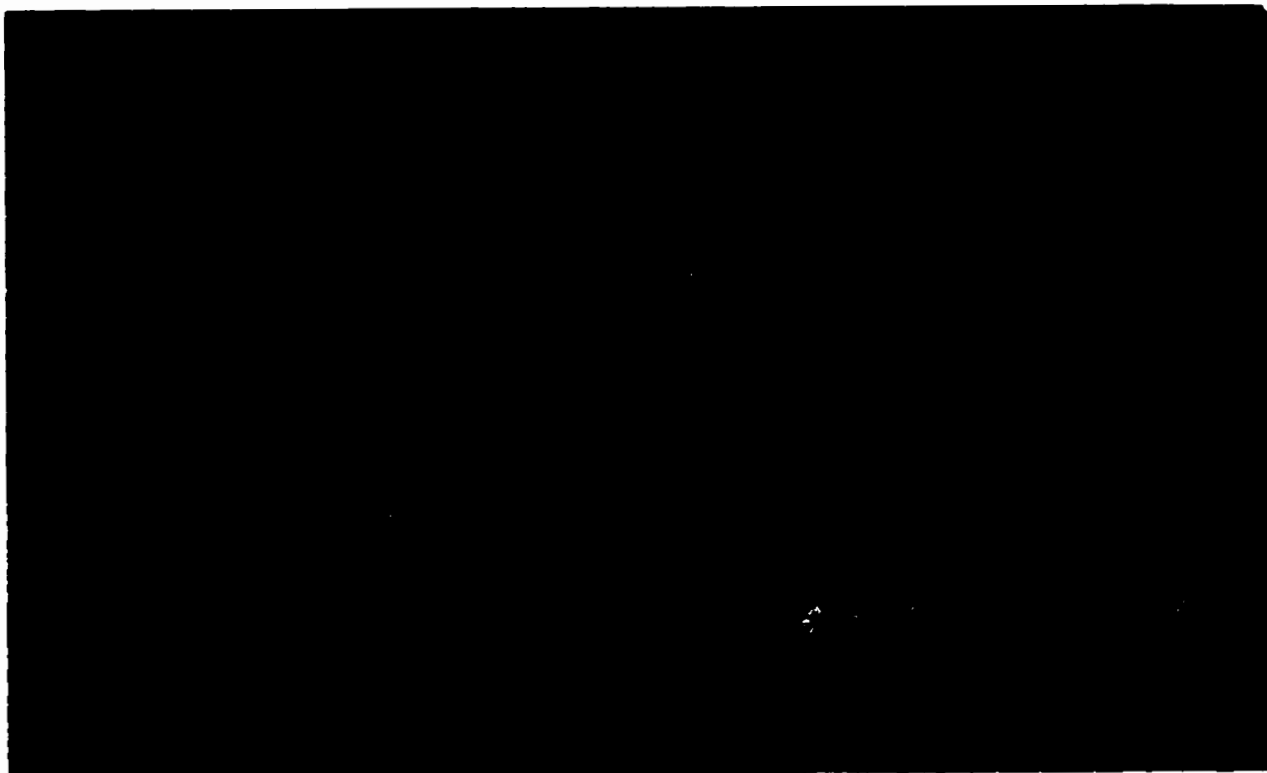


Plate 4-36



Plate 4-37

4.5.4 Late Brittle and Brittle--Ductile Deformation (D₄)

The fourth phase of deformation (D₄) produced ductile to brittle--ductile folds (F₄) and brittle--ductile to brittle faults. The F₄ structures are open folds with S-asymmetry and steeply-dipping axial planes oriented at 035° to 055° (Plate 4-38). Brittle--ductile to brittle failure has commonly occurred in the F₄ structures along planes parallel to the F₄ short limbs (Plates 4-39 and 4-40).

Brittle--ductile to brittle faults associated with D₄ become common in the eastern portion of the Central Zone. A major northerly-trending fault zone transects the entire map area (Figure 4-1). This zone of faults is up to 50 m wide, and consists of faults that are steeply-dipping, predominantly sinistral, have a predominantly north--south orientation (range of 340° to 035°) and commonly contain cataclasite, crush breccia and rare pseudotachylite (Plates 4-40 and 4-41). Sinistral movement is indicated by the S-asymmetry of the F₄ structures (Plates 4-38, 4-39 and 4-40) and by the orientation of tension gashes located proximal to the fault zones (Plate 4-42).

Plates 4-38 through 4-42 (next three pages).

Plate 4-38. Ductile F_4 structure in amphibolite.

Plate 4-39. Brittle-ductile F_4 structure in intermediate rock. Semi-brittle failure along short limb of F_4 structure.

Plate 4-40. Brittle F_4 structure and sinistral brittle fault containing crush breccia and cataclasite in quartzofeldspathic rock.

Plate 4-41. Pseudotachylite in late brittle fault.

Plate 4-42. Tension gashes in epidosite lenses proximal to fault zone indicate sinistral movement.



Plate 4-38

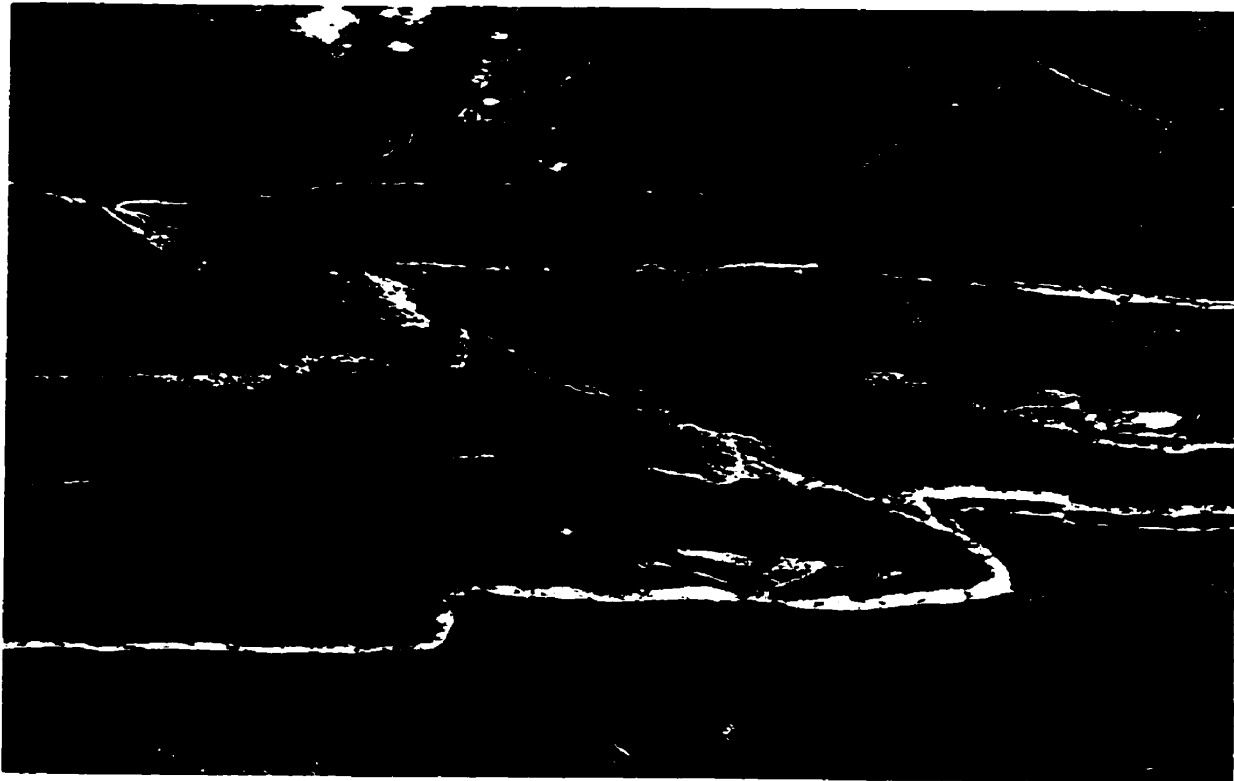


Plate 4-39



Plate 4-40

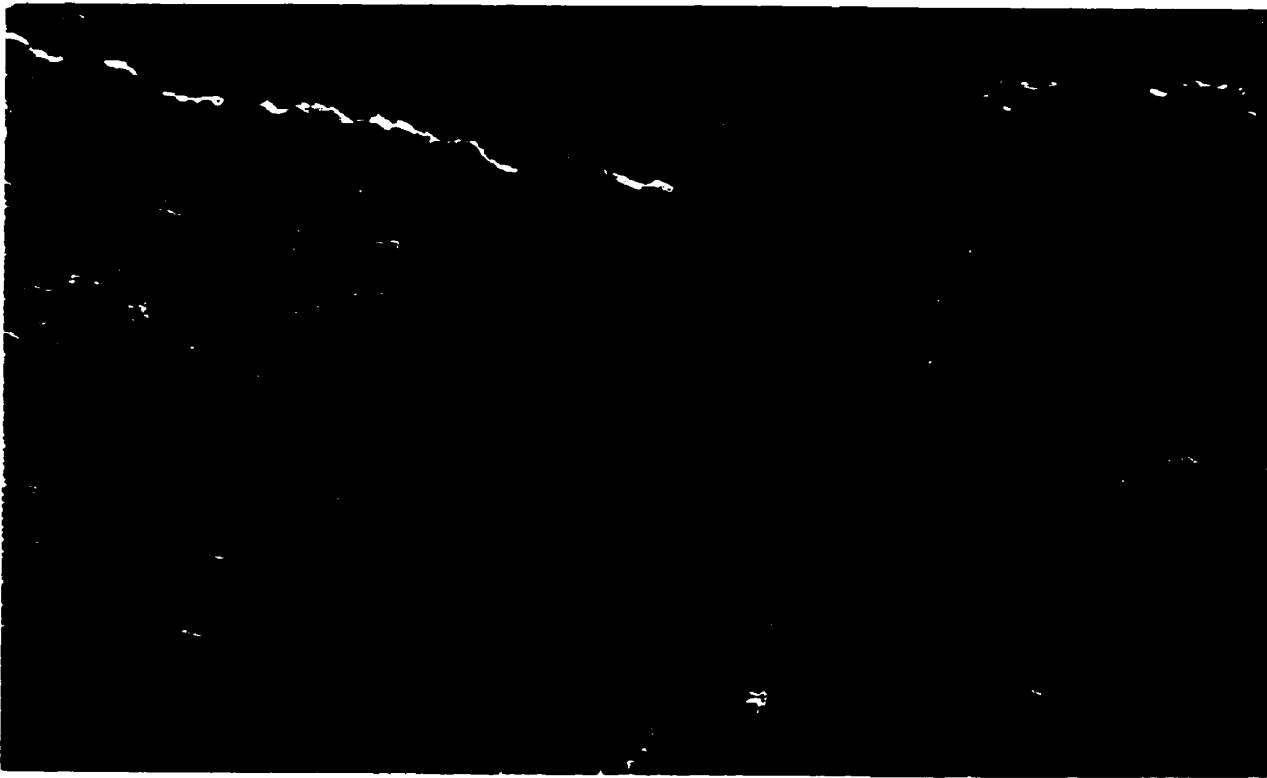


Plate 4-41



Plate 4-42

4.6 Equal Area Stereonet Analysis

4.6.1 First Phase of deformation (D_1)

The S_1 foliation is the dominant fabric in the North Star Lake area. In areas west of the North--South zone structural break that are relatively unaffected by D_2 (subareas 1, 2, 3 and 4) the S_1 foliation is predominantly upright and northerly-trending (Figure 4-1) however, there is an effect of the younger F_2 folds (Figure 4-7).

The S_1 foliation is axial-planar to the F_1 structures. This is diagrammatically shown in Figure 4-8 where the poles to the F_1 axial planes recorded in subareas 1 through 4 would be within the contoured area of the poles to S_1 plot (Figure 4-7).

The maximum concentration of S_1 in subareas 1 through 4 has an orientation of 008/77. The F_1 fold axes recorded in subareas 1 through 4 are gently-plunging and these F_1 fold axes plot proximal to the plane of the maximum concentration orientation of S_1 in these subareas (Figure 4-8). This indicates that the fold axes of these minor F_1 structures lie in the S_1 foliation plane.

The North--South zone (subarea 5) is a zone of concentrated deformation defined by thin north-trending lithological units with layer-parallel foliation (S_1) along and east of Loonhead Creek (Figure 4-2). The S_1 foliations in the subarea 5 (mylonitic fabric, compositional (tectonic) layering and schistosity) are northerly-trending and dip

steeply to the east. The average orientation of these foliations is 010/74 (Figure 4-9) and is near-coplanar to the maximum contour density of the S_1 foliations in subareas 1 through 4 (Figure 4-7).

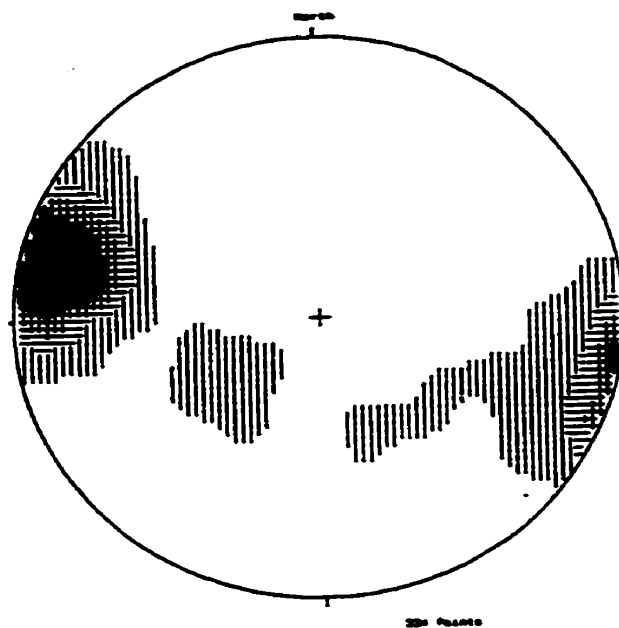


Figure 4-7. Contoured equal area projection of poles to S_1 foliation (subareas 1, 2, 3 and 4). Contour method: Schmidt (1925). Counting area: 0.010. Contour Interval: 2½ points per 1½ area. Maximum contour: 16.

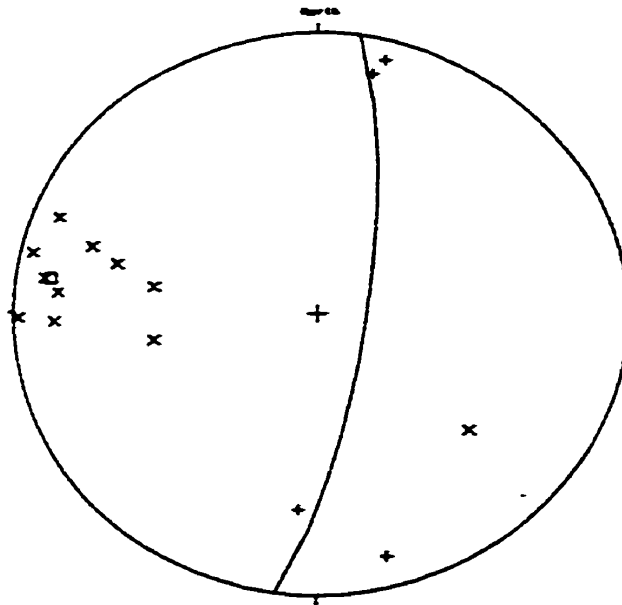


Figure 4-8. Equal area projection of F_1 orientation compared to S_1 maximum contour density (subareas 1, 2, 3 and 4). Pole to F_1 axial plane, x; F_1 fold axis, +; pole to S_1 maximum contour density, box.

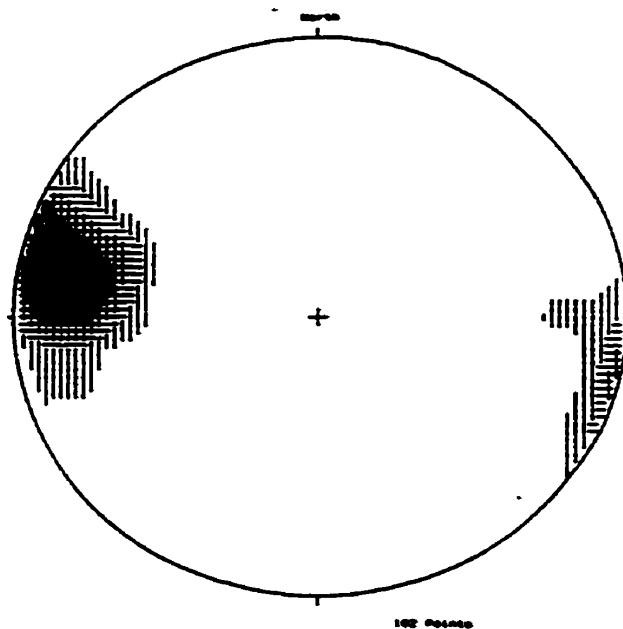


Figure 4-9. Contoured equal area projection of poles to S_1 (subarea 5). Contour method: Schmidt (1925). Counting area: 0.010. Contour interval: 3% points per 1% area. Maximum contour: 27.

4.6.2 Second Phase of Deformation (D_2)

The structures produced during D_2 deformed the D_1 fabrics and structures. This is evident in the hinge areas of the F_{2a} structures where S_1 has gentle to moderate dips in contrast to the steep dips of S_1 on the limbs of the F_{2a} structures. The areas west of the structural break (Figure 4-1) where D_2 structures are best preserved, with minimal overprinting by later deformational events, are subareas 1 through 4 (Figure 4-2). In this area the F_{2a} structures are northerly-trending and upright to steeply-inclined (Figure 4-10).

In vicinity of Face Lake, measurements of S_1 recorded in the southern portion of subarea 1 (Face Lake area) and the northern portion of subarea 4 (Creek Junction area) define gently-plunging, megascopic F_{2a} structures. Geological mapping in this area has defined these F_{2a} structures as a series synform and antiform pairs (Figure 4-1). The average plunge and trend of these F_{2a} structures, as indicated by the pole to the girdle of the S_1 poles, is 26/015 (Figure 4-11).

The megascopic F_{2a} structures in the vicinity of Face Lake can be compared to megascopic F_{2a} structures in the vicinity of Round Lake (Figure 4-1) where geological mapping has also defined a series of synform and antiform pairs (Figure 4-1). In the Round Lake area the average plunge and trend of the megascopic F_{2a} structure, as indicated by the pole to the girdle of the S_1 poles, is 36/015 (Figure 4-12).

The fold axes of the minor D_2 folds in subarea 1 (Face

Lake area) are gently-plunging and northerly-trending. The plunge and trend of these F_{2a} fold axes can be compared to the average plunge and trend of the megascopic F_{2a} in the vicinity of Face Lake (Figure 4-13). The fold axes of the minor D_2 folds in the subarea 2 (Round Lake area) are gently- to moderately-plunging and northerly-trending. The plunge and trend of these F_{2a} fold axes can be compared to the average plunge and trend of the megascopic F_{2a} structures in the vicinity of Round Lake (Figure 4-14).

The minor folds (F_{2b}) in the North--South zone (subarea 5) have upright to steeply-inclined axial planes (Figure 4-15). Comparison of Figure 4-15 with Figure 4-10 diagrammatically shows that the axial planes of the F_{2a} structures in subareas 1 through 4 and the F_{2b} structures in subarea 5 area near-coplanar.

The minor F_{2b} structures have steeply-plunging, southerly-trending fold axes. The average orientation of the plunge and trend of minor F_{2b} structures measured in subarea 5 is 65/170. These measurements were taken on F_{2b} structures located in the portion of subarea 5 located immediately north and south of North Star Lake, proximal to subareas 1 and 4 (Figure 4-2). The comparison of Figure 4-16 with Figure 4-10 diagrammatically indicates that the plunge and trend of the F_{2b} structures are approximately at a 90° angle -- rotated in D_2 axial plane -- to the plunge and trend of the F_{2a} structures in subareas 1 and 4.

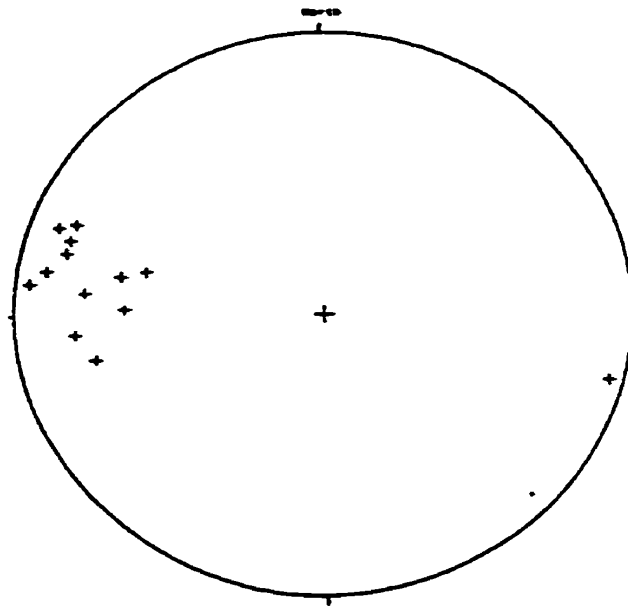


Figure 4-10. Equal area projection of orientation of F_2 axial planes (subareas 1, 2, 3 and 4). F_2 pole to axial plane, +.

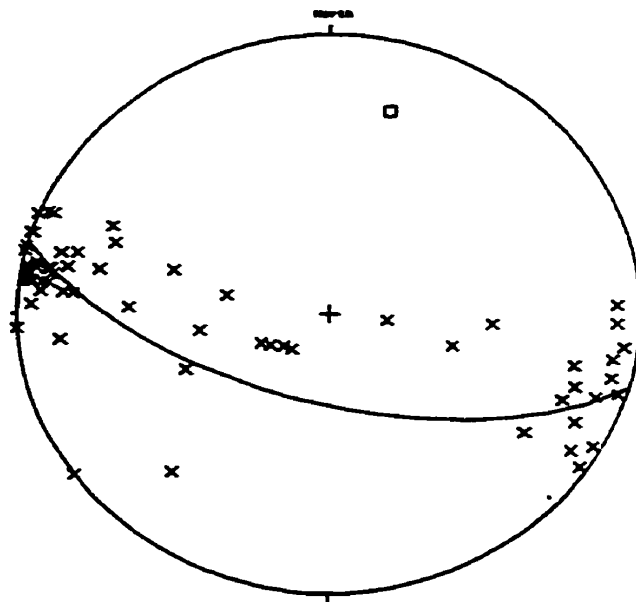


Figure 4-11. Equal area projection of poles to S_1 and girdle of poles to S_1 in the vicinity of Face Lake. Pole to S_1 , x; pole to S_1 girdle, box.

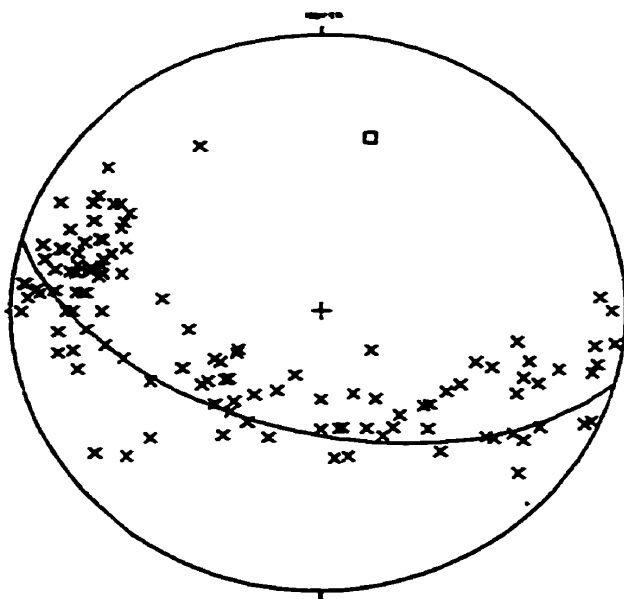


Figure 4-12. Equal area projection of poles to S_1 and girdle of poles to S_1 in the vicinity of Round Lake. Pole to S_1 , x; Pole to S_1 girdle, box.

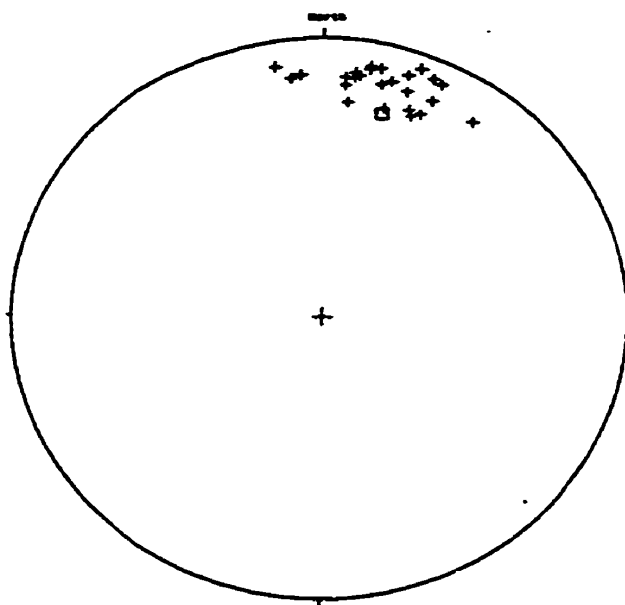


Figure 4-13. Equal area projection of F_{2n} fold axes (subarea 1) compared to girdle of poles to S_1 in vicinity of Face Lake. F_{2n} fold axis, +; pole to S_1 girdle, box.

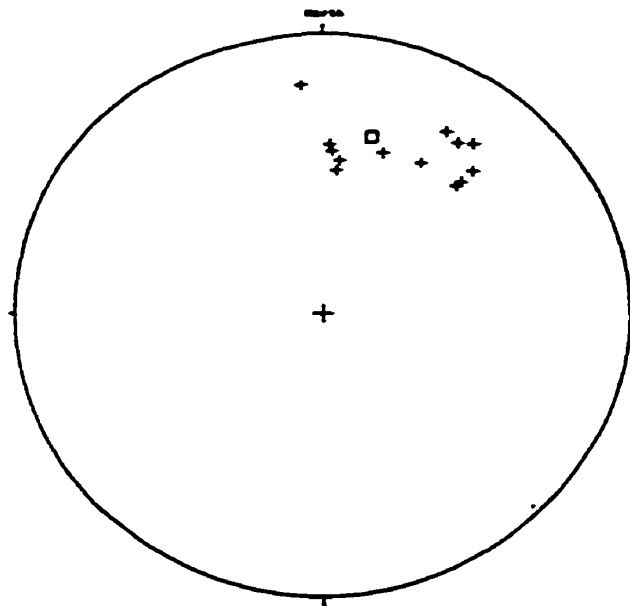


Figure 4-14. Equal area projection of F_2 fold axes (subarea 2) compared to girdle of poles to S_1 in vicinity of Round Lake. F_2 fold axis, +; Pole to S_1 girdle, box.

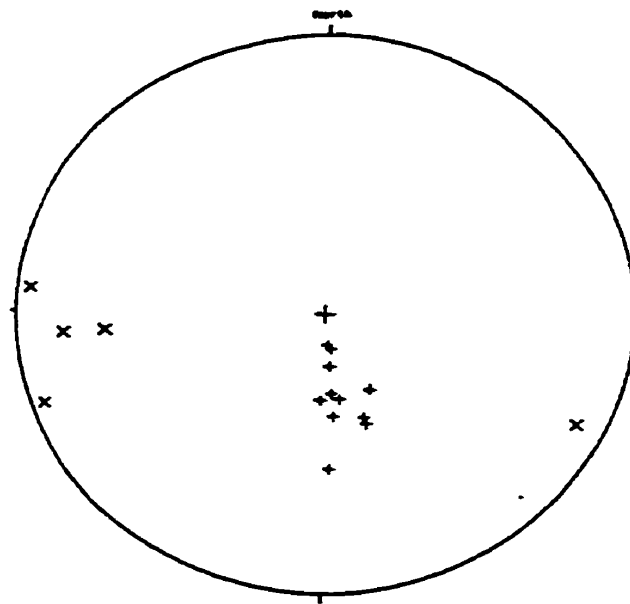


Figure 4-15. Equal area projection of F_2 orientation (subarea 5). F_2 pole to axial plane, x; F_2 fold axis, +.

4.6.3 Third Phase of Deformation (D₃)

The S₃ foliation and the axial planes of F₃ structures trend at approximately 300° to 345° in the southern portion of the map area and approximately 270° to 330° in the northern portion (Figure 4-1). The S₃ foliation is axial-planar to the F₃ structures and these D₃ structures generally are upright to steeply-inclined in the southern portion of the map area and moderately- to steeply-inclined in the northern portion. The F₃ structures have moderately- to steeply-plunging fold axes.

D₃ structures are best developed in subareas 6 and 7 (South North Star area) (Figure 4-2). In these subareas S₃ and F₃ axial planes are northwesterly-trending and upright to steeply-inclined (Figure 4-16). In the area west of North Star Lake (subareas 4, 6 and 7) the effect of D₃ on older (F_{2a}) structures is shown diagrammatically in Figure 4-17. The orientations of the fold axes of F_{2a} structures in subareas 4, 6 and 7 (Figure 4-17) can be compared to the orientations of the fold axes of F_{2a} structures in subareas less effected by D₃ (Figures 4-12 and 4-13).

There is substantial variation in the orientation of the fold axes of F₃ structures in subareas 6 and 7 (Figure 4-2). This area has been further subdivided into a northwest section (subarea 6, Figure 4-2) and a southeast section (subarea 7, Figure 4-2).

In subarea 6 the F₃ fold axes plunge moderately to steeply to the northwest (Figure 4-18) while in subarea 7

these structures plunge moderately to steeply to the southeast (Figure 4-19). This change in plunge may coincide with the axial plane of a large F_2 structure in this area.

The variation across the map area in the orientation of S_3 and the F_3 axial planes can be shown diagrammatically. In the northern portion of the map area (subarea 2, Figure 4-2) these D_3 structures are easterly-trending, generally moderately- to steeply-inclined, and moderately- to steeply-plunging (Figure 4-20). In the southern portion of the map area (subareas 6 and 7, Figure 4-2) the D_3 structures are northwesterly-trending, upright to steeply-inclined, and moderately- to steeply-plunging (Figures 4-16, 4-18 and 4-19).

In the North--South zone (subarea 5 Figure 4-2) intermediate to mafic rocks are compositionally layered. F_3 structures in these rocks are box folds, commonly with better development of the Z-conjugate. Open Z-conjugate folds plunge east--southeast while tight Z-conjugate folds plunge south--southeast. The S-conjugates of these F_3 box folds are predominantly open folds and plunge east--northeast.

The Symmetrical or M-fold F_3 structures in the compositionally layered rocks of the North--South zone are steeply-plunging to the east (Figure 4-20). The orientation of these folds is similar to the orientation of the F_3 structures in the Round Lake area (Figure 4-21).

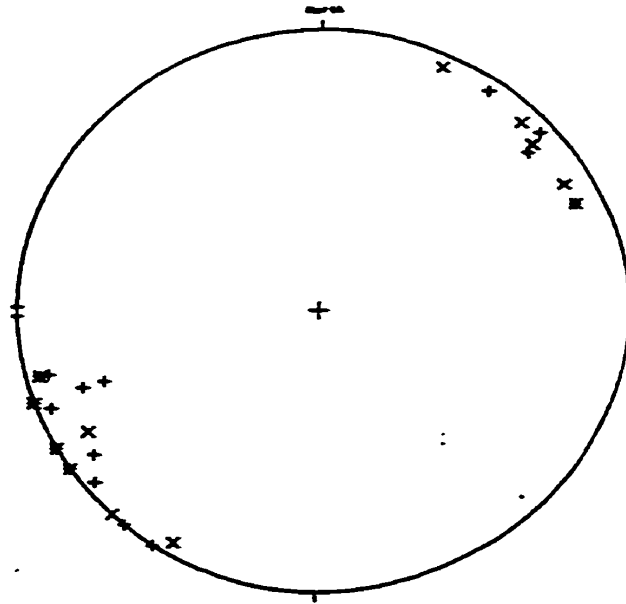


Figure 4-16. Equal area projection of orientation of S_3 foliation and F_3 axial planes, subareas 6 and 7. Pole to S_3 foliation, x; pole to F_3 axial plane, +.

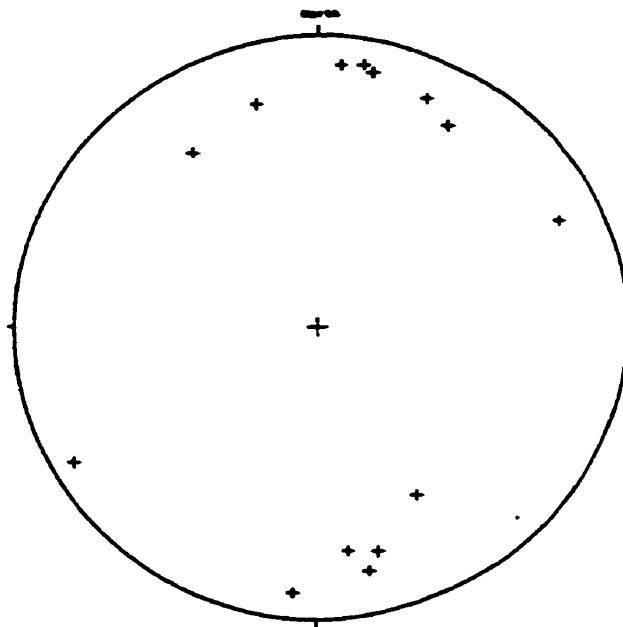


Figure 4-17. Equal area projection of orientation of F_{2a} fold axes, subareas 4, 6 and 7 F_{2a} fold axis, +.

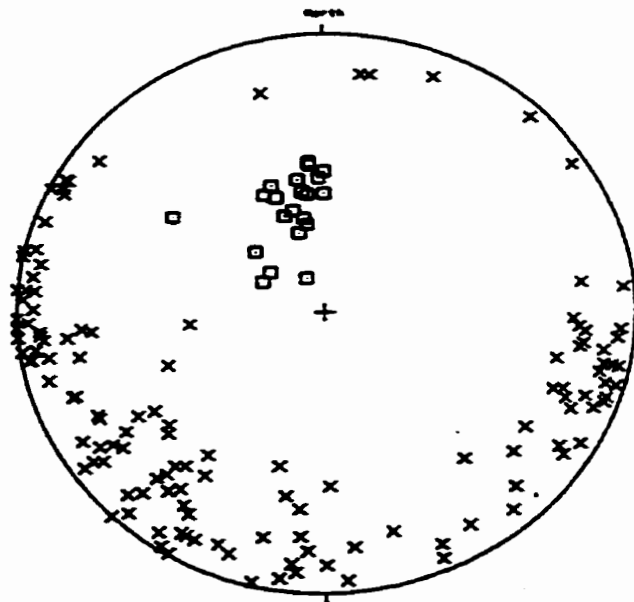


Figure 4-18. Equal area projection of S_1 foliation and F_3 fold axes (subarea 6). Pole to S_1 foliation, x; F_3 fold axis, box.

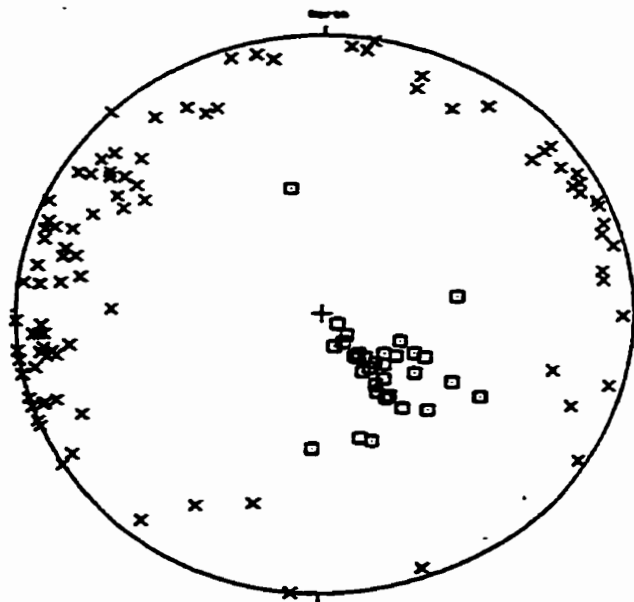


Figure 4-19. Equal area projection of S_1 foliation and F_3 fold axes (subarea 7). Pole to S_1 foliation, x; F_3 fold axis, box.

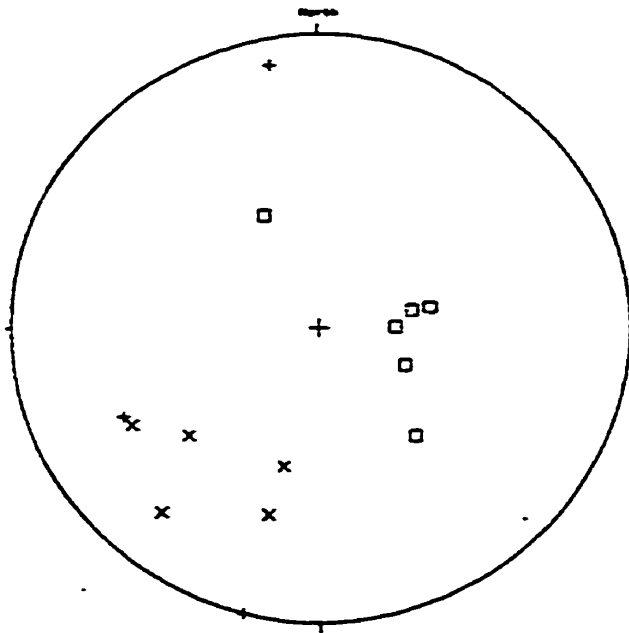


Figure 4-20. Equal area projection of S₃ foliation, F₃ fold axes and F₃ axial planes (subarea 2). Pole to S₃ foliation, x; Pole to F₃ axial plane, +; F₃ fold axis, box.

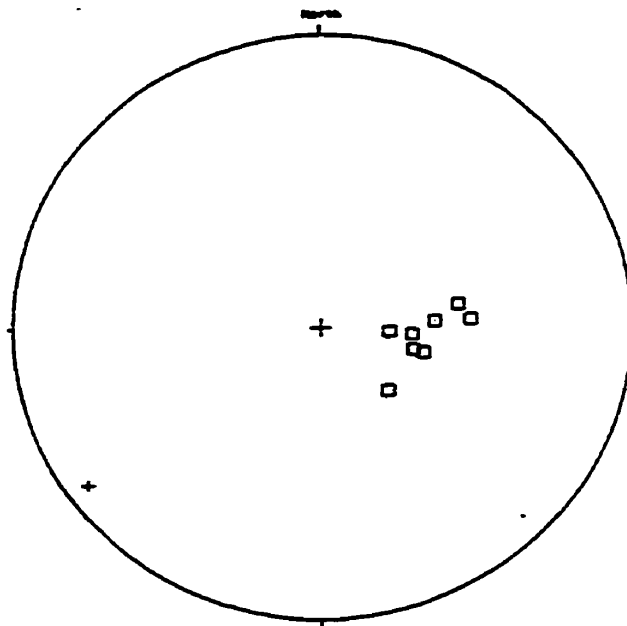


Figure 4-21. Equal area projection of F₃ axial plane and F₃ fold axes (subarea 5). Pole to F₃ axial plane, +; F₃ fold axes, box.

4.7 Microscopic Features

4.7.1 First phase of Deformation (D_1)

The first phase of deformation (D_1) folded the primary layering (S_0) and produced tight to isoclinal, similar folds (F_1) with a well-developed axial-planar foliation (S_1). S_1 is the dominant regional foliation.

The S_1 foliation is well-developed in micaceous felsic rocks and in biotitic amphibolites as a crystallographic preferred orientation of phyllosilicates (Plate 4-43). In the micaceous felsic rocks garnet overprints but is subsequently draped by the S_1 schistosity (Plate 4-44).

A spaced cleavage (S_1) is commonly occurs in quartzo-feldspathic rocks in the North Star Lake area. This spaced cleavage is expressed by biotite-rich domains separated by quartzo-feldspathic--disseminated biotite microlithons.

The North--South zone is a zone of concentrated deformation and fabrics in this zone indicate that at least a portion of the strain was the result of ductile simple shear early in the structural evolution of the North Star Lake area. Winged inclusion geometry suggests a dextral sense of shear.

Some of the quartzo-feldspathic rocks in the North--South zone have an annealed mylonitic fabric. This mylonitic fabric is characterized by thin domains of very fine grained (≤ 0.1 mm) quartz and feldspar separated by flattened lenses and ribbon like veins composed of fine grained quartz (Plate 4-45). The quartzo-feldspathic domains commonly contain

and feldspar porphyroclasts (Plate 4-46).

The mafic rocks in the North--South zone have a well-developed foliation. This foliation is defined by a preferred orientation very fine grained (≤ 0.1 mm) amphibole and flattened lenses of plagioclase and quartz.

Plates 4-43 through 4-46 (next two pages).

Plate 4-43 Fine-grained brown biotite defines S_1 schistosity in felsic rock. Plain light. Scale: 3.2 cm = 1.0 mm.

Plate 4-44 Garnet overprints but is subsequently draped by S_1 schistosity in felsic rock. Plain light. Scale: 3.2 cm = 1.0 mm.

Plate 4-45. Quartz lenses in annealed felsic mylonite (*sensu lato*). X-nicols. Scale: 3.2 cm = 1.0 mm.

Plate 4-46. Feldspar porphyroclast in felsic mylonite (*sensu lato*). X-nicols. Scale: 3.2 cm = 1.0 mm.

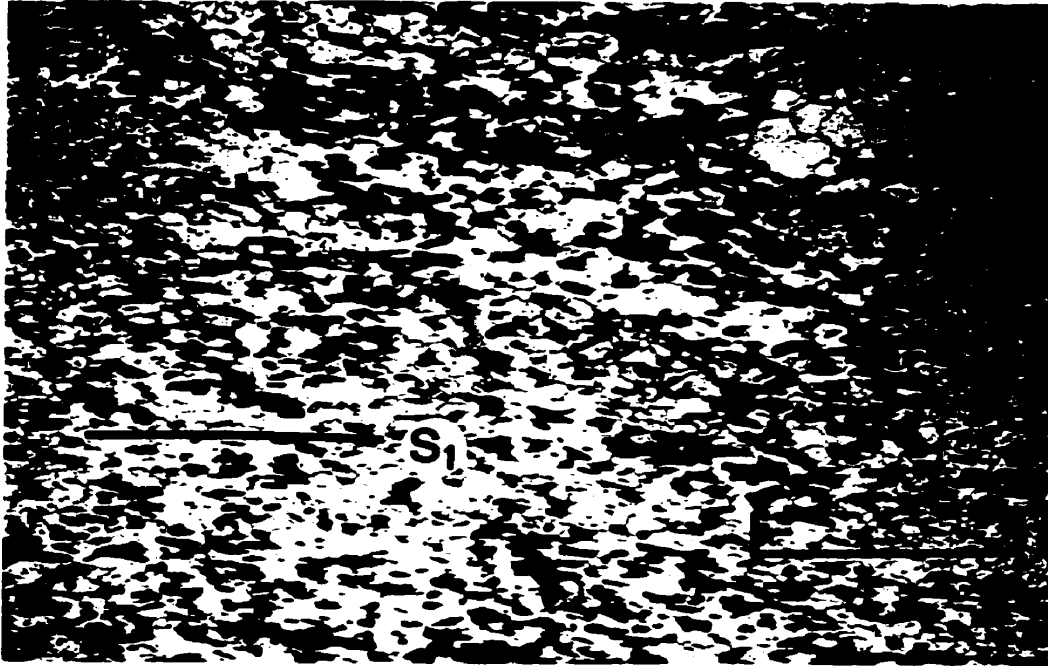


Plate 4-43

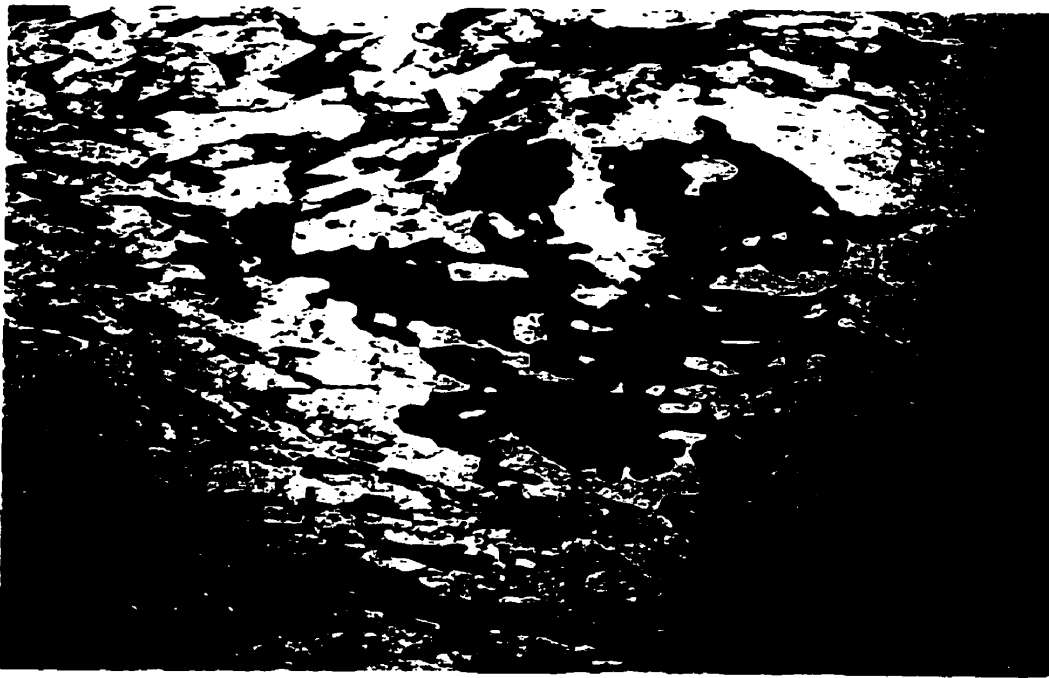


Plate 4-44

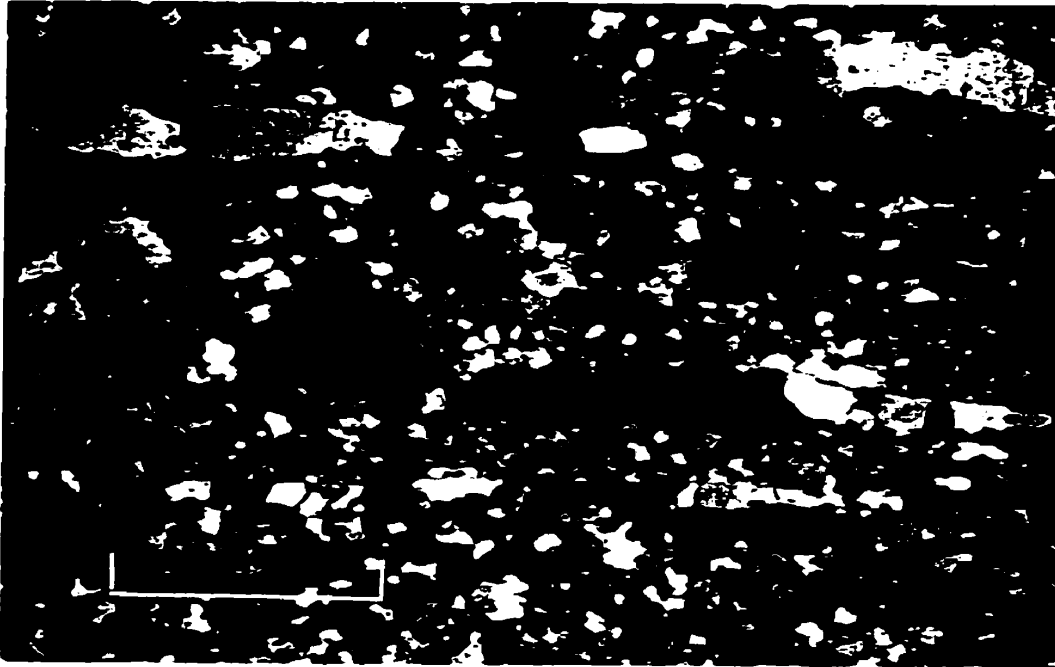


Plate 4-45

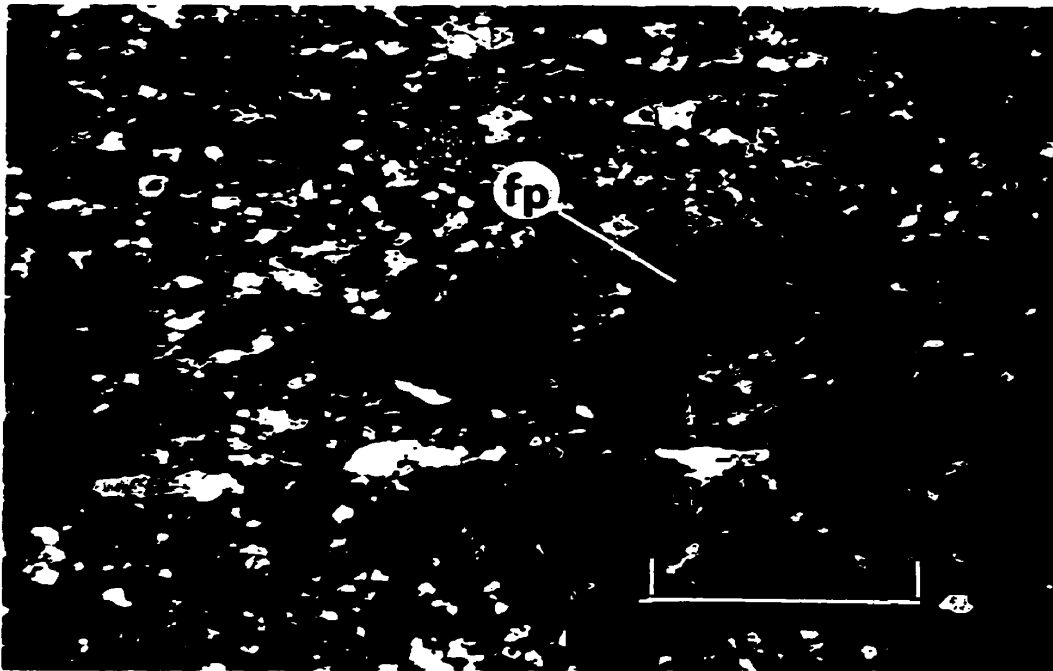


Plate 4-46

4.7.2 Second Phase of Deformation (D_2)

West of the North--South structural break the second phase of deformation produced parallel, open to tight folds (F_2). In the hinge areas of the F_2 structures, D_1 fabrics and structures are flat-lying and have been observed refolded by F_2 .

A distinctive characteristic of D_2 is the development of a prominent lineation (L_2) that has the same orientation of the plunge of the F_2 structures. In amphibolite, this lineation is expressed as a crystallographic preferred orientation of amphibole crystals (Plates 4-47 and 4-48). In quartzo-feldspathic rocks this lineation is expressed by the preferred orientation of quartz rods in L_2 (Plates 4-49 and 4-50).

Some semipelitic rocks have developed a gneissosity (S_2). The leucocratic component of this gneissosity is expressed as quartzo-feldspathic rods, composed of fine to medium grained quartz, K-feldspar and plagioclase, aligned in L_2 (Plates 4-51 and 4-52).

Plates 4-47 through 4-52 (next three pages).

Plate 4-47. Amphibole in hinge area of F_{2a} structure. View parallel to L_{2a} . Plain light. Scale: 1.3 cm = 0.1 mm.

Plate 4-48. Amphibole in hinge area of F_{2a} structure. View perpendicular to L_{2a} . Plain light. Scale: 1.3 cm = 0.1 mm.

Plate 4-49. Quartz rod in felsic rock. View parallel to L_{2a} . Plain light. Scale: 3.2 cm = 1.0 mm.

Plate 4-50. Quartz rod in felsic rock. View perpendicular to L_{2a} . Plain light. Scale: 3.2 cm = 1.0 mm.

Plate 4-51. Leucocratic component of gneissosity in felsic rock. View parallel to L_{2a} . Plain light. Scale: 3.2 cm = 1.0 mm.

Plate 4-52. Leucocratic component of gneissosity in felsic rock. View perpendicular to L_{2a} . Plain light. Scale: 3.2 cm = 1.0 mm.

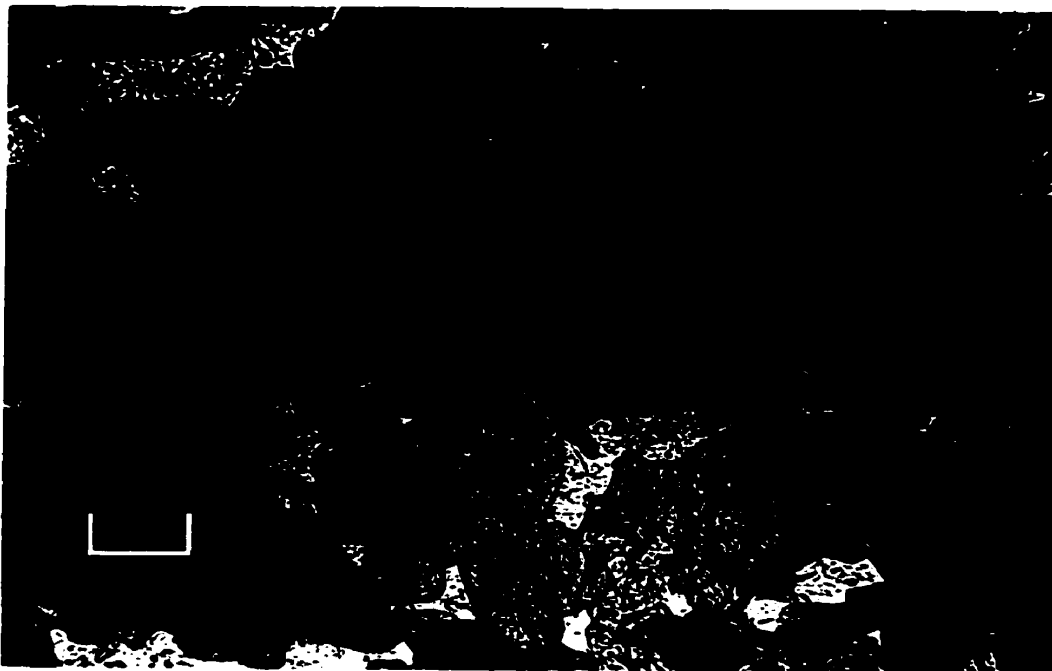


Plate 4-47

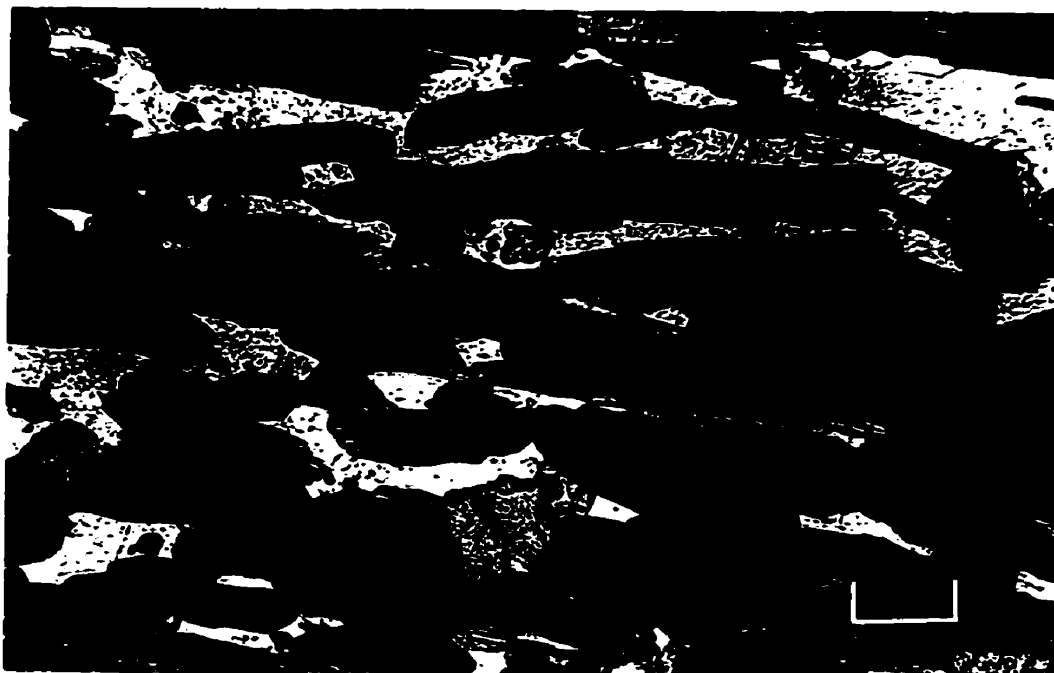


Plate 4-48

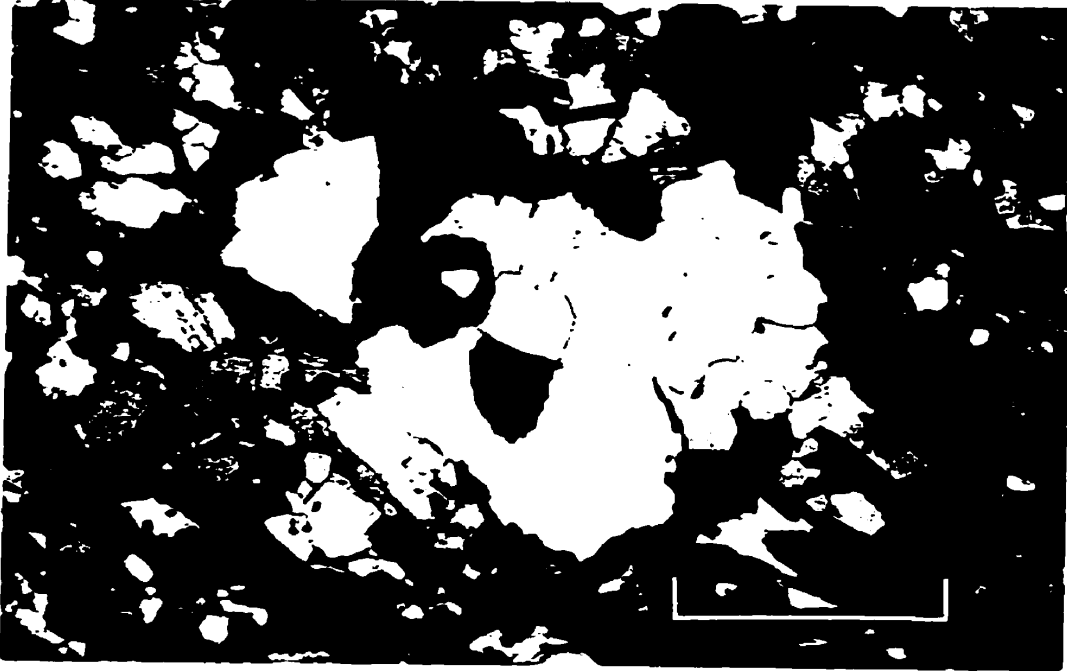


Plate 4-49

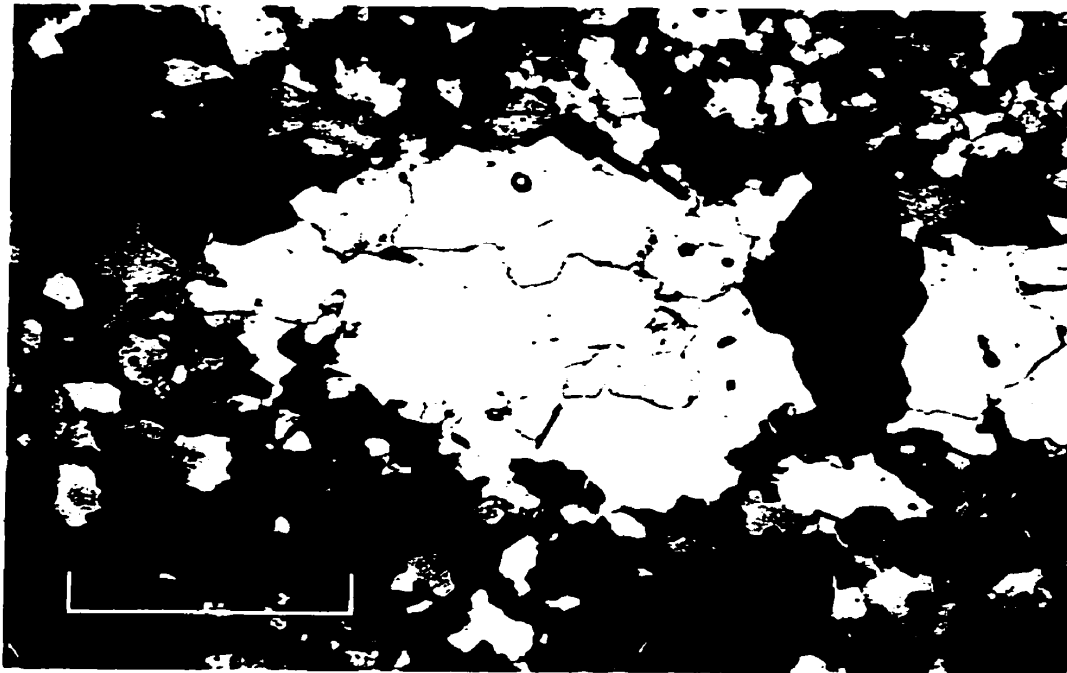


Plate 4-50

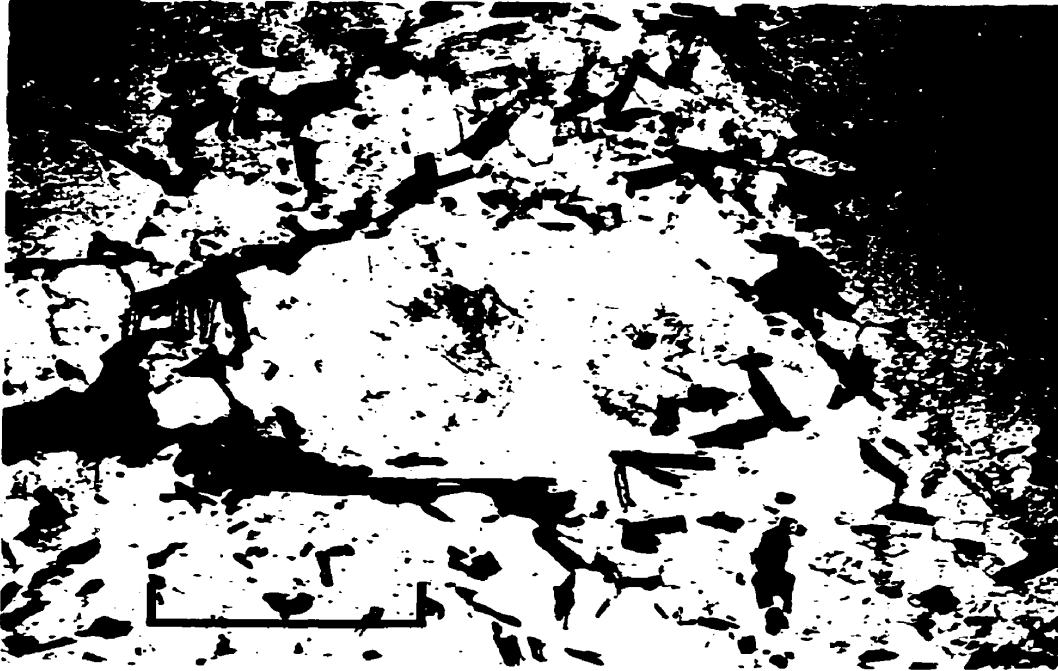


Plate 4-51

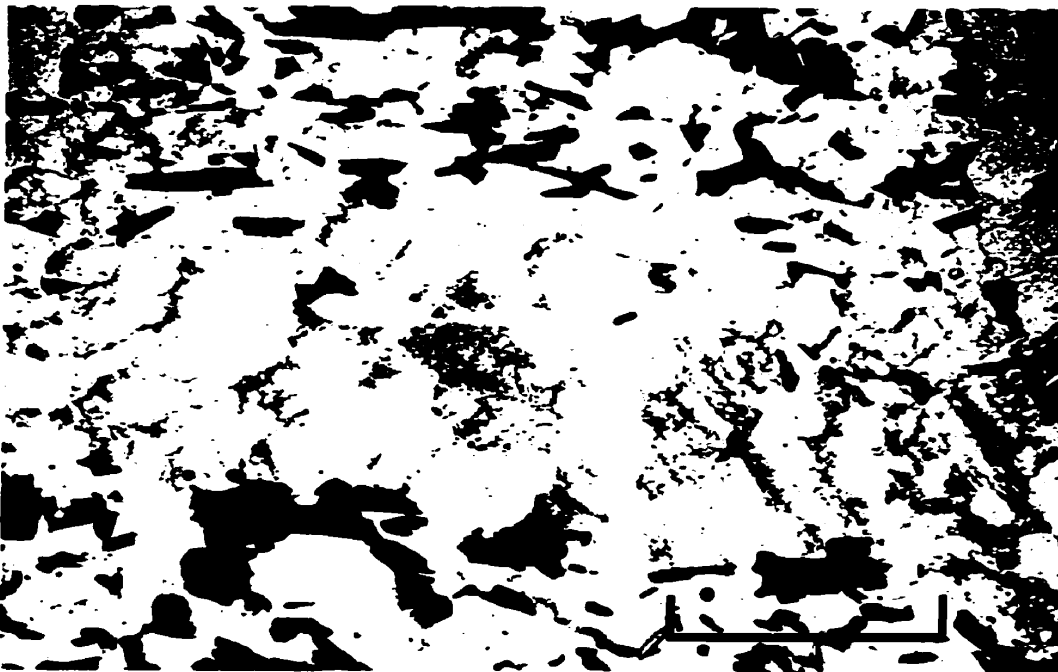


Plate 4-52

4.7.3 Third Phase of Deformation (D_3)

The third phase of deformation produced (D_3) folds (F_3) as well as an axial-planar fabric (S_3) that developed locally in rocks with a strong prior fabric. The F_3 structures exhibit a variety of styles; this variation being the result of differing response of different lithologies to deformation.

In amphibolite F_3 is preserved as crenulate folds approximately 1 cm in wavelength. The amphibole crystals that were aligned in L_1/L_2 have been rotated towards S_3 (Plate 4-53). In these amphibolites there was little, if any, new mineral growth during D_3 . The amphibole crystals were annealed after their rotation towards S_3 since they show only minor strain textures.

Fabrics of the North--South zone were folded during D_3 . In the schistose amphibolite in the North--South zone the strong fabric, defined by very fine grained (≤ 0.1 mm) amphibole and lenses of quartz and plagioclase, was folded to produce crenulate folds (F_3) (Plate 4-54). As with the amphibolite outside of the North--South zone, there was little to no new mineral growth in these amphibolites during D_3 .

Tight flexure to chevron folds (F_3) developed in micaceous quartzo-feldspathic rocks that are characterized by a well-developed fabric (S_1/S_2). These folds commonly have a weakly-developed axial-planar schistosity (S_3) (Plate 4-55).

Plates 4-53 through 4-55 (next two pages).

**Plate 4-53. F_3 crenulate fold in amphibolite. Plain light.
Scale: 3.2 cm = 1.0 mm.**

**Plate 4-54. F_3 crenulate to box fold in amphibolite of
North--South zone. Plain light. Scale: 3.2 cm = 1.0 mm.**

**Plate 4-55. Hinge area of tight flexural fold (F_3) in
micaceous felsic rock. Plain light. Scale: 3.2 cm = 1.0 mm.**

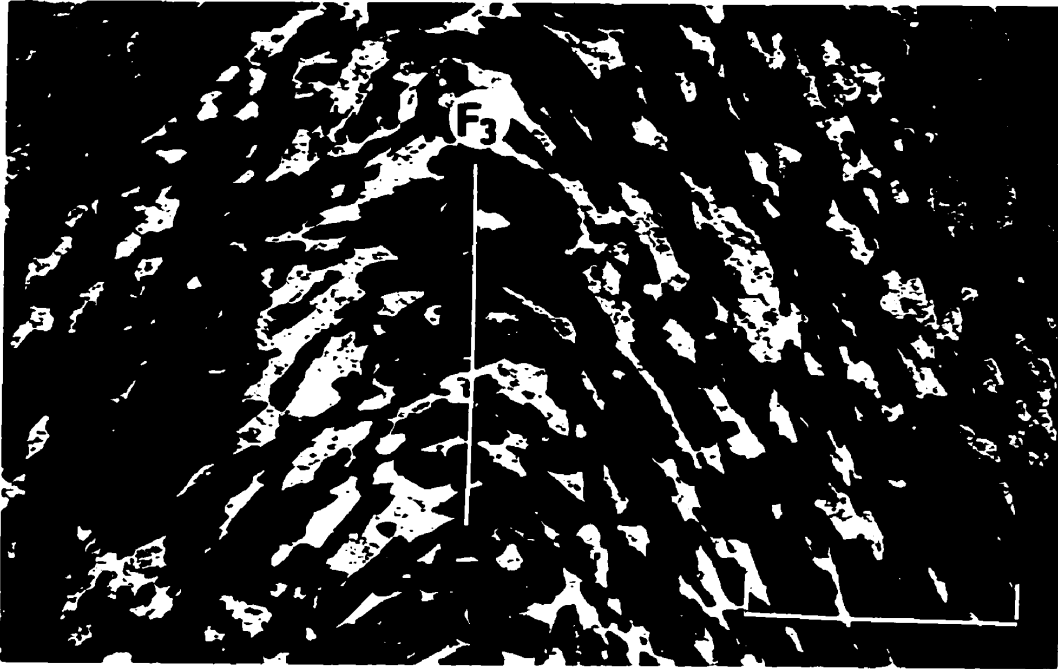


Plate 4-53



Plate 4-54



Plate 4-55

Chapter V

METAMORPHISM IN THE NORTH STAR LAKE AREA

5.1 Introduction

Two phases of prograde regional metamorphism have been identified in the North Star Lake area; these phases of region-wide metamorphism were followed by several minor phases of metamorphism, which show only local expression. Mineral assemblages associated with, and fabrics produced, by the various phases of metamorphism suggest that the rocks in the North Star Lake area followed a clockwise P--T--t evolution with maximum pressure conditions predating maximum temperature conditions. Mineral assemblages associated with the prograde phases of metamorphism indicate a medium-pressure (Barrovian type) regime during the time preceding thermal climax. Temperatures during thermal climax were high enough to cause anatexis in felsic rocks of suitable composition.

A regional metamorphic event (M_1) is associated with the first phase of deformation (D_1). This event produced abundant phyllosilicates (chlorite, muscovite and biotite) and garnet in felsic volcanic and semi-pelitic rocks, and hornblende in mafic volcanic and psammitic rocks. The phyllosilicates and hornblende define a well-developed foliation (S_1) that is axial-planar to isoclinal folds produced during the first phase of deformation.

Peak regional metamorphism is represented by the second metamorphic event (M_2); this event is of amphibolite facies-grade. This phase of metamorphism produced garnet, hornblende, staurolite, and sillimanite or kyanite; and is associated with the second phase of deformation (D_2).

A later phase of metamorphism (M_3) is associated with the third phase of deformation (D_3). This phase of metamorphism resulted in syn-deformational fabrics, such as the growth of biotite and muscovite, that define an axial-planar schistosity (S_3) that occurs locally in the hinge areas of minor F_3 structures. This phase of metamorphism also resulted in post-deformational fabrics, such as the annealing of mineral grains deformed during D_3 and the growth of garnet porphyroblasts that locally overprint D_3 fabrics.

The products of a retrograde metamorphic event (M_4) occur locally in brittle faults. Mineral assemblages associated with this phase of metamorphism are consistent with greenschist facies. Retrograde metamorphism is also suggested by the presence of random-oriented late-chlorite growth in some micaceous felsic rocks unaffected by brittle faults.

The samples for the study of the metamorphism in the North Star Lake area were collected in the vicinity of East--West Creek and in the vicinity of Round Lake (Figure 3-1). Felsic rocks with the mineral assemblage of quartz, muscovite, biotite, chlorite, +/- plagioclase, +/- K-feldspar, +/- garnet, +/- staurolite, +/- kyanite or sillimanite

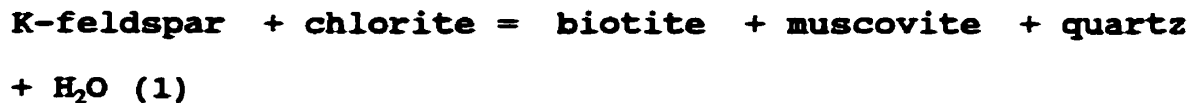
(micaceous felsic volcanic rocks, felsic semi-pelitic rocks, and altered felsic volcanic rocks) were collected. The mineral assemblages found in these muscovite-bearing felsic rock samples may be compared to the AFM diagrams of equilibrium assemblages for pelite, developed by Thompson (1957). Similarly, mafic rocks with mineral assemblage including hornblende, plagioclase, quartz, +/- biotite, +/- garnet were collected and their mineral assemblages were compared to the ACF diagrams of equilibrium assemblages for metabasites, developed by Eskola (1915).

5.2 Description of Metamorphic Events

5.2.1 First Phase of Metamorphism (M_1)

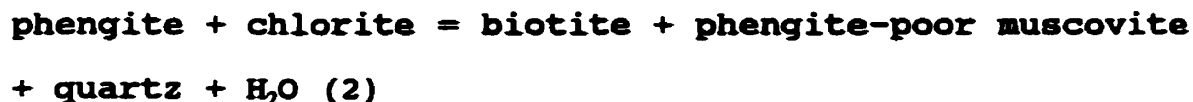
The first phase of metamorphism (M_1) occurred during the first phase of deformation (D_1) that folded the primary layering (S_0) and produced tight to isoclinal folds (F_1). In felsic volcanic and semi-pelitic rocks, chlorite, muscovite and biotite define a schistosity (S_1) that is axial-planar to the F_1 structures (Plate 5-1). This S_1 fabric is defined by hornblende in psammitic and amphibolitic rocks.

The minerals defining the M_1 mineral assemblage in the micaceous felsic rocks of the North Star lake area are biotite, muscovite and quartz; chlorite formed during prograde metamorphism is rare and feldspar is commonly incompletely altered to muscovite. This relict assemblage is possibly the result of the prograde reaction (Yardley, 1989):



The above biotite-in reaction occurs over a fairly narrow temperature range and is indicative of the biotite zone of the Barrovian Zonal Scheme in rocks containing detrital K-feldspar, such as semipelite and greywacke (Yardley, 1989).

In pelitic rocks that lack K-feldspar the biotite-in prograde reaction is the following (Yardley, 1989):



The result of these biotite-in prograde reactions in pelitic and semi-pelitic rocks is that biotite is produced at the expense of chlorite and a potassium-bearing silicate, and the composition of white mica proceeds from phengite towards pure muscovite. The AFM diagram for the biotite zone in pelitic rocks (Figure 5-1a) shows that the compositions of biotite and chlorite cannot vary independently.

The S_1 schistosity is the most prominent regional fabric observed in the North Star Lake area. The development of the S_1 schistosity was contemporaneous with deformation during D_1 . The S_1 schistosity, expressed by the preferred orientation of phyllosilicates, was subsequently folded or overprinted by all other deformational events observed in the area.

In the North Star Lake area, micaceous felsic rocks often contain M_1 garnet porphyroblasts. These garnet porphyroblasts overprint the S_1 fabric but developed while the D_1 stress regime was still active (Plate 5-2). In these micaceous felsic rocks relict chlorite inclusions are commonly observed in M_1 garnet porphyroblasts while the phyllosilicates in the surrounding matrix are biotite and muscovite. The M_1 garnet porphyroblasts have a compositional profile that shows a decrease in $Fe/(Fe+Mg)$ from centre to rim (Figure 5-2).

The next mineral to form after biotite in the Barrovian Zonal Scheme sequence in pelitic rocks is almandine garnet, probably by the prograde reaction (Yardley, 1989):



The occurrence of the various porphyroblasts that develop in a rock is constrained by the bulk composition of the rock. This is shown by the AFM diagrams for different temperatures in the garnet zone of the Barrovian Zonal Scheme as shown in Figures 5-1b through 5-1d. The above prograde garnet-in reaction initially takes place in Fe-rich portions of the rock; with increasing temperature, garnet appears in a wider range of rock compositions, including more Mg-rich rocks (Yardley, 1989).

Iron has a greater affinity for garnet whereas magnesium

has a greater affinity for biotite, however, this effect decreases with increasing temperature (Perchuk *et al.*, 1981; Ferry and Spear, 1979; Ganguly and Saxena, 1984). The above results in a compositional distribution in garnet porphyroblasts. Garnet porphyroblasts that developed in pelitic rocks during a metamorphic regime of increasing temperature will have a profile that shows a decrease in $Fe/(Fe+Mg)$ from centre to rim (Spear *et al.*, 1991).

The S_1 fabric in the semi-pelitic and micaceous felsic rocks in the North Star Lake area is defined by biotite + muscovite +/- chlorite and was subsequently overprinted by garnet. Chloritoid has not been observed in the mineral assemblage that defines the S_1 fabric therefore the bulk chemical composition of these rocks would plot below the garnet--chlorite tie-line of the AFM diagram for the garnet zone of the Barrovian Zonal Scheme (Figure 5-3a).

The mineral assemblage of the mafic rocks of the North Star Lake area are characterized by the presence of hornblende, biotite, quartz, plagioclase and an opaque mineral (probably sphene). Relict S_1 fabrics are less common and when present are defined by a preferred orientation of blue-green hornblende +/- brown biotite. The relict D_1 mineral fabrics are consistent with mineral assemblages of the epidote-amphibolite facies which can be correlated with the garnet zone in pelites (Miyashiro, 1973). The ACF diagram for the epidote-amphibolite facies is shown in Figure 5-4a.

In greenschist facies terranes calcic amphibole found in metabasites typically has a high tremolite component whereas in metabasites of epidote-amphibolite and amphibolite facies calcic amphibole tend to have a composition closer to that of hornblende. Metabasites recrystallized in the epidote-amphibolite facies commonly contain blue-green hornblende. Biotite usually changes from green to brown at metamorphic grades corresponding to approximately the greenschist--amphibolite transition (Miyashiro, 1973).

The first phase of metamorphism was contemporaneous with the first phase of deformation and occurred in a regime of increasing temperature. During the first phase of metamorphism the pressure--temperature regime evolved through the biotite--in reactions and into garnet-in conditions. The mineral assemblages at the peak of the first metamorphic event are consistent with the garnet zone for pelites and the epidote-amphibolite facies for metabasites.

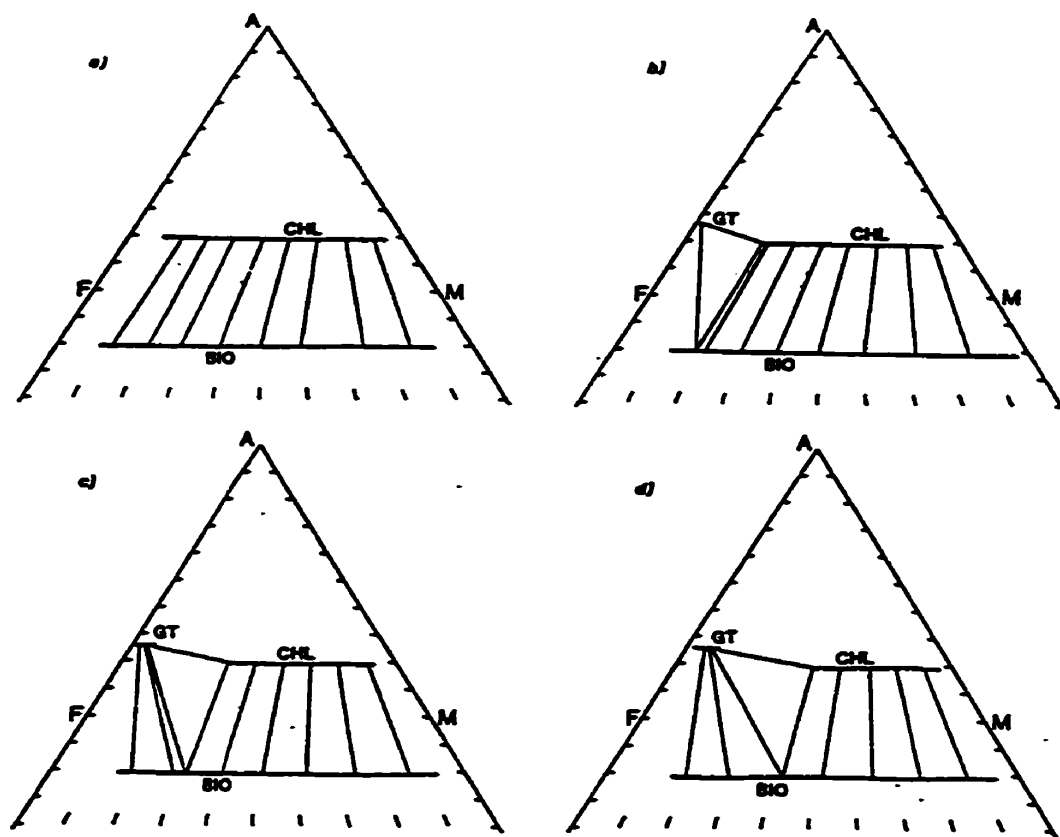


Figure 5-1. AFM projections for the biotite and garnet zones. All assemblages include muscovite, quartz and H₂O. a) Biotite zone, showing trivariant chlorite-biotite field with representative tie-lines connecting coexisting compositions; b) first appearance of garnet, restricted to Fe-rich compositions; c) with increased temperature, garnet is present in a wider range of rocks; d) with further increase in temperature, garnet is present in most normal pelite compositions, and chlorite is absent from more Fe-rich compositions (after Yardley, 1989).

Sample 005, Site 1

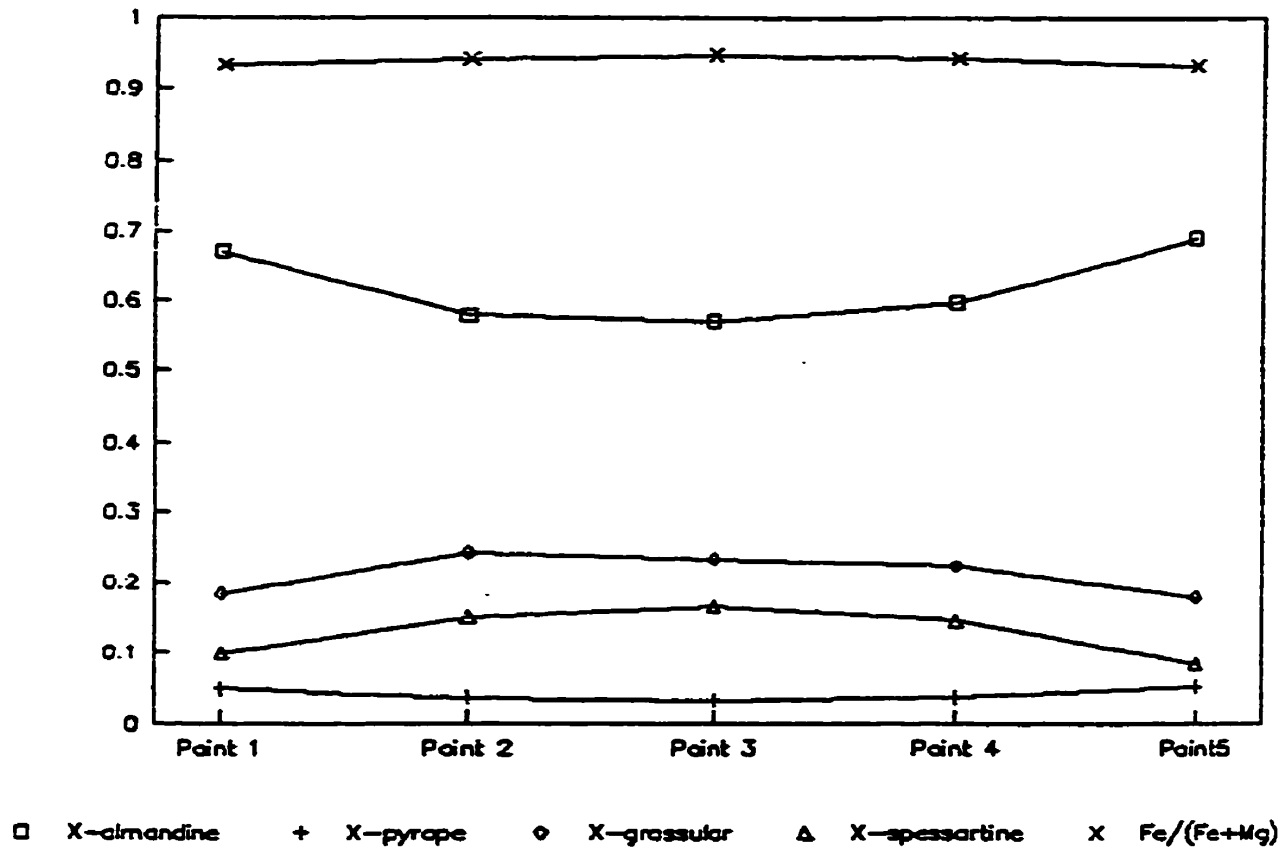


Figure 5-2. M₁ garnet compositional profile.

Plates 5-1 and 5-2 (next page).

Plate 5-1. S_1 defined by biotite and muscovite in micaceous felsic rock. Plain light. Scale: 1.3 cm = 0.1 mm.

Plate 5-2. M_1 garnet with reaction halo; draped by biotite and muscovite. Note chlorite inclusion in garnet. Plain light. Scale: 3.2 cm = 1.0 mm

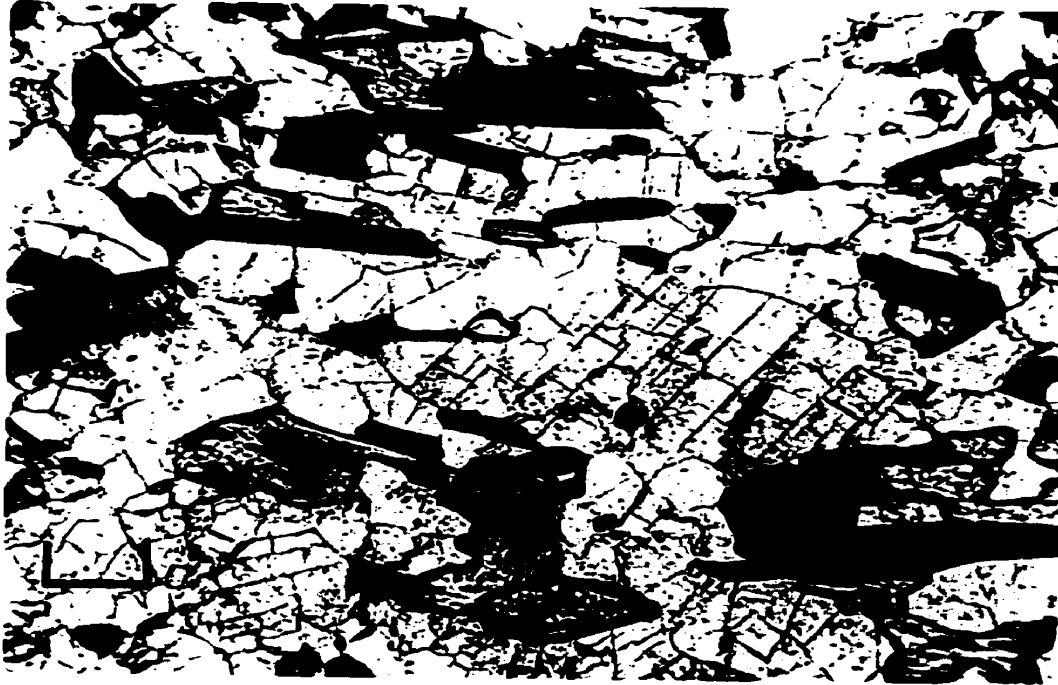


Plate 5-1



Plate 5-2

5.2.2 Second Phase of Metamorphism (M_2)

The second phase of metamorphism (M_2) in the North Star Lake area occurred during and following the second phase of deformation (D_2). This deformational event folded both the primary layering (S_0) and the S_1 foliation; and produced tight to open flexural folds.

The age relationship of the M_2 metamorphic event relative to other deformational and metamorphic events in the North Star Lake area is determined by the following:

- 1) S_1 fabric overprinted by M_2 porphyroblasts.
- 2) development of L_2 mineral lineation fabric parallel to the plunge of F_2 structures.
- 3) M_2 generated granitic mobilizate and metamorphic segregations folded by later (F_3) structures.

Locally, in micaceous felsic rocks, the second phase of metamorphism resulted in the growth of several species of porphyroblasts. These M_2 porphyroblasts (garnet, staurolite, and kyanite or sillimanite) overprint the D_1/M_1 fabrics (Plate 5-3). The presence of these porphyroblasts in micaceous felsic rocks (semipelite) indicate an increasing grade of metamorphism during M_2 . The profiles of late- M_2 garnet, however, indicate near isothermal conditions during the time immediately preceding thermal climax (Figure 5-3).

In the micaceous felsic rocks of the North Star Lake

area, M_2 garnet porphyroblasts overprint the S_1 schistosity and are commonly located in the more biotite-rich layers. These M_2 porphyroblasts typically have quartz-rich reaction haloes that are depleted in M_1 phyllosilicates and contain M_2 biotite (Plate 5-4), suggesting that garnet and biotite were produced at the expense of chlorite and muscovite (reaction 3). These textures suggest that the pressure--temperature conditions in the North Star Lake area were still in the garnet zone of the Barrovian Zonal Scheme at the onset of the second phases of metamorphism and deformation (Figure 5-4a).

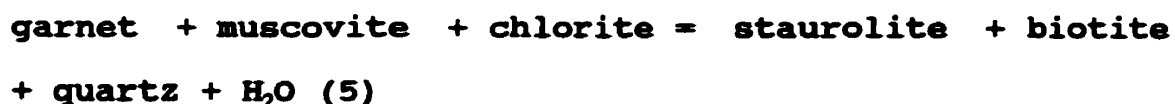
Aluminous felsic rocks of the North Star Lake area (including semi-pelitic and altered felsic volcanic rocks) contain staurolite porphyroblasts with growth texture. The mineral assemblage in these rocks is staurolite, quartz, biotite, muscovite, +/- chlorite, +/- garnet, +/- plagioclase, +/- K-feldspar. In the majority of these aluminous felsic rocks the staurolite is associated with fine- to medium-grained muscovite and biotite (Plate 5-5) and is commonly coexistent with garnet. In some of these rocks, however, garnet has been partially replaced by staurolite.

Occurring after the garnet zone in the Barrovian Zonal Scheme for pelitic rocks is the staurolite zone (Yardley, 1989). The AFM diagram for the staurolite zone is shown in Figure 5-4b. Staurolite porphyroblasts develop in Al-rich, Ca-poor pelitic rocks in the staurolite zone of the Barrovian Zonal Scheme. In pelites that plot above the garnet--chlorite

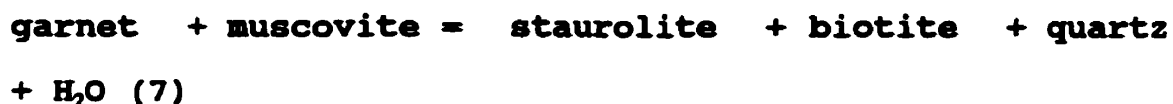
tie-line on the AFM diagram (Figure 5-4a), staurolite is produced by the following reaction (Yardley, 1989):



Although the majority of staurolite-bearing rocks of the North Star Lake area are not true pelites, and would plot below the garnet--chlorite tie-line (Figure 5-4a), their composition allows for the development of staurolite. The growth of staurolite in rocks of suitable composition may be the result of the following prograde reaction (Yardley, 1989):



The above discontinuous reaction takes place at a fixed temperature until one of the reactants has been consumed. Further staurolite may have be produced by the following continuous prograde reactions (Yardley, 1989):

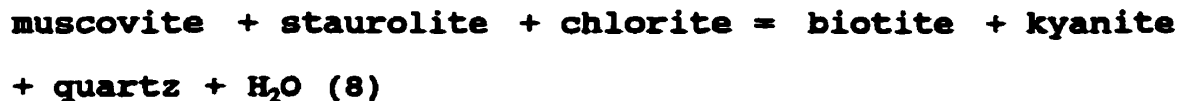


Whether garnet or chlorite is consumed depends on if the

rock plots to the right or to the left of the staurolite--biotite tie-line on the AFM diagram for the staurolite zone (Figure 5-4b). The aluminous felsic rocks that contain the mineral assemblage with coexistent garnet and staurolite would plot to the left of the staurolite--biotite tie-line, whereas those with without garnet, or with garnet partially replaced by staurolite, would plot to the right of the tie-line.

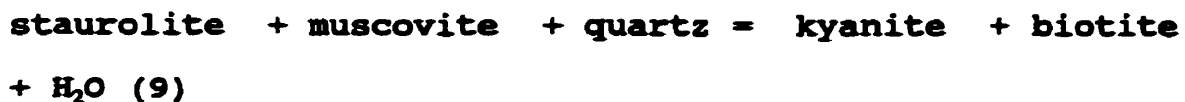
Kyanite porphyroblasts are rare but do occur in some felsic rocks in the North Star Lake area. These unusual rocks contain the assemblage kyanite + biotite + muscovite + quartz; or the assemblage kyanite + staurolite + biotite + muscovite + quartz (Plate 5-6). At one location south of East--West Creek (Figure 3-1) there is an occurrence of an unusual rock with kyanite coexistent with garnet.

Following after the staurolite zone in the Barrovian Zonal Scheme is the kyanite zone (Yardley, 1989). The AFM diagram for the kyanite zone of the Barrovian Zonal Scheme is shown in Figure 5-4c. The first appearance of kyanite is the result of the following discontinuous prograde reaction (Yardley, 1989):



The above reaction takes place in Al and Mg-rich rocks since the assemblage garnet + staurolite + biotite + muscovite

+ quartz is stable to the left of the staurolite--biotite tie-line (Figure 5-4c). Further growth of kyanite takes place by the following continuous reaction (Yardley, 1989):

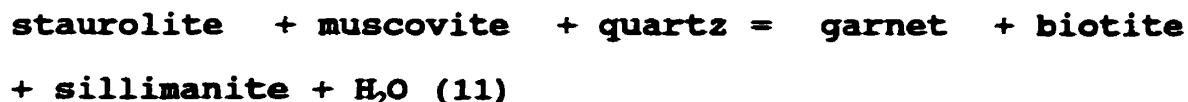


Near Round Lake in the northern portion of the North Star Lake area (Figure 3-1) the assemblage muscovite, biotite, quartz, staurolite, garnet, and sillimanite occurs. This assemblage suggests that reaction of reaction 8 has occurred, however, the aluminosilicate produced was sillimanite, not kyanite.

Following after the kyanite zone in the Barrovian Zonal Scheme is the sillimanite zone. The AFM diagram for sillimanite zone is shown in Figure 5-4d. The onset of the sillimanite zone occurs with the polymorphic transition from kyanite to sillimanite (Yardley):



Within the sillimanite zone further growth of aluminosilicate takes place, and staurolite is consumed in rocks with excess muscovite and quartz by the following reaction (Yardley, 1989):



In the North Star Lake area reactions 9 and 11 do not occur. Staurolite is coexistent with muscovite and quartz for rocks with bulk compositions that plot to the left of the staurolite--biotite tie-line (Figure 5-4c). In the rocks with coexistent kyanite and garnet the garnet probably has a high X_{Mn} component and therefore does not plot on the AFM diagram.

In some areas in the North Star Lake area anatexis has taken place in quartzo-feldspathic felsic rocks and in micaceous felsic rocks. The leucosome material is composed of quartz, K-feldspar, albite, +/- garnet. The leucosome material often occurs in rods with a preferred orientation parallel to the L_2 lineation (Plates 4-19 and 4-20).

Anatexis can take place in quartzo-feldspathic felsic rocks providing there is aqueous fluid phase ($P_{\text{H}_2\text{O}} \geq 3.5$ kbars) and results from the following reactions (Winkler, 1979):

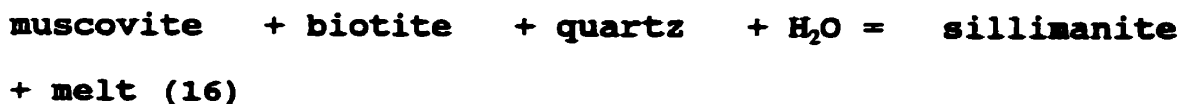


Biotite may also be one of the reactants in the above reactions that produce anatectic melt. The biotite would yield

additional K-feldspar component, and almandine and/or cordierite component to the melt (Winkler, 1979).

In felsic volcanic and semi-pelitic rocks of the North Star Lake area, reactions 12 and 13 have taken place whereas the K-feldspar + muscovite + quartz is coexistent. Biotite has commonly been consumed during the anatexis reaction to produce garnet.

Anatexis can take place in micaceous felsic rocks by the following reactions that require an aqueous fluid phase that dissolves in the product melt (reactions 15 and 16) (Yardley, 1989). Anatexis can also take place through the breakdown of hydrous minerals (reaction 17) (Yardley, 1989):



In the North Star Lake area muscovite is coexistent with quartz and with biotite and quartz.

The development of anatectic neosome is more common in the western portion of the North Star Lake area suggesting that temperatures were higher and/or $P_{\text{H}_2\text{O}}$ was higher in this area.

The amphibolitic rocks of the North Star Lake area are composed of amphibole, quartz, plagioclase (An 80),

+/- garnet, +/- biotite. Blue-green to green amphibole commonly has a preferred orientation and defines the L_2 fabric whereas blue green amphibole commonly defines the S_1 schistosity.

The pressure and temperature regime of the medium-pressure subfacies of epidote-amphibolite facies approximately corresponds the almandine zone of the Barrovian series, while the medium-pressure subfacies of the amphibolite facies approximately corresponds to the kyanite and sillimanite zones of the Barrovian series (Miyashiro, 1973). The ACF diagram for the epidote-amphibolite facies is shown in Figure 5-5a.

Mafic rocks of the epidote-amphibolite facies are characterized by albite + epidote + hornblende +/- almandine. Hornblende is usually blue-green in colour and almandine may occur in mafic rocks with high Fe^{2+}/Mg ratios. The transitional zone between the greenschist and epidote-amphibolite facies occurs under temperature and pressure conditions where the dominant calcic amphibole changes from actinolite to hornblende (Miyashiro, 1973).

Mafic rocks of the amphibolite facies are characterized by andesine or labradorite + hornblende +/- almandine. Hornblende is usually green or brown (Miyashiro, 1973). The ACF diagram for the amphibolite facies is shown in Figure 5-5b.

The second phase of metamorphism in the North Star Lake area was contemporaneous with the second phase of deformation.

Mineral assemblages of the second phase of metamorphism are consistent with the kyanite zone of pelitic rocks and the amphibolite facies of mafic rocks. Fabrics produced during M_2/D_2 were subsequently deformed during later deformational events (Plates 5-7 and 5-8).

Sample 1084, Site 1

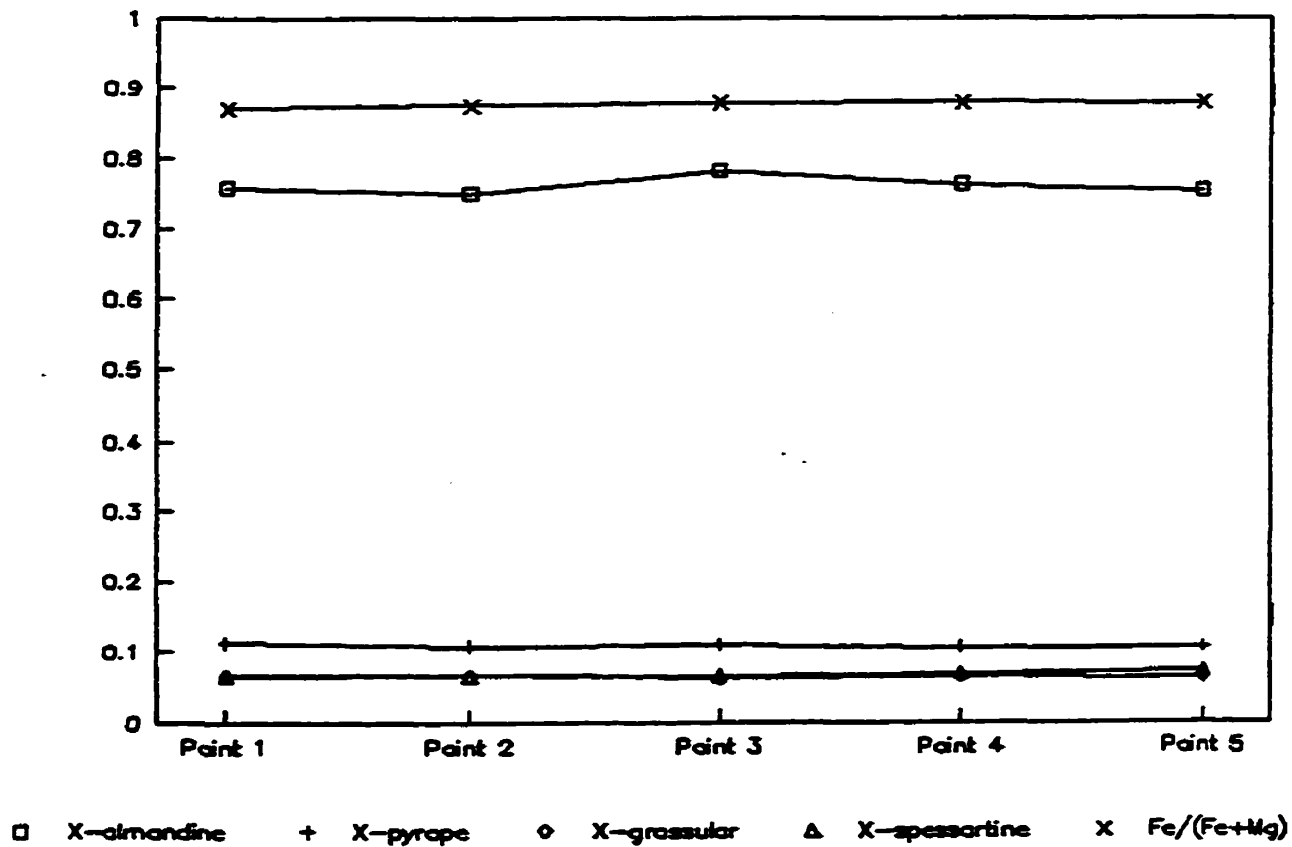


Figure 5-3. M₂ garnet compositional profile.

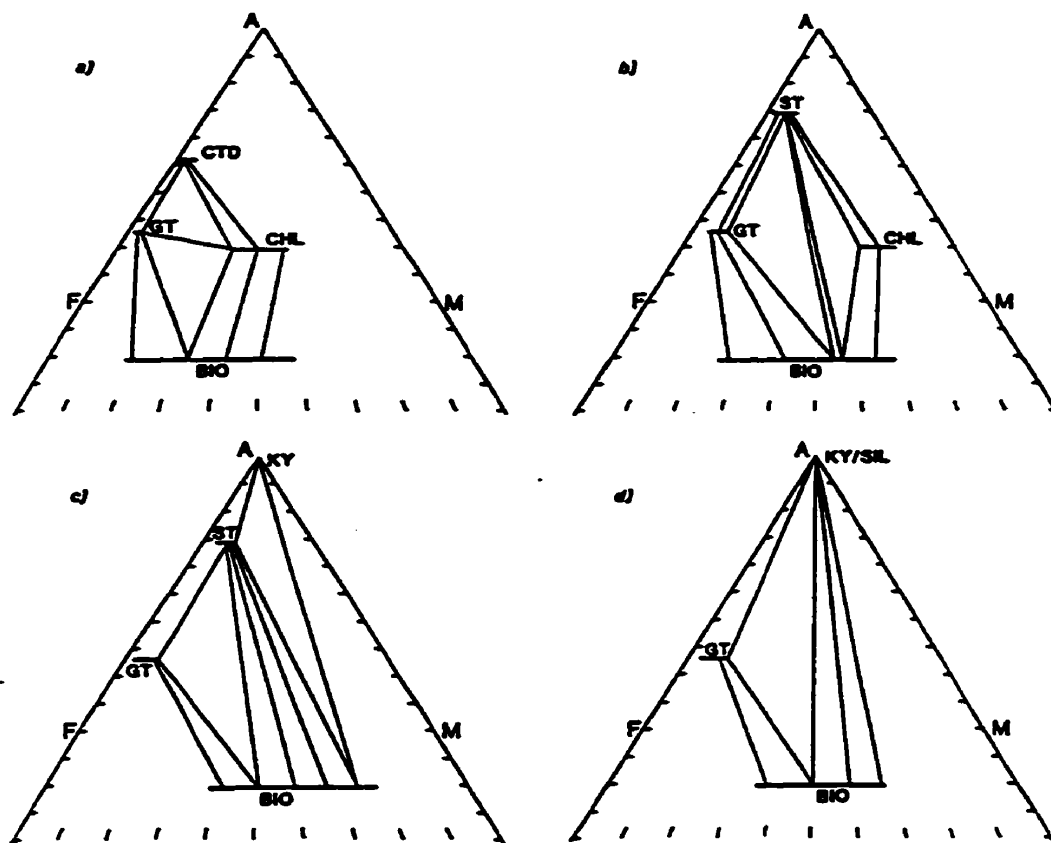


Figure 5-4. AFM projections showing assemblages coexisting with muscovite, quartz and H₂O in Barrovian-type (medium pressure) metamorphism. a) garnet zone, showing divariant and trivariant fields; b) staurolite zone; c) kyanite zone; d) sillimanite zone (after Yardley, 1989).

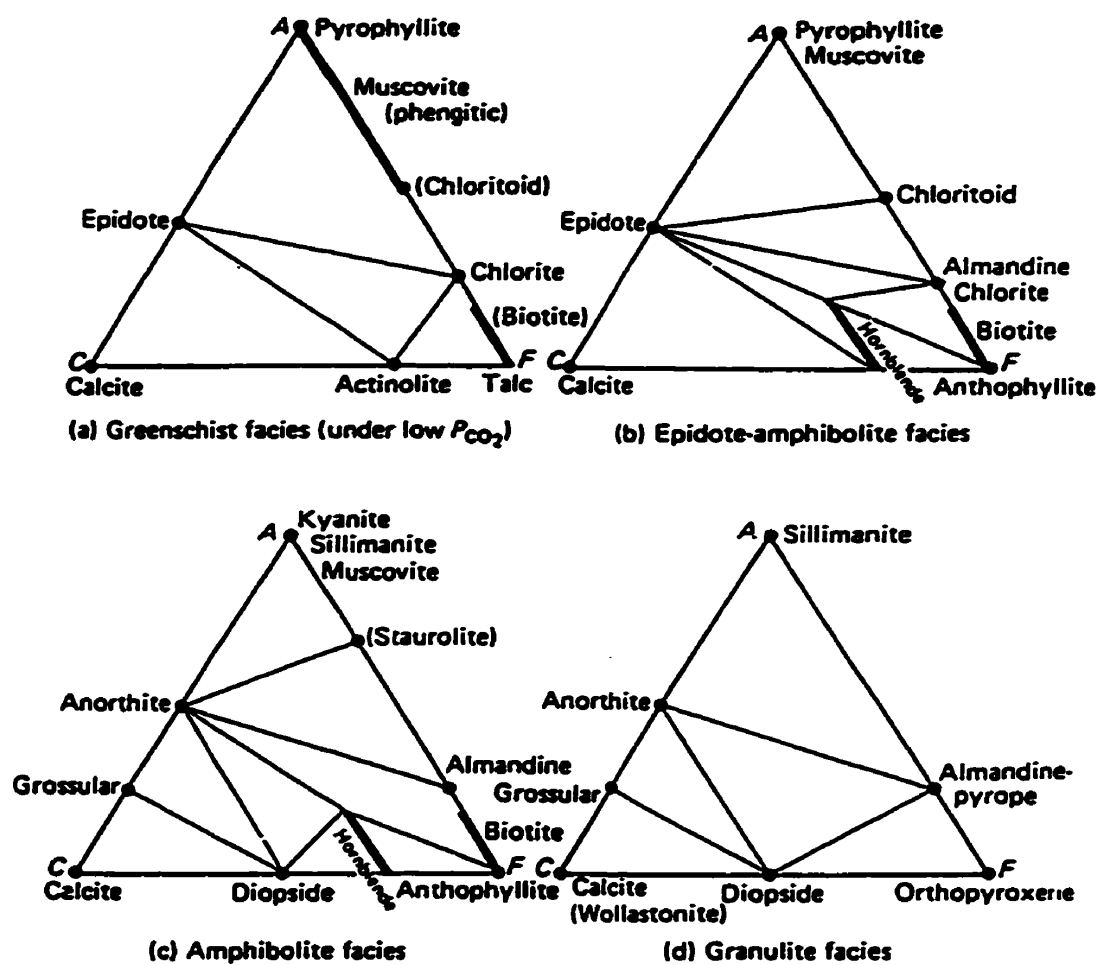


Figure 5-5. ACF diagrams for medium-pressure facies series (after Miyashiro, 1973).

Plates 5-3 through 5-8 (next three pages)

Plate 5-3. M_2 porphyroblasts overprint D_1/M_1 fabrics. M_2 assemblage of staurolite, garnet, biotite, muscovite and quartz.

Plate 5-4. M_2 garnet and biotite. Plain light. Scale: 3.2 cm = 1.0 mm.

Plate 5-5. M_2 assemblage of staurolite, biotite, muscovite and quartz. Plain light. Scale: 1.6 cm = 0.2 mm.

Plate 5-6. M_2 assemblage of kyanite, biotite, muscovite and quartz. Plain light. Scale: 1.6 cm = 0.2 mm.

Plate 5-7. D_2/M_2 fabric (assemblage of staurolite, biotite, muscovite and quartz) deformed by D_3 .

Plate 5-8. D_2/M_2 fabric (leucosome and melanosome material) deformed by D_3 .

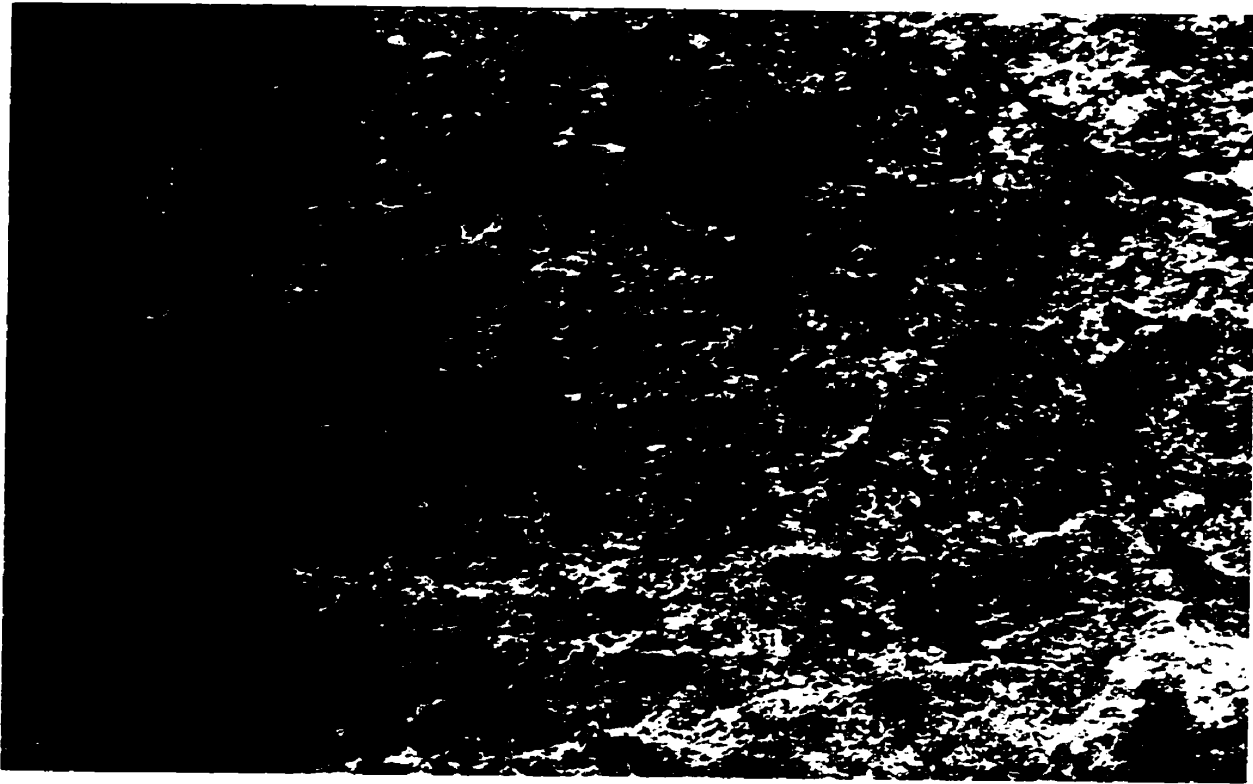


Plate 5-3



Plate 5-4

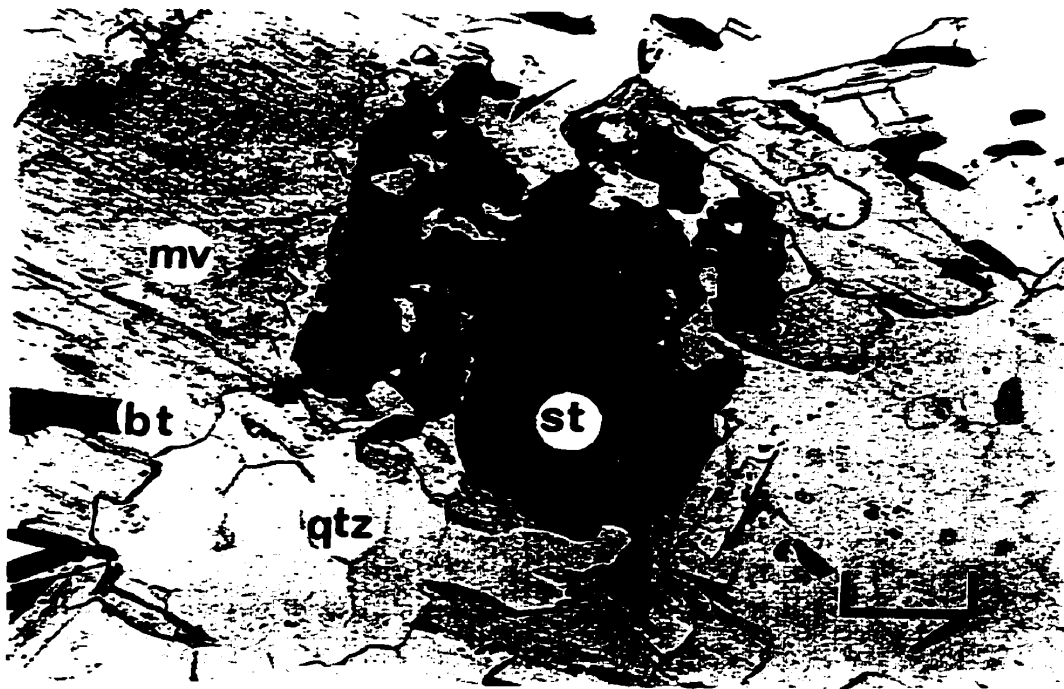


Plate 5-5

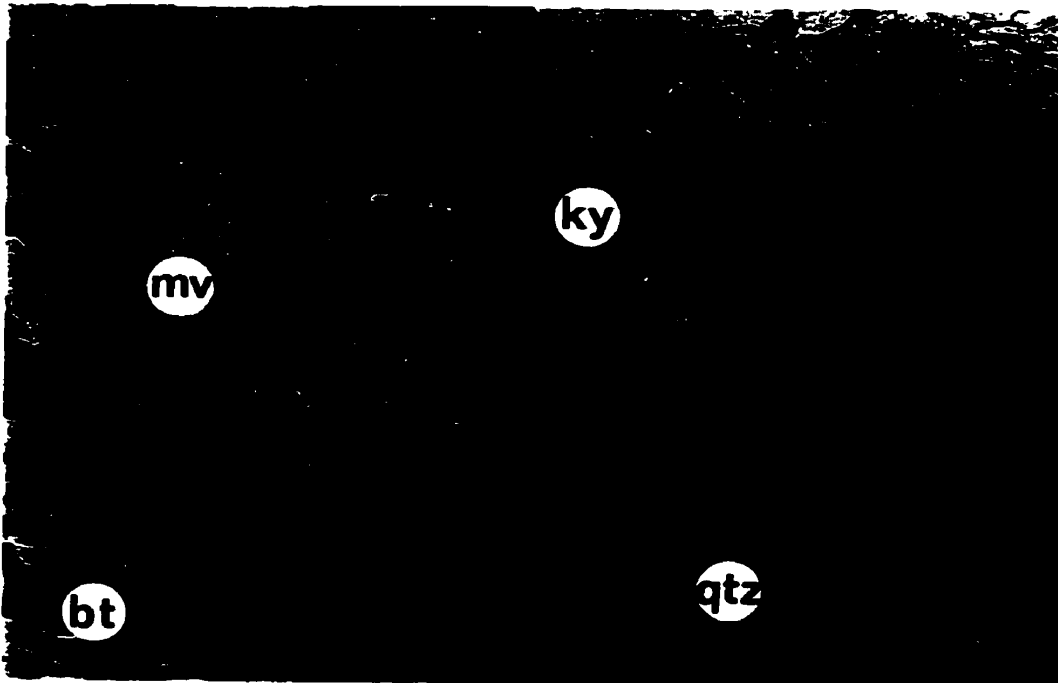


Plate 5-6

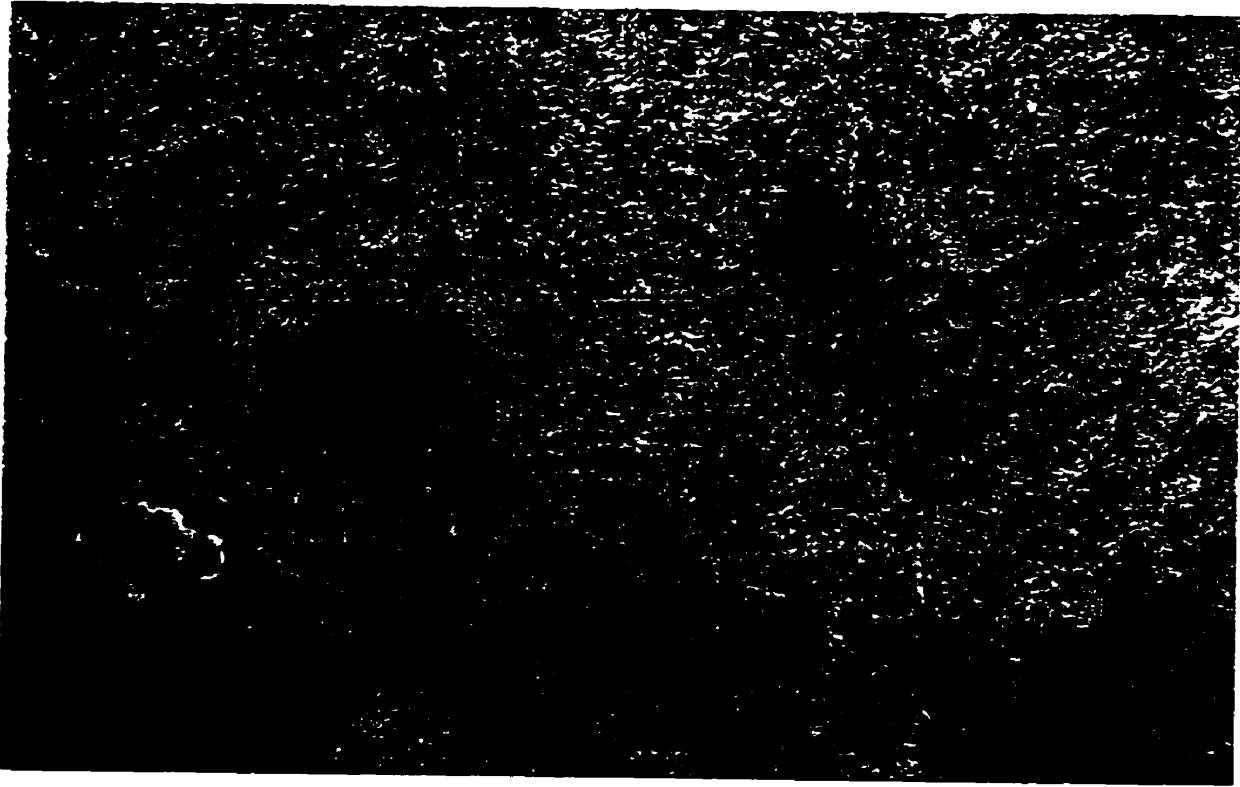


Plate 5-7

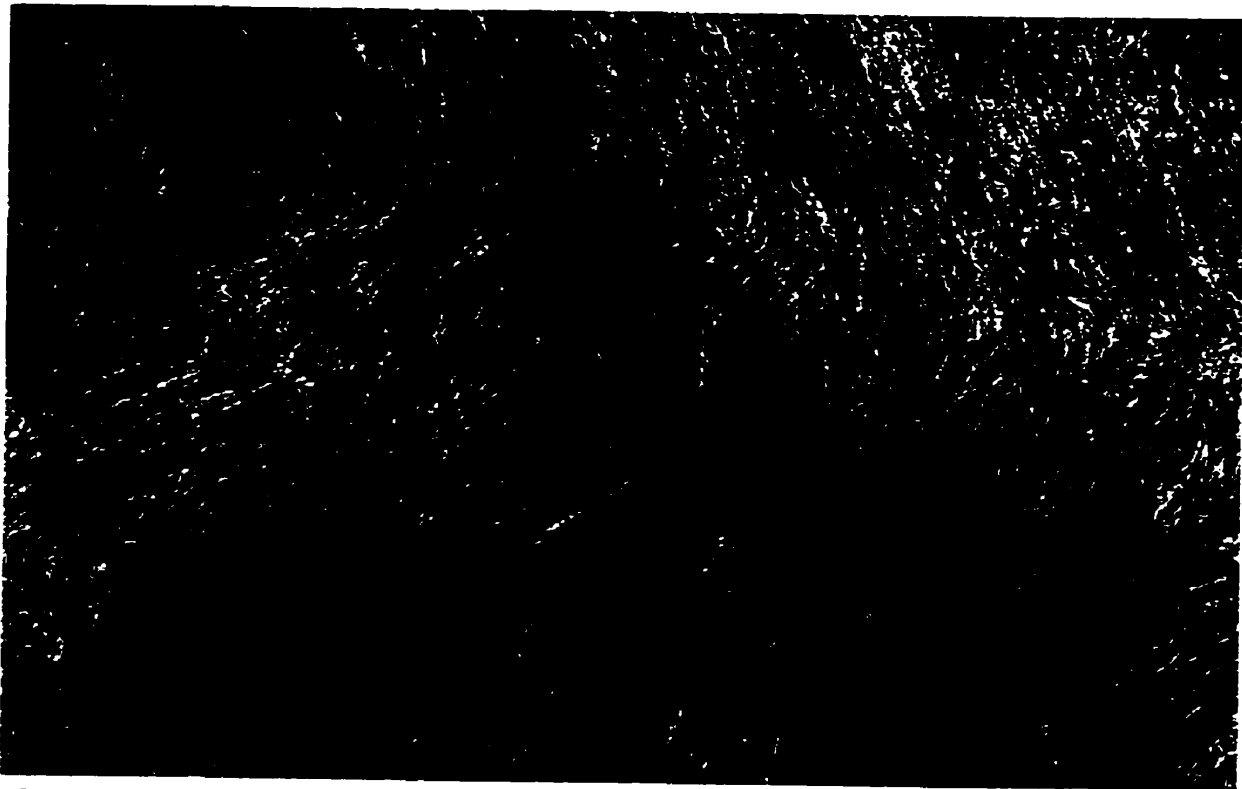


Plate 5-8

5.2.3 Third Phase of Metamorphism (M₃)

The third phase of metamorphism (M₃) is associated with the third phase of deformation (D₃) that produced upright to steeply-inclined flexure folds. This phase of metamorphism is distinguished by:

- 1) the development of axial-planar biotite and muscovite schistosity in the hinge area of minor F₃ folds in felsic rocks.
- 2) the growth of garnet porphyroblasts that overprint D₃ fabrics in amphibolite.
- 3) the annealing of amphibole crystals deformed during D₃.

Muscovite and biotite have grown, and locally, form a schistosity (S₃) that is axial-planar to minor D₃ folds (Plate 5-9). The growth of muscovite and biotite but not chlorite indicates the temperature and pressure regime during M₃ was of amphibolite facies-grade. Chlorite is stable in the lower grade portion of the staurolite zone of the Barrovian Zonal Scheme (Yardley, 1989).

Almandine garnet porphyroblasts overprint D₃ crenulate folds in some amphibolitic rocks (Plate 5-10). The growth of almandine garnet in amphibolite is indicative of medium- to high-pressure metamorphism (epidote-amphibolite to amphibolite facies conditions) (Miyashiro, 1973) however, almandine garnet

porphyroblast growth can occur in hinge areas of crenulate folds in lower pressure regimes (Barker, 1990).

Blue-green hornblende was deformed during D_3 to form crenulate folds (Plate 4-53). This hornblende, although deformed, does not have undulose extinction which indicates that the hornblende crystals have been annealed.

The third phase of metamorphism occurred under pressure--temperature condition equivalent to the staurolite zone for pelites and the amphibolite facies for metabasites. The third metamorphic event produced only a local overprinting of the S_1 fabric suggesting that the pressure conditions during M_3 were lower than those during M_1 when the prominent phyllosilicate fabric was produced.

Plates 5-9 and 5-10 (next page).

Plate 5-9. Biotite and muscovite define S_3 . Plain light. Scale: 3.2 cm = 1.0 mm.

Plate 5-10. F_3 crenulate fold overprinted by late garnet porphyroblast in amphibolite. X-nicols. Scale: 3.2 cm = 1.0 mm.



Plate 5-9

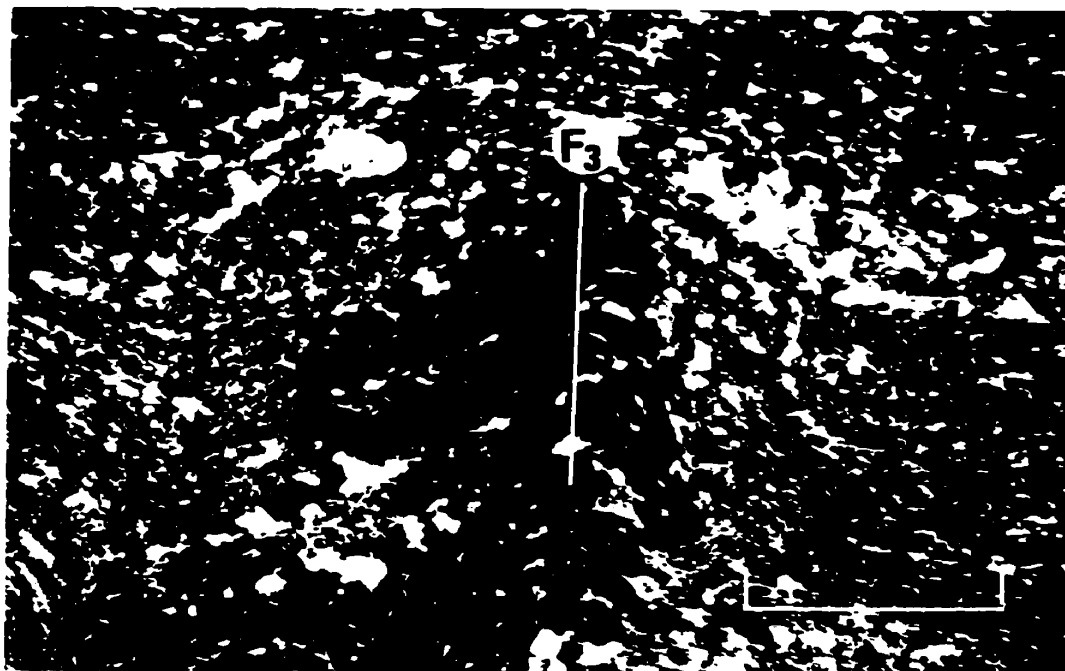


Plate 5-10

5.2.4 Fourth Phase of Metamorphism (M₄) (Retrograde Metamorphism)

The fourth phase of metamorphism (M₄) is retrograde and minerals associated with it are commonly confined to late brittle structures. This phase of metamorphism is distinguished by:

- 1) The occurrence of greenschist facies mineral assemblages (e.g. epidote, calcite, chlorite, quartz and albite) in brittle structures in mafic rocks.
- 2) Random-oriented chlorite and muscovite in some micaceous felsic rocks.

Greenschist facies assemblages are commonly confined to brittle faults (Plate 5-11). Retrograde metamorphism was localized in these brittle structures due to the introduction of aqueous fluids.

Chlorite overprints muscovite and biotite in some micaceous rocks (Plate 5-12). This chlorite has a random orientation suggesting static growth unlike the earlier phyllosilicates which define a schistosity.

Mineral assemblages produced during the retrograde metamorphic events in the North Star Lake area suggest that pressure--temperature conditions were of greenschist facies. Temperatures during this metamorphic event were lower than the temperatures required for biotite stability.

Plates 5-11 and 5-12 (next page).

Plate 5-11. Cataclasite; ductile fabric in North--South zone overprinted by brittle deformation. Retrograde metamorphic mineral assemblage (chlorite, epidote, calcite, albite and quartz). Plain light. Scale: 3.2 cm = 1.0 mm.

Plate 5-12. Poorly-developed S_1 fabric in micaceous felsic rock overprinted by late muscovite. plain light. Scale: 3.2 cm = 1.0 mm.

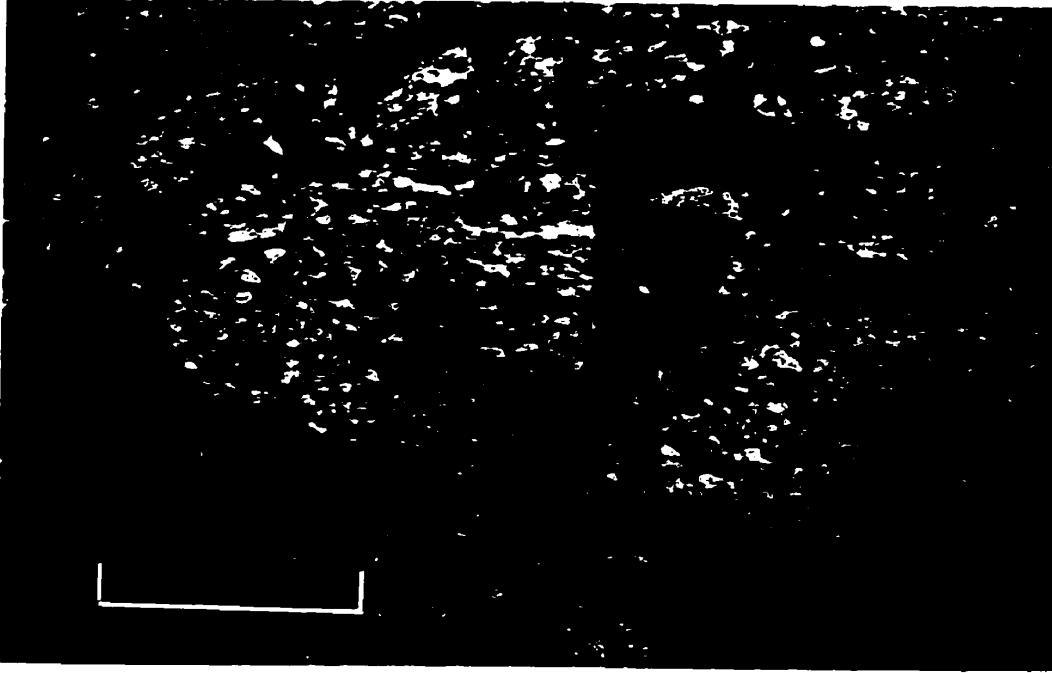


Plate 5-11



Plate 5-12

5.3 Geothermobarometry

The various lithologies in the North Star Lake area provide some opportunities to quantitatively constrain the temperatures of metamorphism. Constraining the pressures of metamorphism is more difficult due to the paucity of coexisting plagioclase, garnet, aluminosilicate, and quartz.

Based on the reaction (3) it is possible to determine the temperature of garnet growth during the late stages of M_1 and during M_2 . The calculation of temperatures is based on the partitioning iron and magnesium between garnet and biotite by the following reaction.



Three different methods of calculating temperatures using the garnet--biotite geothermometer were used. These methods are those defined by Perchuk *et al.*, 1981, Ferry and Spear, 1979, and Ganguly and Saxena, 1984. These methods were used to calculate temperatures at thermal climax since the mineral pair of garnet--biotite is stable from the garnet zone on through the sillimanite zone (Figure 5-3). These methods are summarized in Appendix A.

The method of Perchuk *et al.* (1981) is based on the partitioning of iron and magnesium by reaction 18. Mole fractions of endmembers in both the garnet and the biotite are calculated by assuming $X_{\text{total}} = X_{\text{Fe}} + X_{\text{Mg}} + X_{\text{Mn}}$; the mole fraction of

grossular in the garnet is not considered in calculations using this method. Approximation of the lithostatic pressures is not required in this method. Temperatures calculated using this method are in the range of 465-572 °C.

The method of Ferry and Spear (1979) is based on ideality during the partitioning of iron and magnesium by reaction 18. In garnet the mole fractions of both grossular and spessartine are taken into account since in this method $X_{total} = X_{alm} + X_{prp} + X_{grs} + X_{spes}$. Different calculations were done by assuming pressures of 5, 6, and 7 kbars. Temperatures calculated using this method are in the range of 433-583 °C assuming P=5 kbars, 437-586 °C assuming P=6 kbars, and 440-590 °C assuming P=7 kbars.

The method of Ganguly and Saxena (1984) is based on the quaternary mixing model for Fe--Mg--Ca--Mn endmembers of garnet. Temperatures calculated using this method are in the range of 494-607 °C assuming P=5 kbars, 498-612 °C assuming P=6 kbars, and 501-616 °C assuming P=7 kbars.

Temperatures calculated using biotite--garnet geothermometry on staurolite-bearing rocks may be erroneous. This is the result of the consumption of garnet to produce staurolite by reaction 5. Temperatures calculated for these rocks would be lower than what temperatures actually were (Spear et al., 1991).

5.4 Petrogenetic Grid

A petrogenetic grid for pelitic rocks is shown in (Figure 5-6). Temperatures of peak conditions calculated for staurolite free felsic rocks in the North Star Lake area are in the range of approximately 540-620 °C.

A minimum pressure at a temperature of 620 °C can be approximated at 3.75 kbars due to the lack of cordierite bearing assemblages in the North Star Lake area. This suggests that the metamorphic evolution in the North Star Lake area followed a medium-pressure or Barrovian path.

The maximum pressure at a temperature 670 °C in the North Star Lake area can be constrained at 7.2 kbars by the occurrence near Round Lake of staurolite in equilibrium with quartz and sillimanite.

The assemblage of staurolite + quartz is stable throughout the North Star Lake area. This constrains the temperature to a maximum of 670 °C at a pressure of 7.2 kbars. The reaction producing sillimanite + melt at the expense of albite + muscovite + quartz (reaction 13) constrain the minimum temperature of anatexis at 650 °C at 6.5 kbars.

The first phase of metamorphism resulted in pressure--temperatures evolving through the garnet-in reaction. Profiles of late-M₁ to early-M₂ garnet porphyroblasts suggest that the temperatures in the North Star Lake area were increasing at this time. The development of the prominent regional fabric (S₁) prior to thermal climax suggests that maximum pressure

conditions predated maximum temperature conditions (Brown, 1993). The first phase of metamorphism is associated with the first phase of deformation (Figure 5-6).

Compositional profiles of late-M₂ garnet porphyroblasts suggest that the temperatures were near isothermal during the time of thermal climax. Pressure--temperature conditions can be approximated at 650 °C and 6.5 kbars. The second phase of metamorphism occurred during and after the second phase of deformation (Figure 5-6).

The third phase of metamorphism occurred at similar temperature conditions as the first phase of metamorphism. Pressures must have been substantially less during M₃, since fabrics associated with M₃ (S₃) only locally and weakly overprint the prominent S₁ fabric. The third phase of metamorphism occurred during and after the third phase of deformation (Figure 5-6).

The fourth phase of metamorphism was a retrograde metamorphic event and occurred locally under greenschist facies conditions. The mineral assemblages associated with this metamorphic event suggest that the pressure--temperature conditions in the North Star Lake area were below biotite-in by this time (Figure 5-6).

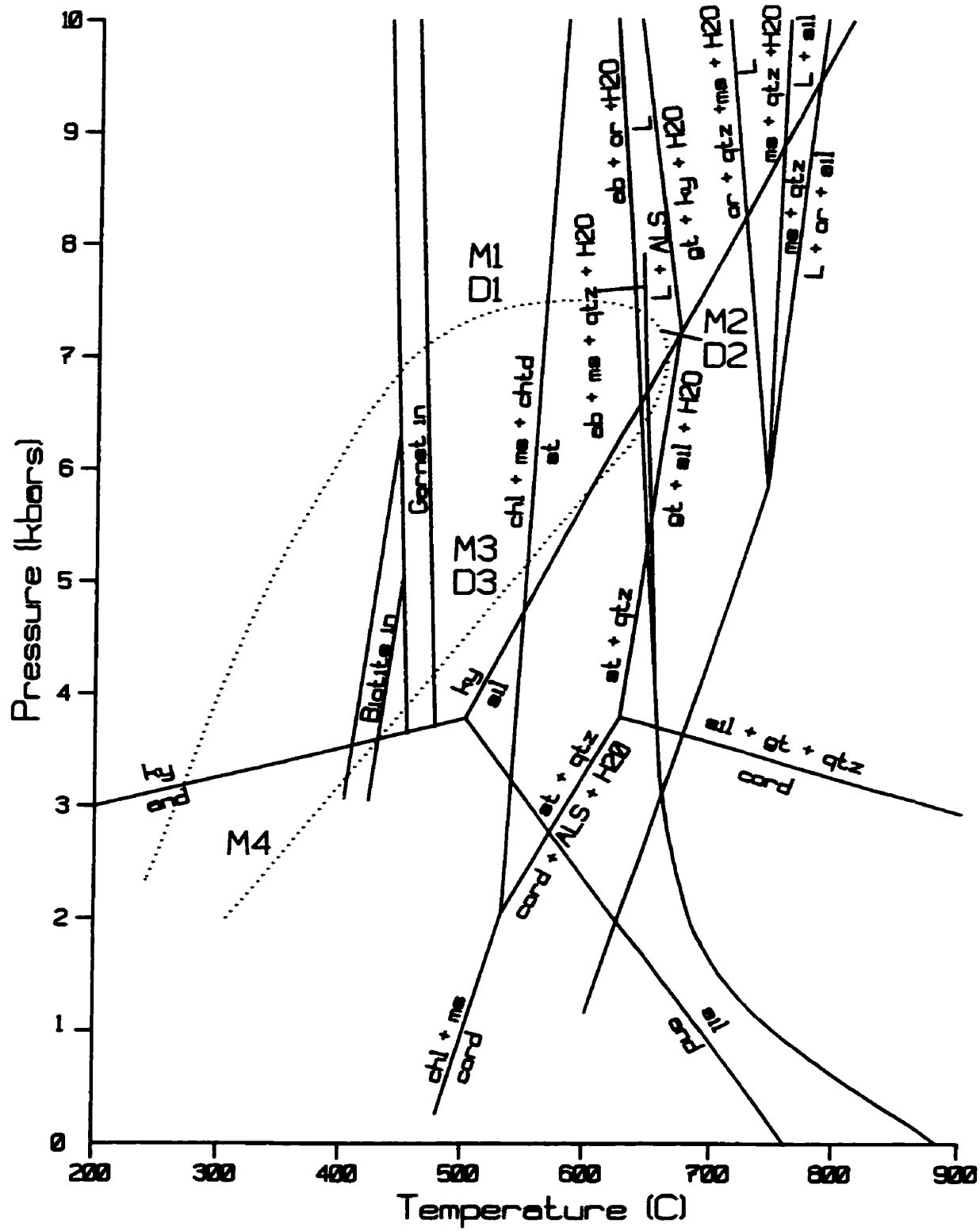


Figure 5-6. Petrogenetic grid for the North Star Lake area.

Chapter VI
STRUCTURAL AND METAMORPHIC HISTORY
OF THE NORTH STAR LAKE AREA

6.1 Introduction

Progressive deformation in the North Star Lake area occurred as a south- to southwest-directed compressive ductile deformation. These ductile phases of deformation (D_1 -- D_3) in the North Star Lake area are associated with a prograde--retrograde metamorphic cycle (M_1 -- M_3).

The heterogeneous non-coaxial strain produced folds whose axes were originally oriented approximately perpendicular to the movement direction and with progressive deformation the fold axes were reoriented by transposition towards parallelism with the south to southwest movement direction (cf. Sanderson, 1973; Escher and Watterson, 1974). With progressive non-coaxial strain the younger folds in low-strain domains are more open and less reoriented towards parallelism than older folds while in high-strain domains transposition is more advanced and most folds approach parallelism (cf. Williams and Zwart, 1977).

Fold style in the North Star Lake area ranges from similar, isoclinal, passive-flow folds that developed during the first phase of deformation (D_1) to parallel, open to tight, flexural folds developed during the third phase of deformation (D_3). This variation in fold style indicates a

transition from homogeneous ductile behaviour early in the structural history of the area to heterogenous elastic--ductile behaviour later in the structural history. The final phase of deformation in the area (D_4) occurred during northwest--southeast compression and produced brittle--ductile to brittle structures.

The North Star Lake area followed a clockwise P--T--t evolution with maximum pressure conditions predating maximum temperature conditions. The prograde phases of metamorphism (M_1 and M_2) indicate a medium-pressure (Barrovian type) regime during the time preceding thermal climax. The clockwise P-T-t evolutionary path in the North Star Lake area suggests that the structural and metamorphic evolution of the area was the result crustal thickening (cf. Brown, 1993).

6.2 Early Deformation in the North Star Lake Area

The initial deformation in the North Star Lake area was the result of intraoceanic tectonics during the period of 1.88--1.87 Ga that juxtaposed the juvenile arc assemblages of the Flin Flon domain into an accretionary complex (cf. Lucas et al., 1996). This initial deformation in the Flin Flon domain predated the deposition of 1.86--1.84 Ga continental and marine sediments and the emplacement of 1.87--1.83 Ga calc-alkaline plutons (Lucas et al., 1996).

Early deformation in the Flin Flon domain has been documented in the areas proximal to the North Star Lake area (Ryan and Williams, 1994, 1995; Syme et al., 1995; Zwanzig, 1995a). The result of the initial deformation in the North Star Lake area was the steepening of the stratigraphy (cf. Lucas et al., 1996). The steepened assemblage was subsequently intruded by the 1.87--1.85 Ga (cf. Whalen, 1993) Gants Lake batholith. Structures that were the result of the initial deformation were not observed in the North Star Lake area likely because of intense later deformation and metamorphism.

6.3 First Deformational Event (D_1) and First Metamorphic Event (M_1) in the North Star Lake Area

The first phase of deformation (D_1) folded the primary layering (S_0) and produced similar, tight to isoclinal folds (F_1) which commonly have a well-developed axial-planar foliation (S_1). The F_1 structures generally are upright, northerly-trending with gentle plunges. The S_1 foliation is the dominant fabric in the North Star Lake area. A lineation (L_1) is commonly well-developed and is near-parallel with the F_1 fold axes.

The S_1 schistosity that developed in micaceous rocks in the North Star Lake area would be classified as coarse continuous cleavage (Figure 4-4). The S_1 spaced cleavage preserved in quartzo-feldspathic rocks in the North Star Lake area would be classified as anastomosing to smooth disjunctive spaced cleavage (Figure 4-4).

The well-developed S_1 schistosity was produced in the North Star Lake area during the first phases of metamorphism (M_1) and deformation (D_1). The grade of metamorphism reached amphibolite facies conditions during this time. Recrystallization is considered to be the dominant process in the development of penetrative foliations under high-grade metamorphic conditions (Ramsey, 1967; Knipe, 1981; Yardley, 1989).

In the quartzo-feldspathic rocks of the North Star Lake area the S_1 foliation is developed as a disjunctive spaced

cleavage expressed by biotite-rich domains (P-domains) that separate quartzo-feldspathic--disseminated biotite microlithons (Q-domains). This S_1 foliation is probably the result of pressure solution however, recrystallization has also taken place since the biotite-rich domains are composed of preferentially orientated biotite and truncated grains are not noted in the microlithons. This process of metamorphic differentiation involves the three processes of pressure solution or selective dissolution, mineral migration and recrystallization (Price and Cosgrove, 1990; Shelly, 1993). At greenschist facies conditions recrystallization becomes dominant (Hatcher, 1990).

The metamorphic differentiation that produced the S_1 disjunctive spaced cleavage in quartzo-feldspathic rocks in the North Star Lake area may be a result of stress heterogeneities in heterogeneous layered rocks (*cf.* Robin, 1979) or stress heterogeneities in phyllosilicate-bearing quartzo-feldspathic rocks (*cf.* Price and Cosgrove, 1990). Conversely, metamorphic differentiation may be the result of strain heterogeneities in heterogeneous rocks (*cf.* Bell et al., 1986).

In some sections in the hinge area of the macroscopic F_1 structure in the Face Lake area (Face Lake synform; Figure 4-1) the thickness of the biotite-rich domains relative to the quartzo-feldspathic--disseminated biotite microlithons is greater and the boundary between the biotite-rich domains and

the microlithons is less distinct than elsewhere in the North Star Lake area. This S_1 foliation is possibly the result of the transposition and metamorphic differentiation of layered rocks (c.f. Price and Cosgrove, 1990).

The S_1 foliations in the North Star Lake area are axial-planar to the F_1 structures in the area. This indicates that these S_1 foliations -- the result of recrystallization -- are approximately parallel to the XY-plane of the D_1 finite-strain ellipsoid (cf. Sanderson, 1973). Planar fabrics that are the result of recrystallization may be geometrically related to the finite-strain ellipsoid in either coaxial or non-coaxial strain regimes (Williams, 1976).

In the Face Lake and Sausage Lake areas (subareas 1 and 3; Figure 4-2) layered psammopelitic rocks have locally undergone the transposition of layering. In these areas the S_1 transposition layering occurs in the hinge area of D_1 folds while on the limbs of these folds layering has remained intact. The transposition of layering is a progressive deformation process that results in the redistribution of existing layering to produce a secondary layering parallel to foliation; as deformation proceeds the transposition layering becomes well-developed in the hinge area of symmetric folds and the short limb and hinge areas of asymmetric folds (Hobbs et al., 1976).

The development of the S_1 transposition layering was consanguineous with the development of the D_1 folds that

contains such layering. This transposition layering is axial-planar to the D_1 folds and therefore parallel to the XY-plane of the D_1 finite-strain ellipsoid, but unlike other S_1 axial-planar foliations in the North Star Lake area it is defined by layering that predates the deformation.

In some areas in the North Star Lake area a well-developed, gently-plunging lineation (L_1) has been noted. This L--S tectonic fabric (as defined by Flinn, 1965) is manifested as the preferred alignment of prolate deformed clasts and of mineral grains and aggregates. The principle axes and planes of the finite-strain ellipsoid in the North Star Lake area may be determined from the principle axes and planes of originally-spherical deformed objects (cf. Flinn, 1962). An L--S tectonic fabric has developed of which the planar element is parallel to the XY-plane and linear element is parallel to the X-axis (cf. Escher and Watterson, 1974).

A simple shear model (Escher and Watterson, 1974) has been proposed in which the Y-axis of the finite-strain ellipsoid remains parallel to the deformation boundary; while with increased deformation the X- and Z-axes are progressively reoriented (Figure 6-1). The D_1 linear fabric or extension lineation (transverse extension lineation of Escher and Watterson, 1974) in the North Star Lake area defines the X-axis of the D_1 finite-strain ellipsoid. This linear fabric is transverse to the deformation boundary or zone of concentrated deformation; the North--South zone.

The D_1 linear fabric in the North Star Lake area suggests that the North Star Lake area underwent non-coaxial strain during the first phase of deformation. Regional extension lineations at destructive plate margins coincide with known relative motions of the converging plates (Shackleton and Ries, 1984). In a ductile shear zone the azimuth of the extension lineation defines the horizontal direction of crustal shortening (Escher and Watterson, 1974). The gently-plunging, northerly-trending orientation of the D_1 linear fabric suggests that the non-coaxial strain during D_1 was the result of northerly-southerly crustal shortening.

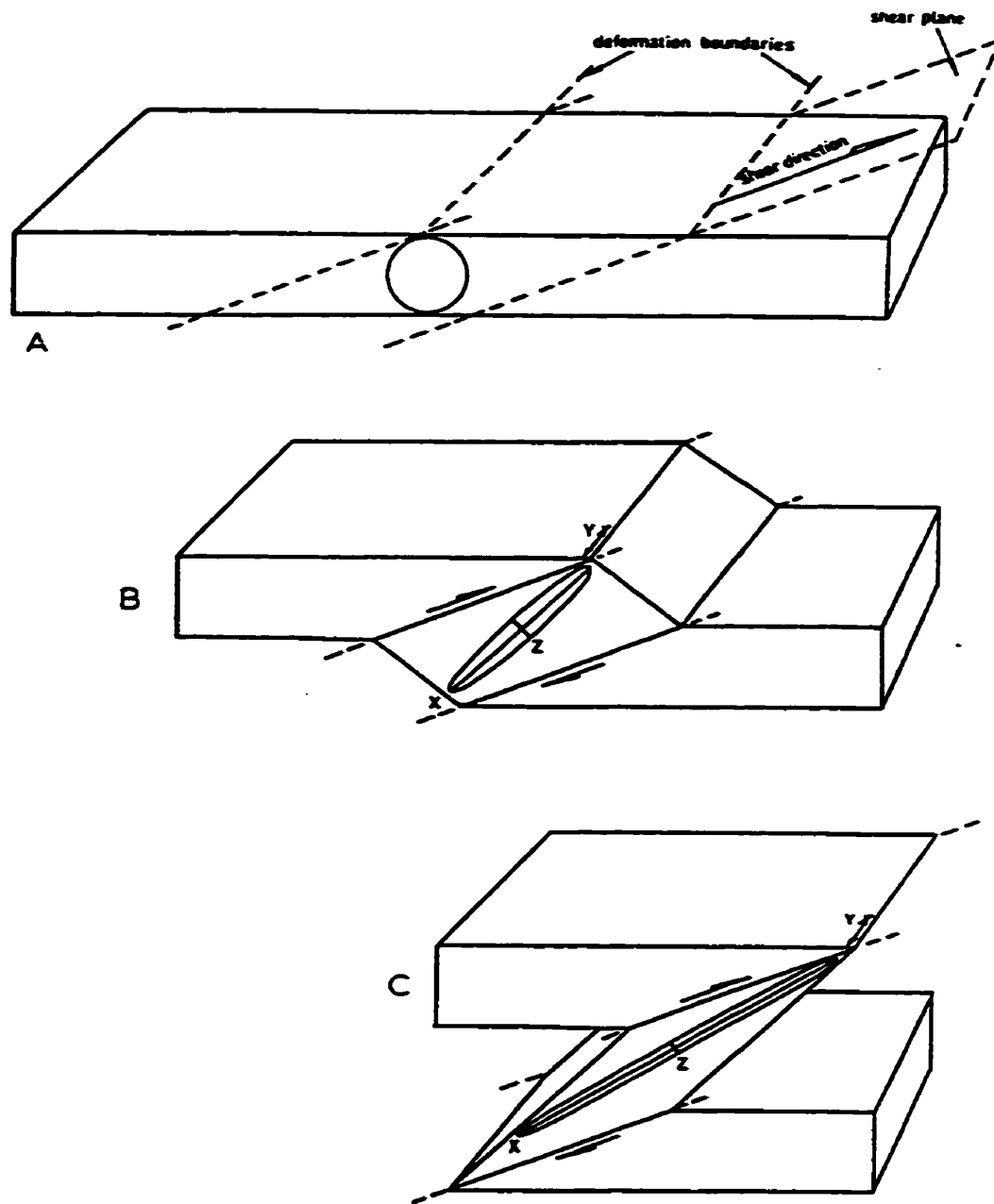


Figure 6-1. Displacement by progressive simple shear showing relationship of geometrical and geological elements (from Escher and Watterson, 1974).

In the area along, and immediately to the east of, Loonhead Creek thin lithologic units generally strike north--south (Figure 3-2) and define a zone of concentrated deformation (North--South zone). The eastern long limb of the macroscopic F_1 structure (Face Lake synform; Figure 4-1) is located in this area along and immediately east of Loonhead Creek. Some of the fabrics in the North--South zone indicate that at least a portion of the strain was in the form of ductile simple shear.

In the North--south zone rare examples of winged inclusion geometry and porphyroclast fracture patterns suggest a dextral sense of shear. Foliations (S_1) in the North--South zone (compositional (tectonic) layering in intermediate to mafic rocks, and a well-developed schistosity in mafic rocks) are, in some locations, possibly the result of ductile simple shear.

There are some rocks in the North--South zone that possibly contain mylonite fabrics (*sensu lato*). These felsic rocks are characterized by thin (<0.5 cm) lenses and veins, composed of fine-grained (<0.5 mm) quartz. These lenses and veins are separated by quartzo-feldspathic domains composed of very fine-grained (≤ 0.1 mm) anhedral quartz and feldspar grains. The quartz lenses and veins along with disseminated fine-grained biotite define the S_1 foliation.

The quartz grains in the lenses and veins commonly contain dynamic recrystallization textures. These textures

include undulose extinction, subgrains and new grains. The edges of the quartz grains in the lenses and veins and the outer edges of those lenses and veins are irregular to sutured. Locally however, quartz grains in the lenses and veins have a near granoblastic texture and are non- to slightly-undulose indicating that some static recrystallization has occurred.

Rocks in the North--South zone commonly contain feldspar crystals that are possibly porphyroclasts. In the felsic rocks of the North--South zone feldspar crystals have irregular to sutured edges, are commonly undulose and commonly have a texture similar to mortar texture. The fine-grained mortar surrounding the porphyroclast is commonly overprinted by muscovite. Locally feldspar crystals in the rocks of the North--South zone are fractured.

A rock will undergo deformation when acted upon by a superimposed shear stress. The mineral constituents of the rock may deform in either a brittle fashion by fracturing (brittle failure) or a ductile fashion by crystal--plastic processes. The primary factors that influence the deformation style are temperature and strain rate; low temperatures and high strain rates favour brittle deformation while high temperatures and low strain rates favour ductile deformation (Barker, 1990).

In crystalline quartzo-feldspathic crust cataclasite (*sensu lato*) is generated by elasto-frictional (EF)

behaviour while mylonite (*sensu lato*) is generated by quasi-plastic (QP) behaviour (Sibson, 1977). The EF/QP transition (*i.e.* brittle--ductile transition) is at approximately 300°C and 10-15 km depth and corresponds approximately to the lower boundary of greenschist facies conditions (Sibson, 1977).

The development of mylonite fabrics (*sensu lato*) in quartzo-feldspathic crust has been summarized by Barker (1990). Early in the development of a quartzo-feldspathic mylonite intracrystalline slip occurs in quartz resulting in undulose extinction. With continuing ductile deformation subgrains, deformation bands and deformation lamellae develop in quartz while large feldspar porphyroclasts undergo brittle fragmentation and may develop deformation twins. The internal dislocation density is reduced by recovery and dynamic recrystallization resulting in the development of subgrains and new grains. Serration and new grain development at porphyroclast edges occurs. At high strain and/or temperatures the elongation of quartz grains and lenses will result in quartz ribbons. Behrmann and Mainprice (1987) state that feldspar ductility may be present under amphibolite facies conditions.

Prior to end of D_1 the area of the North--South zone along Loonhead Creek was probably the eastern long limb of the macroscopic F_1 structure (Face Lake synform; Figure 4-1). This area is dominated by layered rocks (psammite?) and at the time at or near the end of D_1 , but prior to subsequent

deformations, the dominant regional fabric (S_1) was subparallel to parallel to layering (S_0), either primary or transposed. In addition, the S_1 fabric is commonly well-developed in the layered psammitic rocks elsewhere in the North Star Lake area. These factors would have resulted in a regional zone of weakness that could have been exploited by a shear couple with a northerly trend.

The folds produced during the first phase of deformation in the North Star Lake area are of the similar style (class 2 of Ramsey (1967)) with well-developed axial-planar fabrics. These folds developed under amphibolite facies conditions and are interpreted to be passive folds; the result of passive-flow (cf. Price and Cosgrove, 1990, Hatcher, 1990). Passive-flow is the most likely mechanical process required to produce these similar style folds (cf. Hatcher, 1990). Ideal similar style folds are rare in nature; it is common to have a spectrum of fold styles of a range of class 1C to class 3 (Hobbs et al., 1976).

Passive folds in the North Star Lake area were the result of layered rocks subject to a compressive stress regime when the competency contrast between layers is small. The difference in competence between rock layers becomes less as metamorphic grade increases and therefore passive folds are the dominant fold style in high-grade metamorphic terranes (Price and Cosgrove, 1990).

In the North Star Lake area the fold axes of F_1

structures area near-parallel to the (L_1) extension lineations. In mobile thrust belts, fold axes can be reoriented towards parallelism with extension lineations (Sanderson, 1973; Escher and Watterson, 1974; Williams, 1978; Shackleton and Ries, 1984).

Folds that develop in a mobile thrust belt originally form with the fold axes near-parallel to the Y-axis of the finite-strain ellipsoid and upon further deformation the fold axes rotate towards the X-axis (Sanderson, 1973). This reorientation occurs in contemporary folds (as defined by Escher and Watterson, 1974) and can also occur in pre-existing folds (Escher and Watterson, 1974). Williams (1978) in a study of the Lakesfjord Nappe in Norway found that distal contemporary folds are oblique to the extension lineation while contemporary folds proximal to the thrust plane are near-parallel to the extension lineation.

The D_1 fabrics and folds in the North Star Lake area suggest that the area developed in a non-coaxial strain regime proximal to a thrust plane during D_1 . High-grade metamorphic conditions existed during D_1 as expressed by the amphibolite facies M_1 mineral assemblage and the similar style of the D_1 folds. The concentrated dextral ductile simple shear deformation in the North--South zone suggests that this area was a thrust plane during D_1 . The boundary between the Kisseynew and Flin Flon domains is immediately north of the North Star Lake area and a zone of thrust sheets and fold

nappes developed early in the structural history of this area (cf. Lucas et al., 1994b; Norman et al., 1995; Connors, 1996). The northerly-trending, gently-plunging F_1 fold axes and near-parallel L_1 extension lineation suggest that during D_1 the North Star Lake area was proximal to thrust planes in a regime of northerly--southerly crustal shortening.

6.4 Second Deformational Event (D_2) and Second Metamorphic Event (M_2) in the North Star Lake Area

The second phase of deformation (D_2) produced open to tight folds (F_2) that generally have northerly-trending and moderately- to steeply-inclined, easterly-dipping axial planes. In the area west of the North--South zone structural break the F_2 structures (F_{2a}) predominantly have northerly- to northeasterly-trending, gently- to moderately-plunging fold axes while east of the structural break the F_2 structures (F_{2b}) have southerly-trending, moderately- to steeply-plunging fold axes.

In the hinge areas of the F_{2a} structures, D_1 fabrics and structures are gently-inclined. In the F_{2a} hinge areas a fabric is locally expressed in quartzo-feldspathic rocks as a poorly-developed fracture cleavage (S_{2a}). On the limbs of the F_{2a} structures the S_1 foliation is coplanar to near-coplanar with the S_{2a} foliation.

A distinctive characteristic of D_2 is the development of a prominent linear fabric (L_{2a}) that is near-parallel with the

plunge of the northerly- to northeasterly-trending, gently-plunging F_2 fold axes. In amphibolite, this lineation is expressed as a crystallographic preferred orientation of amphibole crystals. In quartzo-feldspathic rocks this lineation is expressed by the preferred orientation of quartz rods.

Further evidence of extension during D_2 are boudinage structures. These boudinage structures, such as boudinaged amphibolite dykes and quartz veins are preserved on the limbs of F_2 structures.

In the area southwest of Face Lake, immediately south of East--West Creek (Figure 3-2), semipelitic rocks have developed a prominent gneissosity (S_2). The distribution of the gneissosity appears to have been controlled by compositional variations in the original lithological package. The leucocratic component of this gneissosity defines the L_2 fabric.

In the area along Loonhead Creek immediately north of North Star Lake the trend of a prior fabric (S_1) is gently-inclined, predominantly clockwise to the trend North--South zone structural break (Figure 4-1). Within the North--South zone in this area F_2 structures, exclusively with Z-asymmetry, are common. The D_1 fabrics within the North--South zone predate the F_2 structures. This indicates that the North--South zone was active over a long period of time; probably from D_1 and definitely through D_2 . Simple shear deformation was

not pervasive throughout the North-South zone during D_2 , since D_1 features are commonly preserved.

Dennis and Secor (1987) describe the development of fabrics in shear zones in which an older schistosity became reactivated. These features are known as extensional crenulation cleavage (Hatcher, 1990). In the case where the prior fabric is inclined gently clockwise to the shear couple (Figure 6-2) the development of reverse-slip crenulations (RSC) would compensate for movement normal to the shear zone walls. This normal movement would result from movement on one S-surface becoming 'locked' and transferred to an adjacent S-surface. In the North Star Lake area this mechanism produced the F_2 structures.

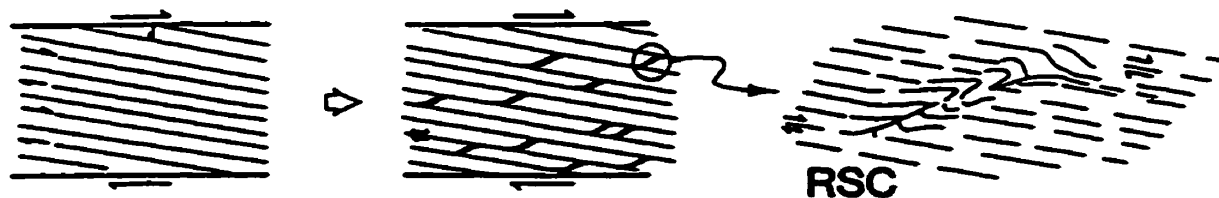


Figure 6-2. Development of reverse-slip crenulations (C) compensates for movement normal to shear-zone walls (S) where the original foliation is gently inclined clockwise to shear-zone movement direction; RSC: reverse-slip crenulations. (after Dennis and Secor, 1987).

The fold style of the F_2 structures is that of open to tight, parallel to similar geometry (class 1C to class 2 of Ramsey, 1967). The dominant process involved in the

development of folds during D_2 would have been flexural-flow (cf. Price and Cosgrove, 1990; Hatcher, 1990).

The second phase of deformation in the North Star Lake area was contemporaneous with the peak of metamorphism (M_2), therefore took place under high-grade metamorphic conditions. This would have resulted in rheological conditions similar to those of the first phase of deformation; high ductility rheology of the rocks in and reduced ductility contrast between individual layers of differing lithologies. The second phase of deformation, however, was affected by pervasive fabrics that developed during the first phases of deformation and metamorphism and resulted in increased intrinsic anisotropy of the rocks in the North Star Lake (cf. Ramsey and Huber, 1987). At similar temperature conditions, the ductility contrast between individual layers governs whether flexural-flow or passive-flow folds form (Donath and Parker, 1964).

The minor folds of the North--South zone (F_{2a}) are tight, similar to chevron, exclusively have Z-asymmetry and fold the compositional layering and S_1 foliation. The axial planes of these folds have an orientation similar to those of F_{2a} however, these folds plunge steeply in a southerly direction (Figure 4-1).

It is probable that the F_{2a} and the F_{2b} structures were contemporaneous. Both postdate the first phase of deformation (D_1) and were subsequently deformed during the third phase of deformation (D_3). A significant indication of the relationship

between the F_{2a} and F_{2b} structures is the North--South zone structural break that occurs in the North Star Lake area. F_{2a} structures occur to the west, while F_{2b} structures occur immediately to the east of this structural break. In mobile thrust belts folds and linear fabrics may be reoriented towards parallelism with the a -kinematic axis (Escher and Watterson, 1974; Williams and Zwart, 1977; Shackleton and Ries, 1984) however, this requires large shear strains (Skjernaa, 1980; Mies, 1993). The D_2 structures to the west of the North--South zone structural break have possibly undergone higher shear strains than those to the east of the structural break.

According to Syme et al. (1995) the North--South zone is the northerly extension of the West Reed--North Star shear zone. This shear zone can be traced northward from the Phanerozoic cover through the North Star Lake area to the Dow Lake area (Syme et al., 1995; Zwanzig, 1995a).

The West Reed--North Star shear zone is classified by Syme et al. (1995) as a post-peak of metamorphism structure (their D_{3a}). This D_{3a} shear zone correlates well with an earlier shear zone (their D_1) and deforms the earlier shear zone foliation (their S_1). This suggests that the strong anisotropy developed during D_1 localized the subsequent D_{3a} strain (Syme et al., 1995). This is similar to the interpretation of Zwanzig (1995a) who considers this structure in the Dow Lake area to be a high-strain zone that predated the development of

the regional foliation and peak of metamorphism.

The S_1 fabric described by Syme et al. (1995) is a penetrative grain-scale fabric that is parallel to centimetre- to metre-scale compositional layering; S_1 mylonites (*sensu lato*) have been recognized however, the subsequent D_2 fabric obscures much of the earlier fabrics. This is similar to the fabric described in the North--South zone of the North Star Lake area however, Syme et al. (1995) state that the D_1 shear fabrics are older than the isoclinal folds (their F_2) in the File Lake area.

In the North Star Lake area the earlier fabrics in the North--South zone are considered contemporaneous with the macroscopic D_1 fold (Face Lake synform; Figure 4-1) and the penetrative S_1 fabrics. This suggests that the North--South zone is possibly an attenuated long limb of the macroscopic D_1 fold that underwent dextral simple shear during D_2 . The northerly- to northeasterly-trending, gently- to moderately-plunging F_2 and L_2 fabric suggest that the North Star Lake area underwent continued non-coaxial strain during D_2 as a result of south--southwesterly-directed transport. M_2 mineral assemblages and F_2 fold style indicate that D_2 occurred at amphibolite facies conditions.

6.5 Third Deformational Event (D₃) and Third Metamorphic Event (M₃) in the North Star Lake Area

Examples of S₃ schistosity (coarse continuous cleavage) occur in micaceous felsic rocks in the area west of North Star Lake. This fabric is the result of recrystallization and is expressed as a preferred orientation of M₃ biotite and muscovite that define the XY-plane of the D₃ finite strain ellipsoid.

Well-developed examples of S₃ also occur in amphibolitic rocks that have a strong D₁ and/or D₂ foliation. In these rocks S₃ defines the D₃ XY-plane and is preserved as a upright to steeply-inclined crenulation cleavage that overprints the D₁/D₂ fabric. In such amphibolites F₃ is preserved as crenulate folds ≤ 1 cm in wavelength.

Crenulation cleavage (crenulate folds or microfolds) is the result of the formation of regular microfolds -- generally with a form close to similar (class 2 of Ramsey, 1967) in style -- in a pre-existing fine lamination or fabric. The wavelength of these microfolds is a function of the spacing of the pre-existing fabric; wavelengths in coarser grained rocks (schists and mica-rich gneisses) are approximately 1 cm, while those in finer grained rocks (phyllites, slates and shales) are approximately 1 mm (Ramsey and Huber, 1987).

Powell (1979) classified crenulation cleavage into either zonal or discrete types (Figure 4-4). The crenulation cleavage in the North Star Lake area is the zonal type with silicate-

rich (Phyllosilicate or inosilicate) domains (P-domains) and quartz-rich domains (Q-domains). Preferential solution and crystallization results in P-domains in the limb regions of the microfolds and Q-domains in the hinge areas (Barker, 1990). Zonal crenulation cleavage is common in both low- to medium-grade metamorphic rocks while discrete crenulation cleavage tends to be found only in low-grade metamorphic rocks (Barker, 1990).

The development of crenulation cleavage has been summarized by Barker (1990). This development begins with the initial microfolding or crinkling of a prior fabric. The initial stage is dominated by the deformation and rotation of phyllosilicate and/or inosilicate minerals. With further compression the crystallization of new phyllosilicate and/or inosilicate minerals parallel to the microfold axial surfaces become dominant. Further increase in strain tightens the microfolds and stress induced chemical potential gradients between the hinge and limb regions leads to the development of P-domains and Q-domains.

The variation in fold style exhibited by the F_3 structures is the result of differing response to deformation of different lithologies. The factor that greatly influences rock deformation style is anisotropy which is either the intensity and spacing of prior fabrics in the rock or the thickness of rock layers and the ductility contrast between those layers (Ramsey and Huber, 1987).

The F_3 structures in the North Star Lake area are interpreted to be buckle folds; the result of pure shear compression subparallel to layering in anisotropic or multilayered rocks (cf. Ramsey and Huber, 1987). The dominant mechanism involved in the formation of the F_3 structures is interpreted to be flexural-slip (cf. Price and Cosgrove, 1990; Hatcher, 1990). Locally tangential longitudinal strain folds occur (cf. Price and Cosgrove, 1990; Hatcher, 1990).

Ramsey and Huber (1987) discuss a model on fold morphology for buckle folds developed in single layers (Figures 6-3). In this model a competent layer (thickness d and viscosity μ_1) is embedded in a matrix with a viscosity μ_2 and infinite thickness. The minimum initial wavelength (W_i) is given by the following equation:

$$W_i = 2\pi d(\mu_1/6\mu_2)^{1/3}$$

It can be seen from this equation that the initial wavelength is directly proportional to the thickness of the competent layer and the cube root of the viscosity contrast between the competent and incompetent materials. The dependence of fold style on the viscosity contrast (μ_1/μ_2) on single layer buckle folds with competent layer thickness (d) constant is shown in Figure 6-4.

Ptygmatic folds commonly developed during D_3 in quartz veins that lie within the older S_1 foliation. These folds are

best developed in quartz veins in amphibolite. This fold style would result from a high viscosity contrast between the competent single layer (quartz vein) and the incompetent matrix (amphibolite) (Figure 6-3a).

During D_3 , cusped and lobate folds developed at the contacts between amphibolite dykes and the quartzo-feldspathic country rocks in the area west of North Star Lake. This indicates a low viscosity contrast between the quartzo-feldspathic country rock and the relatively incompetent amphibolite dykes (Figure 6-3b). In these situations the incompetent material forms the single layer; opposite to the situation shown in Figure 6-3b. The symmetry of the cusped and lobate folds are dependant upon the orientation of the amphibolite dyke relative to the X-Y plane of the D_3 finite-strain ellipsoid.

Open to tight, parallel, flexural-slip F_3 structures with wavelengths of approximately 1 m are preserved in layered mafic and felsic sequences. In unit 5 south of North Star Lake (Figure 3-2) the thicknesses of the felsic layers are approximately 1 m, and are less than the thicknesses of the relatively incompetent mafic layers. Flexural-slip occurred as a result of well-developed older fabric (S_1) in the felsic layers (cf. Price and Cosgrove, 1990). The fold morphology of the felsic layers is that of a single layer buckle fold with a moderate viscosity contrast between the competent felsic layer and the incompetent mafic matrix (Figure 6-4).

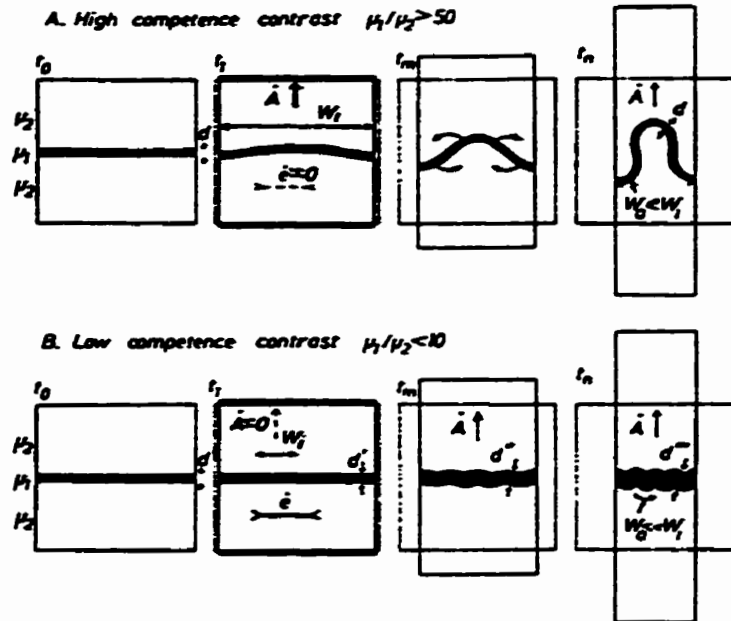


Figure 6-3. Theory of the progressive evolution of fold shapes in single competent layers (From Ramsey and Huber, 1987). W_i , initial dominant wavelength; W_n , arc length between adjacent like points; $\dot{\lambda}$, amplification rate; ϵ , layer-parallel shortening; d , layer thickness (from Ramsey and Huber, 1987).

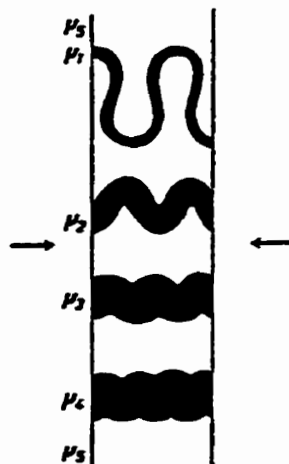


Figure 6-4. The spectrum of fold shapes produced by buckling a competent layer in a less competent host material; $\mu_1 > \mu_2 > \mu_3 > \mu_4 > \mu_5$ (from Ramsey and Huber, 1987).

Ramsey and Huber (1987) discuss six models on fold morphology for buckle folds developed independently of gravitational force in regularly alternating multilayers (Figure 6-5). The rock multilayers consist of an infinite stack of alternating competent layers (thickness d_1 and viscosity μ_1) and incompetent layers (thickness d_2 and viscosity μ_2). In these models the variation in fold morphology is dependant upon the viscosity contrast (μ_1/μ_2) and the ratio of incompetent to competent layer thickness ($n=d_2/d_1$).

The first model (Model A of Ramsey and Huber, 1987) has the conditions of a low ductility contrast (μ_1/μ_2) and a high ratio of incompetent to competent later thickness (n) (Figure 6-5a). The fold wavelength is small relative to the layer thickness and the rate of layer-parallel shortening ($\dot{\epsilon}$) initially predominates over the amplification rate ($\dot{\lambda}$). The high total layer-parallel shortening (ϵ) relative to total wave amplification (λ) resulted in the D_3 cusate-lobate folds described previously in single layer buckle fold theory.

Crenulate folds (microfolds) that developed in amphibolite during D_3 are characterized by a crenulation of a well-developed older fabric (S_1/S_2). Crenulate folds in the North Star Lake area that have not undergone significant solution and migration of mineral species have the form described in the second model (Model B) of Ramsey and Huber (1987). In this model the viscosity contrast (μ_1/μ_2) between

the competent and incompetent layers is low and the ratio of incompetent to competent layer thickness (n) is moderate (Figure 6-5b). A moderate value of n indicates that the incompetent and competent layer thicknesses are approximately equal. Folds developed under these conditions by layer-parallel shortening are harmonic. Because of the similarities in thickness and ductility between the thin amphibole-rich and quartzo-feldspathic layers the layers undergo similar modifications (slight thickening in hinge areas and slight thinning of limbs) and the fold style approaches that of the similar (class 2) fold.

In the North--South zone in layered felsic material minor irregular folds and a conjugate set of fractures occur. In the third model (Model C of Ramsey and Huber, 1987) the viscosity contrast (μ_1/μ_2) between the competent and incompetent layers and the ratio of incompetent to competent layer thickness (n) are low (Figure 6-5c). The initial wavelength is irregular and fold hinges tend to localise at layer contact irregularities. Strong layer-parallel shortening predominates over buckle fold development. The multilayer shows deformation approaching homogenous strain and fabrics commonly have a regular orientation (*i.e.* little cleavage refraction) throughout the multilayer. Commonly buckling may be insignificant and deformation occurs as conjugate shears.

Rare examples of harmonic D_3 folds occur in the North Star Lake area in layered mafic and felsic rocks. These D_3

folds are similar to those described in the fourth model (Model D) of Ramsey and Huber (1987). In this model the viscosity contrast (μ_1/μ_2) between the competent and incompetent layers and the ratio of incompetent to competent layer thickness (n) are high (Figure 6-5d). In a multilayer with these conditions there is little initial layer-parallel shortening and the amplification rate is high. The initial wavelength is large relative to the competent layer thickness and contact strain effects between adjacent competent layers results in a harmonic fold pattern. The competent layers usually have a parallel (class 1B) form while the incompetent layers have a class 3 form.

Chevron folds (F_3) have developed in micaceous quartzofeldspathic rocks that are characterized by a well-developed earlier schistosity. These folds have the form described in the fifth model (Model E) of Ramsey and Huber (1987). In this model the viscosity contrast (μ_1/μ_2) between the competent and incompetent layers is high and the ratio of incompetent to competent layer thickness (n) is moderate (Figure 6-5e). The amplification rate is high and layer-parallel shortening is low. The interaction between competent layers results in harmonic folds. Since there is limited incompetent material there is insufficient material for physical migration to produce a class 2 fold form in the incompetent layers; the result is that the folds in the multilayer are of a chevron style. Displacement is accommodated layer-parallel simple

shear in the incompetent layers.

Box folds (F_3) have overprinted the tectonic layering fabric of the banded intermediate to mafic rocks of the North--South zone. The process that results in conjugate kink folds (box folds) is described in the sixth model (Model F) of Ramsey and Huber (1987). In this model the viscosity contrast (μ_1/μ_2) between the competent and incompetent layers is high and the ratio of incompetent to competent layer thickness (n) is low (Figure 6-5f). During buckle folding the initial fold wavelength is poorly defined which results in fold axial surfaces oriented subperpendicular to the layering. Rotation takes place only in the areas where layering is non-parallel to the compressive stress. Within the kink zones layer-parallel simple shear takes place in the thin incompetent layers. The kinked limbs increase in strength by sideways migration and should the migration of one axial surface pass through the axial surface of its conjugate irregular chevron folds are produced.

In the Face Lake and Sausage Lake areas, on the limbs of earlier structures, the F_3 structures are commonly preserved as open folds with wavelengths that range from 1 m to several metres, fold the S_1/S_2 foliation and rotate the L_1/L_2 lineation. These flexural open folds are the result of minor layer-parallel compressive stress.

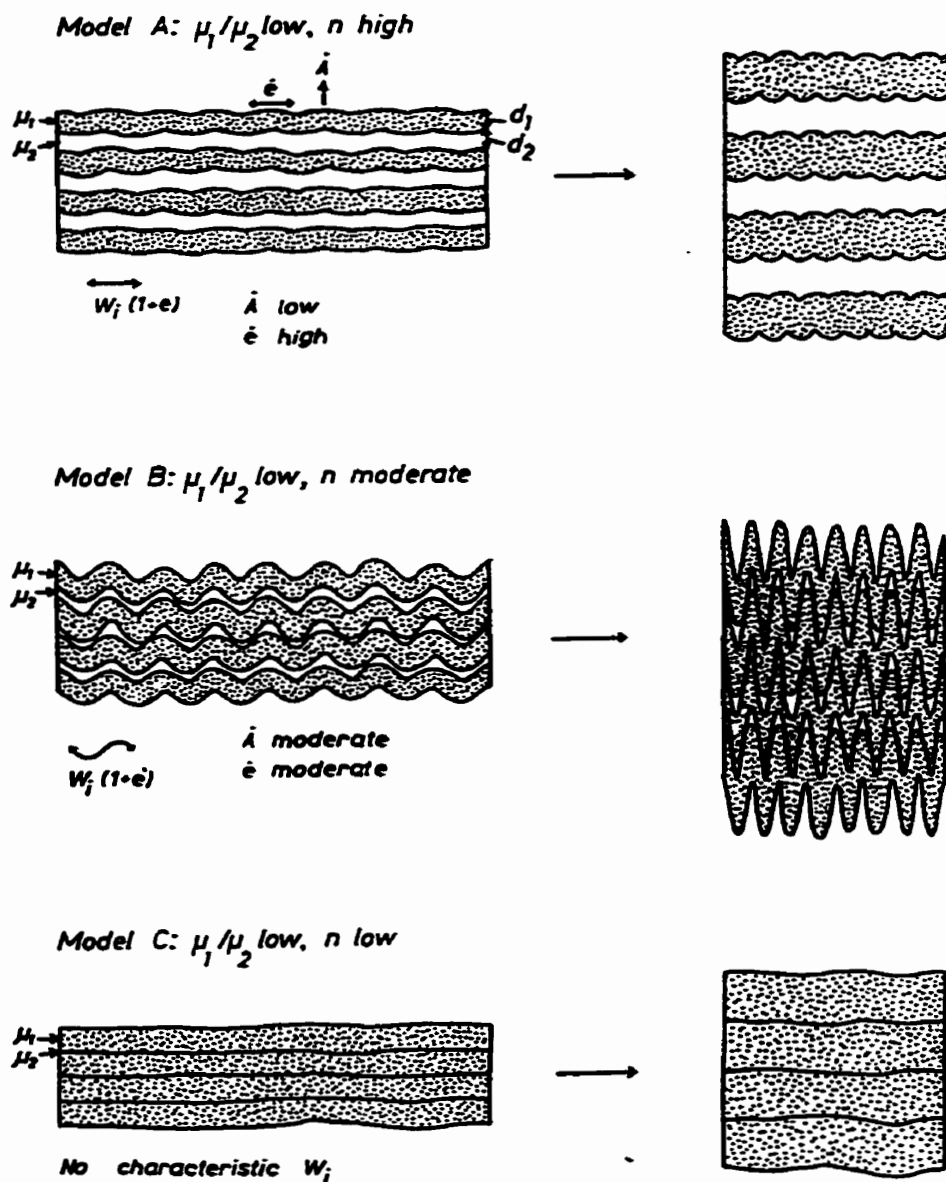
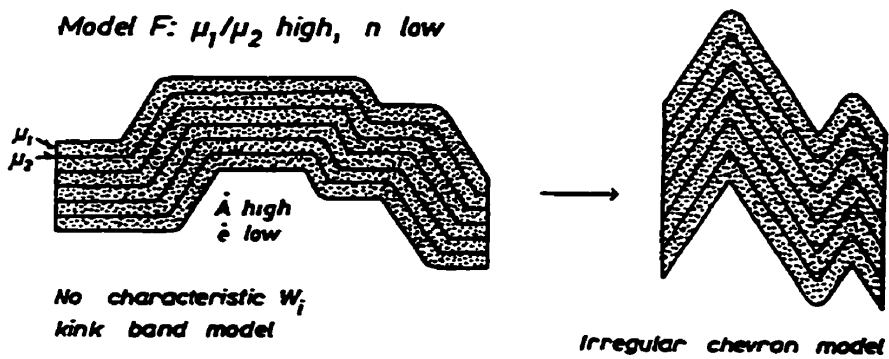
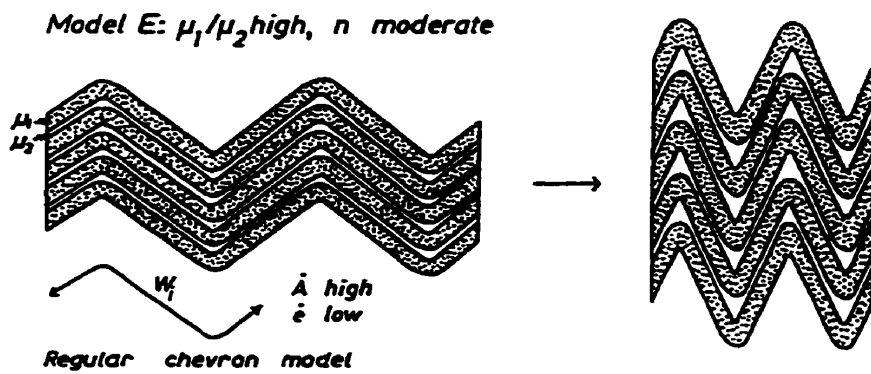
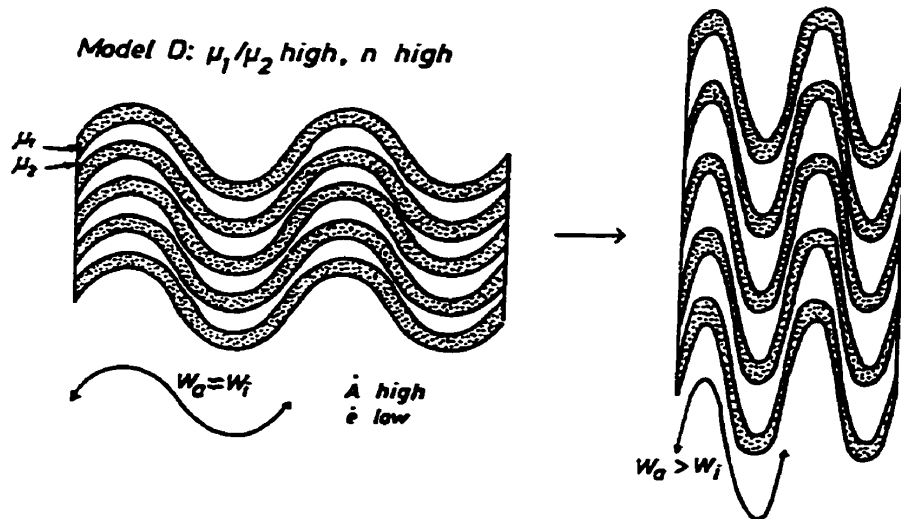


Figure 6-5. Models of folds developed in regularly alternating competent layers of thickness and viscosity d_1 , μ_1 and d_2 , μ_2 respectively and with $n = d_2/d_1$. W_i is the initial wavelength, \dot{A} is the buckle fold amplification rate, \dot{e} is the later parallel shortening rate, and e is the total layer parallel extension (from Ramsey and Huber, 1987). Continued on following page.



In the North Star Lake area D_3 structures and fabrics resulted from continued northeast--southwest compression. The F_3 structures developed approximately perpendicular to the southwest-directed movement direction however, non-coaxial strain was not great enough to result in the rotation of F_3 fold axes towards subparallelism with the transport direction (cf. Escher and Watterson, 1974; Williams and Zwart, 1977; Shackleton and Ries, 1984). The D_3 fabrics and structures developed under waning amphibolite facies metamorphic conditions.

6.6 Late Deformation and Metamorphism in the North Star Lake Area

Brittle to brittle--ductile faults and brittle conjugate fractures produced during the fourth phase of deformation (D_4) crosscut earlier fabrics and occur throughout the map area. These faults locally contain crush breccia, cataclasite and pseudotachylite.

The mineral growth associated with the fourth phase of metamorphism (M_4) is commonly confined to late brittle structures. Retrograde metamorphism was localized in these brittle structures probably due to the introduction of aqueous fluids. Locally, random-oriented retrograde M_4 metamorphic mineral growth occurred outside of the brittle structures.

Mineral assemblages produced during the M_4 retrograde metamorphism in the North Star Lake area suggest that pressure--temperature conditions were of greenschist facies. Temperatures during this metamorphic event were lower than the temperatures required for biotite stability.

A large, predominantly brittle fault zone transects the mapped area. This fault zone is north-trending, steeply-dipping and structures preserved within the fault zone indicate sinistral movement. The north--south orientation of this sinistral fault zone indicates that the North Star Lake area underwent northwest--southeast compression during the fourth phase of deformation.

CHAPTER VII
DISCUSSION AND CONCLUSIONS

7.1 The Structural and Metamorphic Evolution of the North Star Lake Area Within the Context of the Trans-Hudson Orogen

The eastern portion of the Flin Flon domain -- which includes the North Star Lake area -- and the adjacent southern flank of the Kiseynew domain have undergone progressive deformation (Krause and Williams, 1995; Norman et al., 1995; Connors, 1996) as defined by Tobisch and Paterson (1988). This progressive deformation was coeval with a prograde--retrograde metamorphic cycle that occurred over a period of 30 Ma (Norman et al., 1995) and was contemporaneous with the development of collisional thrusts during the period of 1.83--1.80 Ga that resulted in the Amisk collage overthrust by the Kiseynew domain and the Snow Lake arc segment (Lucas et al., 1996).

Progressive deformation paths (first defined by Flinn, 1962) may be recognized by the refolding and reorientation of folds in shear zones; a process dominated by non-coaxial deformation (Bell, 1978; Mawer and Williams, 1991). In ductile shear zones the rotation of linear fabrics to near-parallelism with the a -kinematic axis requires large shear strains (Skjerna, 1980; Mies, 1993). In mobile thrust zones, fold axes may be reoriented to near-parallelism with extension lineations and the direction of transport (Escher and Williams, 1974; Shackleton and Ries, 1984).

Seismic reflection data collected by the LITHOPROBE program across the Trans-Hudson Orogen of Manitoba and Saskatchewan has produced images of the Flin Flon and Kisseynew domains (internal zone of the Reindeer zone) juxtaposed against the Archean Superior craton. The internal zone has undergone crustal-scale or "thick-skinned" deformation that has resulted in substantial crustal shortening (White et al., 1994).

This thesis and other recent work on the southern flank of the Kisseynew domain and the eastern portion of the Flin Flon domain (Figure 7-1) has produced new geological data (Zwanzig and Schledewitz, 1992; Krause and Williams, 1994a, 1994b, 1995; Ryan and Williams, 1994, 1995; Syme et al., 1995; Norman et al., 1995; Zwanzig, 1995a; Connors, 1996) and allows for an attempt at correlation on the metamorphic and structural evolution of the area (Tables 7-1 and 7-2).

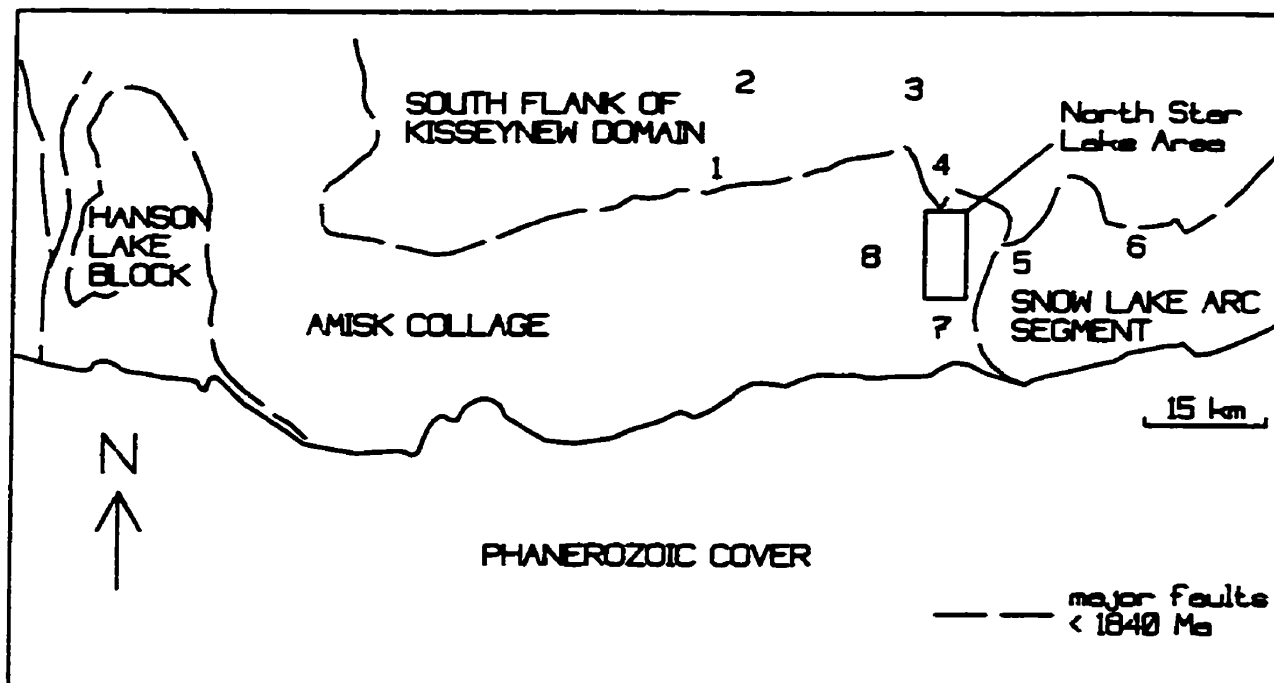


Figure 7-1. Location of areas of recent studies in the eastern portion of the Flin Flon domain and the southern flank of the Kiseynew domain. 1) Kiseynew--Cleunion Lakes area; 2) Kississing Lake area; 3) Batty Lake area; 4) Dow Lake area; 5) File Lake area; 6) Snow Lake area; 7) Reed Lake area; 8) Elbow Lake area.

Early deformation

Accretion of Flin Flon domain

1.88--1.87 Ga

Initial movement on North--South zone?

Gants Lake batholith

1.87--1.85 Ga

First phase of deformation (D₁) and first phase of metamorphism (M₁)

South--southwest-directed transport

Development of regional foliation during amphibolite facies-grade metamorphism.

Development of isoclinal, passive-flow folds and reorientation of fold axes and linear fabrics near-parallel to X-axis of finite strain ellipsoid.

Reorientation of foliation and fold axial planes near-parallel to XY-plane of finite strain ellipsoid.

Dextral (?) movement on North--South zone.

Norris Lake pluton

1.83 Ga

Second phase of deformation (D₂) and second phase of metamorphism (M₂)

Continued south--southwest directed transport

Amphibolite facies-grade metamorphism. Peak metamorphism (M₂) 1820--1805 Ma.

Development of open to tight, flexural-flow folds and reorientation of fold axes and linear fabrics near-parallel to X-axis of finite strain ellipsoid.

Reorientation of fold axial planes near-parallel to XY-plane of finite strain ellipsoid.

Dextral movement on North--South zone.

Third phase of deformation (D₃) and third phase of metamorphism (M₃)

Northeast--southwest compression

Development of open to tight flexural-slip folds perpendicular to compression.

Local expression of amphibolite facies-grade metamorphism.

Fourth phase of deformation (D₄) and fourth phase of metamorphism (M₄)

Northwest--southeast compression

North-trending, sinistral regional fault zone.

Local expression of greenschist facies-grade metamorphism.

Table 7-1. Structural and metamorphic history of the North Star Lake area.

Cleunian-- Kisseynew Lakes area (Norman et al., 1995)	Kississing--Batty Lakes area (Zwanzig and Schledewitz, 1992)	File Lake area (Connors, 1996)	Reed (Syme 1995)
D ₁ --M ₁ Intra-arc rifting 1836--1827 Ma.	D ₁ Pre-Missi deformation	D ₁ Accretion of volcanic terranes 1880--1870 Ma.	D ₁ Early West Star (1870)
D ₂ --M ₂ Hudsonian orogeny 1827--1800 Ma. Southwestward shortening. Prograde-- retrograde metamorphic cycle.	D ₂ --D ₃ Southerly to southwesterly transport. Prograde-- retrograde metamorphic cycle.	D ₂ Southwest-directed fold thrust belt. 1841--1805 Ma.	D ₂ Colli defor
F ₁ isoclinal folds.	D ₂ Early fold nappes, southerly transport.	D _{2a} 1841--1832 Ma. Isoclinal folds and thrust faults.	D _{2a} Contr Kisse <1842
F ₂ tight to isoclinal folds. M ₂ peak (1818 Ma).	D ₂ Pre- to peak- metamorphism.	Calc-alkaline plutons (1832 Ma).	Reed (1830)
F ₃ tight folds. Retrograde metamorphism.	D ₃ Recumbent to reclined folds. Southwesterly transport.	D _{2b} Continued folding and faulting. Peak metamorphism (1820--1805 Ma).	D _{2b} Colli exot block Peak (1820)
F ₄ parallel folds.	Peak- to late- metamorphism (1815 Ma).	D _{2c} Backfolding near Amisk and Kisseynew contact.	Reed (1830)
D ₃ East--west shortening. Conjugate kink bands.	D ₃ Northwest-- southeast compression. Waning metamorphism.	D ₃ Northwest-- southeast shortening. 1805--1800 Ma.	D ₃ Colli Super (<1810 React West Star
D ₄ Brittle deformation.		D ₄ Brittle--ductile faulting.	D ₄ --D ₅ Post- transp (1800-

Table 7-2. Struc
proximal to the



Lake area
et al.,
)

deformation;
Reed--North
shear zone.
--1840 Ma).

sional
nation.

action of
new basin
-->1840 Ma.

lake pluton
Ma).

ion with
c' Archean
(<1830).
etamorphism
-1805 Ma).

ion with
or craton
Ma).
vation of
eed--North
hear zone.

ollision
ression
-1700 Ma).

ural and metamorphic characteristics of areas
North Star Lake area.

Dow Lake area
(Zwanzig, 1995a)

D₁
Intermittent
terrane fragment
assembly.

D₂
Tectonic burial
of Flin Flon
domain.
Metamorphic peak.

D₃--D₄
Uplift and
continued
convergence.

D₃
Southwest-verging,
folds.

D₄
Open east--
northeast-trending
arch.

Snow Lake area
(Krause and
Williams, 1994a;
1994b; 1995)

D₁--D₂
Convergence of
Flin Flon and
Kisseynew domains.

D₁
Isoclinal folds
and related
southwest-directed
thrusting
(<1836 Ma).

D₂
Isoclinal folds,
Southwest-directed
thrusting.
Peak metamorphism
(1810 Ma).

D₃
Collision with
Superior craton.
Large scale folds.

D₄
Waning stages of
convergence.

Elbow Lake area
(Ryan and Williams,
1994, 1995)

D₁
Early accretionary
complex (<1876 Ma).

D₂
Magmatic-arc
(1876--1845 Ma).

D₃
Continentalization
(1835--1800 Ma).
Peak metamorphism
(1820--1810 Ma).

D₄
Segmentation of Flin
Flon domain (<1800
Ma).



7.1.1 Early Deformation

Early in its history The North Star Lake area -- as part of the volcano-plutonic assemblage of the Flin Flon domain -- underwent amalgamation into an accretionary complex. This amalgamation (described by Lucas et al., 1996) occurred during the period of 1.88--1.87 Ga. The accretionary complex was intruded by magmatic-arc plutons -- such as the 1.87--1.85 Ga Gants Lake batholith (cf. Whalen, 1993)-- and unconformably overlain by volcanic and sedimentary rocks during the period of 1.87--1.84 Ga (Lucas et al., 1994a; 1996). Magmatic-arc plutons -- such as the ca. 1.83 Ga Norris Lake pluton (cf. Connors, 1996) -- were emplaced during the arc magmatism of the Snow Lake arc segment during the period of 1.84 to 1.83 Ga (Lucas et al., 1994a). Heat advected into the accretionary complex by the plutonism associated with the arc magmatism resulted in extensive contact metamorphism (Lucas et al., 1996).

The amalgamation of the accretionary complex and the development of post-accretion magmatic-arc resulted in steeply-dipping stratigraphy and structures in the North Star Lake area prior to the plutonism related to the arc magmatism (cf. Lucas et al., 1996). Field evidence in the low-grade areas of the Amisk Collage suggests that early structures and fabrics would have been steepened prior to the development of the magmatic-arc (Lucas et al., 1996). Early deformation in the Flin Flon domain has been documented in the areas proximal

to the North Star Lake area (Ryan and Williams, 1994, 1995; Syme et al., 1995; Zwanzig, 1995a).

Ryan and Williams (1994, 1995) have described an early shear foliation in the Elbow Lake area that predates the contact metamorphism associated with the intrusion of magmatic-arc plutons. Syme et al. (1995) regard the southern extension of the North--South zone in the Reed Lake area as an early shear zone. This structure -- which they refer to as the West Reed--North Star shear zone -- extends northward from the Reed Lake area through the North Star Lake area to the Dow Lake area (Zwanzig, 1995a). In the Reed Lake area the West Reed--North Star shear zone appears to be synmagmatic and therefore probably was active during the 1.87--1.84 Ga post-accretion magmatic-arc system (Syme et al., 1995). In the Dow Lake area the early fabrics within the shear zone have been annealed, indicating a pre-peak metamorphism age for the initial movement in the zone (Zwanzig, 1995a).

Zwanzig and Schledewitz (1992) have described an early deformation in the southern flank of the Kisseynew domain that steepened stratigraphy and the margins of early plutons. This deformation occurred prior to the deposition of the 1.85--1.83 Ga Missi Group fluvial--alluvial sediments. An early high-temperature deformational and metamorphic event in the southern flank of the Kisseynew domain is described by Norman et al. (1995) and is interpreted by those workers to have been the result of extension in an intra-arc basin.

7.1.2 Collision Tectonics, Deformation and Metamorphism

Progressive deformation in the North Star Lake area occurred as a southwest-directed compressive deformation (D_1 -- D_3) associated with a prograde--retrograde metamorphic cycle (M_1 -- M_3), similar to the deformation and metamorphism described in the eastern portion of the Flin Flon domain (Krause and Williams, 1994a, 1994b, 1995; Connors, 1996) and on the southern flank of the Kisseynew domain (Zwanzig and Schledewitz, 1992; Norman et al., 1995). This progressive deformation was the result of collision tectonics achieved by the contraction of the Kisseynew basin in a southwest-directed fold--thrust belt and its subsequent overthrusting of the Flin Flon domain volcano-plutonic terrane (Zwanzig and Schledewitz, 1992; Norman et al., 1995; Connors, 1996). On the southern flank of the Kisseynew domain southwest-directed compressive deformation began approximately 1830 Ma with peak of metamorphism occurring at approximately 1818 Ma (Norman et al 1995). Southwest-directed thrusting and continued until approximately 1805 Ma (Connors, 1996).

Partitioning of deformation resulted in a concentration of non-coaxial strain along the boundary of the Flin Flon and Kisseynew domains (Norman et al., 1995; Connors, 1996) and in eastern portion of the Flin Flon domain (Krause and Williams, 1994a, 1994b, 1995; Connors, 1996); immediately north and east of the North Star Lake area, respectively. Seismic reflection profiles of the Trans-Hudson Orogen in Manitoba and

Saskatchewan obtained from the LITHOPROBE program data are interpreted as a series of stacked thrust sheets essentially confined to the crust (Lucas et al., 1994). On the southern flank of the Kiseynew domain seismic reflections are interpreted by Lucas et al. (1994) as a stack of thrust sheets and fold nappes with a major footwall ramp at the northern margin of the Flin Flon domain. The structures that juxtapose the Flin Flon and Kiseynew domains are interpreted to have been localized near the ancestral Kiseynew sedimentary basin margin (Lucas et al., 1994; Norman et al., 1995; Connors, 1996).

On the southern flank of the Kiseynew domain, a south-to southwest-directed, progressive, compressive deformation cycle was coeval with a prograde--retrograde metamorphic cycle (Zwanzig and Schledewitz, 1992; Norman et al., 1995). In the heterogeneous non-coaxial model of Norman et al. (1995) the progressive compressive deformation cycle on the southern flank of the Kiseynew domain produced a succession of folds. The heterogeneous non-coaxial strain produced folds whose axes were originally oriented approximately perpendicular to the southwest-directed movement direction and with progressive deformation the fold axes were reoriented by transposition towards parallelism with this movement direction (cf. Sanderson, 1973; Escher and Watterson, 1974). Younger folds in low-strain domains are more open and less reoriented towards parallelism than older folds while in high-strain domains

transposition is more advanced and most folds approach parallelism (cf. Williams and Zwart, 1977). In the model of Norman et al. (1995) the heterogeneous non-coaxial strain path for the Kiseynew gneisses had a southwesterly movement direction over the Flin Flon domain. The Flin Flon domain is interpreted by Norman et al. (1995) to have behaved as a relatively rigid block. In the Kiseynew domain the high-strain domain is proximal to the contact with the Flin Flon domain while the intermediate- and low-strain domains are further removed (Norman et al., 1995).

The contact between the Kiseynew metasedimentary rocks and the Amisk volcano-plutonic assemblage lies along early (≥ 1.83 Ga) faults (Syme et al., 1995; Zwanzig, 1995a; Connors, 1996). In the Dow Lake and the File Lake areas (Figure 7-2) this contact lies along the Loonhead Lake fault (Connors, 1996; Zwanzig, 1995a). In the File Lake area this contact is also located along the Morton Lake fault (Syme et al., 1995; Connors, 1996) and the Woosey fault (Connors, 1996).

The Loonhead Lake fault and early folds are the earliest post-Missi structures in the Dow Lake area and predate the development of the regional foliation (Zwanzig, 1995a). Initial movement on the fault possibly transported older Amisk rocks to the north or east over Kiseynew basin rocks and the fault was subsequently overturned during later deformational events (Zwanzig, 1995a, 1995b). Syme et al. (1995) correlate

the Morton Lake fault zone with the early fabrics and isoclinal folds in the Reed Lake and the southern File Lake areas (Figure 7-3) and interpret these structures to be the result of the closure of the Kisseynew basin at approximately 1.84 Ga. The Morton Lake fault zone is considered to be the bounding structure between the Amisk collage and the Snow Lake arc segment (Lucas *et al.*, 1996) and therefore originated during the 1.88--1.87 Ga accretionary stage of the Flin Flon domain and was subsequently reactivated during the *ca.* 1.84 Ga closure of the Kisseynew basin. Connors (1996) considers the Morton Lake and Loonhead Lake faults to be south-verging thrusts of the same deformational event.

In the Snow Lake arc segment the initial imbrication of the 1.85 Ga Kisseynew turbidites with the older volcano-plutonic assemblages occurred prior to the onset of the 1.84--1.83 Ga magmatism (Connors, 1996). Early folds in the Snow Lake arc segment and the southern flank of the Kisseynew domain are isoclinal and predate the peak of metamorphism (Krause and Williams, 1994a; 1994b; 1995; Norman *et al.*, 1995; Connors, 1996).

In the North Star Lake area the initial southerly- to southwesterly-directed deformation (D_1) produced tight to isoclinal folds (F_1) with well-developed axial-planar foliation (S_1). F_1 fold axes were reoriented towards parallelism with the northerly-trending, gently-plunging L_1 fabric and the southerly- to southwesterly-directed transport

direction. D_1 predated the ca. 1.83 Ga Norris Lake pluton as seen the random orientation of S_1 fabrics in xenoliths within the pluton.

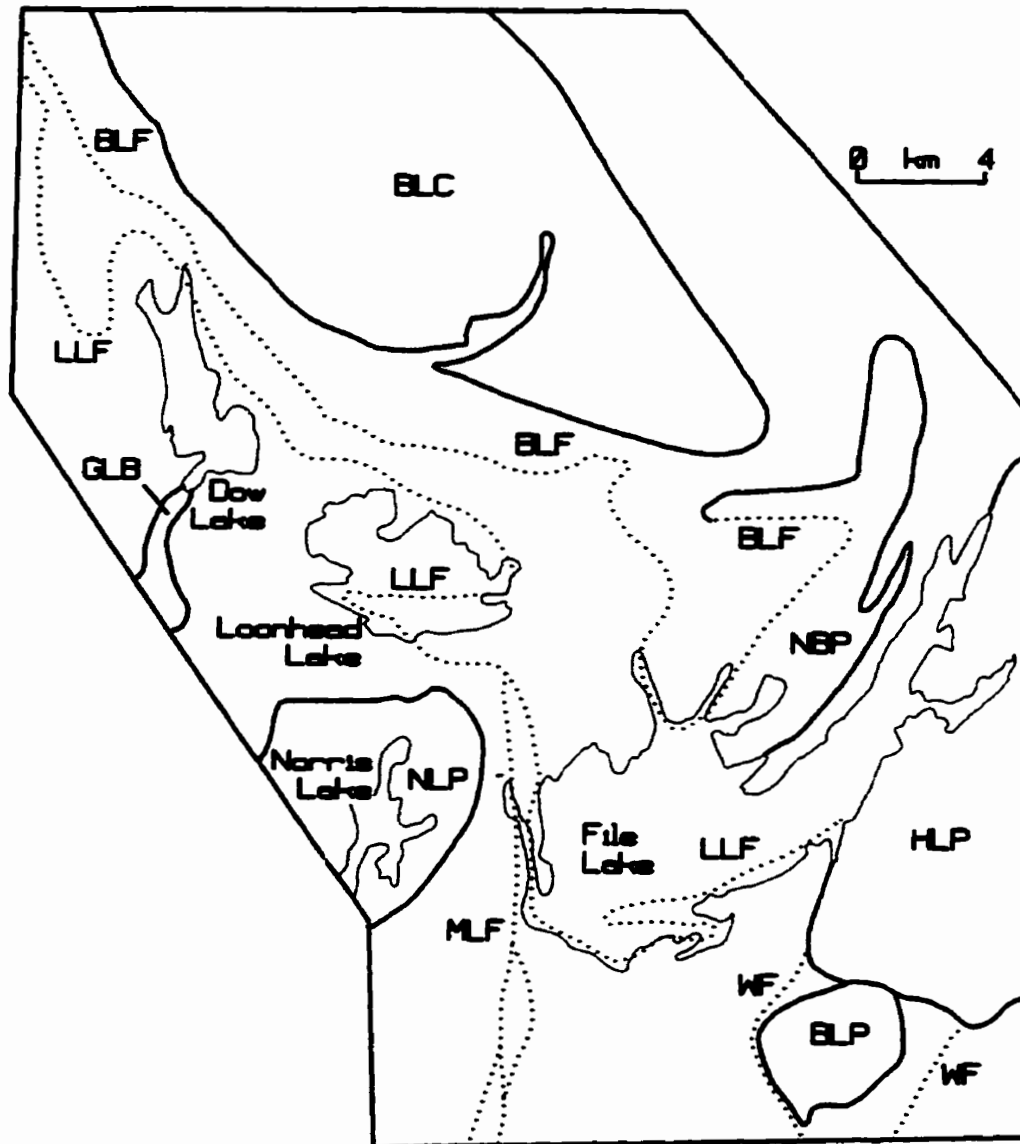


Figure 7-2. Dow Lake and File Lake areas (after Connors, 1996). Dotted line, early (≥ 1830 Ma) faults; BLF, Beltz Lake fault; LLF, Loonhead Lake fault; MLF, Morton Lake fault; WF, Woosey fault; BLC, Batty Lake complex; GLB, Gants Lake batholith; NLP, Norris Lake pluton; NBP, Nelson Bay pluton; HLP, Ham Lake pluton; BLP, Barron Lake pluton.

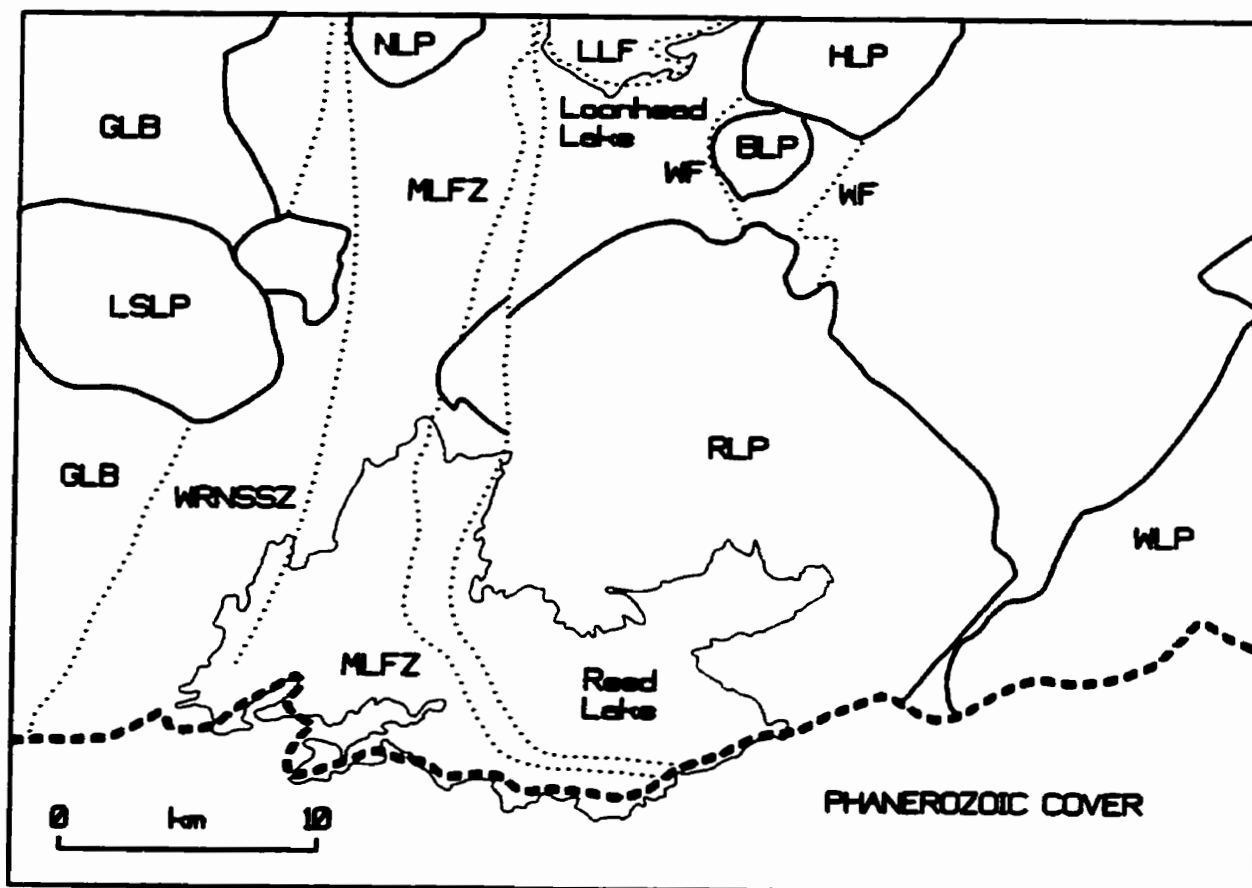


Figure 7-3. Reed Lake and southern File Lake areas (after Syme et al., 1995). Dotted line, early (≥ 1830 Ma); WRNSSR, West Reed--North Star shear zone; MLFZ, Morton Lake fault zone; LLF, Loonhead Lake fault; WF, Woosey fault; GLB, Gants Lake batholith; LSLP, Little Swan Lake pluton; HLP, Ham Lake pluton; BLP, Barron Lake pluton; RLP, Reed Lake pluton; WLP, Wekusko Lake pluton.

At the time of the peak of metamorphism southwest-directed progressive deformation continued along the southern flank of the Kisseynew domain (Zwanzig and Schledewitz, 1992; Norman et al., 1995) and eastern portion of the Flin Flon domain (Krause and Williams, 1994a; 1994b; 1995; Connors,

1996). In the northern portion of the eastern Flin Flon domain -- proximal to the contact with the Kisseynew domain -- the dominant regional foliation was produced at this time, whereas in areas to the south the dominant regional foliation predates the peak of metamorphism (Zwanzig, 1995a; Connors, 1996.) The dominant regional foliation in the northern portion of the eastern Flin Flon domain is interpreted to be the result of high-temperature protracted ductile deformation under mid-crustal conditions (Zwanzig, 1995a). Folds produced at this time contain a well-developed, gentle east- to northeast-plunging lineation (Zwanzig, 1995a; Connors, 1996). A regional fault (Fairwind Lake--Beltz Lake fault) produced at this time is interpreted to be a southwest-verging structure (Connors, 1996).

In the North Star Lake area (F_2) folds that are approximately contemporaneous with the peak of metamorphism (M_2) fold the older regional foliation (S_1). West of the North--South zone structural break F_2 fold axes (F_{2a}) and the contemporaneous extension lineation (L_{2a}) have gentle northerly-plunges suggesting that they have been rotated towards parallelism with the earlier F_1 fold axes and the south--southwest transport direction. F_2 fold axes to the east of the North--South zone structural break (F_{2b}) are less evolved and have steep southerly-plunging fold axes.

The F_3 structures in the North Star Lake area postdate the peak of metamorphism however, these folds are interpreted

to be the result of continued southwest-directed transport. Similar deformation occurred on the southern flank of the Kisseynew domain (Norman et al., 1995) and in the eastern portion of the Flin Flon domain (Krause and Williams, 1994a; 1994b; 1995). Backfolding along the faulted Flin Flon--Kisseynew boundary occurred in the File Lake area during the waning stages of southwest-directed deformation (Connors, 1996).

Subsequent to the southwest-directed progressive deformation and the associated prograde--retrograde metamorphic cycle the Flin Flon and Kisseynew domains underwent northwest--southeast to east--west compression (Zwanzig and Schledewitz, 1992; Norman et al., 1995; Syme et al., 1995; Connors, 1996). This switch from southwest-directed transport to northwest--southeast compression is possibly the result of the collision of the Reindeer zone with the Superior craton (Krause and Williams, 1994a, 1994b; Syme et al., 1995). The Flin Flon and Kisseynew domains underwent ductile to brittle deformation under waning-metamorphic conditions (Zwanzig and Schledewitz, 1992; Ryan and Williams, 1994, 1995; Norman et al., 1995; Syme et al., 1995; Connors; 1996). In the North Star Lake area the northwest--southeast compression resulted in brittle--ductile to brittle faults. These <1800 Ma structures played a significant role in the segmentation of the Flin Flon and Kisseynew domains (Lucas et al., 1994).

7.2 Conclusions

The North Star Lake area lies within the Flin Flon domain that, along within the southern flank of the Kisseynew domain, is part of the internal zone of the Reindeer zone of the Trans-Hudson Orogen. The structural and metamorphic evolution of the North Star Lake (Table 7-1) area can be correlated with the structural and metamorphic evolution of the eastern portion of the Flin Flon domain and the southern flank of the Kisseynew domain (Table 7-2).

The initial deformation in the North Star Lake area was the result of the accretion of the Flin Flon domain. This initial deformation (described by Lucas *et al.*, (1996)) juxtaposed the juvenile arc assemblages of the Flin Flon domain, by intraoceanic tectonics during the period of 1.88--1.87 Ga, into an accretionary complex prior to the deposition of continental and marine sediments during the period of 1.86--1.84 Ga and the emplacement of 1.87--1.83 Ga calc-alkaline plutons.

The result of the initial deformation in the North Star Lake area was the steepening of the stratigraphy. The primary layering would have been steep-dipping prior to the emplacement of the 1.87--1.85 Ga Gants Lake Batholith and the development of the associated contact aureole. Structures that were the result of the initial deformation were not observed in the North Star Lake area because of intense later deformation and metamorphism.

In the North Star Lake area a progressive deformation cycle (D_1 -- D_3) and a contemporaneous prograde--retrograde metamorphic cycle (M_1 -- M_3) occurred subsequent to the initial deformation. The North Star Lake area underwent progressive deformation as a result of south--southwest-directed thrusting associated with the closure of the Kisseynew basin and the overthrusting of the Amisk collage by the Kisseynew domain and the Snow Lake arc segment. Progressive deformation commenced prior to the emplacement of the ca. 1.83 Ga Norris Lake pluton.

The prograde--retrograde metamorphic cycle in the North Star Lake area followed a clockwise, medium-pressure (Barrovian type) P--T--t path with maximum pressure predating maximum temperature. Peak metamorphism (M_2) is associated with the second phase of deformation (M_2) and culminated at medium-pressure amphibolite facies conditions. Peak metamorphism would have occurred at approximately 1.820--1.805 Ga, similar to areas proximal to the North Star Lake area.

The progressive deformation cycle in the North Star Lake area produced a succession of folds (F_1 -- F_3) which initially formed perpendicular to the south--southwest-directed movement vector. The fold axes of early folds (F_1 and F_2) and the linear fabrics of early phases of deformation (L_1 and L_2) were reoriented towards parallelism with the transport direction. Later folds (F_3) are less evolved and therefore did not reorient toward parallelism with the transport direction.

The final deformation (D_4) in the North Star Lake area produced brittle--ductile to brittle structures. This deformation occurred under greenschist facies conditions in a northwest--southeast compressive stress regime.

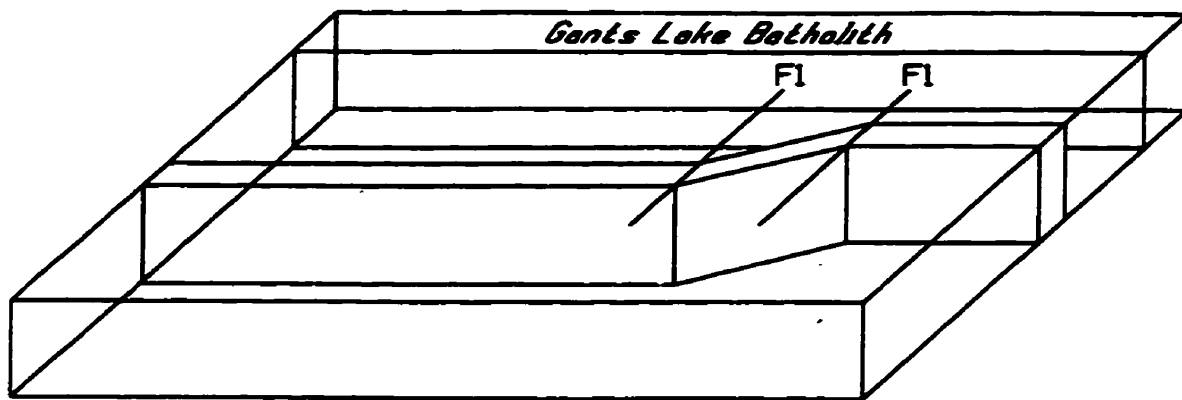
During the first phase of deformation (D_1) in the North Star Lake area (Figure 7-4) folds (F_1) initially developed perpendicular to the south--southwest transport-direction (Figure 7-4a). The D_1 linear structures (fold axes and lineations) were subsequently reoriented by non-coaxial strain towards parallelism with the direction of transport (Figure 7-4b). Primary layering and planar fabrics were transposed during D_1 towards parallelism with the XY-plane of the finite-strain ellipsoid and linear fabrics define the X-axis. The XY-plane of the finite-strain ellipsoid is subparallel to the thrust plane that occurred in the area of the North--South zone. In plan view this plane is oriented parallel to the dextral shear couple and the maximum principle stress is oriented parallel to the transport direction (Figure 7-4c).

The dominant regional foliation (S_1) developed during the first phase of deformation (D_1) and the contemporaneous first phase of metamorphism (M_1) and was the result of recrystallization and metamorphic differentiation during medium-pressure amphibolite facies conditions. Transposition of the primary layering (S_0) occurred locally in the hinge areas of F_1 structures. An L--S fabric developed at this time

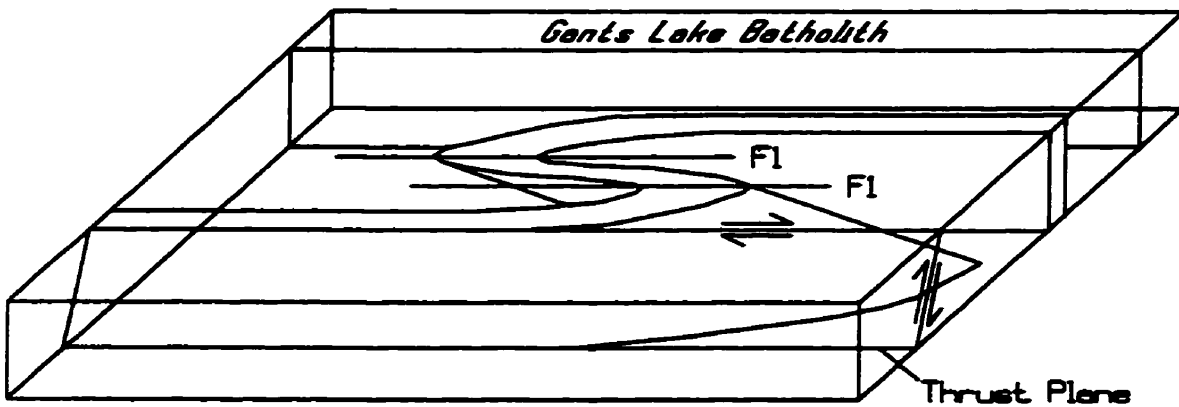
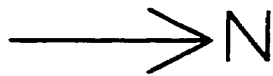
by recrystallization of mineral grains and distortion of primary features.

The North--South zone has been interpreted in the Reed Lake area as an early (>1.87 Ga) shear zone (Syme et al., 1995) and has been extrapolated to the Dow Lake area (Zwanzig, 1995a). It is unclear if the North--South zone is the continuation of the structure referred to by Syme et al. (1995) as the West Reed--North Star shear zone or a D_1 thrust plane and attenuated limb of the D_1 Face Lake synform. The orientation of the early fabrics within the North--South zone and the orientation of the (D_1) extension lineations and F_1 fold axes west of the North--South zone suggest that the eastern portion of the North Star Lake area overthrust the western portion (Figure 7-4b). This is consistent with the Amisk collage overthrust by the Snow Lake arc segment (described by Lucas et al., 1996).

The folds that developed during D_1 are tight to isoclinal, similar style folds that were the result of passive-flow. These passive-flow folds were the result of low ductility contrast between layers during deformation. The low ductility contrast was a result of the high-grade conditions and the low intrinsic anisotropy (paucity of prior fabric) of the rocks at the that time.



a)



b)

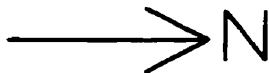
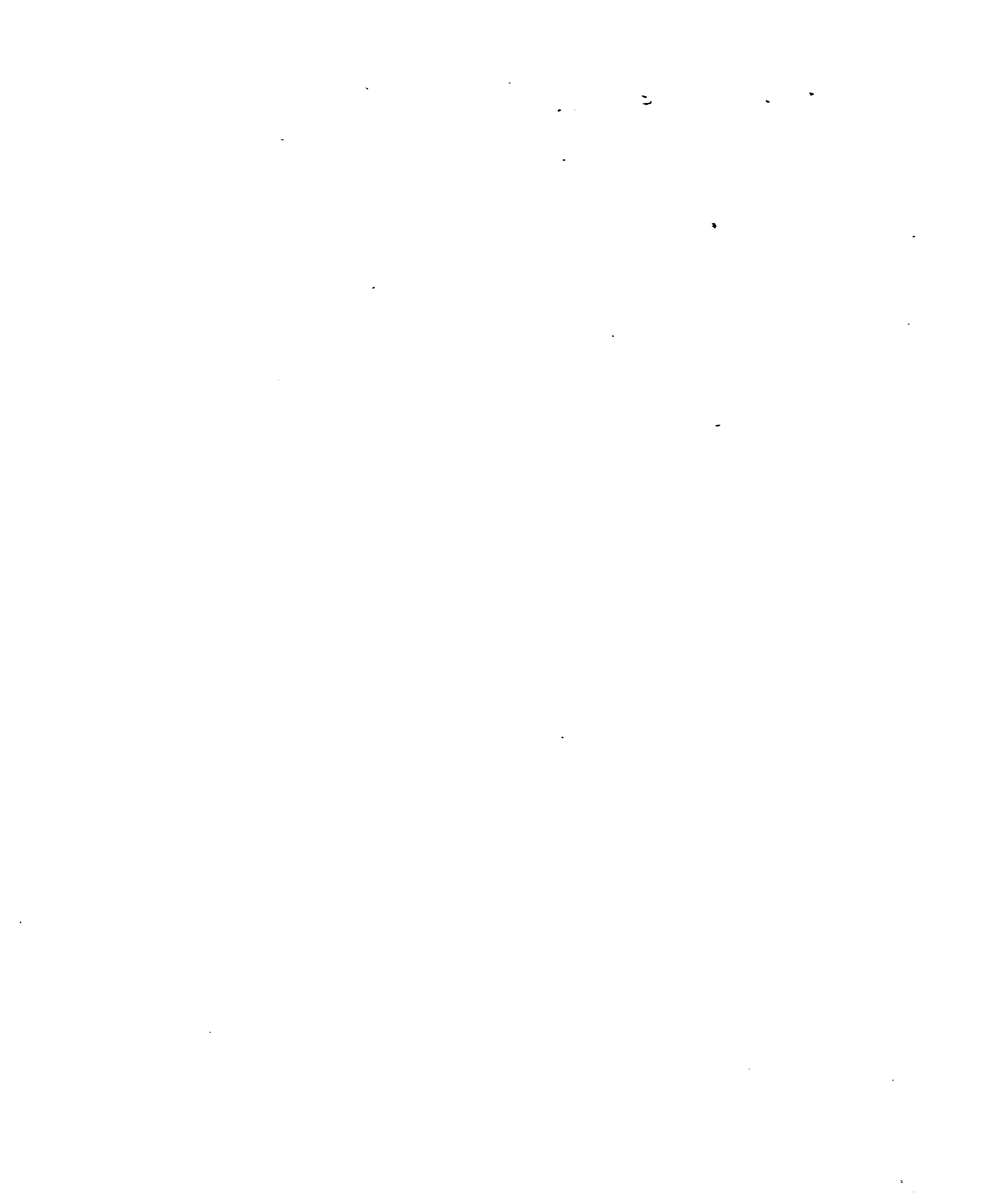
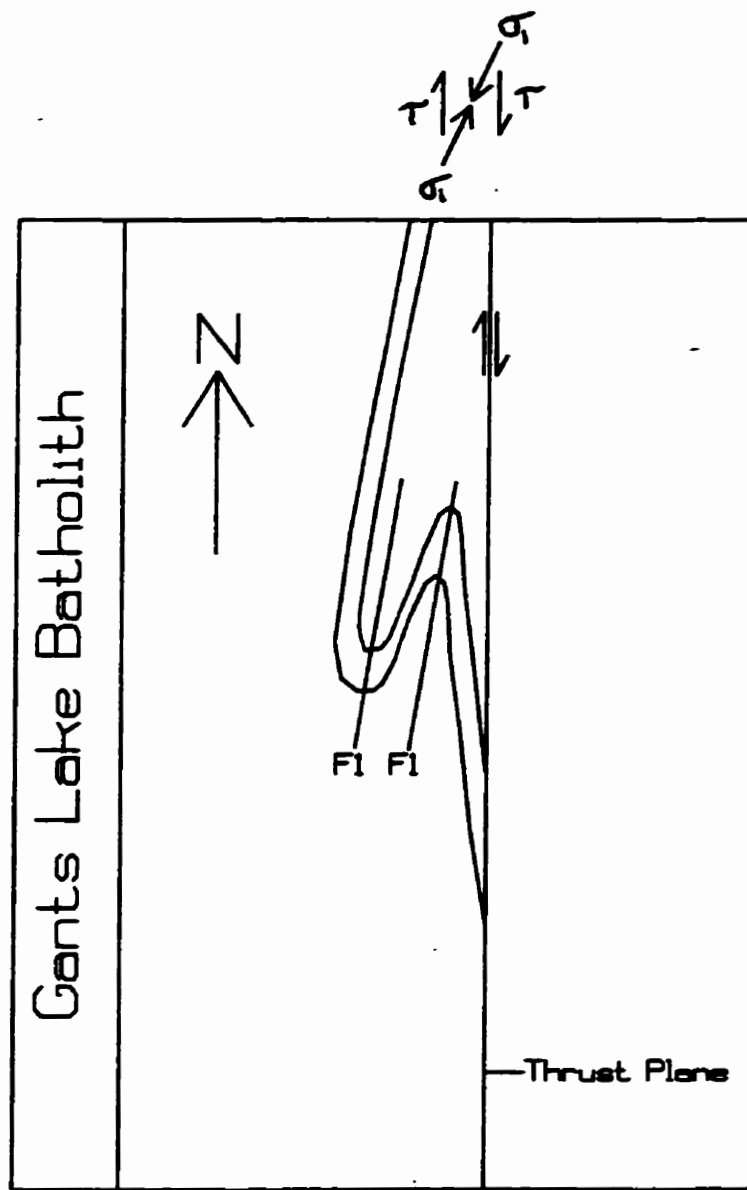
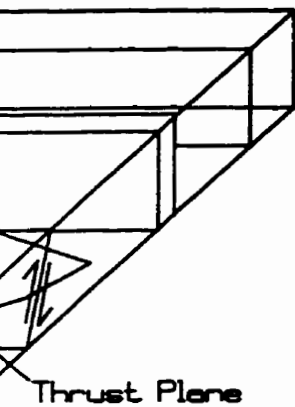
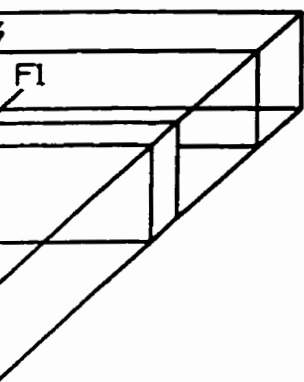


Figure 7-4. Diag area during the first phase of deformation. c) first phase of principle stress





c)

Figure 7-4. Diagram of the development of the North Star Lake area during the first phase of deformation. a) beginning of first phase of deformation. b) end of first phase of deformation. c) plan view of North Star Lake area at end of first phase of deformation and orientation of maximum principle stress and dextral shear couple.



Continued south--southwest-directed transport during the second phase of deformation (D_2) (Figure 7-5) produced a new generation of structures (F_{2a}) that initially developed perpendicular to the direction of transport (Figure 7-5a). West of the North--South zone structural break linear fabrics and the fold axes of the F_{2a} structures were reoriented by non-coaxial strain towards parallelism with the transport direction (Figure 7-5b). F_{2a} structures east of the North--South zone structural break were not reoriented towards parallelism due to either lower non-coaxial strain in this area or because strain occurred along planar surfaces. In plan view the North--South zone structural break is oriented parallel to the dextral shear couple and the maximum principle stress is oriented parallel to the transport direction (Figure 7-5c).

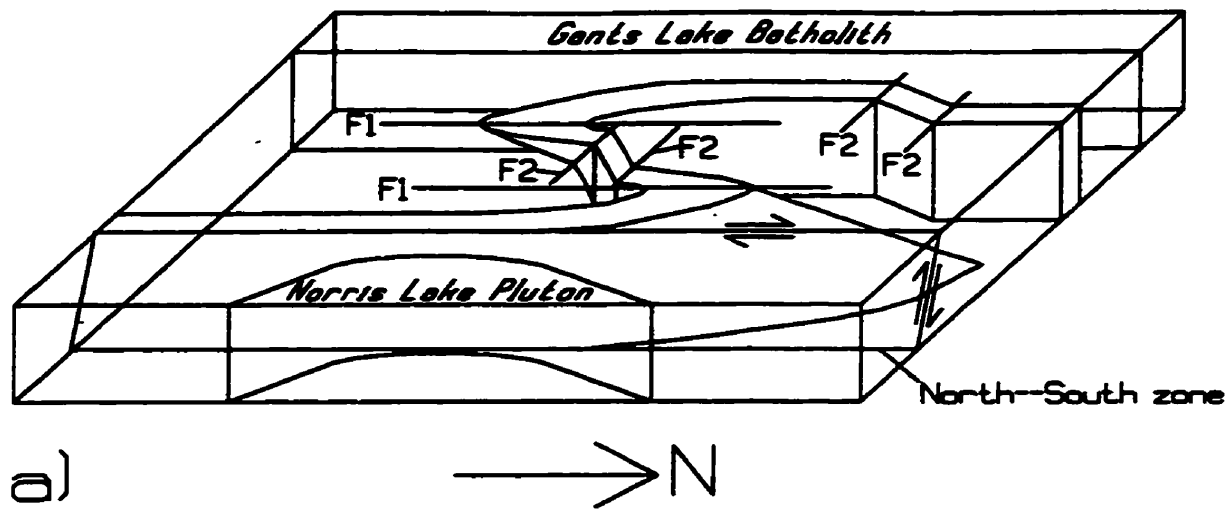
A linear fabric (L_{2a}) developed near-parallel to the direction of transport in the area west of the North--South structural break during the second phase of deformation (D_2) and the contemporaneous second phase of metamorphism (M_2). The L_{2a} fabric was the result of the continued recrystallization of mineral grains and the distortion of primary features. In some micaceous felsic rocks a gneissosity (S_{2a}) defines the L_{2a} fabric.

The area of the North--South zone was an area of deformational reactivation during D_2 . This zone was possibly active prior to D_1 (cf. Syme et al., 1995) and acted as a

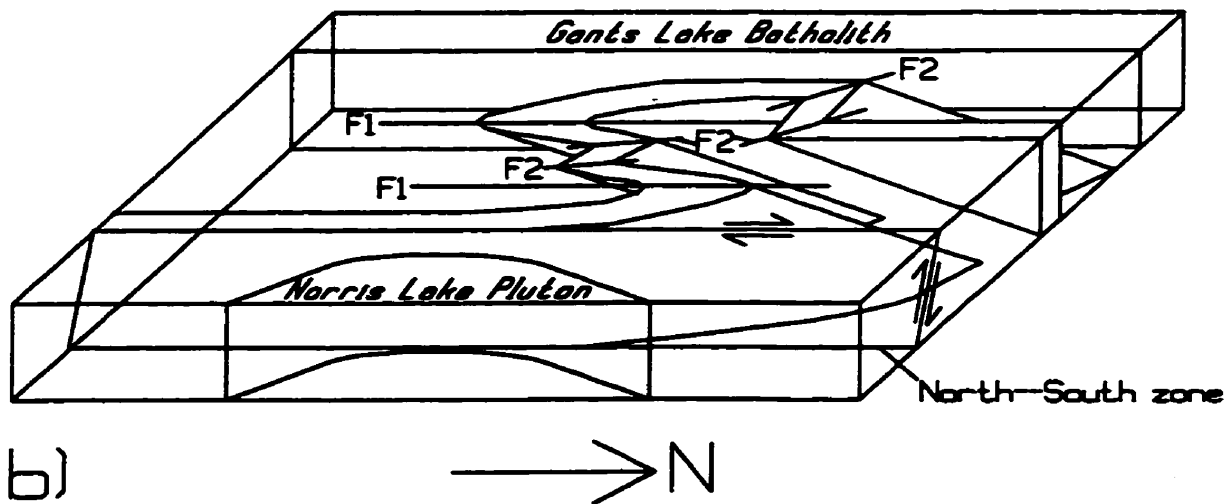
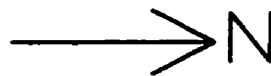
shear plane or decollement during D_1 and D_2 . The orientation of the principle stresses during D_2 would result in a dextral shear couple oriented subparallel to the of the trend North--South zone (Figure 7-5c). Reverse-slip crenulations (F_{2b}) with Z-asymmetry developed during D_2 and are interpreted to be the result of the dextral shear couple inclined clockwise at a small angle to the foliation within the zone.

The F_1 structures and the F_{2a} structures west of the North--South zone structural break are commonly near-coaxial and near-coplanar. This indicates that continued south--southwest-directed transport during D_2 resulted in continued reorientation of fold axes and linear fabrics towards near-parallelism with the transport direction and the transposition of planar features towards sub-parallelism with the thrust plane. In some areas (eg. subarea 3, Figure 4-2) however, the F_{2a} fold axes have a variable orientation. This suggests that the F_{2a} structures in this area are less evolved than the F_{2a} structures elsewhere in the North Star Lake area.

Peak metamorphism (M_2) in the North Star Lake area is associated with D_2 and was of medium-pressure amphibolite facies conditions. Peak metamorphism in the North Star Lake would have occurred at 1820--1805 Ma -- which is the time of peak metamorphism in the File Lake area (Connors, 1996).



a)



b)

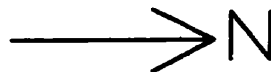
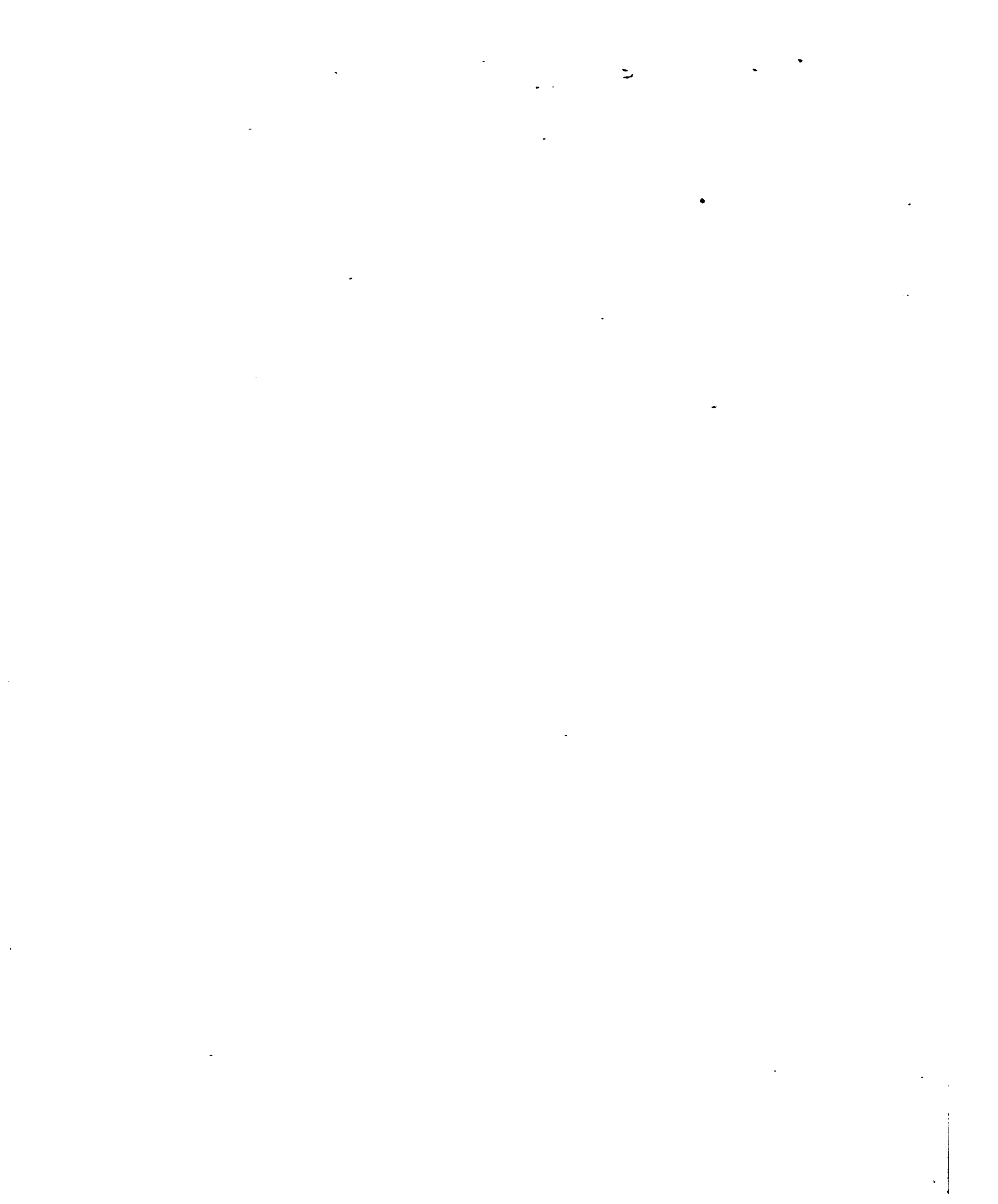
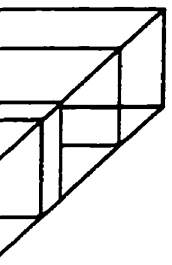
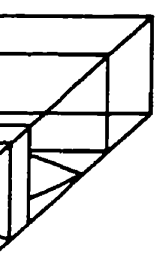


Figure 7-5
 area durin
 second ph
 deformatiic
 second ph
 principle

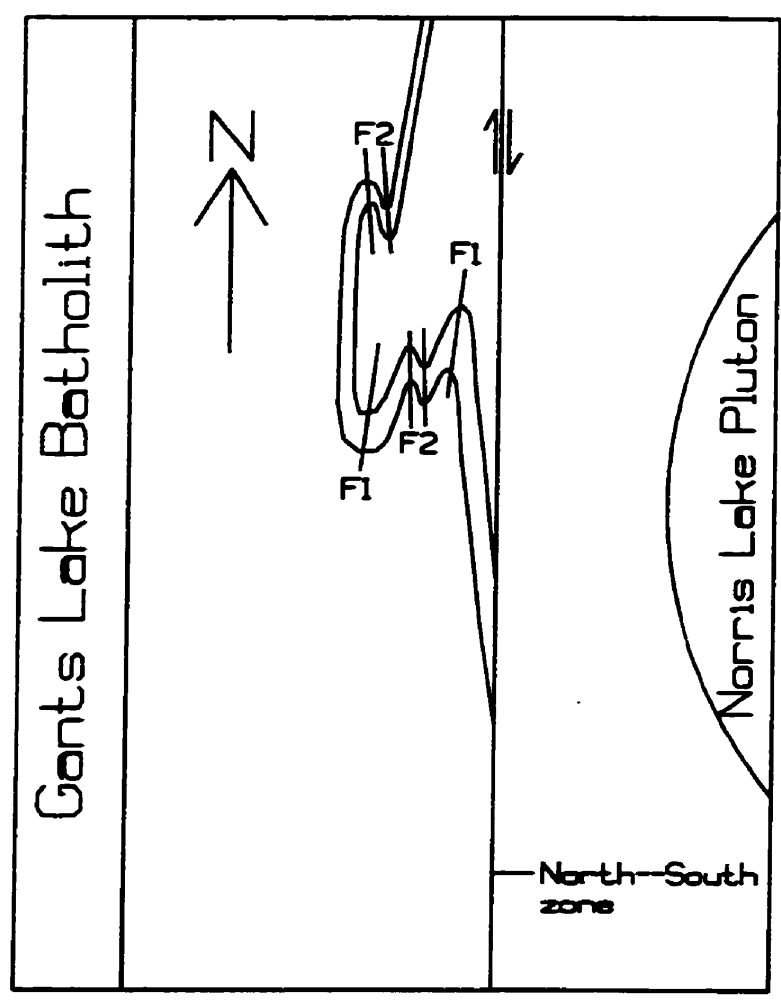
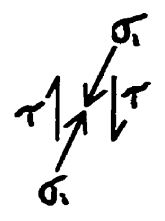




South zone



South zone

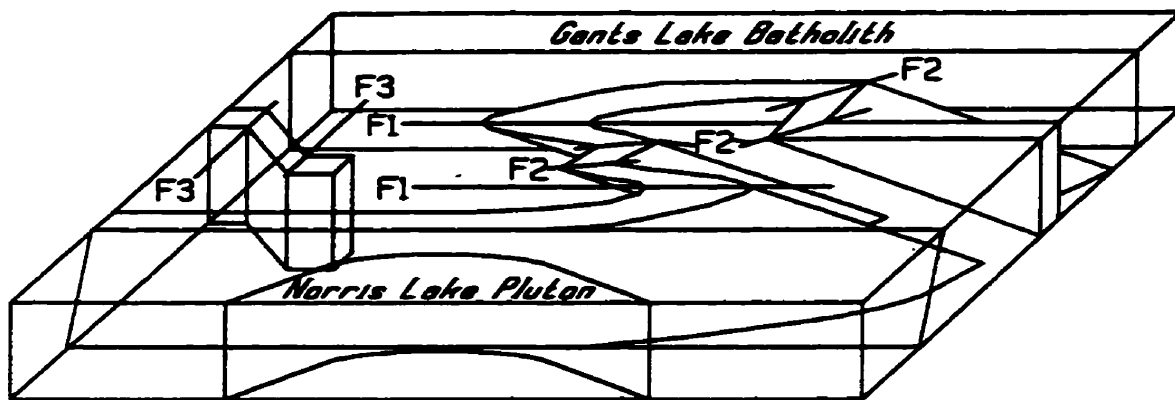


c)

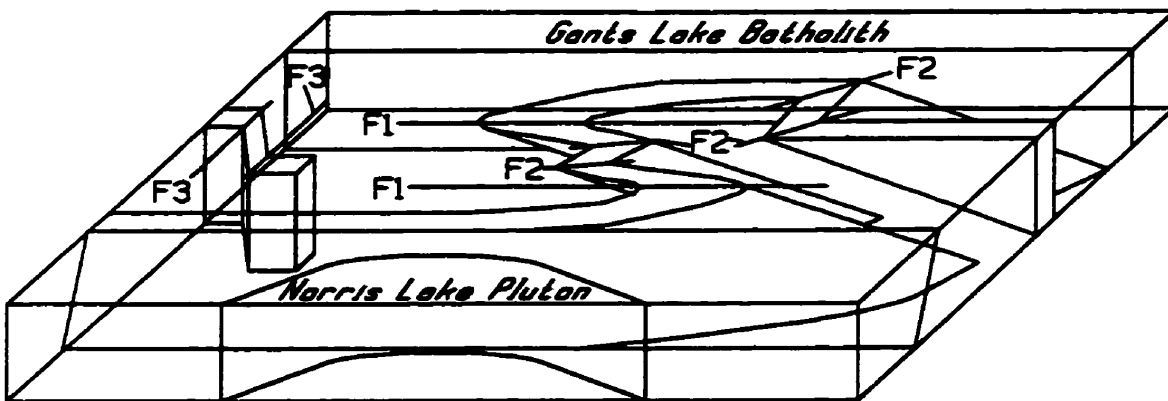
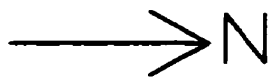
Figure 7-5. Diagram of the development of the North Star Lake area during the second phase of deformation. a) beginning of second phase of deformation. b) end of second phase of deformation. c) plan view of North Star Lake area at end of second phase of deformation and orientation of maximum principle stress and dextral shear couple.



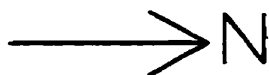
Continued southwest-directed compression in the North Star Lake area occurred subsequent to the peak of metamorphism under waning amphibolite facies conditions (Figure 7-6). The folds (F_3) that developed during the third phase of deformation (D_3) are predominantly flexural-slip buckle folds that locally contain an axial-planar foliation (S_3). The D_3 structures and fabrics developed perpendicular to the southwest transport or compression direction (Figure 7-6a). The F_3 structures were tightened but were not reoriented towards parallelism with the transport direction (Figure 7-6b). In plane view the F_3 fold axes are perpendicular to the northeast--southwest orientation of the maximum principle stress (Figure 7-6c).



a)



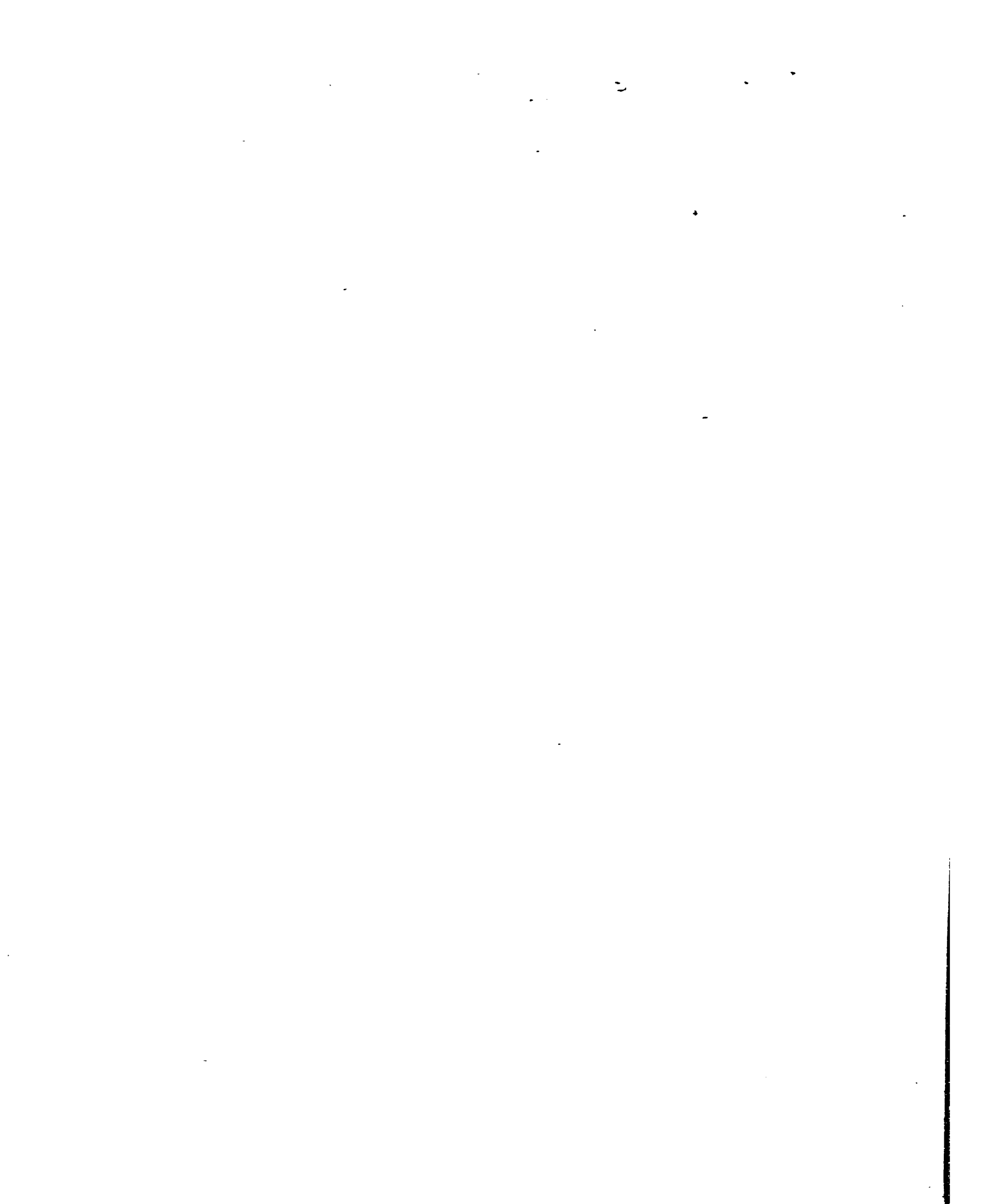
b)

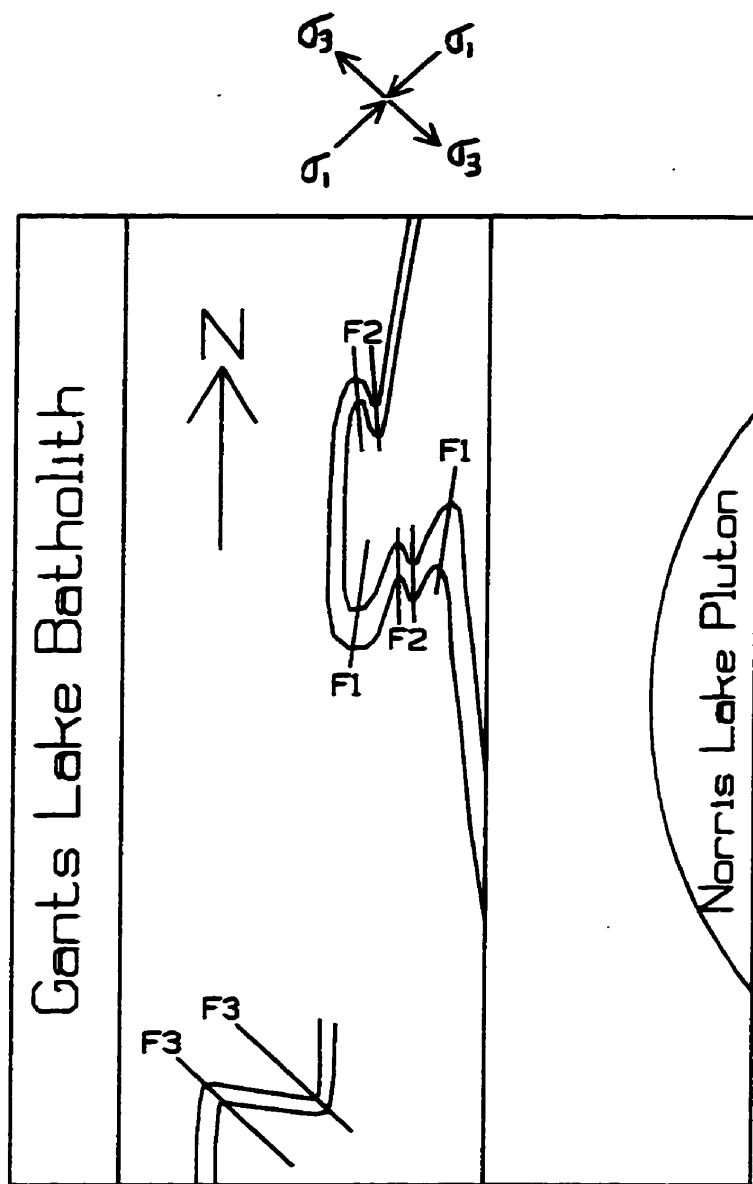


Gents Lake Batholith

c)

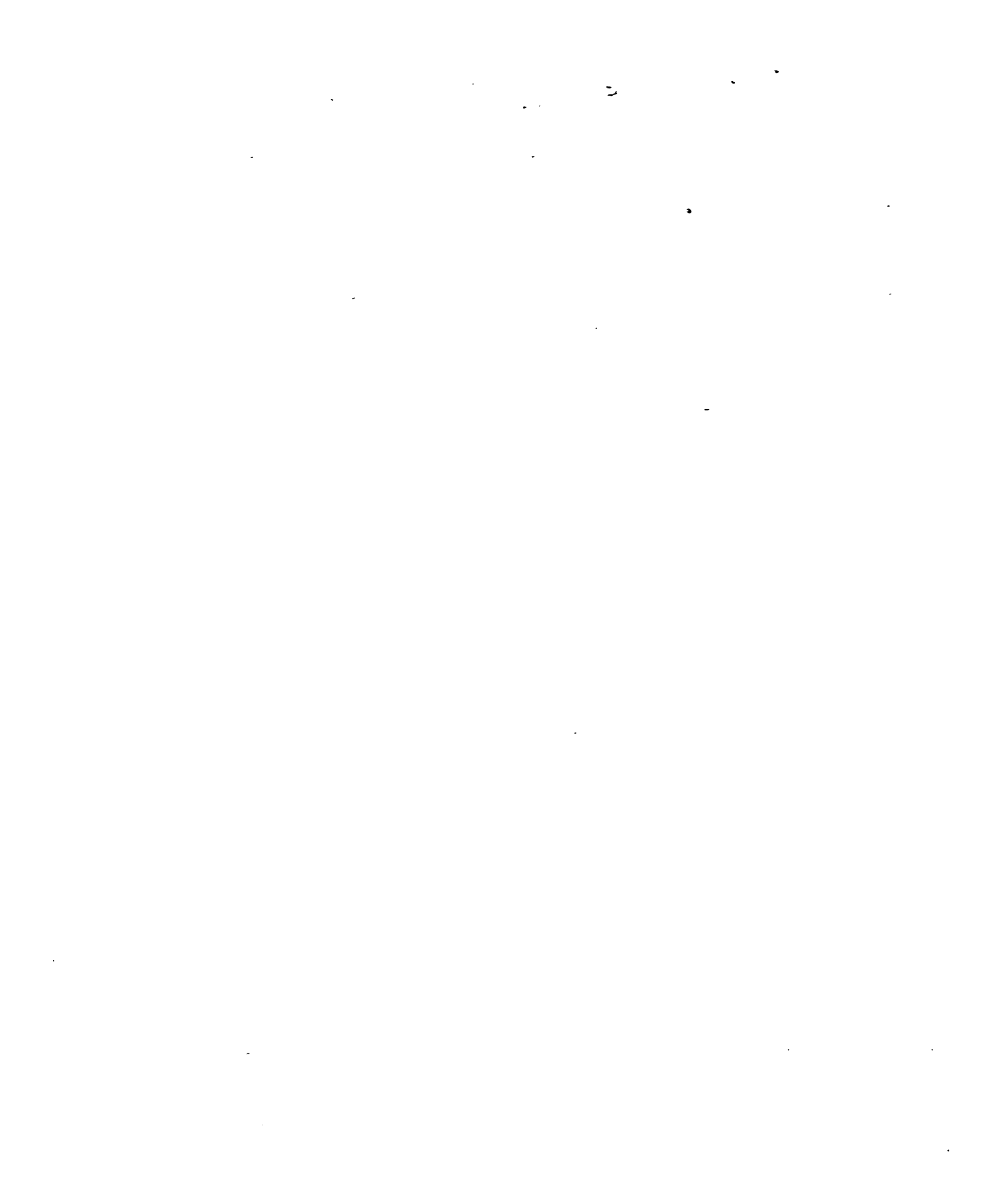
Figure 7-6. Diagram area during the third phase of deformation. c) plan view during the third phase of deformation.





c)

Figure 7-6. Diagram of the development of the North Star Lake area during the third phase of deformation. a) beginning of third phase of deformation. b) end of third phase of deformation. c) plan view of North Star Lake area at end of third phase of deformation and orientation of maximum and minimum principle stresses.



The final deformation (D_4) in the North Star Lake area resulted in brittle-ductile to brittle structures under greenschist facies conditions. This phase of deformation was the result of northwest--southeast compression (Figure 7-7) during uplift of the North Star Lake area. The north-trending brittle fault zone is oriented parallel to the sinistral shear couple. An east-trending fault possibly exists in the area along East--West Creek (Figure 3-2). There is no outcrop exposure of this assumed fault however, the outcrop pattern of the lithological units suggests dextral movement.

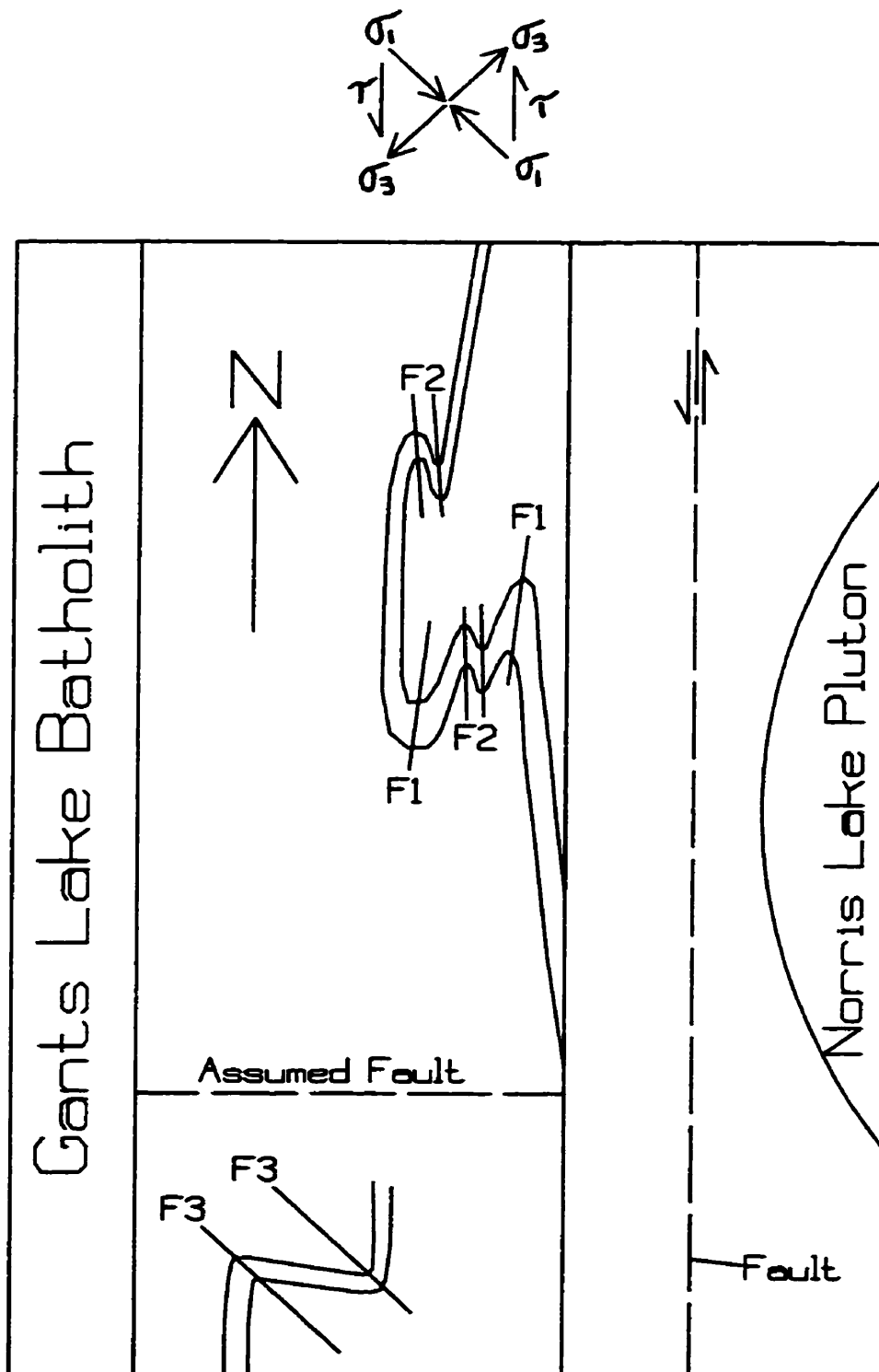


Figure 7-7. Plan view of the North Star Lake area during the fourth phase of deformation and orientation of maximum and minimum principle stresses and sinistral shear couple.

REFERENCES

Ayed, A.E. (1994): North Star Lake diatremes; B.Sc. Thesis, University of Manitoba.

Ayed, A.E. and Halden, N.M. (1993): North Star Lake breccia pipes (NTS 63K/15); in Manitoba Energy and Mines, Geological Services Branch, Report of Activities 1993, p.73-77

Bailes, A.H. (1971): Preliminary compilation of the geology of the Snow Lake--Flin Flon Sherridon area; Manitoba Mines Branch, Geological Paper 1/71, 27 pages.

Bailes, A.H. (1980): Geology of the File Lake area; Manitoba Energy and Mines, Mineral Resources Division, Geological Paper 78-1, 134 pages,

Bailes, A.H. and McRitchie, W.D. (1978): The transition from low to high grade metamorphism in the Kisseynew Sedimentary Gneiss Belt, Manitoba; in Fraser, A. and Heywood, W.W. (eds.); Metamorphism in the Canadian Shield; Geological Survey of Canada, Paper 78-10, p. 155-177.

Bailes, A.H. and Syme, E.C. (1987): Geology of the Flin Flon--White Lake Area; Manitoba Energy and Mines, Geological Report GR 87-1, 313 pages.

Bailes, A.H., Syme, E.C., Galley, A., Price, D.P., Skirrow, R. and Zeilke, D.J. (1987): Early proterozoic volcanism, hydrothermal activity, and associated ore deposits at Flin Flon and Snow Lake, Manitoba; Field Trip Guidebook, GAC-MAC Joint Annual Meeting, Saskatoon, Saskatchewan, 95 pages.

Barker, A.J. (1990): Introduction to Metamorphic Textures and Microstructures; Blackie, 162 pages.

Barrow, G. (1893): On an intrusion of muscovite--biotite gneiss in the south-eastern Highlands of Scotland, and its accompanying metamorphism; Quarterly Journal of the Geological Society of London, 49, p. 330-358.

Behrman, J.H. and Mainprice, D. (1987): Deformation mechanisms in a high-temperature quartz--feldspar mylonite: evidence for superplastic flow in the lower continental crust; Tectonics, 140, p.297-305.

Bell, T.H. (1978): Progressive deformation and reorientation of fold axes in a ductile mylonite zone: The Woodroffe Thrust; Tectonophysics, 44, p. 285-320.

Bell, T.H., Rubenach, M.J. and Fleming, P.D. (1986): Porphyroblast nucleation, growth and dissolution in regional metamorphic rocks as a function of deformation partitioning during foliation development; *J. Metam. Geol.*, 4, p. 37-67.

Bleeker, W. (1990): New structural--metamorphic constraints on Early Proterozoic oblique collision along the Thompson Nickel Belt, Manitoba; in Lewry, J.F. and Stauffer, M.R. (eds.); *The Early Proterozoic Trans-Hudson Orogen of North America*; Geological Association of Canada, Special Paper 37, p. 57-73.

Brown, M. (1993): P--T--t evolution of orogenic belts and the causes of regional metamorphism; *Journal of the Geological Society, London*, 150, p.227-241.

Bruce, E.L. (1918): Amisk--Athapapuskw Lakes district; Geological Survey of Canada, Memoir 105, 130 pages.

Connors, K.A. (1996): Unravelling the boundary between turbidites of the Kisseynew belt and volcano-plutonic rocks of the Flin Flon belt, Trans-Hudson Orogen, Canada; *Can. J. Earth Sci.*, 33, p. 811-829.

Dennis, A.J. and Secor, D.T. (1987): A model for the development of crenulations in shear zones with applications from the southern Appalachian Piedmont; *Journal of Structural Geology*, 8, p. 809-817.

Donath, F.A. and Parker, R.B. (1964): Folds and folding; *G.S.A. Bull.*, 75, p. 45-62.

Elliot, D. (1965): The quantitative mapping of directional minor structures; *Journal of Geology*, 73, p. 865-880.

Eskola, P. (1915): On the relations between the chemical and mineralogical composition in the metamorphic rocks of the Orijarvi region; *Bull. Comm. geol. Finlande*, No. 44.

Escher, A. and Watterson, J. (1974): Stretching fabrics, folds and crustal shortening; *Tectonophysics*, 22, p.223-231.

Ferry, J.M. and Spear, F.S. (1978): Experimental calibration of the partitioning of Fe and Mg between biotite and garnet; *Contributions to Mineralogy and Petrology*, 66, p. 113-117.

Fleuty, M.J. (1964): The description of folds; *Proc. Geol. Assoc.*, 75, Pt. 4, p. 461-489.

Flinn, D. (1962): On folding during three-dimensional progressive deformation; *J. Geol. Soc. Lond.*, 118, p. 385-428.

Flinn, D. (1965): Deformation in metamorphism; in Pitcher, W.S. and Flinn, G.W. (eds.); Controls of Metamorphism; Oliver and Boyd, p. 46-72.

Ganguly, J. and Saxena, S.K. (1984): Mixing properties of aluminosilicate garnets: constraints from natural and experimental data, and applications to geothermo-barometry; American Mineralogist, 69, p. 88-97.

Geological Survey of Canada (1990): Map C 21509 G, Magnetic anomaly map (residual total field), NTS 63K/15; 1: 50 000

Gordon, T.M., Hunt, P.A., Bailes, A.H. and Syme, E.C. (1990): U-Pb ages from the Flin Flon and Kisseynew belts, Manitoba: chronology of crust formation at an Early Proterozoic accretionary prism; in Lewry, J.F. and Stauffer, M.R., (eds.); The Early Proterozoic Trans-Hudson Orogen of North America; Geological Association of Canada, Special Paper 37, p. 177-199.

Green, A.G., Hajnal, Z. and Weber, W. (1985): An evolutionary model of the western Churchill Province and the western margin of the Superior Province in Canada and the north-central United States; Tectonophysics, 116, p. 281-322.

Hajnal, A. and Lewry, J. (eds.) (1992): LITHOPROBE Trans-Hudson Orogen Transect, Report 26.

Hajnal, A. and Lewry, J. (eds.) (1993): LITHOPROBE Trans-Hudson Orogen Transect, Report 34.

Hajnal, A. and Lewry, J. (eds.) (1994): LITHOPROBE Trans-Hudson Orogen Transect, Report 38.

Hajnal, A. and Lewry, J. (eds.) (1995): LITHOPROBE Trans-Hudson Orogen Transect, Report 48.

Halden, N.M., Clark, G.S., Corkery, M.T., Lenton, P.G. and Schledewitz, D.C.P. (1990): Trace-element and Rb-Sr whole-rock isotopic constraints on the origin of the Chipewyan, Thorsteinson, and Baldock batholiths, Churchill Province, Manitoba; in Lewry, J.F. and Stauffer, M.R., (eds.); The Early Proterozoic Trans-Hudson Orogen of North America; Geological Association of Canada, Special Paper 37, p. 201-214.

Hammer, S. and Passchier, C. (1991): Shear-sense indicators: a review; Geological Survey of Canada, Paper 90-17, 72 pages.

Hatcher, R.D.Jr. (1990): Structural Geology: Principles, Concepts and Problems; Merrill, 531 pages.

Hobbs, B.E, Means, W.D. and Williams, P.F. (1976): An Outline of Structural Geology; John Wiley and Sons, 571 pages.

Hoffman, P.F. (1981): Autopsy of Athapuscow Aulacogen: a failed arm affected by three collisions; in Campbell, F.H.A. (ed.); Proterozoic Basins of Canada; Geological Survey of Canada, Paper 81-10, p. 97-102.

Hoffman, P.F. (1988): United plates of America, the birth of a craton: Early Proterozoic assembly and growth of Laurentia; Annual Review of Earth and Planetary Sciences, 16, p. 543-603.

Hoffman, P.F. (1990): Subdivision of the Churchill Province and the extent of the Trans-Hudson Orogen; in Lewry J.F. and Stauffer, M.R., (eds.); The Early Proterozoic Trans-Hudson Orogen of North America; Geological Association of Canada, Special Paper 37, p. 15-39.

Klasner, J.S. and King, E.R. (1990): A model for tectonic evolution of the Trans-Hudson Orogen in North and South Dakota; in Lewry, J.F. and Stauffer, M.R., (eds.); the Early Proterozoic Trans-Hudson Orogen of North America; Geological Association of Canada, Special Paper 37, p. 271-285.

Knipe, R.J. (1981): The interaction of deformation and metamorphism in slates; Tectonophysics, 78, p.249-272.

Krause, J. and Williams, P.F. (1994a): Structure of the Squall Lake area, Snow Lake (NTS 63K/16). in Manitoba Energy and Mines, Geological Services Branch, Report of Activities 1994, p. 189-193.

Krause, J. and Williams, P.F. (1994b): Cleavage development and timing of metamorphism in the File Lake Formation across the Threehouse Synform, Snow Lake, Manitoba: A new paradigm; in Hajnal, A. and Lewry, J., (eds.); LITHOPROBE Trans-Hudson Orogen Transect, Report 38, p.230-260.

Krause, J. and Williams, P.F. (1995): The thermometamorphic history of the Snow Lake area, Manitoba, revisited; in Hajnal, A. and Lewry, J., (eds.); LITHOPROBE Trans-Hudson Orogen Transect, Report 48, p. 206-212.

Lewry, J.F. and Collerson, K.D. (1990): The Trans-Hudson Orogen: extent, subdivisions, and problems. in Lewry, J.F. and Stauffer, M.R., (eds.); The Early Proterozoic Trans-Hudson Orogen of North America; Geological Association of Canada, Special Paper 37, p.1-14.

Lewry, J.F., MacDonald, R., Livesey, C., Meyer, M.T., Van Schmus, W.R. and Bickford, M.E. (1987): U-Pb geochronology of accreted terranes in the Trans-Hudson Orogen in northern Saskatchewan; in *Geochemistry and Mineralization of Proterozoic Volcanic Suites*; Geological Society of London, Special Publication 33, p. 146-166.

Lewry, J.F., Thomas, D.J., Macdonald, R. and Chiarenzelli, J. (1990): Structural relations in accreted terrains of the Trans-Hudson Orogen, Saskatchewan: telescoping in a collisional regime?; in Lewry, J.F. and Stauffer, M.R., (eds.); *The Early Proterozoic Trans-Hudson Orogen of North America*; Geological Association of Canada, Special Paper 37, p. 75-94.

Lucas, S.B., Stern, R.A., Fedorowich, J. and Ansdell, K. (1994a): A brief history of the Flin Flon belt; *LITHOPROBE Trans-Hudson Orogen Transect, Report 38*, p. 251-260.

Lucas, S.B., White, D., Hajnal, Z., Lewry, J., Green, A., Clowes, R., Zwanzig, H., Ashton, K., Schledewitz, D., Stauffer, M., Norman, A., Williams, P.F. and Spence, G. (1994b): Three-dimensional collisional structure of the Trans-Hudson Orogen, Canada; *Tectonophysics*, 232, p. 161-178.

Lucas, S.B., Stern, R.A., Syme, E.C., Reilly, B.A. and Thomas, D.J. (1996): Intraoceanic tectonics and the development of continental crust: 1.92-1.84 Ga evolution of the Flin Flon Belt, Canada; *GSA Bulletin*, 108, p. 602-629.

Mawer, C.K. and Williams, P.F. (1991): Progressive folding and foliation development in a sheared, coticule--bearing phyllite; *Journal of Structural Geology*, 13, p.539-555.

McGlynn, J.C. (1959): Elbow--Hemming Lakes area, Manitoba; *Geological Survey of Canada, Memoir 305*, 72 pages.

Mies, J.W. (1991): Planar dispersion of folds in ductile shear zones and kinematic interpretation of fold-hinge girdles; *Journal of Structural Geology*, 13, p. 281-297.

Miyashiro, A. (1973): *Metamorphism and Metamorphic Belts*; George Allen and Unwin, 492 pages.

Mukherjee, A.C., Stauffer, M.R. and Baadsgaard, H. (1971): The Hudsonian Orogeny near Flin Flon, Manitoba: a tentative interpretation of Rb/Sr and K/Ar ages; *Can. J. Earth Sci.*, 8, p. 939-946.

Norman, A.R., Williams, P.F. and Ansdell, K.M. (1995): Early Proterozoic deformation along the southern margin of the Kisseynew gneiss belt, Trans-Hudson Orogen: a 30 Ma progressive deformation; *Can. J. Earth Sci.*, 32, p. 875-894.

Norquay, L.I. and Halden, N.M. (1992): Structural observations in the North Star Lake area (NTS area 63K/15); in *Manitoba Energy and Mines, Geological Services Branch, Report of Activities 1992*, p. 19-22.

Norquay, L.I., Prouse, D.E., Bieri, M. and Gale, G.H. (1991): Geology of the North Star Lake area (part of NTS 63K/15NE); in *Manitoba Energy and Mines, Minerals Division, Report of Activities 1991*, p. 31-39.

Norquay, L.I., Prouse, D.E., Heine, T.H. and Gale, G.H. (1992): Geological investigations in the North Star Lake area (NTS area 63K/15); in *Manitoba Energy and Mines, Geological Services Branch, Report of Activities 1992*, p. 23-27.

Norquay, L.I., Prouse, D.E. and Gale, G.H. (1993): Geological investigations in the North Star Lake area (NTS 63K/15); in *Manitoba Energy and Mines, Geological Services Branch, Report of Activities 1993*, p.78-83.

Norquay, L.I., Prouse, D.E. and Gale, G.H. (1994): North Star Lake (NTS 63K/15NE4); *Manitoba Energy and Mines, Preliminary Map 1994S-2*, 1:10 000.

Norquay, L.I., Prouse, D.E. and Gale, G.H. (1994): North Star Lake (NTS 63K/15SE4); *Manitoba Energy And Mines, Preliminary Map 1994S-3*, 1:10 000.

Norquay, L.I., Prouse, D.E. and Gale, G.H. (1994): The North Star Lake project (NTS 63K/15); in *Manitoba Energy and Mines, Geological Services Branch, Report of Activities 1994*, p. 83-84.

Perchuk, L.L, Podlesskii, K.K. and Aranovich, L.Ya. (1981): Calculation of thermal properties of end-member minerals from natural parageneses; in *Newton, R.C., Navrotsky, A. and Wood, B.J. (eds.); Thermodynamics of Minerals and Melts; Springer-Verlag*, p. 112-129.

Powell, C.McA. (1979): A morphological classification of rock cleavage; *Tectonophysics*, 58, p. 21-34.

Price, N.J. and Cosgrove, J.W. (1990): *Analysis of Geological Structures; Cambridge University Press, Cambridge*, 502 pages.

- Prouse, D.E. and Gale, G.H. (1993): North Star Lake (63K/15SE1); Manitoba Energy and Mines, Preliminary Map 1993-3, 1:5000
- Ramsey, J.G. (1967): Folding and Fracturing of Rocks; McGraw Hill, 568 pages.
- Ramsey, J.G. and Huber, M.I. (1983): The Techniques of Modern Structural Geology, Volume 1: Strain Analysis; Academic Press, 307 pages.
- Ramsey, J.G. and Huber, M.I. (1987): The Techniques of Modern Structural Geology, Volume 2: Folds and Fractures; Academic Press, 388 pages.
- Robin, P.Y.F. (1979): Theory of metamorphic segregation and related processes. *Geochim. Cosmochim. Acta*, 43, p. 1587-1600.
- Ryan, J.J. and Williams, P.F. (1994): Tectonometamorphic history of the Elbow Lake shear zone, Flin Flon--Snow Lake greenstone belt, Manitoba. in Hajnal, A and Lewry J. (eds.); LITHOPROBE Trans-Hudson Orogen Transect, Report 38, p. 221-229.
- Ryan, J.J. and Williams, P.F. (1995): The Elbow Lake area: a long-lived deformation corridor. in Hajnal, A. and Lewry, J. (eds.); LITHOPROBE Trans-Hudson Orogen Transect, Report 48, p. 156-161.
- Sanderson, D.J. (1973): The development of fold axes oblique to the regional trend; *Tectonophysics*, 16, p.55-70.
- Sibson, R.H. (1977): Fault rocks and fault mechanisms; *J. Geol. Soc. Lond.*, 133, p. 191-213.
- Shackleton R.M. and Ries, A.C. (1984): The relation between regionally consistent stretching lineations and plate motions; *Journal of Structural Geology*, 6, p. 111-117.
- Shelley, D. (1993): *Igneous and Metamorphic Rocks Under the Microscope: Classification, Textures, Microstructures and Mineral Preferred Orientations*; Chapman and Hall, 445 pages.
- Skjærnaa, L. (1980): Rotation and deformation of randomly oriented planar and linear structures in progressive simple shear; *Journal of Structural Geology*, 2, p. 101-109.
- Spear, F.S., Kohn, M.J., Florence, F.P. and Menard, T. (1991): A model for garnet and plagioclase growth in pelitic schists: implications for thermobarometry and P--T path determinations; *J. metamorphic Geol.* 8, p. 683-696.

- Stauffer, M.R. (1974): Geology of the Flin Flon area: a new look at the Sunless City; Geoscience Canada, 1, p. 217-242.**
- Stauffer, M.R. (1984): Manikewan: an Early Proterozoic ocean in central Canada, its igneous history and orogenic closure; Precambrian Research, 25, p. 257-281.**
- Stauffer, M.R., Mukherjee, A.C. and Koo, J. (1975): The Amisk Group: an Aphebian(?) island arc deposit; Can. J. Earth Sci., 12, p. 2021-2035.**
- Stauffer, M.R. (1990): The Missi Formation: an Aphebian molasse deposit in the Reindeer Lake Zone of the Trans-Hudson Orogen, Canada; in Lewry, J.F. and Stauffer, M.R., (eds.); The Early Proterozoic Trans-Hudson Orogen of North America; Geological Association of Canada, Special Paper 37, p. 121-141.**
- Stockwell, C.H. (1935): Gold deposits of the Elbow--Morton Lakes area, Manitoba; Geological Survey of Canada, Memoir 186, 74 pages.**
- Stockwell, C.H. (1961): Structural provinces, orogenies and time classification of rocks of the Canadian Shield; in Lowden, J.A. (ed.); Age Determinations by the Geological Survey of Canada; Geological Survey of Canada, Paper 6-17, p. 108-118.**
- Syme, E.C. (1990a): Stratigraphy and geochemistry of the Lynn Lake and Flin Flon metavolcanic belts, Manitoba; in Lewry, J.F. and Stauffer, M.R., (eds.); The Early Proterozoic Trans-Hudson Orogen of North America; Geological Association of Canada, Special Paper 37, p. 143-161.**
- Syme, E.C. (1990b): Elbow Lake project (part of NTS 63K/15); in Manitoba Energy and Mines, Minerals Division, Report of Activities 1990, p. 49-57.**
- Syme, E.C. (1991): Elbow Lake project -- Part A: Supracrustal rocks and structural setting; in Manitoba Energy and Mines, Minerals Division, Report of Activities 1991, p. 14-27.**
- Syme, E.C. (1992): Elbow Lake project -- Part A: Supracrustal rocks; in Manitoba Energy and Mines, Geological Services Branch, Report of Activities 1992, p. 32-46.**
- Syme, E.C., Bailes, A.H., Price, D.P. and Zeilke, D.V. (1982): Flin Flon volcanic belt: geology and ore deposits at Flin Flon and Snow Lake, Manitoba; Field Trip Guidebook 6, GAC-MAC Joint Annual Meeting, Winnipeg, Manitoba, 91 pages.**

Syme, E.C., Bailes, A.H. and Lucas, S.B. (1995): Geology of the Reed Lake area (parts of NTS 63K/9 and 10); in Manitoba Energy and Mines, Geological Services Branch, Report of Activities 1995, p. 42-60.

Thompson, J.B. (1957): The graphical analysis of mineral assemblages in pelitic schists; *American Mineralogist*, 42, p. 842-858.

Torbish, O.T. and Paterson, S.R. (1988): Analysis and interpretation of composite foliations in areas of progressive deformation; *Journal of Structural Geology*, 10, p. 745-755.

Trembath, G.D., Norquay, L.I. and Gale, G.H. (1990): Mineral investigations in the North Star Lake area (NTS 63K/15); in Manitoba Energy and Mines, Minerals Division, Report of Activities 1990, p. 77-79.

Van Hise, C.R. (1896): Principles of North American pre-Cambrian geology; in U.S Geological Survey 16th. Annual report, p. 571-843.

Weber, W. (1990): The Churchill-Superior Boundary Zone, southeast margin of the Trans-Hudson Orogen: a review; in Lewry, J.F. and Stauffer, M.R., (eds.); *The Early Proterozoic Trans-Hudson Orogen of North America*; Geological Association of Canada, Special Paper 37, p. 41-55.

Weber, W. and Scoates, R.F.J. (1978): Archean and Proterozoic metamorphism in the northwestern Superior Province and along the Churchill--Superior boundary, Manitoba; in Frasier, J.A. and Heywood, W.W. (eds.); *Metamorphism in the Canadian Shield*; Geological Survey of Canada, Paper 78-10, p. 5-16.

Whalen, J.B. (1991): Elbow Lake project -- Part B: Granitoid rocks; in Manitoba Energy and Mines, Minerals Division, Report of Activities 1991, p. 28-30.

Whalen, J.B. (1992): Elbow Lake project -- Part B: Granitoid rocks; in Manitoba Energy and Mines, Geological Services Branch, Report of Activities 1992, p. 47-51.

Whalen, J.B. (1993): Granitoid rocks of the Elbow Lake sheet (NTS 63K/15); in Manitoba Energy and Mines, Geological Services Branch, Report of Activities 1993, p. 86-89.

Winkler, H.G.F. (1979): *Petrogenesis of Metamorphic Rocks*, 5th ed.; Springer--Verlag, 348 pages.

Williams G.D. (1978): Rotation of contemporary folds into the X direction during overthrust processes in Laksefjord, Finnmark; *Tectonophysics*, 48, p.29-40.

Williams P.F. (1976): Relationship between axial-plane foliations and strain; *Tectonophysics*, 30, p.181-196.

Williams, P.F. and Zwart, H.J. (1977): A model for the development of the Seve--Koli Caledonian Nappe Complex; in Saxena, K. and Bhattacharji, S. (eds.); *Energetics of Geological Processes*; Springer--Verlag, p.169-187.

White, D.J. and Lucas, S.B. (1994): A closer look at the Superior Boundary zone. in Hajnal, A and Lewry, J. (eds.); *LITHOPROBE Trans-Hudson Orogen Transect, Report 38*, p. 35-41.

White, D.J., Lucas, S.B., Hajnal, Z., Green, A.G., Lewry, J.F., Weber, W., Bailes, A.H., Syme, E.C. and Ashton, K. (1994): Paleo-Proterozoic thick-skinned tectonics: Lithoprobe seismic reflection results from the eastern Trans-Hudson Orogen; *Can. J. Earth Sci.*, 31, p. 458-469.

Yardley, B.W.D. (1989): *An Introduction to Metamorphic Petrology*; Longman Scientific and Technical, 247 pages.

Zwanzig, H.V. (1990): Kisseynew gneiss belt in Manitoba: stratigraphy, structure, and tectonic evolution; in Lewry, J.F. and Stauffer, M.R., (eds.); *The Early Proterozoic Trans-Hudson Orogen of North America*; Geological Association of Canada, Special Paper 37, p. 95-120.

Zwanzig, H.V. (1995a): Alternative structural restorations of the Flin Flon Belt--Kisseynew Boundary Zone; in Hajnal, A. and Lewry, J., (eds.); *LITHOPROBE Trans-Hudson Orogen Transect, Report 48*, p. 135-142.

Zwanzig, H.V. (1995b): Geology of the Dow Lake area (parts of NTS 63K/15 and 63N/2); in Manitoba Energy and Mines, Geological Services Branch, *Report of Activities 1995*, p. 19-23.

Zwanzig, H.V. and Schledewitz, D.C.P. (1992): Geology of the Kississing--Batty Lakes area: interim report; Manitoba Energy and Mines, Open File OF92-2.

APPENDIX A

1) Perchuk et al., 1981

$$\ln K_D = (X_{Mg}/1-X_{Mg})^{M_1} (1-X_{Mg}/X_{Mg})^{C_2}$$

$$K_D = Mg/(Mg+Fe+Mn)$$

2) Ferry and Spear, 1979

$$T = (12454 + 0.057P) / (4.662 - 3R \ln(X_{prp}/X_{alm}) / X_{phi}/X_{ann})$$

P = pressure in bars

R = gas constant (1.987 cal/mole°K)

3) Ganguly and Saxena, 1984

$$T = [1175 + 9.45P + (W_{FeMg}(X_{alm} - X_{prp}) + 3000(X_{grs} + X_{spe})) / R] / [\ln((X_{alm}/X_{prp}) / X_{ann}/X_{phi}) + 0.782]$$

P = pressure in bars

R = gas constant (1.987 cal/mole°K)

$$W_{FeMg} = 200((X_{prp}/(X_{prp} + X_{alm})) + 2500((X_{alm}/(X_{prp} + X_{alm})))$$

Sample		1)	2)	3)
201				
X_{ann}	0.5372	T=540°C	P=5kbars	P=5kbars
X_{phi}	0.4611		T=539°C	T=533°C
X_{Mn-Bt}	0.0016			
X_{alm}	0.8167		P=6kbars	P=6kbars
X_{prp}	0.1104		T=543°C	T=537°C
X_{grs}	0.0251		P=7kbars	P=7kbars
X_{spe}	0.0461		T=547°C	T=541°C
1084				
X_{ann}	0.4758	T=508°C	P=5kbars	P=5kbars
X_{phi}	0.5220		T=497°C	T=494°C
X_{Mn-Bt}	0.0022			
X_{alm}	0.7560		P=6kbars	P=6kbars
X_{prp}	0.1129		T=500°C	T=498°C
X_{grs}	0.0642		P=7kbars	P=7kbars
X_{spe}	0.0651		T=504°C	T=501°C

Sample		1)	2)	3)
1125B site 1				
X_{ann}	0.6047	T=543°C	P=5kbars	P=5kbars
X_{phl}	0.3919		T=538°C	T=579°C
$X_{\text{Ms-Bt}}$	0.0034			
X_{alm}	0.8068		P=6kbars	P=6kbars
X_{prp}	0.0821		T=542°C	T=583°C
X_{grs}	0.0994		P=7kbars	P=7kbars
X_{spcs}	0.0241		T=546°C	T=586°C
1125B site 2				
X_{ann}	0.5958	T=572°C	P=5kbars	P=5kbars
X_{phl}	0.4029		T=578°C	T=595°C
$X_{\text{Ms-Bt}}$	0.0013			
X_{alm}	0.8090		P=6kbars	P=6kbars
X_{prp}	0.0972		T=582°C	T=599°C
X_{grs}	0.0877		P=7kbars	P=7kbars
X_{spcs}	0.0116		T=586°C	T=603°C
1136				
X_{ann}	0.5829	T=550°C	P=5kbars	P=5kbars
X_{phl}	0.4171		T=547°C	T=563°C
$X_{\text{Ms-Bt}}$	0.0000			
X_{alm}	0.8759		P=6kbars	P=6kbars
X_{prp}	0.1011		T=551°C	T=567°C
X_{grs}	0.0224		P=7kbars	P=7kbars
X_{spcs}	0.0269		T=554°C	T=570°C
1138				
X_{ann}	0.7282	T=527°C	P=5kbars	P=5kbars
X_{phl}	0.2594		T=578°C	T=607°C
$X_{\text{Ms-Bt}}$	0.0123			
X_{alm}	0.7239		P=6kbars	P=6kbars
X_{prp}	0.0458		T=582°C	T=612°C
X_{grs}	0.0329		P=7kbars	P=7kbars
X_{spcs}	0.2121		T=586°C	T=616°C

Sample		1)	2)	3)
2008				
X_{ann}	0.5706	T=566°C	P=5kbars	P=5kbars
X_{phl}	0.4283		T=572°C	T=569°C
X_{Mn-Bt}	0.0011			
X_{alm}	0.8215		P=6kbars	P=6kbars
X_{prp}	0.1075		T=576°C	T=573°C
X_{grs}	0.0471		P=7kbars	P=7kbars
X_{spcs}	0.0223		T=580°C	T=577°C
3026				
X_{ann}	0.6503	T=465°C	P=5kbars	P=5kbars
X_{phl}	0.3482		T=433°C	T=516°C
X_{Mn-Bt}	0.0016			
X_{alm}	0.7902		P=6kbars	P=6kbars
X_{prp}	0.0449		T=437°C	T=519°C
X_{grs}	0.1056		P=7kbars	P=7kbars
X_{spcs}	0.0728		T=440°C	T=522°C
3076				
X_{ann}	0.5887	T=562°C	P=5kbars	P=5kbars
X_{phl}	0.4094		T=583°C	T=596°C
X_{Mn-Bt}	0.0019			
X_{alm}	0.8058		P=6kbars	P=6kbars
X_{prp}	0.1008		T=586°C	T=600°C
X_{grs}	0.0376		P=7kbars	P=7kbars
X_{spcs}	0.0632		T=590°C	T=604°C